

Carnegie Mellon University

CARNEGIE INSTITUTE OF TECHNOLOGY

THESIS

SUBMITTED IN PARTIAL FULFILLMENT OF THE REQUIREMENTS

FOR THE DEGREE OF Doctor of Philosophy

TITLE Assessment of Solid Sorbent Systems for Post Combustion Carbon Dioxide Capture at Coal-Fired Power Plants

PRESENTED BY Justin Glier

ACCEPTED BY THE DEPARTMENT OF

Engineering and Public Policy

Edward Rubin
ADVISOR, MAJOR PROFESSOR

December 22, 2015
DATE

Douglas Sicker
DEPARTMENT HEAD

December 22, 2015
DATE

APPROVED BY THE COLLEGE COUNCIL

Vijayakumar Bhagavatula
DEAN

December 23, 2015
DATE

Assessment of Solid Sorbent Systems for Post-Combustion Carbon Dioxide Capture at Coal-Fired Power Plants

Submitted in partial fulfillment of the requirements for the degree of

Doctor of Philosophy

In

Engineering & Public Policy

Justin C. Glier

Bachelor of Science, Environmental Soil Science, University of Delaware

Master of Engineering, Engineering, University of Arizona

Carnegie Mellon University

Pittsburgh, PA

November 2015

Acknowledgments

This work was supported by the U.S. Department of Energy's National Energy Technology Laboratory (DOE/NETL).

First, I would like to thank my wonderful girlfriend, Lauren Arnita, who has been a patient and unwavering source of happiness and understanding. You have made the past few years ever better through your love, humor, and empathy. I love you very much. To my parents, Geoff and Jan Glier. You instilled in me a passion for the environment and a sense of urgency for finding a balance between progress and preservation. Our many "forest marches" together throughout the years has taught me the value of making your own fun. You both have given me so much and I am eternally grateful. To my sister, Jennifer Glier, whose drive and unflagging determination has been a constant source of inspiration. Finally, thank you to all the wonderful friends I have made during my time at Carnegie Mellon. You have all made the journey worth while.

Next, I would like to thank Hari Mantripragada. Your guidance and never-ending support made all the difference during this endeavor. I learned a lot over the years under your mentorship, and I really appreciate the time and effort you have invested into this work. Your patience and understanding have been invaluable in getting this thesis finished. I hope to cultivate the same positive and long lasting influence that you have on others, every day. I wish you all the best and hope that many people have the benefit of your guidance in the future. Thank you as well to Professor Ed Rubin. Your hard work has been an inspiration, as has your graceful acceptance of everything that goes with it. Thank you for your patience, your compassion, and for teaching me the value of nuance. I am eternally grateful for the opportunity to have learned from you.

In our research group, I would like to thank in particular Peter Versteeg and Kyle Borgert. I have learned great and many things from our conversations. Your feedback, troubleshooting, and help with this work have greatly improved it. Thank you as well to Scott Matthews for teaching the best class I have

ever had. Your commitment, approachability, and style are an inspiration and I wish you great success in the years to come.

I am also beholden to several colleagues at NETL for their help and attention to detail including, Mac Gray, David Miller, and Nick Seifert. A special thank you to Dan Fauth and Jim Hoffman for your generous open door policy and tolerance of my abuse of said policy. Finally, I would also like to thank my committee chair Ed Rubin, committee members Paul Fischbeck, Holly Krutka, Hari Mantripragada, and Jeff Sirola and the many other great professors and the fantastic staff in the Department of Engineering and Public Policy. You made my time here an experience to remember.

Abstract

In an effort to lower future CO₂ emissions, a wide range of technologies are being developed to scrub CO₂ from the flue gases of fossil fuel-based electric power and industrial plants. This thesis models one of several early-stage post-combustion CO₂ capture technologies, solid sorbent-based CO₂ capture process, and presents performance and cost estimates of this system on pulverized coal power plants.

The spreadsheet-based software package Microsoft Excel was used in conjunction with AspenPlus modelling results and the Integrated Environmental Control Model to develop performance and cost estimates for the solid sorbent-based CO₂ capture technology. A reduced order model also was created to facilitate comparisons among multiple design scenarios. Assumptions about plant financing and utilization, as well as uncertainties in heat transfer and material design that affect heat exchanger and reactor design were found to produce a wide range of cost estimates for solid sorbent-based systems. With uncertainties included, costs for a supercritical power plant with solid sorbent-based CO₂ capture ranged from \$167 to \$533 per megawatt hour for a first-of-a-kind installation (with all costs in constant 2011 US dollars) based on a 90% confidence interval. The median cost was \$209/MWh.

Post-combustion solid sorbent-based CO₂ capture technology is then evaluated in terms of the potential cost for a mature system based on historic experience as technologies are improved with sequential iterations of the currently available system. The range costs for a supercritical power plant with solid sorbent-based CO₂ capture was found to be \$118 to \$189 per megawatt hour with a nominal value of \$163 per megawatt hour given the expected range of technological improvement in the capital and operating costs and efficiency of the power plant after 100 GW of cumulative worldwide experience.

These results suggest that the solid sorbent-based system will not be competitive with currently available liquid amine-systems in the absence of significant new improvements in solid sorbent properties and process system design to reduce the heat exchange surface area in the regenerator and cross-flow heat exchanger. Finally, the importance of these estimates for policy makers is discussed.

Contents

Acknowledgments	1
Abstract	3
Contents	4
List of Tables	13
List of Figures	19
1. The role of carbon capture and storage in climate change mitigation	23
1.1. Carbon dioxide emissions and electric power	23
1.2. Why the interest in carbon capture and storage?.....	25
1.3. Overview of current options for carbon dioxide capture and storage (CCS).....	26
1.3.1. The current state of post-combustion carbon capture and storage	28
1.3.2. Commercial projects for carbon capture and storage	29
1.3.3. Full-scale demonstration plants	29
1.3.4. The drawbacks of solvent-based systems	32
1.4. Why study solid sorbents for post-combustion carbon capture?.....	35
1.5. Current status of solid sorbent-based carbon capture technology	36
1.6. Scope and objectives of this thesis.....	38
1.7. Organization of thesis	39
2. Sorbent characteristics	40
2.1. Chemical and physical adsorbents	40
2.2. Solid sorbents properties and materials for post-combustion applications.....	41
2.3. Chemical degradation	44
2.3.1. Influence of nitrogen	45
2.3.2. Influence of water.....	46
2.3.3. Influence of sulfur dioxide, nitrogen oxides, and oxygen	49

2.4.	Physical attrition.....	51
2.5.	Treatment of degradation and attrition.....	52
2.6.	Reaction kinetics.....	52
2.7.	Sorbents modelled in this thesis.....	54
2.8.	Conclusion.....	56
3.	The solid sorbent process for coal-based CCS	58
3.1.	Introduction.....	58
3.2.	Adsorption/desorption cycles	59
3.2.1.	Temperature-swing adsorption.....	59
3.2.2.	Pressure-swing cycles	60
3.2.3.	Liquid-solid heat exchange.....	63
3.2.4.	Solid-gas heat exchange.....	64
3.3.	Gas-solid system designs	64
3.3.1.	Fixed bed reactors	65
3.3.2.	Moving bed reactors.....	66
3.3.3.	Bubbling and circulating fluidized-bed reactors.....	67
3.3.4.	Cascading bed reactors	68
3.4.	Process design choice	69
4.	Process performance model	73
4.1.	Model objective.....	73
4.2.	Process mass balance	73
4.2.1.	Flue gas pre-treatment.....	75
4.2.2.	Flue gas blower	77
4.2.3.	Adsorber	77
4.2.4.	Flue gas cyclones	84
4.2.5.	Cold-side heat exchanger	85

4.2.6.	Regenerator.....	86
4.2.7.	Hot-side heat exchanger	95
4.2.8.	Discarded solids separation	96
4.2.9.	Discarded solids treatment.....	98
4.2.10.	Solid sorbent storage and handling area	98
4.2.11.	Closing the mass balance	104
4.3.	Quantifying rich and lean CO ₂ loading.....	105
4.3.1.	The Langmuir equations for modelled solid sorbents	105
4.3.2.	Influence of water on solid sorbent capacity	113
4.3.3.	Kinetics and carbon dioxide loading	114
4.3.4.	Actual rich and lean loading	116
4.4.	Energy balance.....	118
4.4.1.	Flue gas pre-treatment and blower	120
4.4.2.	Cooling duty.....	122
4.4.3.	Heating duty	126
4.4.4.	Auxiliary electrical load.....	131
4.5.	Performance estimators.....	137
4.5.1.	Total CCS electricity requirements	137
4.5.2.	Energy penalty.....	139
4.5.3.	Specific solid requirement	139
4.5.4.	Net plant efficiency.....	139
4.6.	Performance calculation procedure	140
4.7.	Chapter conclusion	142
5.	Performance model case studies for a full-scale system	143
5.1.	Baseline assumptions about the power plant.....	143
5.2.	Case Study #1: The “ideal sorbent” performance model	146

5.2.1.	Case Study #1 calculation.....	149
5.2.2.	Case Study #1 discussion.....	171
5.3.	Performance model sensitivity studies.....	172
5.3.1.	Solid sorbent variables.....	174
5.3.2.	Adsorber design variables.....	180
5.3.3.	Regenerator design variables.....	181
5.3.4.	CO ₂ capture efficiency.....	182
5.4.	Case Study #2: Effects of SO ₂ impurities.....	184
5.4.1.	Case study #2 calculation	185
5.4.2.	Case study #2 discussion.....	196
5.5.	Case study #3: Effect of water vapor impurities	196
5.5.1.	Case study #3 calculation	197
5.5.2.	Case study #3 discussion.....	208
5.6.	Case study #4: Effects of water and SO ₂ impurities.....	208
5.6.1.	Case study #4 calculation	209
5.6.2.	Case study #4 discussion.....	220
5.7.	Summary results for Case Studies #1 through #4.....	222
5.8.	Effect of solid purge fraction.....	224
5.9.	Case Studies #5 and #6: Systems informed by CCSI's model	226
5.10.	Performance case studies based on expert elicitation	230
5.11.	Characterization of performance uncertainty and variability	237
5.12.	Chapter conclusion	240
6.	Process cost model	242
6.1.	Cost estimation method	242
6.2.	Process facilities capital (PFC).....	243
6.2.1.	Flue gas pre-treatment system	247

6.2.2.	Flue gas blower	248
6.2.3.	CO ₂ adsorber	248
6.2.4.	Cyclone bank	250
6.2.5.	Cold-side heat exchanger	250
6.2.6.	Regenerator	252
6.2.7.	Hot-side heat exchanger	254
6.2.8.	Product gas drying and compression.....	256
6.2.9.	Solid sorbent storage and staging	257
6.2.10.	Conveyor systems	257
6.2.11.	Heat exchange circulation pump	258
6.2.12.	Heat exchange circulation compressor.....	258
6.2.13.	Steam extractor	258
6.3.	Total plant cost (TPC)	259
6.4.	Total capital requirement (TCR)	261
6.5.	Operation and maintenance costs	262
6.5.1.	Fixed O&M costs.....	263
6.5.2.	Variable O&M	264
6.5.3.	Total O&M cost summary.....	270
6.6.	Overall cost metrics	271
6.6.1.	Cost of electricity generation	272
6.6.2.	Cost of CO ₂ avoidance.....	273
6.7.	Illustrative cost model results	274
6.7.1.	Adsorber costs	274
6.7.2.	Regenerator cost	277
6.7.3.	Solid purge fraction.....	280
6.8.	Characterization of parameter uncertainty and variability.....	282

6.9.	Chapter conclusion	284
7.	Model applications	285
7.1.	Baseline plant characteristics.....	286
7.2.	Case studies with solid sorbent-based CO ₂ capture	290
7.2.1.	Power plants with idealistic CO ₂ capture (Case Studies 1-4).....	292
7.2.2.	Power plants with CCSI response surface model (Cases 5 and 6).....	293
7.2.3.	Power plants with present-case elicitation results (Cases 7-10).....	293
7.2.4.	Power plants with future-case elicitation results (Cases 11-14).....	294
7.2.5.	Case study discussion	295
7.3.	Cost uncertainty for solid sorbent systems	299
7.4.	Probabilistic uncertainty analysis.....	301
7.5.	Estimating future costs.....	304
7.5.1.	Introduction.....	305
7.5.2.	Application of technology learning curves.....	306
7.5.3.	Future cost results	309
7.6.	Achieving low cost solid sorbent-based CO ₂ capture	311
7.7.	Technological maturity of solid sorbent systems.....	314
7.8.	Chapter conclusion	315
8.	Summary and conclusions	317
8.1.	Thesis summary	317
8.2.	Main results and implications	319
9.	References	321
10.	Appendices	337
	Appendix A: Characterization of uncertainty and variability	337
	Appendix B: Expert elicitation form	340
	Appendix C: Flue gas pre-treatment (Direct Contact Cooler and Polishing Scrubber).....	364

General application	364
Performance model development	366
Performance model	372
Appendix D: Flue gas blower design.....	386
Appendix E: Heat exchanger design.....	387
Appendix F: Derivation of the degraded solid flow rate at the adsorber inlet.....	388
Mass flow rate of SO ₂ entering the system.....	389
Mass flow rate of adsorbed SO ₂ at the adsorber inlet.....	389
Mass flow rate of degraded solid sorbent.....	391
Solid composition	391
Sensitivity to purge fraction.....	392
Appendix G: CCSI performance and cost model data matching exercise	393
Appendix H: Adsorber response surface model	396
Matching CCSI adsorber modelling results	396
CCSI adsorber sensitivity analysis data	398
Appendix I: Probability distributions for solid sorbent system performance model parameters	
402	
CO ₂ capture efficiency (%)	403
Maximum CO ₂ loading (moles CO ₂ /kg dry solid sorbent).....	403
Heat of reaction.....	404
Solid heat capacity	405
Adsorber Temperature	406
Adsorber equilibrium CO ₂ pressure.....	406
Adsorber pressure drop.....	406
Adsorption Kinetics.....	407
Adsorber overall heat transfer coefficient	408
Regeneration temperature.....	409

CO ₂ outlet pressure	410
Regeneration kinetics	410
Regenerator overall heat transfer coefficient.....	411
Cross-flow HX solid temp. at hot-side outlet.....	413
Flue gas blower efficiency	413
Solids purge fraction.....	413
Water uptake (% removed from flue gas).....	414
Water regeneration efficiency	414
Water influence on CO ₂ Capacity	415
CO ₂ product pressure	416
CO ₂ compressor efficiency	416
Solid sorbent cost.....	417
CO ₂ transport cost.....	418
Appendix J: Case study generation and cost data.....	418
Case study #1: Ideal solid sorbent system without degradation.....	418
Case study #2: Ideal with SO ₂ degradation.....	421
Case study #3: Ideal with water degradation.....	423
Case study #4: Ideal with SO ₂ and water degradation.....	425
Case study #5: CCSI model without SO ₂ degradation.....	427
Case study #6: CCSI model with SO ₂ degradation.....	430
Case study #7: Present case without degradation.....	432
Case study #8: Present case with SO ₂ degradation	434
Case study #9: Present case with water degradation	436
Case study #10: Present case with SO ₂ and water degradation	439
Case study #11: Future case without degradation.....	441
Case study #12: Future case with SO ₂ degradation	443

Case study #13: Future case with water degradation	446
Case study #14: Future case with SO ₂ and water degradation.....	448
Appendix K: Financial assumptions for the baseline power plant.....	450

List of Tables

Table 1.1: Current and projected global generation of electricity by fuel source.....	24
Table 1.2: Installed electrical generation capacity and net electricity production by type.....	24
Table 1.3: Planned and active commercial post-combustion capture processes at power plants that capture, transport, and sequester CO ₂	31
Table 1.4: CO ₂ capture costs for post-combustion CO ₂ capture systems.	34
Table 1.5: Potential advantages and challenges for solid sorbent-based post-combustion CO ₂ capture	36
Table 2.1: List of parameters used in the performance and cost models describing the solid sorbent.	42
Table 2.2: Advantages and disadvantages of the leading solid sorbents being considered for use in a carbon capture system	43
Table 4.1: Flue gas constituents used as inputs to the solid sorbent model.....	75
Table 4.2: Reactor bed designs commonly used for solid-gas reactors and the resulting equilibrium pressures.....	107
Table 4.3: Properties of the solid sorbents discussed in this work	111
Table 4.4: Thermodynamic properties of the heat exchanger fluid circulating through the cold-side heat exchangers.	123
Table 4.5: Thermodynamic properties of the heat exchanger fluid circulating through the cold-side heat exchangers.	127

Table 4.6: Reference values and assumptions for the solid sorbent-based CO ₂ capture system.	132
Table 5.1: Configuration parameters for the baseline power plant used to evaluate the solid sorbent-based CO ₂ capture system	143
Table 5.2: Summary table of constant values relating to the performance model shown in Chapter 4.	145
Table 5.3: Flue gas conditions and molar composition upon entering the CO ₂ capture system for Case Study #1.	146
Table 5.4: Baseline configuration for the solid sorbent-based CO ₂ capture system for Case Study #1.	148
Table 5.5: Changes in the input parameters for Case Study #2 as different from those used in Case Study #1.	185
Table 5.6: Flue gas conditions and molar composition upon entering the CO ₂ capture system for Case Study #2.	186
Table 5.7: Changes in the input parameters for Case Study #2 as different from those used in Case Study #1.	197
Table 5.8: Flue gas conditions and molar composition upon entering the CO ₂ capture system for Case Study #3.	198
Table 5.9: Changes in the input parameters for Case Study #3 as different from those used in Case Study #1.	209
Table 5.10: Flue gas conditions and molar composition upon entering the CO ₂ capture system for Case Study #4.	210

Table 5.11: Performance results for solid sorbent system using performance parameters informed by deterministic CCSI model results.....	223
Table 5.12: Changes to the performance parameter values used for the CCSI case studies. ...	228
Table 5.13: Performance results for solid sorbent system using performance parameters informed by deterministic CCSI model results.....	229
Table 5.14: Performance parameter values for the elicited performance scenarios	231
Table 5.15: Degradation parameter values used in the elicited performance scenarios	234
Table 5.16: Results for the Present case scenarios.	235
Table 5.17: Results for the Future case scenarios.	237
Table 5.18: Solid sorbent system performance model parameters and uncertainties for system which would be built using today's state-of-the-art solid sorbent system.	238
Table 6.1: List of equipment and process areas and the reference source used for cost data...	247
Table 6.2: Nomenclature and temperature values used to calculate the logarithmic mean temperature difference in the cold-side heat exchanger	252
Table 6.3: Derivation of the temperatures for the solid and team used to calculate the heat exchange surface area and steam requirements for the regenerator.	254
Table 6.4: Nomenclature and temperature values used to calculate the logarithmic mean temperature difference in the hot-side heat exchanger	256
Table 6.5: Process contingency cost guidelines.....	260
Table 6.6: Project contingency costs	260

Table 6.7: Solid sorbent capital cost model parameters and nominal values	262
Table 6.8: Solid sorbent O&M cost model parameters and nominal values.	271
Table 6.9: Solid sorbent system cost model parameters and uncertainties for system that would be built using today's state-of-the-art solid sorbent system.....	283
Table 7.1: Baseline PC power plant assumptions for the reference (no CO ₂ capture) case and CCS-equipped cases.....	286
Table 7.2: Summary of IECM results for the reference supercritical power plant without CO ₂ capture.....	290
Table 7.3: Differences in parameter values for the initial 14 case studies.	291
Table 7.4: Summary of case study supercritical PC plants with idealized solid sorbent-based CO ₂ capture.....	292
Table 7.5: Summary of case study results for supercritical PC plants with CO ₂ capture using CCSI's response surface models.....	293
Table 7.6: Summary of case study results for supercritical PC plants with CO ₂ capture using the present case performance and cost models.....	294
Table 7.7: Summary of case study results for supercritical PC plants with CO ₂ capture using the future case performance and cost models.....	295
Table 7.8: CO ₂ capture system direct capital cost estimates for select cases.....	296
Table 7.9: Breakdown of CO ₂ capture and storage system total capital requirement (TCR) by cost component for FOAK systems	297
Table 7.10: Summary of results for the initial 14 case studies	299

Table 7.11: Summary data for the probabilistic LCOE uncertainty distributions representing the 90th percentile and median.....	304
Table 7.12: Summary of “best estimate” learning rates for capital and O&M costs	308
Table 7.13: Cost estimates for FOAK power plants with CO ₂ capture derived for solid sorbent-based systems for the Present Case with water and SO ₂ degradation (Case Study #10).....	309
Table 7.14: NOAK cost estimates for the best available CO ₂ control technology for post-combustion application.	311
Table 7.15: An example of modifications to the solid sorbent-based CO ₂ capture system that could result in a system capable of meeting DOE’s goals for post-combustion CCS technologies.....	313
Table 7.16: An example of modifications to the solid sorbent-based CO ₂ capture system that could result in a system capable of meeting DOE’s goals for post-combustion CCS technologies.....	315
Table 10.1: The constants used in the Antoine Equation are temperature dependent across the range of expected operation of the DCCPS.....	375
Table 10.2: Input and output properties for the DCCPC process model.....	385
Table 10.3: Specifications for the induced draft blower developed by CCSI.	386
Table 10.4: Specifications for the cold-side cross-flow heat exchanger	387
Table 10.5: Specifications for the hot-side heat exchanger	388
Table 10.6: Calculations used to calculate the flow rate of adsorbed flue gas constituents.	393
Table 10.7: The results from a data validation procedure in which the performance variables were adjusted in order to reproduce the results published by CCSI.....	394

Table 10.8: Summary of the kinetic parameter value calculated for each of the 49 sensitivity cases derived using CCSI's adsorber model.	398
Table 10.9: Aspen Custom Modeler input parameters used by CCSI to predict loading response in the adsorber.	398
Table 10.10: Outputs of NETL's solid sorbent-based CO ₂ capture adsorber model.	399
Table 10.11: Case studies varying the solid sorbent flow rate	399
Table 10.12: Case studies varying the flue gas flow rate entering the adsorber.....	400
Table 10.13: Case studies varying the inlet flue gas CO ₂ mole fraction	401
Table 10.14: Case studies varying the inlet flue gas water concentration	401
Table 10.15: Case studies varying the inlet solid sorbent temperature	402
Table 10.16: Nominal performance and cost values for Case study #1.	419
Table 10.17: Nominal performance and cost values for Case study #2.	421
Table 10.18: Nominal performance and cost values for Case study #3.	423
Table 10.19: Nominal performance and cost values for Case study #4.	425
Table 10.20: Nominal performance and cost values for Case study #5.	427
Table 10.21: Nominal performance and cost values for Case study #6.	430
Table 10.22: Nominal performance and cost values for Case study #7.	432
Table 10.23: Nominal performance and cost values for Case study #8.	434
Table 10.24: Nominal performance and cost values for Case study #9.	436

Table 10.25: Nominal performance and cost values for Case study #10.	439
Table 10.26: Nominal performance and cost values for Case study #11.	441
Table 10.27: Nominal performance and cost values for Case study #12.	443
Table 10.28: Nominal performance and cost values for Case study #13.	446
Table 10.29: Nominal performance and cost values for Case study #14.	448
Table 10.30: Baseline plant financial assumptions.....	451

List of Figures

Figure 1.1: Historical and projected global greenhouse gas emissions and CO ₂ concentrations and estimates of the associated average equilibrium temperature increase.....	26
Figure 1.2: Simplified schematic of a coal-fired power plant with a generic post-combustion CO ₂ capture system	28
Figure 1.3: The Boundary Dam CO ₂ capture facility located in Saskatchewan, Canada.	32
Figure 1.4: The solid sorbent skid located at the National Carbon Capture Center located at the Plant Gaston generating station in Wilsonville, AL.....	37
Figure 2.1: Microgranular appearance of a calcium-based sorbent	48
Figure 2.2: Kinetic adsorption for a primary-functionalized ion exchange resin	54
Figure 3.1: Generic solid sorbent based CO ₂ capture system	59
Figure 3.2: Temperature swing cycle for solid sorbent-based CO ₂ capture.....	60
Figure 3.3: Pressure swing cycle for solid sorbent-based CO ₂ capture	62
Figure 3.4: Diagram of the solid-liquid heat exchange system.....	63
Figure 3.5: Reactor bed designs for CO ₂ capture.....	65
Figure 3.6: Process flow diagram for solid sorbent-based CO ₂ capture adapted from the CCSI design	70
Figure 4.1: Mass flow diagram of a carbon capture system.....	74
Figure 4.2: A mass flow diagram of the flue gas pre-treatment unit and blower unit.....	76

Figure 4.3: Mass balance diagram of a solid sorbent-based adsorber unit	78
Figure 4.4: Mass flow diagram of the cyclone unit.....	85
Figure 4.5: A mass flow diagram of the cold-side heat exchanger.....	86
Figure 4.6: Mass flow diagram of the regenerator.....	87
Figure 4.7: Mass flow diagram of the hot-side heat exchanger.....	96
Figure 4.8: Mass flow diagram for discarded solids separation.....	97
Figure 4.9: Diagram of the degradation products treatment area.....	98
Figure 4.10: Langmuir isotherm of an ion exchange resin with primary benzyl amine.....	109
Figure 4.11: A Langmuir isotherm for BrightBlack™	109
Figure 4.12: Results of the data fitting exercise for the amine resin based solid sorbent.....	112
Figure 4.13: Summary of the energy balance for a solid-sorbent CO ₂ capture system.....	119
Figure 5.1: Tornado diagram showing the parameters demonstrating the largest influence on the specific solid requirement for the CCS system	173
Figure 5.2: A tornado graph indicating the change in the plant efficiency for a +/-10% change in the input of ten important variables.	174
Figure 5.3: The solid sorbent loading for the amine resin solid sorbent	176
Figure 5.4: Influence of the Langmuir parameter on rich and lean loadings	177
Figure 5.5: The influence of the heat of reaction between CO ₂ and the sorbent on CO ₂ loading in the adsorber (rich) and regenerator (lean) using the nominal ideal case study process conditions.....	178
Figure 5.6: Ratio of the working capacity versus the maximum capacity for the two amine solid sorbents considered in this work.....	179
Figure 5.7: Influence of the equilibrium pressure on rich loading.....	181
Figure 5.8: Performance model results for the lean CO ₂ loading as a function of CO ₂ pressure and temperature.....	182
Figure 5.9: Influence of CO ₂ capture efficiency on the rich loading in the adsorber vessel for the bounding conditions of the inlet and outlet CO ₂ pressures.....	183
Figure 5.10: Specific solid requirement as a function of the CO ₂ capture efficiency. Additional solid sorbent is required as the equilibrium pressure departs from the ideal case.	184
Figure 5.11: Mass flow rate of solids at the adsorber inlet as a function of the CO ₂ capture efficiency	222

Figure 5.12: Specific solid requirement as a function of the solid purge fraction	224
Figure 5.13: Flow rates of heat exchange fluids in the adsorber, regenerator, and cross-flow heat exchangers as a function of the solid purge fraction for Case study #4. (water and SO ₂ degradation)...	226
Figure 6.1: Method of cost assessment	243
Figure 6.2: Direct capital cost of the adsorber as a function of the overall heat transfer coefficient and adsorber temperature for Case study #1.	275
Figure 6.3: Log mean temperature difference and cooling requirement as a function of the outlet solid temperature.....	276
Figure 6.4: The adsorber heat exchange surface area requirement normalized by the quantity of CO ₂ and expressed as a function of the adsorber temperature.....	277
Figure 6.5: Direct capital cost of the regenerator as a function of the overall heat transfer coefficient and regenerator temperature for Case study #1	278
Figure 6.6: The regenerator surface area requirement as a function of the maximum solids temperature.....	279
Figure 6.7: LCOE and solid flow rate as a function of the solid purge fraction.....	281
Figure 7.1: Scaling functions for the total capital and operating costs for the PC power plant without CO ₂ capture as a function of the gross electrical output.....	289
Figure 7.2: Breakdown of the levelized cost of electricity separated by the costs associated with the CO ₂ capture system and the balance of the plant (BOP).	298
Figure 7.3: A tornado diagram indicating the change in the levelized cost of electricity for a +/- 10% change in the input of ten important parameters.....	300
Figure 7.4: Probability distribution for the levelized cost of electricity with only the uncertainties in the performance parameters of the solid sorbent system considered.....	303
Figure 7.5: Probability distribution for the levelized cost of electricity for the Present Case scenario	303
Figure 7.6: Projections of future LCOE for supercritical power plants equipped with solid sorbent-based CO ₂ capture and storage.....	310
Figure 10.1: Process flow diagram for solid sorbent-based CO ₂ capture adapted from the CCSI design.	344
Figure 10.2: Illustration of the flue gas pre-treatment process.	365
Figure 10.3: Block flow diagram representing the stream flows accounted for in the direct contact cooler and polishing scrubber model.....	367
Figure 10.4: Water vapor saturation curve used in the flue gas pre-treatment process.	369
Figure 10.5: The latent heat of vaporization of water is temperature dependent.	371

Figure 10.6: Elicited responses for the Present Case maximum CO ₂ loading.	404
Figure 10.7: Elicited responses for the Future Case maximum CO ₂ loading.	404
Figure 10.8: Elicited responses for the Present-Case adsorber kinetic parameter.	408
Figure 10.9: Elicited responses for the Future Case kinetic parameter.	408
Figure 10.10: Expert elicitation responses for the Present Case overall adsorber heat transfer coefficient.	409
Figure 10.11: Expert elicitation responses for the Future Case overall adsorber heat transfer coefficient.	409
Figure 10.12: Expert responses for the present case regeneration (desorption) kinetic parameter.	411
Figure 10.13: Expert responses for the Future Case regenerator (desorption) kinetic parameter.	411
Figure 10.14: Expert responses for the Present Case regenerator overall heat transfer coefficient.	412
Figure 10.15: Expert responses for the Future Case regenerator overall heat transfer coefficient.	412
Figure 10.16: Expert responses for the Present Case influence of water on CO ₂ loading.	415
Figure 10.17: Expert responses for the Future Case influence of water on CO ₂ loading.	416
Figure 10.18: Present Case expert elicitation responses regarding the cost of solid sorbent. ...	417
Figure 10.19: Future Case expert elicitation responses for the cost of solid sorbent.	418

1. The role of carbon capture and storage in climate change mitigation

1.1. Carbon dioxide emissions and electric power

Today, approximately 32 gigatonnes of CO₂ out of 49 gigatonnes of CO₂-equivalent emitted globally from anthropogenic sources are the result of burning fossil fuels (IPCC, 2007; Carbon Dioxide Information Analysis Center, 2013);. Through power plant combustion processes, fossil fuels were responsible for producing nearly 63% of the world's net generated electricity in 2010 (IEA, 2013). Moreover, the global use of fossil fuels is forecasted to rise over the coming decades as global living standards increase. The International Energy Agency (IEA), for example, projects electricity generated by fossil fuels to increase by an average of over 3% annually between 2010 and 2040 (IEA, 2014).

Table 1.1 describes the breakdown of net power generation throughout the world. Coal is the primary fuel source for electricity generation because the technology is relatively inexpensive and there is a large global reserve. The U.S., China, and India in particular have large reserves of coal, and China and India's use of coal continues to expand as a result of a growth in generation capacity. As of September 2015, The World Resources Institute (WRI) identified 1,199 coal plants in planning across 59 countries, with about three-quarters in China and India. The capacity of the new plants adds up to 1,400GW of electricity production capacity, the equivalent of adding another China – the world's biggest emitter. Today, China hosts approximately 620 of the 2300+ coal-fired power stations throughout the world (WRI, 2015).

Table 1.1: Current and projected global generation of electricity by fuel source (trillion kilowatt-hours), 2010-2040 (from IEA 2013). Combined generation of electricity by liquids, natural gas, and coal amount to a 3% increase annually

Generation Fuel Source	2010	2020	2030	2040	Avg. Annual Change
Liquids	0.9	0.8	0.7	0.7	-1
Natural Gas	4.5	5.5	7.2	9.4	2.5
Coal	8.1	10.1	12.3	13.9	1.8
Nuclear	2.6	3.6	4.8	5.5	2.5
Renewables	4.2	6.5	7.9	9.6	2.8
Total World	20.2	26.6	33	39	2.2

Table 1.2 describes the breakdown of nameplate capacity and net electricity generation in the United States. According to the latest available Annual Energy Outlook produced by DOE's Energy Information Administration (2015), the U.S. continues to remain heavily dependent on fossil fuels for powering the electric grid with 330 GW capacity of coal and 488 GW capacity of natural gas. Combined, these two sources were responsible for producing 70% of the nation's electricity in 2013.

Table 1.2: Installed electrical generation capacity and net electricity production by type (U.S. Energy Information Administration, 2015)

Energy source	U.S. installed capacity, 2013 (GW)	U.S. generation, 2013 (million megawatt-hours)
Coal	329.8	1,581
Petroleum	49.8	27
Natural gas	488.2	1,125
Nuclear	104.4	789
Hydroelectric conventional	78.6	269
Hydroelectric pumped storage	21.6	-5
Renewables	82.7	254
Other	8.9	26
Total*	1,164.0	4,066

Electricity production at a single power plant can lead to a significant mass flow of CO₂ emissions into the environment. For example, a typical 550 MWe coal-fired power plant with a standard suite of environmental controls emits about 3-4 million tonnes of CO₂ per year, or about 0.3-0.4% of a GtCO₂/year (for a sense of this scale, refer to the y-axis of the left frame in Figure 1.1 shown in GtCO₂/year). For

larger plants, the emissions can be significantly higher. For example, the Robert W. Scherer Electric Generating Plant in Juliette, Georgia has a nameplate capacity of 3.52 GW_e and released 21 million tonnes of CO₂ during 2011, or the equivalent of 0.4% of the total U.S. CO₂ emissions during that year (EARPC, 2013).

1.2. Why the interest in carbon capture and storage?

As anthropogenic greenhouse gas emissions increase atmospheric greenhouse gas concentrations, the resulting climate system warming poses an increasingly serious environmental challenge. According to the Intergovernmental Panel on Climate Change (IPCC), it is now “very likely” that these emissions are responsible for most of the recent measured global average surface temperature increase, totalling about 0.65°C or 0.10 - 0.16°C per decade between 1956 and 2005 (IPCC, 2007). As shown in Figure 1.1, equilibrium global temperatures depend on the concentration of atmospheric greenhouse gas emissions (*ibid*). Rising global temperatures increase the risk of extreme changes in the climate and impacts natural systems supporting water availability, species habitat, and food production.

A significant global reduction in greenhouse gas emissions is required to limit these risks and impacts (IPCC, 2007; NAS, 2011). In particular, there is some consensus that this warming should be limited to 2°C above pre-industrial levels (IPCC, 2007; NAS, 2011), requiring an 80%-85% decrease in global CO₂ emissions by mid-century (IPCC, 2007) . If these goals to reduce the risks associated with climate change are to be met, a large reduction in CO₂ emissions is needed.

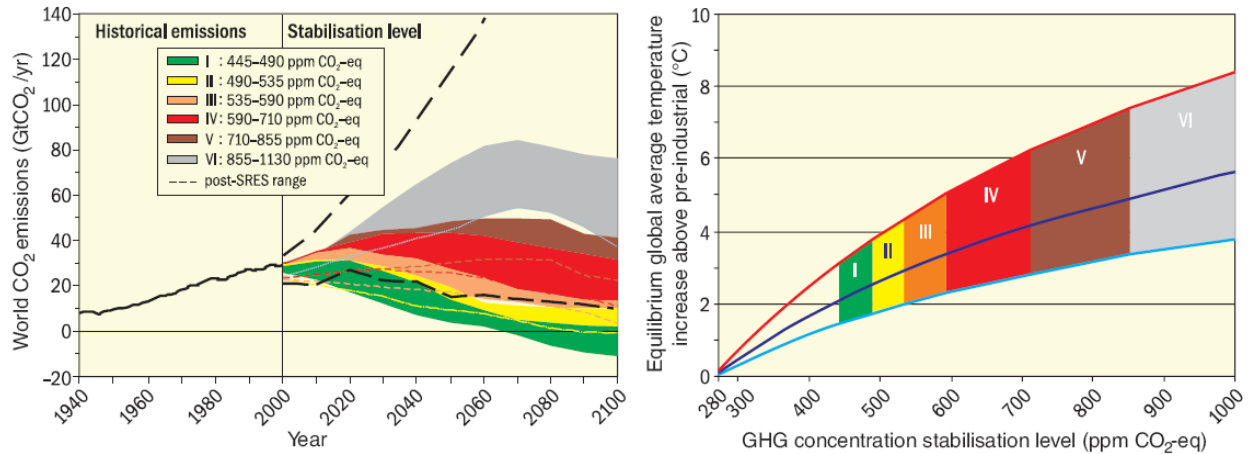


Figure 1.1: Historical and projected global greenhouse gas emissions and CO₂ concentrations (left) and estimates of the associated average equilibrium temperature increase (right) (IPCC, 2007)

One approach to CO₂ emission reductions from large point sources is carbon capture and storage (or sequestration) (CCS). CCS could significantly reduce CO₂ emissions from coal and natural gas-fired power plants as well as from other large industrial sources. CCS involves two steps: 1) capturing the CO₂ emitted during fuel combustion/conversion; and 2) transporting and injecting the CO₂ in an appropriate geologic formation. In a power plant equipped with CCS, CO₂ in the combustion gases is selectively captured and purified using a CO₂ capture process instead of being vented to the atmosphere. The CO₂ is then compressed to form a liquid-like supercritical fluid that is stored in an underground formation. The potential for CCS to reduce CO₂ emissions is significant because of the broad use of fossil fuels in electric power generation. Many organizations acknowledge the potential of CCS, recognizing it as a useful component in large scale, fossil fuel-based processes while transitioning to a less carbon-intensive economy (IPCC, 2014; MIT, 2007; RFF, 2003). CCS is also thought to be a key part of a least-cost climate strategy (IPCC, 2014).

1.3. Overview of current options for carbon dioxide capture and storage (CCS)

There are several different power plant designs that could be used for both power production and simultaneous CO₂ capture. These include post-combustion capture in which a CO₂ scrubbing system is added to the end of a power plant flue gas stream (DOE/NETL, 2013); pre-combustion capture in which

fuel is converted into H_2 and CO_2 and then separated so that the H_2 can be combusted while the CO_2 is sent to storage (DOE/NETL, 2010); and oxy-combustion capture in which air is separated into N_2 and O_2 and the fuel is combusted with O_2 resulting in a concentrated CO_2 stream which can be sent to storage (DOE, 2014). Each of these technologies has advantages and disadvantages under different circumstances. However, in their current state of development, these technologies are expensive and have not been proven at full commercial scale. A growing community of universities, government labs, and industrial partners are investigating CCS technology options in a collective effort to discover capture processes that will prove competitive with other electricity generation technologies in a carbon constrained regulatory future. The CCS community is working to advance these technologies through pilot and demonstration phases towards commercialization.

The technology investigated in this thesis is a post-combustion CO_2 capture technology. The plant configuration with post-combustion capture, shown in Figure 1.2, is the most likely to be competitive as a retrofit option for existing power plants (DOE/NETL, 2010). This is an important consideration because a large portion of future power sector CO_2 emissions will emanate from existing power plants, and post-combustion CO_2 capture may be a useful technology to reduce CO_2 emissions at these plants (ITFCCS, 2010). In addition, other industrial point sources account for a significant amount (19%) of greenhouse gas emissions (IPCC, 2007) and post-combustion capture can also be applied to many of these industries including those involved in the production of liquid fuels, cement, pulp and paper, ammonia, iron, and steel (IPCC, 2014; ITFCCS, 2010). The development of post-combustion CO_2 capture technologies is being done in this context.

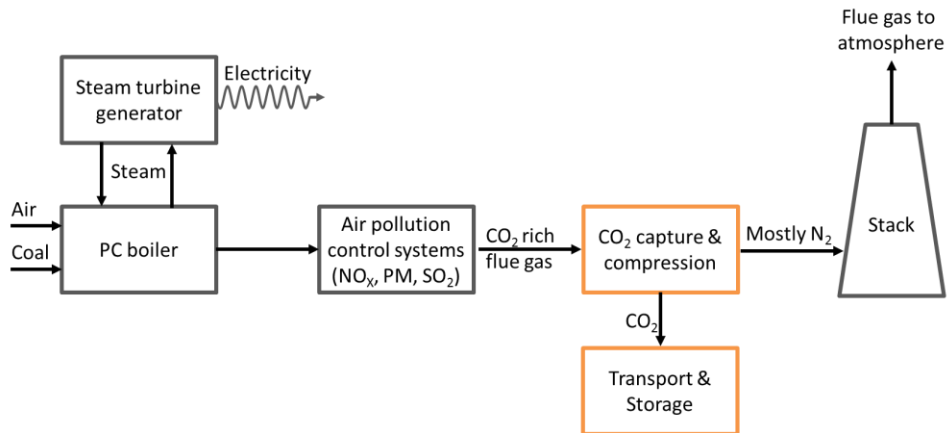


Figure 1.2: Simplified schematic of a coal-fired power plant with a generic post-combustion CO₂ capture system. Other major air pollutants (nitrogen oxides, particulate matter and sulfur dioxide) are removed from the flue gas prior to CO₂ capture

1.3.1. The current state of post-combustion carbon capture and storage

In recent years, carbon capture research and development programs have expanded rapidly throughout the world; thus, any summary of “current” activities and projects is soon out of date. For this reason, it is difficult to be comprehensive in covering all post-combustion capture-related activities. Rather, this section attempts to synthesize key findings from the literature and from online databases which track and report on the status of CO₂ capture technology developments. Excellent publicly available databases and CCS project status reports are maintained by organizations including the U.S. Department of Energy’s National Energy Technology Laboratory (DOE/NETL), the International Energy Agency’s Greenhouse Gas Control Program (IEAGHG), the Scottish Carbon Capture and Storage organization (SCCS), the Massachusetts Institute of Technology (MIT), and the Global Carbon Capture and Storage Institute (GCCSI). In many cases, the information from public databases and reports presented below has also been supplemented and checked by additional data from companies and research groups involved in capture technology development and testing. In each one of the sections below, the objective is to summarize the status of post-combustion capture technology developments (as of September 2015).

1.3.2. Commercial projects for carbon capture and storage

Post-combustion CO₂ capture systems have been in use commercially for many decades, mainly in industrial processes for purifying natural gas streams, though they have also been used to on combustion-based flue gas. The first process for separating CO₂ from a gas stream was patented over 80 years ago (Bottoms, 1930) using an amine solvent. Since that time, amine-based systems have remained the preferred method used to meet CO₂ product specifications in industries ranging from natural gas production to the food and beverage industry (CO₂ Capture Project, 2008). There are hundreds of commercial aqueous systems currently in operation and most are used for removing acid gases from a product stream and the captured CO₂ is typically vented to the atmosphere (Versteeg, 2012).

The history of commercial experience has advanced liquid solvent-based scrubbing to the technological forefront in terms of readiness for CCS deployment at coal-fired power plants (Rochelle, 2009; Sintef, 2013). Today, a number of vendors currently offer commercial post-combustion processes, including the Cansolv™ CO₂ capture system, the Fluor Daniel Econoamine FG Plus™ process, the HTC Pureenergy process, the Mitsubishi Heavy Industries KS-1 solvent process, and the Shell Carbonate Slurry Process.

1.3.3. Full-scale demonstration plants

Although several CO₂ capture systems have operated commercially for nearly two decades on a portion of power plant flue gases, it not until this year (2015) that an integrated CO₂ capture and storage process has been applied to the full flue gas stream of a modern coal-fired or natural gas-fired power plant. Demonstration of post-combustion CO₂ capture at the commercial full-scale is widely regarded as crucial for gaining the acceptance of this technology by electric utility companies and by the institutions that finance and regulate power plant construction and operation.

Several large-scale CCS projects are actively injecting CO₂ into suitable geologic formations or are in the planning phase that will combine post-combustion CO₂ capture, transport, and storage. Table

1.3 lists the features and locations of the major post-combustion capture demonstration projects at power plants throughout the world as of September 2015. Several of these CO₂ capture systems will transport the captured CO₂ via pipeline to a geological storage site, often in conjunction with enhanced oil recovery (EOR) in order to improve the project economics. Most of the projects have completed front-end engineering design (FEED) studies and are awaiting final investment decisions that are expected to be announced later this year.

Table 1.3: Planned and active commercial post-combustion capture processes at power plants that capture, transport, and sequester CO₂ (Global CCS Institute, 2015; MIT, 2015)

Project name and location	Stage	Fuel	Year of start-up	Storage type	Approx. capture plant capacity (net)	Capture system type (vendor)	CO ₂ captured (10 ⁶ tonnes/yr.)
Boundary Dam, (Saskatchewan, Canada)	Active	Coal	2014	EOR	110 MW	Cansolv	1
Bow City Power Project (Alberta, Canada)	Planned	Coal	2017	EOR	Two 500 MW units	Cansolv	1
Getica (Gorj County, Romania)	Planned	Coal	2015	Deep saline	330 MW	Advanced amine/chilled ammonia	1.5
Industrikraft Møre AS Norway, (Møre og Romsdal, Norway)	Planned	Natural gas	2016	N/A	250 MW	Sargas' Stargate 250	1.4
Korea-CCS 1 (Korea)	Planned	Coal	N/A	Deep Saline	300-500 MW	Unknown	1.5
Petra Nova CCS Project, (Texas, USA)	Planned	Coal	2016	EOR	250 MW	MHI's KM-CDR	1.4
Peterhead Gas CCS Project (Aberdeenshire, Scotland)	Planned	Coal	2018	Depleted reservoir	385 MW	Cansolv	1
Rotterdam (ROAD) (Rotterdam, The Netherlands)	Planned	Coal	2017	Depleted reservoir	250 MW	Unknown	1.1
Sinopec Shengli Oil, (Dongying, China)	Planned	Coal	2016	EOR	101-250 MW	Unknown	1
Porto Tolle (Porto Tolle, Italy)	Planned	Coal	2016	Deep Saline	250 MW	Aker Clean Carbon	1
Surat Basin (Queensland, Australia)	Planned	Coal	2018	Deep saline	240 MW	Amine	>2.5
Taweelah (Abu Dhabi, UAE)	Planned	Natural gas	2018	EOR	Unknown	Unknown	2

Included in this list is the Boundary Dam project led by the government owned utility company, SaskPower. This is the world's first full-scale post-combustion coal-fired CCS process and began injecting CO₂ as part of an enhanced oil recovery operation during the middle half of 2014. The \$1.35 billion dollar retrofit of an existing coal-fired unit produces 110 MW of base-load electricity while capturing approximately 1 million tonnes of CO₂ per year. Figure 1.2 shows a photograph of the Boundary Dam carbon capture facility located in Saskatchewan, Canada.



Figure 1.3: The Boundary Dam CO₂ capture facility located in Saskatchewan, Canada. Photo courtesy of SaskPower, Inc.

At present, the technologies that are being incorporated into the designs of initial large-scale post-combustion demonstration plants use liquid amines for CO₂ capture. These technologies represent the best available practice for post-combustion CO₂ capture and will most likely become the technologies chosen for the first generation of post-combustion CCS.

1.3.4. The drawbacks of solvent-based systems

Liquid solvent-based CCS technologies are a promising near-term solution for achieving commercial CCS, but the technology faces several technological limitations that have led to an expansion of research into alternative methods for CCS. These hurdles include a high energy penalty, high parasitic load, and additional consumption of water (DOE/NETL, 2010; DOE/NETL, 2012). Higher solvent concentrations can be beneficial by reducing the energy requirements of a CO₂ capture process since there is less water in the solution that requires heating in the regeneration process. Capital costs are also reduced since higher solvent concentrations lead to smaller equipment sizes. On the other hand, many solvents such as amines are highly corrosive and higher concentrations often drive up costs in the form of

chemical additives or more costly construction materials in order to prevent corrosion. The addition of a CO₂ capture and compression system will also increase water consumption by an estimated 90% for a subcritical pulverized coal (PC) plant and 87% for a supercritical PC plant (Gerdes & Nichols, 2009). Trade-offs among these factors underlie some of the differences in capture system designs offered by different vendors.

Even as solvent-based CO₂ capture technologies overcome the current setbacks related to performance and cost, implementing solvent-based CCS will remain expensive. Table 1.4 lists the predicted CO₂ capture costs for post-combustion capture from coal-fired power plants equipped with mature liquid-amine systems. On average, these organizations predict an estimated 63% increase in the levelized cost of electricity. By contrast, the U.S. Department of Energy has set a target for post-combustion capture of capturing 90% of CO₂ at no more than a 35 percent increase in the cost of electricity compared to those same plants without CCS (DOE/NETL, 2012). For this reason, the research community continues to investigate alternative post-combustion CO₂ capture technologies.

Table 1.4: CO₂ capture costs for post-combustion CO₂ capture systems. All dollar amounts have been converted to 2011 dollars using the CPI inflation rate. Data is sourced from IEA's 2011 report in the cost and performance of CO₂ capture from power generation (Finkenrath, 2011).

Regional focus	OECD													China	Avg. (OECD)	
Year of cost data	2005	2005	2005	2005	2007	2007	2007	2007	2007	2007	2009	2009	2009	2009		
Year of publication	2007	2007	2007	2007	2009	2009	2009	2009	2010	2010	2009	2009	2009	2009		
Organization	CMU	MIT	GHG IA	GHG IA	EPRI	EPRI	EPRI	MIT	NETL	NETL	GCCSI	GCCSI	GHG IA	NCEC		
Original Data as published (converted to USD)																
Region	US	US	EU	EU	US	US	US	US	US	US	US	US	EU	CHN		
Specific fuel type	Bit. coal	Lignite	Bit. coal	Bit. coal	Sub-bit. coal	Sub-bit. coal	Bit. coal	Bit.+10% biomass	Bit. coal							
Power plant type	SCPC	CFB	USCPC	USCPC	SCPC	USCPC	SCPC	SCPC	SCPC	Sub.PC	SCPC	USCPC	SCPC	USCPC		
Net power output w/o capture (MW)	528	500	758	758	600	600	600	500	550	550	550	550	519	824	582	
Net power output w/ capture (MW)	493	500	666	676	550	550	550	500	550	550	550	550	399	622	545	
Net efficiency w/o capture, LHV(%)	41.3	36.5	44.0	44.0	39.2	39.8	40.0	40.4	41.2	38.6	41.4	46.8	44.8	43.9	41.4	
Net efficiency w/ capture, LHV(%)	31.4	26.7	34.8	35.3	28.2	28.8	29.1	30.7	29.9	27.5	29.7	34.9	34.5	31.1	30.9	
CO ₂ emissions w/o capture (kg/MWh)	811	1030	743	743	879	865	836	830	802	856	804	707	754	797	820	
CO ₂ emissions w. capture (kg/MWh)	107	141	117	92	124	121	126	109	111	121	112	95	73	106	111	
Capital cost w/o capture (USD/kW)	1442	1330	1408	1408	2061	2089	2007	1910	2024	1996	2587	2716	1710	856	3135	
Capital cost w/ capture (USD/kW)	2345	2270	1979	2043	3439	3485	3354	3080	3570	3610	4511	4279	2790	1572	3135	
Relative decrease in net efficiency	24%	27%	21%	20%	28%	28%	27%	24%	28%	29%	28%	26%	23%	25%	25%	
Re-evaluated data (2011 USD)																
Overnight cost w/o capture (USD/kW)	1508	1868	1720	1720	2580	2615	2512	2391	2203	2172	2409	2529	1873	938	2162	
Overnight cost w/ capture (USD/kW)	2664	3404	2581	2664	4596	4657	4482	4116	4148	4195	4485	4255	3263	1838	3808	
LCOE w/o capture (USD/MWh)	50	9	69	69	62	63	73	70	65	66	70	70	78	51	66	
LCOE w/ capture (USD/MWh)	80	84	95	97	107	109	121	112	113	117	121	112	118	80	107	
Cost of CO ₂ avoided (USD/tCO ₂)	43	40	42	42	60	61	68	58	69	69	74	68	59	42	58	
Relative increase in overnight cost	77%	82%	50%	55%	78%	78%	78%	72%	88%	93%	86%	68%	74%	96%	75%	
Relative increase in LCOE	59%	73%	38%	40%	72%	72%	67%	60%	73%	77%	73%	59%	52%	57%	63%	

Notes: Data cover only CO₂ capture and compression but not transport and storage. Overnight costs include owner's engineering, procurement, and construction (EPC), and contingency costs, but not interest during construction (IDC). A 15% contingency based on EPC cost is added for unforeseen technical or regulatory difficulties for CCS cases, compared to a 5% contingency applied for non-CCS cases. IDC is included in LCOE calculation. Fuel price assumptions differ between regions.

1.4. Why study solid sorbents for post-combustion carbon capture?

Among the many process technology options proposed for CO₂ capture from flue gases, there is significant interest in using solid sorbent-based processes as an alternative separation technique. Like the liquid system, the adsorption processes (as opposed to absorption) reversibly captures CO₂ using a pressure and/or temperature swing approach. The CO₂ is later purified and compressed for storage at the generation station. This process is thought to have several potential advantages compared to other separation techniques, the foremost advantage being a reduced energy consumption in the regeneration process (DOE/NETL, 2013). Early investigations into the use of solid sorbent-based post-combustion CO₂ capture indicated significant potential improvements in performance over traditional liquid amine technologies as shown in Table 1.5. Most notably, solid sorbents may have lower costs for implementation (SRI International, 2013; Tarka & Ciferno, 2005).

The benefits claimed for an advanced sorbent could be significant if they can be realized. For example, the theoretical energy consumption of a dry sorbent system may be significantly reduced compared to the liquid because of the absence of large amounts of water in the structure of the adsorbing material. Moreover, the heat capacity of solid sorbent is comparatively lower than that of an aqueous amine solvent (Samanta, et al., 2012). Further perceived advantages include greater selectivity for CO₂, ease of handling, and lower water requirements (Glier & Versteeg, 2012; Samanta, et al., 2012). These early predictions set a “best case” scenario of reduced sorbent cost, high selectivity for CO₂, and regeneration energy; and predict an increase in the levelized cost of electricity (LCOE) of about 21% over the cost without CCS (Samanta, et al., 2012). Later estimates are often higher because they are based on specific solid sorbent data. System designs based on experimental solid sorbent data require higher direct capital costs and high energy penalties because the systems must accommodate non-ideal system behavior such as material fouling, water adsorption, and non-ideal heat transfer (Green, 2008; Seider, 2014).

Table 1.5: Potential advantages and challenges for solid sorbent-based post-combustion CO₂ capture (ADA-ES, 2011; Choi, et al., 2009; Tarka & Ciferno, 2005)

Potential advantages	Challenges
Chemical sites provide large capacities and fast kinetics, enabling capture from streams with low CO ₂ partial pressure	Heat required to reverse chemical reaction
Higher capacities on a per mass or volume basis than similar wet-scrubbing chemicals	Heat management in solid systems is difficult, which can limit heat capacity and/or create operational issues when adsorption reaction is exothermic
Lower heating requirements than wet-scrubbing in many cases (CO ₂ and heat capacity dependent)	Pressure drop can be large in flue gas applications
Dry process- potential for a lower sensible heat requirement	Sorbent attrition may be high

1.5. Current status of solid sorbent-based carbon capture technology

Development of solid sorbent systems for carbon capture is still in the early stages. As an example, consider that no solid sorbent system has been demonstrated under steady-state operation capable of treating a volume of flue gas greater than the equivalent of a 1 MW coal-power plant. Yet, innovation in this field has been prolific in the past decade, particularly between 2011 and 2013 and new designs may outperform the current “state of the art” system (Li, et al., 2013) as defined by DOE (DOE/NETL, 2012). As of this writing, there are two pilot-scale solid sorbent-based carbon capture plant built or in operation. The first is located at Alabama Power’s James H. Miller Electric Generating Station near Birmingham, Alabama. This system is capable of handling a nominal gas flow rate of 3,500 acfm, or the equivalent of approximately 1 MW (Starns, et al., 2012). The primary purpose of this slipstream test facility is to demonstrate solid sorbent technology at a small scale and collect data regarding several key aspects of the technology, including the regeneration energy, process conditions, and the purity of the product stream (*ibid*). As part of this \$20 million dollar effort, ADA-ES, Inc. and its partners will refine the conceptual design of a commercial solid sorbent-based, post-combustion CO₂ capture technology through slipstream pilot testing and process modelling (DOE, 2010).

A second pilot scale facility, shown in Figure 1.4, is ongoing at the National Carbon Capture Center located in Wilsonville, Alabama. This facility will be capable of treating 0.5 MW of flue gas and has

a similar stated purpose of determining the effect of fluid velocity and flue gas contaminants, evaluating construction materials, and determining the efficiency of thermal recovery (Jones, 2014; SRI International, 2013).

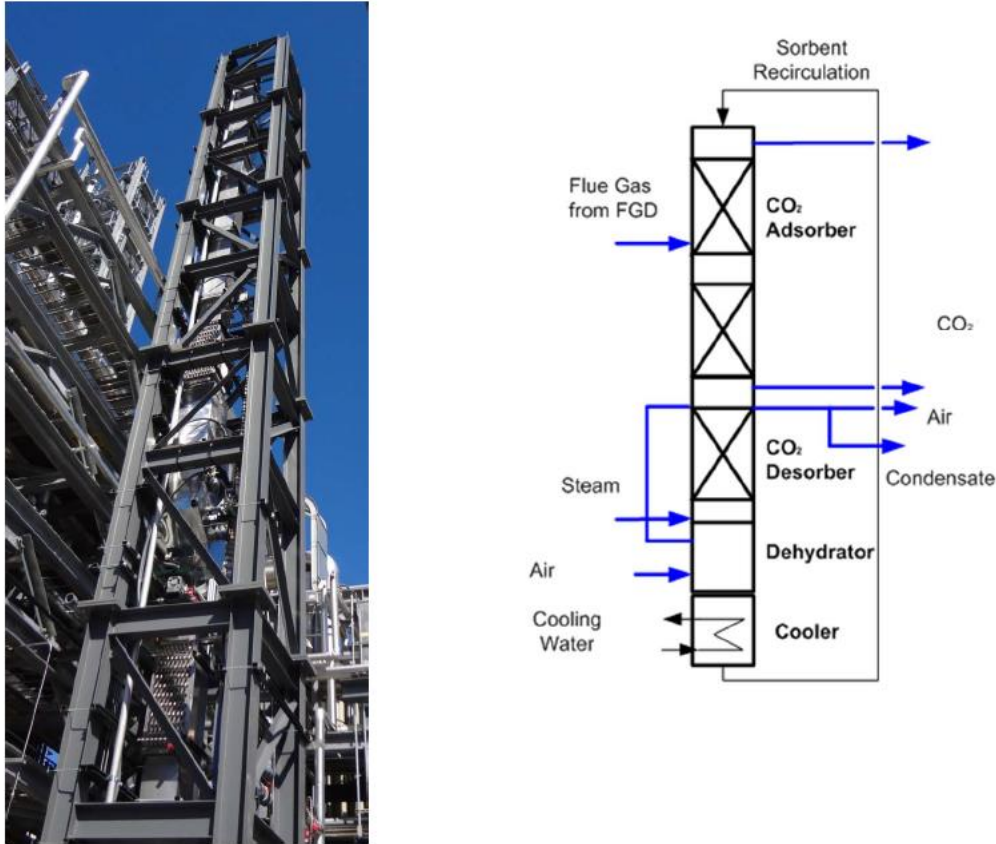


Figure 1.4: The solid sorbent skid located at the National Carbon Capture Center located at the Plant Gaston generating station in Wilsonville, AL. The solid sorbent facility (shown left) is a vertically stacked unit comprised of an adsorber, regenerator, and heat management equipment (SRI International, 2013). The process diagram (right) shows the arrangement of the testing unit.

Another group currently investigating solid sorbents is the Carbon Capture Simulation Initiative (CCSI). This is a partnership among national laboratories, industry, and academic institution working to develop and deploy state-of-the-art computational modelling and simulation tools to accelerate the commercialization of carbon capture technologies (CCSI, 2015). One of the most pertinent publications released by this group is a process model of the solid sorbent process based on high-resolution simulation of the solid and gas interactions occurring in several of the process vessels. This particular

publication represents the most current, publically available design for a solid sorbent-based CO₂ capture process.

1.6. Scope and objectives of this thesis

The discussion in the previous section shows that solid sorbents are one of several early-stage alternatives that may allow CCS to reach the DOE's goal of achieving 90 percent CO₂ capture while keeping the increase in the cost of electricity below 35 percent. To date, however, there are no publicly available tools allowing researchers to compare solid sorbents to other emerging and commercial CO₂ capture technologies. This thesis seeks to address this need by developing a transparent, flexible tool for modeling the performance and economics of a full-scale solid sorbent system to assess whether a full-scale solid sorbent system represents a viable low-cost alternative to the current state of the art or other competing CCS systems. To that end, this thesis presents an evaluation of solid sorbent-based CO₂ capture systems by:

- Developing a techno-economic model suitable for preliminary design and analysis that identifies key CCS process and power plant system parameters for a new coal-fired power plant;
- Presenting multiple case studies demonstrating the model's functionality to aid users in their modeling efforts;
- Estimating the performance and cost of a full-scale solid sorbent system built using today's state-of-the-art solid sorbent technology as a function of sorbent properties and system design (including the effects of uncertainties);
- Developing a strategy for integrating the CO₂ capture process model with the Integrated Environmental Control Model as a means of estimating the performance and cost of a fully-integrated coal-fired power plant
- Estimating the performance and costs of a full-scale solid sorbent system based on expert judgments about future improvements in solid sorbent technology (including the effects of uncertainties);

- Determine the first-of-a-kind (FOAK) and Nth-of-a-kind (NOAK) cost of a fully integrated power plant equipped with the solid sorbent-based CO₂ capture process under uncertainty
- Recommending pathways for realizing potential improvements in solid sorbent-based CO₂ capture technology

1.7. Organization of thesis

This chapter has briefly introduced the connection between CO₂ emissions and climate change and has established that post-combustion-based CCS could be a useful technology for significantly reducing CO₂ emissions at large point sources. It has also defined the scope of this thesis to an investigation of the performance and economics of solid sorbent post-combustion technology with a focus on coal-fired power plant applications. Chapter 2 provides a literature review and an initial assessment of solid sorbents. Chapter 3 describes the current designs considered for solid-gas reactors and heat transfer processes, and defines the current state-of-the-art for solid sorbent-based CO₂ capture. Chapter 4 then describes the performance model used to assess the solid sorbent-based CO₂ capture process based on key performance parameters and assumptions regarding the CO₂ capture process and overall power plant. Chapter 5 demonstrates the functionality of the performance model and describes several case studies describing various outlooks using published data and expert elicitations regarding the performance of the sorbent material and process. Chapter 6 presents a process cost model for implementing a full-scale system. Chapter 7 exercises the performance and cost models to compare various operating scenarios, estimate a range of present costs under uncertainty, and project future costs using an established learning curve method. Finally, in Chapter 8, the results are summarized and general conclusions drawn on this approach to CO₂ capture.

2. Sorbent characteristics

This chapter discusses the properties and types of solid sorbents relevant to the performance and cost of post-combustion CO₂ capture. The chapter begins with a discussion of the reaction mechanisms of solid sorbents and their relevance to CO₂ capture. The discussion then broadens to include a range of factors that affect the CO₂-capture process, such as the interactions between the solid sorbent and other flue gas components, sorbent attrition and degradation, and the influence of reaction kinetics. The chapter concludes with a summary description of the solid sorbents that are modeled in later chapters.

2.1. Chemical and physical adsorbents

Solid sorbents are small porous particles which can selectively react with gaseous chemical species (in this case, CO₂), thereby removing the species from a gas mixture. The mechanism for adsorbing CO₂ is characterized by the heat of adsorption, which is a direct measure of the binding strength of a fluid molecule and the surface. Molecules of CO₂ may be held loosely by weak intermolecular forces, termed “physiosorption,” or strongly via covalent bonding, termed “chemisorption.”

Generally, physiosorption occurs when the heat of adsorption is less than approximately 40 kJ per mole of CO₂, while chemisorption occurs with the heats of adsorption greater than 60 kJ per mole (Yang, 2003). Physiosorption is characterized by a moderate heat of adsorption (less than 2-3 times the latent heat of evaporation) and monolayer or multilayer coverage (i.e. CO₂ molecules may stack through the formation of reactive products). Physiosorption is also a rapid and reversible process.

Chemisorption, on the other hand, is characterized by higher magnitude heats of adsorption (typically greater than 2-3 times the latent heat of vaporization), highly specific sites of adsorption, monolayer coverage only, and possible dissociation of CO₂ bonds. In addition, chemisorption is a comparatively slow process due to the electron transfer occurring as the adsorbate bonds to the solid

sorbent's reactive sites, as well as the activation barrier that needs to be overcome in order to form the bound complex. Nonetheless, CO₂ uptake has been demonstrated to be very rapid (Wilcox, 2012).

These characterizations of physisorbents and chemisorbents are rules of thumb, however, and exceptions do exist. For instance, the heat of physisorption of CO₂ in some zeolites has been reported to be as high as 210 kJ/mol CO₂ (Shen, et al., 2000), with heats of chemisorption known to extend from as low as 60 kJ/mol to over 420 kJ/mol. Nonetheless, research regarding the application of solid sorbents for CO₂ capture has tended to focus on the use of chemisorbents for post-combustion application since the higher heats of adsorption allow the solid to undergo larger changes in CO₂ capacity without inducing large changes in gas pressure (DOE/NETL, 2013; Drage, et al., 2012). Moreover, the selectivity of chemisorbents for CO₂ tends to be higher than physisorbents making them more ideal for post-combustion application, as discussed in section 2.3. The range of materials under investigation for post-combustion CO₂ capture is discussed in the next section.

2.2. Solid sorbents properties and materials for post-combustion applications

Choosing a viable sorbent for CO₂-capture is not a straightforward process because there are many important characteristics which can affect the overall process performance. The ideal adsorbent would have high selectivity for CO₂ adsorption, high CO₂ capacity, infinite chemical and thermal stability, infinite regenerability, fast adsorption and desorption kinetics, and low regeneration energy requirements. This material would also be capable of capturing CO₂ in a wide range of operating conditions found in post-combustion setting, including natural gas and pulverized coal-fired power plants (Choi, et al., 2009).

Adsorption can be described by the Langmuir model, which assumes an adsorbate (in this case, CO₂) behaves as an ideal gas at isothermal conditions. At these conditions, the adsorbate's partial pressure is related to the molar concentration adsorbed on the solid sorbent. The adsorbent is assumed to be an ideal solid surface composed of distinct reactive sites capable of binding the adsorbate. Several other parameters in this model are used to describe the concentration of adsorbate as it exists in the gas

and solid form. Among these terms are the heat of reaction between the solid sorbent and adsorbate, the maximum capacity of the solid sorbent for the adsorbate, and the Langmuir parameter, a characteristic of the particular adsorbent-adsorbate reaction. Details regarding the Langmuir method and Langmuir parameter are discussed in Section 4.3.

The solid sorbent parameters shown in Table 2.1 are used throughout the performance model in order to calculate the mass of solids, liquids, and gases flowing throughout the system and the cost model presented in Chapter 6 to calculate the capital and operating cost of CCS.

Table 2.1: List of parameters used in the performance and cost models describing the solid sorbent.

Parameter name	Description and use
Maximum CO ₂ capacity	Defines the saturated loading of CO ₂ exposed to post-combustion concentrations of CO ₂ . At maximum CO ₂ capacity, all reactive sites are effectively occupied by CO ₂ . This value represents CO ₂ capacity after repeated adsorption/desorption cycling, thus accounting for physical attrition occurring over long periods of use (moles CO ₂ /kg solid sorbent)
Langmuir parameter	Isotherm equation parameter (1/Pa)
Heat of reaction	Refers to the reaction between the sorbent and CO ₂ and required in order to calculate the latent heat requirements in the adsorber and regenerator (kJ/mol CO ₂)
Heat capacity	Heat capacity of the solid sorbent. This parameter is needed in order to calculate the sensible heat requirement in the adsorber and regenerator (kJ/kg solid sorbent)
Material cost	Used to calculate the cost of fresh solid sorbent (\$/kg solid sorbent)

Solid sorbent research for CCS is an active field with many materials under investigation for use in post-combustion systems. These materials include hydrotalcites (Choi, et al., 2009; D'Alessandro, et al., 2010), modified zeolites (Banerjee, et al., 2008), graphites (Zhao, et al., 2012), and carbon nanotubes (Lu, et al., 2008) among others. These materials are being developed and tested at universities, government laboratories, and by private institutions worldwide in order to “tune” the properties according to the demands of a post-combustion system. Many of these adsorbents perform strongly in ideal, bench-scale tests but have yet to be tested under realistic conditions and/or show potential for application pending further research and development. Table 10.1 lists the advantages and disadvantages of several solid sorbents currently under investigation for use in post-combustion capture.

Table 2.2: Advantages and disadvantages of the leading solid sorbents being considered for use in a carbon capture system

Solid sorbent type	Advantages	Disadvantages	Sources
Physical sorbents			
Activated Carbon (e.g. BrightBlack®, NoritAC)	Good stability over repeated adsorption/desorption cycles	Low CO ₂ capacity (2-3 mol/kg)	(SRI International, 2013)
	Resistant to poisoning and degradation by flue gas constituents	Relatively soft—possible attrition problems	
	Low energy of adsorption	Potential affinity for water	
	Responds well to pressure swings	Oxidation due to water Temperature instability	
Metal Organic Frameworks (e.g. zeolitic imidazolate, 13X, MOF-2, Cu(BTC))	Potentially high adsorption capacity (at high pressure)	Highly impacted by water	(Siriwardane, et al., 2001), (Ritter, 2013), (Chuang, 2013), (Lang, 2013), (Li, et al., 2013)
	Low energy of adsorption	Moderately high cost	
	High durability and regenerability		
	Generally rapid adsorption		
Chemical adsorbents			
Supported amines (MCM-41, MCM-41-PEI, APS-MCM-48, TRI-PE-MCM-41, supported PEI, supported APTES, DBU-3)	High adsorption capacity (2-5 mol/kg)	Degraded by acid gases and oxygen	(Gray, et al., 2008; Hicks, et al., 2008; Jones, 2013; Nelson, 2013)
	Moderately fast kinetics	Potential thermal stability issues	
	Low attrition when bound to a stabilizing substrate	High cost of production Possible corrosion and material handling issues	
Alkali Earth Metal Oxides (e.g. Calcium carbonates)	High Adsorption capacity (2-18 mol/kg)	Temperature degradation (pore blockage and sintering)	(Gray, et al., 2008), (Plaza, et al., 2007), (Radosz, et al., 2008), (Lu, et al., 2008), (Alptekin, 2013)
	Inexpensive and abundant	Non-selective for acid gases	
		Low to moderate reaction kinetics	
		High heat of adsorption	
Alkali Metal Oxides and Silicates	Potentially high CO ₂ capacity	Very high heat of reaction	(Elliott, 2013; Krishnan, 2013; Nelson, et al., 2009; Nelson, 2013; Shigemoto, et al., 2006)
	Relatively inexpensive and mildly abundant	Moderate reaction kinetics	

This study utilizes an amine-based resin solid sorbent in order to demonstrate the functionality of the performance and cost models. The decision to model this solid sorbent is two-fold. First, this solid sorbent was selected for use in a demonstration plant located at Plant Miller near Birmingham, Alabama.

As part of their inclusion in this project, published data is available regarding the basic characteristics of this solid sorbent (Sjostrom, et al., 2011). In addition, this solid sorbent represents the current, proven state-of-the-art regarding solid sorbent performance. The characteristics used to model this solid sorbent may be modified to represent many of the other adsorbents as data for these materials becomes available. More details regarding the method used in this work based on published data is available in Appendix A.

In the following sections, the properties of the above-mentioned solid sorbents are analyzed in terms of their applicability to CO₂ capture. These issues include the selectivity of the solid sorbent for CO₂ over other flue gas constituents, degradation, cost, and kinetic limitations among others. Additional information regarding the advantages and disadvantages of these materials can be found in any of the excellent reviews of solid sorbent materials are available in the literature (Choi, et al., 2009; D'Alessandro, et al., 2010; Samanta, et al., 2012).

2.3. Chemical degradation

Interaction between the solid sorbent and the variety of species present in flue gas is an issue for most adsorbent materials. Materials that rely on physical adsorption of CO₂, such as zeolites, are often prone to degradation by molecules of similar size and shape to CO₂, e.g. elemental nitrogen and oxygen. Those using chemical reaction mechanisms such as amines and metal oxides are prone to degradation by the presence of acid gases such as SO₂ and NO₂ or are oxidized in the presence of O₂ (Berger & Bhowan, 2011). Water may also exhibit an important influence as well depending on the affinity of the material for water and the specifics of the process configuration. The effects of these constituents on specific sorbent classes is somewhat known, and reviews of these interactions are available although detailed information on specific solid sorbent reactions is often sparse. A review of these effects and the

modeling method used to address them are presented in this section (Choi, et al., 2009; D'Alessandro, et al., 2010; Drage, et al., 2009).

2.3.1. Influence of nitrogen

Many solid sorbents exhibit an affinity for molecular nitrogen (N_2). This is particularly problematic since nitrogen is the primary constituent in conventional post-combustion flue gas streams. Even a weak affinity for nitrogen may therefore degrade performance as reactive sites used to adsorb CO_2 are occupied or inhibited by nitrogen, thereby lowering the material's CO_2 adsorption capacity. Published literature addressing the uptake of nitrogen by CO_2 adsorbents typically addresses this concern by using a ratio comparing the uptake of CO_2 to N_2 , generally called the selectivity coefficient. Table 2.2 lists seven solid sorbents representing three major material classes and the relative affinity of each for nitrogen obtained from the relevant literature. This table shows that physisorbents have lower selectivity compared to chemisorbents. Hence, chemisorbents make more sense for post-combustion applications.

Table 2.2: CO₂/N₂ selectivity for different materials at room temperature and high CO₂ concentration. Adapted from (Belmabkhout, et al., 2011)

Material class	Physical or chemical	Materials	CO ₂ conc. (%)	CO ₂ vs. N ₂ selectivity	Reference
Zeolite	Physical	13X	50	23	(Cavenati, et al., 2004)
Metal Organic Framework	Physical	Cu-BTC ¹ (MOF)	14.9	20	(Yang, et al., 2007)
Activated Carbon	Physical	NoritAC	20	14	(Dreisbach, et al., 1999)
Supported Amine	Chemical	MCM-41	20	12	(Belmabkhout & Sayari, 2009)
Supported Amine	Chemical	MCM-41-PEI ²	4	>1000	(Xu, et al., 2003; Xu, et al., 2005)
Supported Amine	Chemical	APS ³ -MCM-48	50	>100	(Kim, et al., 2005)
Supported Amine	Chemical	TRI-PE-MCM-41	20	infinite	(Belmabkhout, et al., 2011)

¹Copper(II) benzene-1,3,5-tricarboxylate

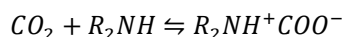
²Polyethylenimine

³Aminopropyltriethoxysilane

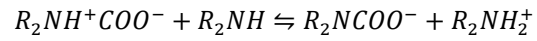
2.3.2. Influence of water

The interaction between water and solid sorbents is unique among the non-CO₂ flue gas constituents. In some cases, water increases the overall solid's capacity for CO₂ by offering additional chemical reaction pathways (such as the formation of carbonates, bicarbonates, or the zwitterion intermediates with polyethylenimine (PEI) (Yue, et al., 2008). One commonly suggested chemistry for reaction of CO₂ with primary or secondary amines is shown below (using secondary amines as the example) (Sanz, et al., 2010; Vaidya & Kenig, 2007).

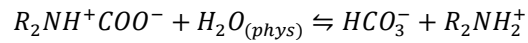
First, CO₂ reacts with an amine to form a zwitterion:



The zwitterions can then react with another amine to form a carbonate ion and protonated amine:



If water is present in within the system, the zwitterions may also react with the water to form bicarbonate and a protonated amine instead:



The products of these reactions may also serve as nucleation sites for the formation of additional layers of carbonates, thereby creating additional mechanisms for capturing CO₂.

However, water may also decrease CO₂ capacity by competitively adsorbing to reactive sites as seen in several families of promising adsorbents including zeolites and metal organic frameworks (MOFs). Water can also interfere by blocking pore pathways through sorbent swelling or by capillary blockage, as seen in Figure 2.1 (Choi, et al., 2009).

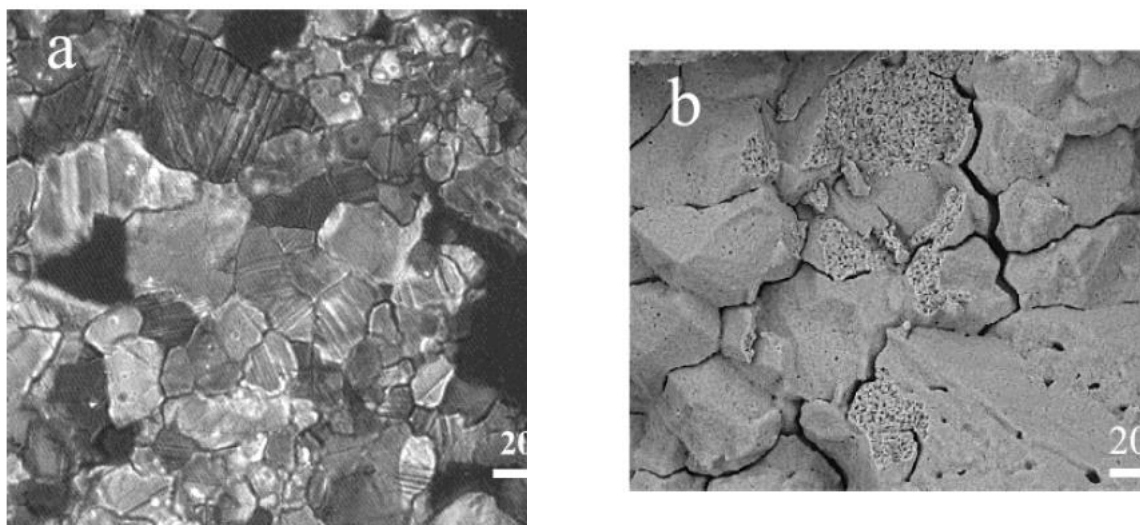


Figure 2.1: Microgranular appearance of a calcium-based sorbent. (a) Parent limestone, transmitted light optical micrograph, and (b) limestone after 40 calcination/carbonation cycles (SEM). Like many materials, calcium oxides swell when reacting with water. Though chemical reactions are the primary cause of lost CO₂ capacity for some sorbents, non-reaction mechanisms like pore closure can significantly limit the availability of internal surface area for additional CO₂ uptake. SEM pictures are publically available from (Abanades & Alvarez, 2003)

Physical adsorption of water (through capillary action) also may restrict gas flow in the solid and, in some cases, reduce the capacity of the solid sorbent for adsorbing CO₂. Because of this, more solid sorbent is needed to achieve the same level of CO₂ capture. Additionally, these mechanisms may lead to higher sensible and latent heat requirements, thereby increasing the heat exchange surface area necessary in order to maintain the adsorption and desorption process temperatures. Hence, the adsorption of water by the solid sorbent is a potential concern due to its indirect influence on equipment size.

One way of mitigating water adsorption is by dehumidifying the flue gas through pre-treatment steps prior to the CO₂ capture process. Another option is to rely on hydrophobic adsorbents, which avoid or at least mitigate interaction with water. Choosing a water-tolerant adsorbent may lead to significant cost savings if the material can be produced without substantial increase to the cost of the adsorbent (Marx, et al., 2013). This interaction is the reason why a tolerance of water is often considered the second most important criterion when evaluating a new sorbent following CO₂ selectivity (ibid).

Though it is known that water plays an important role in the performance of a sorbent, the available data regarding the reaction mechanisms for CO₂ uptake do not accurately account for the influence of water on sorbent loading. This is the case when:

- The interaction between the sorbent and water is not strictly caused by competing reaction mechanisms, but by physical changes to the solid sorbent such as pore closure or multi-layer reactions (Figure 2.2 below) (Abanades & Alvarez, 2003); and
- For many sorbents, data is not yet available regarding the performance of the solid under “wet” flue gas conditions such as those found in a post-combustion setting.

In rare cases, there are kinetic models that account for the numerous possible reactions between the adsorbent, water, and CO₂ for specific solid sorbents. The U.S. Department of Energy’s National Energy Technology Laboratory (DOE/NETL) has invested significant resources, for example, to estimate the equilibrium and kinetic parameters for one of their most promising internally developed solid sorbents, NETL-32D (Lee, et al., 2011). Most solid sorbents, however, have not received the same level of scrutiny. Multi-reaction data for most promising solids are absent from the literature for either propriety reasons or lack of dedicated resources.

An alternative method of modelling the effect of water on CO₂ capacity is to adjust the maximum equilibrium CO₂ capacity of the solid based on the observed influence of water. The advantage of this method is that the effect can be applied as either a positive or negative influence on CO₂ uptake without regard to the specific cause of the change. In this work, a parameter for water loss ($q_{\text{water loss}}$) is used to alter the availability of reactive sites (q_{maximum}) based on the positive or negative influence of water. Details regarding this method are discussed in Section 4.3.

2.3.3. Influence of sulfur dioxide, nitrogen oxides, and oxygen

Many adsorbent materials are susceptible to degradation by acid gases present in the flue gas. The extent to which these constituents pose a concern depends on the concentration and uptake of each

constituent. A typical flue gas produced by a plant under the U.S. New Source Performance Standards in contains about 4% O₂, less than 0.01% NO and SO₂, and less than 0.001% NO₂ (40 C.F.R. §60). Unfortunately, data regarding the uptake of these constituents on the solid sorbent are sparse, particularly in the case of oxygen and nitrogen oxides, although limited data is available on some of the more prominent sorbents. In general, physical sorbents are prone to degradation by molecules of similar shape to CO₂ including N₂ and O₂. These constituents occupy the reactive sites and prevent the uptake of CO₂ (Bollini, et al., 2011). Chemical adsorbents are often subject to denaturing and irreversible reactions of acid gases (SO₂, NO_x, and NO₂) and O₂. Amine-based sorbents, for example, have been found to be prone to degradation from SO₂ through a practically irreversible chemical reaction (Diaf & Beckman, 1995; Diaf, et al., 1994; Sjoström, et al., 2011). Moreover, oxidation of solid sorbents in the presence of oxygen becomes prevalent at temperatures above 100°C as a result of a Schiff-base reaction (Ahmadalinezhad, et al., 2013; Drage, et al., 2009).

Oxidation of the solid sorbent is important in the context of post-combustion CO₂ capture given the range of temperatures under consideration for this process. Current formulations of many of the more prominent solid sorbents, including NETL-32D, do not include corrosion inhibitors common in liquid systems that deter degradation of the solid. Moreover, it is unclear whether the additives and other inhibition methods used in liquid systems are applicable to solid systems because of the proprietary nature of commercially available liquid systems.

Despite the lack of data available regarding the influence of these constituents, the inclusion of water and SO₂ degradation in this work is necessary because of the severity of their impact on the performance of a solid sorbent system, as shown in Chapters 5 and 7. Depending on the properties of the specific adsorbent used in a capture system, some pre-treatment of the flue gas may be capable of mitigating the water and SO₂ degradation issues discussed in this section.

2.4. Physical attrition

Most sorbents are subject to some level of attrition caused by physical weathering in addition to the chemical degradation processes discussed in the previous section. Consensus in the literature is that the rate of solids attrition depends on the toughness of the material, the degree of particle fluidization, and the weight of the solid bed in a solid-gas reactor bed (Shih, et al., 2003). Merrick and Highley (1974) found that the total rate of fines by abrasion in a fluidized bed was proportional to the bed weight and velocity (Merrick & Highley, 1974). Their study used the particle size and reactor bed dimensions to predict the reduction in particle size over a wide range of bed dimensions. Lin et al. found that the production of particle fines in a char and sand fluidized bed increases exponentially with the excess velocity (Lin, et al., 1980). Shamlou et al. reported that the breakage of the solid material could occur by purely hydrodynamic effects in the fluidized bed (Shamlou, et al., 1990). They further conclude that the primary mechanism for material breakdown in a fluidized bed is the removal of single particles or small groups of particles from the surface of the parent material. Ray et al. proposed a mechanical model to assess the effects of various mechanical factors on the attrition rate for a bubbling bed. This model predicted that larger coal and smaller limestone were more desirable for reducing attrition in a coal combustor (Ray, et al., 1987). Lee et al. observed that the weight of the solid in a fluidized bed would approach a constant value, so they introduced a minimum weight of the bed material into the first-order attrition rate model (Lee, et al., 1993). Cook et al. further proposed a modified second-order model using a minimum weight and excess velocities for lime sorbent in a circulating fluidized bed adsorber and expressed the attrition rate in an Arrhenius form (Cook, et al., 1996). Mathur and Epstein indicated that a smaller diameter of the gas inlet, a higher gas flow rate, and a deeper bed of solids resulted in a larger attrition in a sprouting bed reactor (Mather & Epstein, 1974).

Because data is sparse, solid sorbent attrition rates are not addressed as a unique parameter in this work. Rather, its influence on the solid sorbent's capacity for CO₂ is reflected in the value for maximum CO₂ capacity (q_{maximum}) discussed in section 4.3. Particle fines that are generated from physical

attrition are removed from the circulating solid stream as part of the solid purge stream (see Section 4.2.8).

2.5. Treatment of degradation and attrition

Although attrition and degradation can be minimized through effective material and reactor design, losses to the initial capacity will occur as the material undergoes repeated cycling through the CO₂ capture process. The lost capacity must be replaced by removing material, called “purge”, from the system and replacing it with fresh adsorbent. This constant replenishing process ensures that the system maintains a constant CO₂ capacity. More details on how these effects are modeled are provided in Chapter 4.

2.6. Reaction kinetics

CO₂ adsorption and desorption kinetics are critical to the effectiveness of any solid sorbent. For a given reactor size, fast reaction rates increase the working capacity of the solid sorbent and reduce the required solid flow rate. Conversely, the same solid sorbent with slow reaction rates reduce the working capacity resulting in higher solid flow rates. The design of the solid sorbent is key to achieving fast reaction rates as well as high capacities. Very high surface areas are required for optimal capacity, which requires the materials to have very fine pores and high permeability. Transport of the flue gas through these pores occurs by various diffusion mechanisms depending on the pore size, and understanding these mechanisms is essential for the effective design of sorbents for CO₂ capture since transport rates define the limits on the cycle times that may be possible. The significance of rate limiting mechanisms has also been shown in previous experiments of Yue (2008) and Xiaochun (2002) regarding amine-functionalized (chemisorption) and metal organic framework (physisorption), respectively (Xiaochun, et al., 2002; Yue, et al., 2008).

Due to the exothermic nature of the adsorption reaction, an increase in temperature typically causes a decrease in adsorption capacity. However, due to diffusion limitations in the smaller pores, an increase in temperature results in an increase in the diffusion rate, leading to enhanced capacity at higher temperatures. Xiaochun, et al. (2002) found that their solid sorbent, a silica-supported polyethylenimine (PEI)-modified material (MCM-41-PEI), increased in CO₂ capacity across a temperature range of 323 to 348 K where it exhibited a maximum and decreased thereafter (Xiaochun, et al., 2002). When pore size becomes restrictive, as it is for some microporous sorbents, and certainly for supported amine-based solid sorbents, the pore openings become restricted and diffusional limitations becoming more important than thermodynamic limitations.

Some of the fastest reaction kinetics for solid sorbents can be found in zeolites, reaching their equilibrium capacity within 1-5 minutes in most cases (Choi, et al., 2009). Primary amines also exhibit fast reaction kinetics as shown in Figure 2.2. In a bench-scale, fixed bed adsorption experiment, Alesi and Kitchin (2012) characterized this solid sorbent using a 10 volume % CO₂ at equilibrium pressures and temperatures. This sorbent achieves 80% maximum loading within 2 minutes, but has a long tail at the higher end of the adsorption curve indicating an abrupt shift in the rate of adsorption. A much longer time is therefore required in order to reach full equilibrium (Alesi, Jr & Kitchin, 2012). This 2-phase adsorption profile is typical of amine-based solids (Wilcox, 2012). The equilibrium design used by CCSI, for example, uses a 32 minute residence time in order to achieve full loading on mixed-amine based solid (Lee, et al., 2011). The CO₂ loading profile for this solid sorbent has a long tail at the higher end of the adsorption curve, and the abrupt shift in adsorption rate indicates a sharp drop-off in the rate of adsorption. However, given the space and cost restrictions for the application of CO₂ capture systems, it is doubtful that commercial reactor vessels will be constructed which will allow the solid sorbent to reach full equilibrium. The extent to which the adsorbent approaches the equilibrium loading is therefore an important constraint.

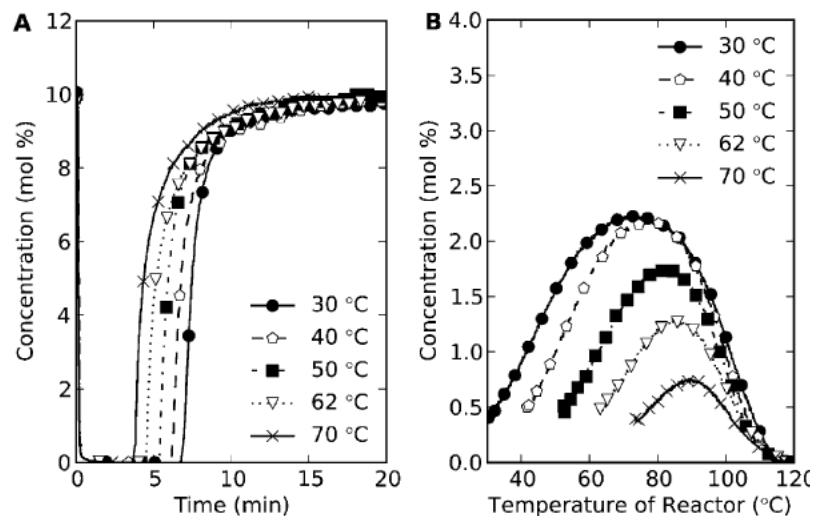


Figure 2.2: Kinetic adsorption for a primary-functionalized ion exchange resin (Alesi, Jr & Kitchin, 2012).

The kinetics of sorbent reactions are difficult to model precisely using standard kinetic parameters for two reasons: First, the interactions between the sorbent and flue gas are complex and often poorly understood; and second, there is little data regarding the kinetic parameters for many of the more promising solid sorbents. For these reasons, a traditional approach using reaction rate constants for one or more reactions is ill-suited for this reduced-order approach.

An alternative method used in this work is to adjust the equilibrium loadings based on a working knowledge of the adsorbent and the CO₂ capture system. Two kinetic parameters (k_A and k_R) are used to adjust the loading in the adsorber and regenerator vessels. The utility of these parameters and the method for quantifying the influence of kinetics on CO₂ uptake are elaborated in Section 4.3.

2.7. Sorbents modelled in this thesis

Based on the considerations above, amine-based solid sorbents were selected as the basis for a model of current post-combustion CO₂ capture system designs using solid sorbents. From this category, two solid sorbents were selected for use in this work. The first is a primary benzyl amine-based ion exchange resin. This material was selected based on its use as the first solid sorbent tested in the pilot unit at the test facility located at Southern Company's Plant Miller located in Wilsonville, AL (Sjostrom S.,

2013), combined with the availability of performance and cost data. The second solid sorbent is a supported amine developed by researchers at NETL. This sorbent, called 32D, was chosen based on its use in the CCSI modelling studies discussed in Section 1.5. Table 2.3 lists the characteristics for these solid sorbents.

Table 2.3: Comparison of adsorbents and the specific values for several key solid sorbent parameters considered in this thesis.

Sorbent	Units	Amine resin¹	Supported amine²
Heat of reaction	kJ/mol CO ₂	-60	-67
Langmuir constant ³	1/Pa	4.92*10 ⁻¹⁴	4.92*10 ⁻¹⁴
Manufacturing cost	\$/kg	2.27	2.27
Maximum CO ₂ loading	mol CO ₂ /kg sorbent	2.9	3.5
Solid heat capacity ⁴	kJ/kg-K	1.05	1.0

¹Values for the amine resin sorbent are from (DOE/NETL, 2013) under project NT-0004343

²Estimated from published data (DOE/NETL, 2012)

³Estimated from published data (DOE/NETL, 2013)

⁴Solid heat capacity measured at standard pressure and temperature (1 atm, 15°C)

Preliminary performance results for the amine resin solid sorbent were reported by ADA-ES as part of the May 2013 DOE/NETL Technology Update (DOE/NETL, 2013). This data shows that this material is able to achieve a working capacity of approximately 7% by weight (or 1.6 moles CO₂ per kilogram of solid sorbent) in a laboratory setting. This is nearly an 80% improvement versus the working capacity of aqueous monoethanolamine (MEA) provided in the 2010 version DOE Baseline Report (DOE/NETL, 2010).

The amine solid sorbents listed in Table 2.3 are the most promising solid sorbents for which there is publically available data. However, they represent only two materials among many potential alternatives. In order to also represent potential near-term improvements in the performance of solid sorbents, an expert elicitation was conducted to estimate the characteristics of alternative solid sorbent materials as elaborated in Appendix B. This exercise consisted of telephone or in-person interviews with twelve experts in the area of solid sorbent technology who addressed several key characteristics of

present and near-term future solid sorbents under certain conditions. The solid sorbent characteristics addressed in this elicitation exercise include:

- a. Maximum solid sorbent loading
- b. Influence of water on maximum CO₂ loading
- c. Adsorber kinetics
- d. Regenerator kinetics
- e. Cost of solid sorbents

The basic characteristics of the present and future-case theoretical solid sorbents modelled in this work are shown in Table 2.4. A more detailed description of these solid sorbents is presented in Chapter 5, which includes additional information regarding the treatment of degradation, kinetics and other performance characteristics of the material. The questionnaire used in this exercise is included in Appendix B.

Sorbent	Units	Present solid sorbent	Future solid sorbent
Heat of reaction	kJ/mol CO ₂	-60	-60
Langmuir constant	1/Pa	4.92*10 ⁻¹⁴	4.92*10 ⁻¹⁴
Manufacturing cost	\$/kg	4.30	2.70
Maximum CO ₂ loading	mol CO ₂ /kg sorbent	2.9	3.9
Solid heat capacity	kJ/kg-K	1.0	1.0

2.8. Conclusion

This chapter reviewed the current state of the art for solid sorbent materials for CO₂ capture and discussed the characteristics of solid sorbents that are important for the CO₂ capture process. The chapter began by describing two general classifications for solid sorbents (physiosorbents and chemisorbents) based on the adsorption mechanism. The Langmuir method was then presented as a means of describing adsorption, followed by a description of the basic material properties that determine CO₂ uptake. More advanced material properties were then discussed including attrition, interaction with

other flue gas species, and rate-limited adsorption. The chapter concluded with a description of the best available solid sorbent species based on currently available data and an expert elicitation exercise. Chapter 3 next describes the post-combustion CO₂ capture process that uses these solid sorbent materials downstream from other pollution control systems in a coal-fired power plant.

3. The solid sorbent process for coal-based CCS

This chapter provides a review of the solid sorbent-based CO₂ capture process. Several concepts relating to solid-based gas separation systems are reviewed, including the two adsorption/desorption mechanisms and four categories of reactors considered for post-combustion capture. The chapter concludes by proposing a process design for CO₂ capture that will serve as the basis of the performance and cost assessment presented in later chapters.

3.1. Introduction

The basic setup for a solid sorbent system consists of an adsorber unit designed to separate CO₂ from the flue gas by selectively adsorbing CO₂ and a regenerator that releases the CO₂ from the solids as a concentrated stream. Figure 3.1 shows a generic system diagram describing the CO₂ capture system starting downstream of an optional flue gas pre-treatment unit. There are multiple designs possible for several of the steps involved in the capture although most solid sorbents that use amine-based solid sorbents share this basic process design.

In this type of system, flue gas enters the adsorber where it comes in contact with solid material. CO₂ is selectively adsorbed on the solid sorbent and the “clean” flue gas is released to the atmosphere and the CO₂ rich solids are transported to the regenerator. The conditions in the regenerator are such that the adsorbed CO₂ is released from the solid (often with water vapor and trace gases like SO₂ and N₂). Downstream from the capture system, the CO₂-rich gas stream is dewatered and pure CO₂ is compressed for transport via pipeline to a CO₂ storage site. Meanwhile, the CO₂-lean solids are transported back to the adsorber where the cycle begins again. In a non-ideal process, a portion of the returning solids are discarded and replaced with fresh solids in order to maintain consistent CO₂ adsorption capacity in the face of material wear and degradation.

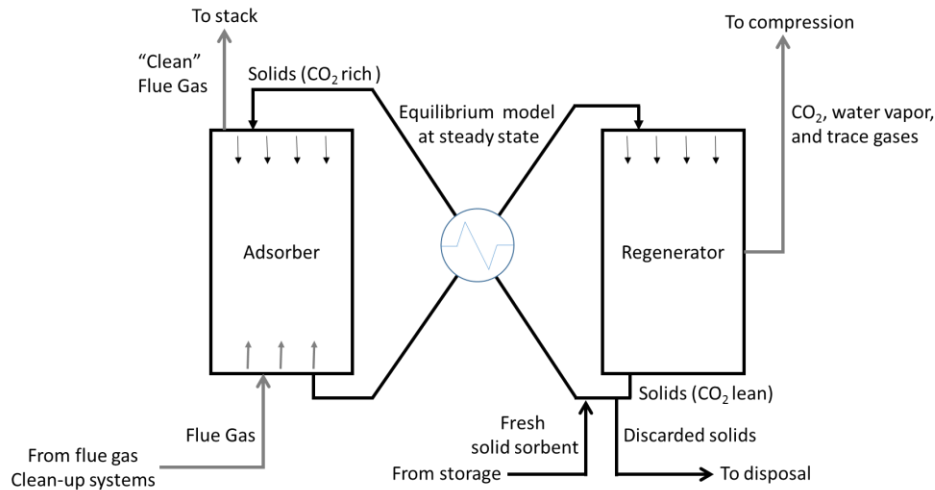


Figure 3.1: Generic solid sorbent based CO₂ capture system consisting of an adsorber, regenerator, and an optional cross-flow heat exchange process.

3.2. Adsorption/desorption cycles

Two basic methods are used for changing the loading of CO₂ on the solid sorbent in a full-scale operation: temperature swing adsorption (TSA) and pressure swing adsorption (PSA). These methods are discussed in greater detail below.

3.2.1. Temperature-swing adsorption

Figure 3.2 shows an example of a temperature-swing cycle, in which a feed stream containing CO₂ at a partial pressure of p_1 is passed through the adsorber vessel at a temperature of T_1 . The initial loading is expressed as x_1 in units of moles of CO₂ per mass of sorbent. After sufficient contact time has passed to allow adsorption of flue gas CO₂ by the solid sorbent, the solids are transferred to the regeneration cycle where the sorbent temperature is increased to T_2 (either directly with a hot purge gas or indirectly by heating the solids using an indirect heat exchanger) with the desorption process establishing a new equilibrium loading, x_2 . The net removal capacity (*i.e.*, working capacity or delta loading) of the bed can be determined from the difference between x_1 and x_2 .

In particular, for thermal regeneration of CO₂ with steam at 130-150°C, regeneration is the most steam-intensive step of the process, with typical steam consumption values of 0.2-0.4 kg per kg of carbon (McCabe, et al., 2005). Temperature swing adsorption is being considered for many adsorbents which exhibit a strong dependence on temperature for CO₂ affinity (DOE/NETL, 2013; Jones, 2013). For chemisorbents, temperature swing adsorption is the preferred method because of the strong relationship between temperature and the solid sorbent's CO₂ capacity.

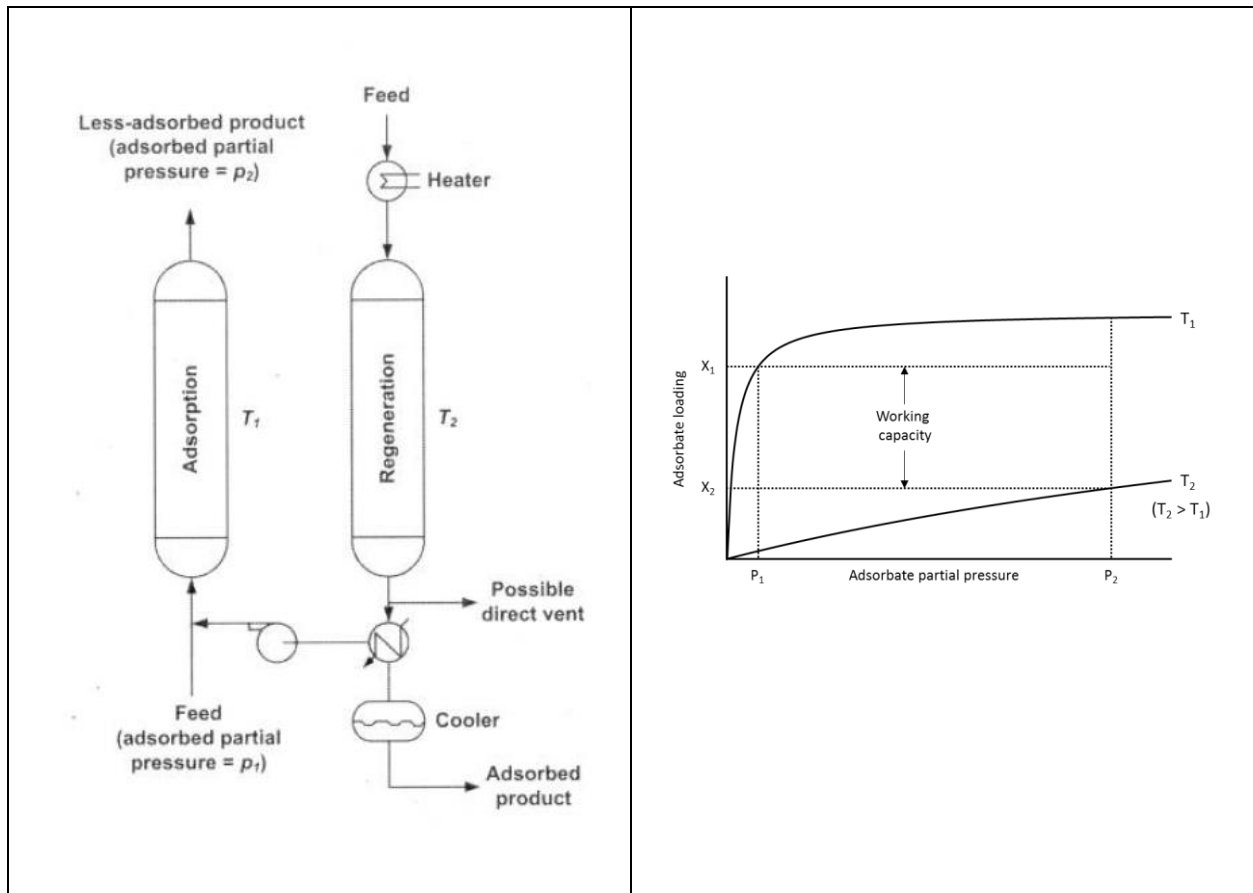


Figure 3.2: Temperature swing cycle (Keller, et al., 1987). The graph at the right shows the difference in adsorbate loading as a function of temperature and partial pressure in the two reactor vessels.

3.2.2. Pressure-swing cycles

Figure 3.4 represents a pressure-swing cycle in which the partial pressure of the adsorbate can be reduced by lowering the total pressure of the gas. The lower the total pressure during the regeneration

step, the lower the lean loading. This difference in adsorbate pressure has the desirable effect of increasing the working capacity of the solid sorbent in the CO₂ capture system. Such a system could theoretically lead to higher working capacity than a temperature swing system, depending on the time required to load, depressurize, regenerate, and repressurize a bed in a fixed bed design, and the total pressure drop, which can be achieved in other system designs (Wilcox, 2012). A design capable of achieving very short residence times, on the order of seconds rather than minutes, would make the pressure-swing cycle an option for bulk-gas separation processes.

One advantage of a pressure swing system is its ease of application to a combination adsorption/desorption unit. This type of system is one potential design that has received attention, though the energy penalty for a commercial-scale chamber under a vacuum appears cost prohibitive. Nonetheless, pressure swing adsorption is being considered for adsorbents that exhibit a strong dependence on pressure for CO₂ affinity and may therefore be the preferred system for physiosorbents (Ritter, 2013).

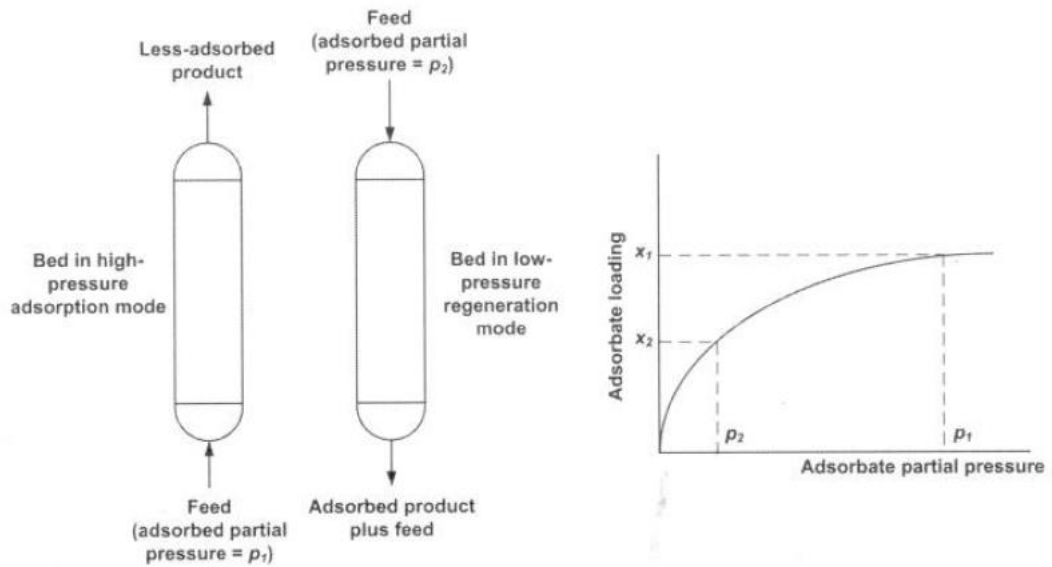


Figure 3.3: Pressure swing cycle (Keller, et al., 1987). The graph at the right shows the difference in adsorbate loading as a function of partial pressure in the two reactor vessels.

A disadvantage of this process for post-combustion CO₂ capture applications would be the required compression costs of handling large flow rates. This method may be more attractive for pre-combustion CO₂ capture in which the feed is already at an elevated pressure.

3.2.3. Liquid-solid heat exchange

Between the adsorber and regenerator units, heat exchangers are used to transfer recovered heat from the hot solids exiting the regenerator to the cooler solids prior to entering the regenerator. Pre-heating the solids reduces the steam demand necessary to heat the solids in the regenerator. The design of the solid-liquid heat exchangers is adapted from the published work completed by the CCSI group (DOE/NETL, 2012). This work assumes single pass, counter-current flow of the solids through the cross-flow heat exchanger based on the CCSI design. Water is used as the heat transfer fluid, which is vaporized using heat from the hot solids leaving the regenerator and condensed as heat is transferred to the solids leaving the adsorber. A pump and a compressor are provided to move the heat exchange fluid between the heat exchange vessels as shown in Figure 3.5.

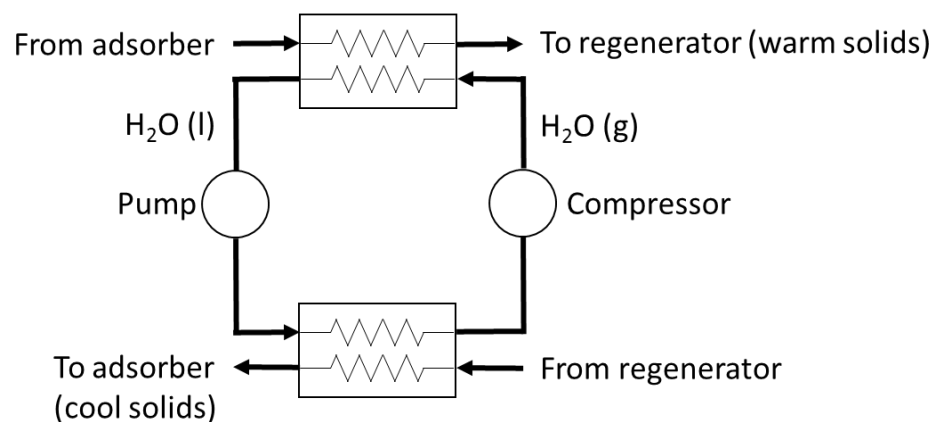


Figure 3.4: Diagram of the solid-liquid heat exchange system. The heat exchange fluid (water/steam) circulates through the tube side while solids circulate through the shell side.

The heat exchange vessels are sized using design correlations proposed by Seider *et al.* (Seider, 2014). The heat exchanger design is a shell-and-tube type made with carbon steel as reported by CCSI (DOE/NETL, 2012). This design has the advantage of being relatively easy to maintain and since the tube bundle can be pulled out from the shell. However, this type of heat transfer system is complicated and has a high manufacturing cost (China-OGPE, 2014). Nonetheless, the shell and tube design is used in this model in order to conform to the CCSI design discussed in Section 3.4.

3.2.4. Solid-gas heat exchange

Although flue gas may enter the adsorber at a relatively low temperature (40-60°C), the thermal energy of the entering solid stream is very large and necessitates further cooling. Two notable studies have incorporated internal or external heat exchange as part of the adsorber process area to cool the solids and dissipate the heat generated by the exothermic reaction between CO₂ and the solid sorbent. In the first of these studies by CCSI, the solids are cooled from 391K (118°C) to 313K (40°C) within the adsorber by indirect heat exchange with cooling water (DOE/NETL, 2012) (including the heat released in the reaction between CO₂ and sorbent). The second study, performed by Stantec, Inc. and included in ADA's 2012 final technical report to NETL integrates a rotary contact cooler prior to adsorber entry (ADA-ES, 2011). This work used the internal heat exchange design specified by CCSI to remain consistent with their modeling efforts.

3.3. Gas-solid system designs

There are four general types of solid-gas reactors associated with separation via adsorption on a large-scale: fixed bed, moving bed, fluidized bed, and cascading bed design. Though there are variations on each of these processes, examples of each are shown in Figure 3.2. A review of the basic concepts, their application, and the relative merits for each design are reviewed in this section.

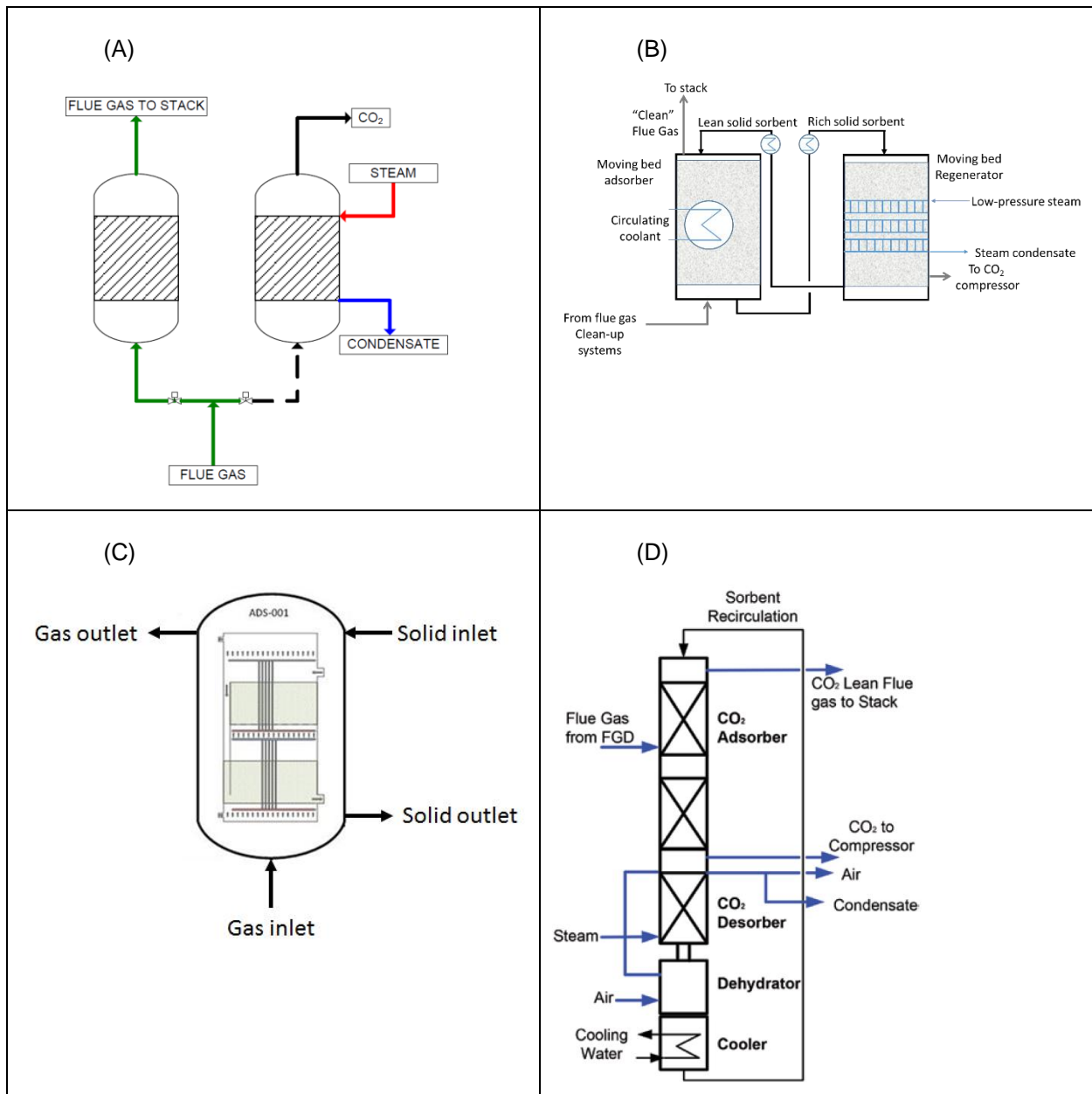


Figure 3.5: (A) Fixed bed system (Tarka & Ciferno, 2005); (B) Moving bed system. Schematic courtesy of SRI and NETL (SRI International, 2013); (C) fluidized (bubbling) bed reactor (DOE/NETL, 2011); (D) Cascading bed reactor (DOE/NETL, 2012)

3.3.1. Fixed bed reactors

A fixed bed is a type of reactor in which the solids remain stationary while gas flows over or through the solid material. Reactor vessels using this design typically consists of two or more cylindrical

vessels packed with solid sorbent in order to allow for continuous operation of the process (as opposed to batch operation) (Tarka & Ciferno, 2005). The gas to be scrubbed enters the first reactor and passes through the solid sorbent, as shown in Figure 3.2(A). While the first reactor is processing the gas flow, solid sorbent in one or more additional reactors is being regenerated. Prior to breakthrough (when all of the solid sorbent becomes saturated), flow is switched from the first reactor to a freshly regenerated one. The near-saturated reactor is then regenerated by cycling the temperature or pressure of the vessel. In most cases, the CO₂ is removed using either hot inert gas or steam, which condenses in the bed, raising the bed temperature and providing sufficient energy for desorption.

The exiting gas stream is a mixture of CO₂ with either an inert gas or water, which would have to be further separated or condensed using a separation step downstream of the fixed bed unit. While the fixed bed was initially an attractive option (in part because of its application in the bio-solids separation industry), it has since has lost favor due to a high pressure drop and/or high area footprint which is attributed in part to the slow desorption kinetics and low heat transfer characteristics (Tarka & Ciferno, 2005; Wilcox, 2012).

3.3.2. Moving bed reactors

Moving bed reactors (shown in Figure 3.2B) are similar to fixed beds in that the solids are densely packed within the vessel. In the moving bed design, however, the solids move through the bed along with the reactants. Moving bed reactors offer several advantages for CO₂ capture, including a reduced footprint and a smaller pressure drop compared to a fixed bed design. Moreover, moving beds are used in bulk solid operations to heat, cool, and dry materials including fertilizers, polymers, sugars, minerals, oilseeds, and grains and may therefore be used for either an adsorber or regenerator (Solex Thermal Science, 2015). Several researchers have recommended the moving bed regenerator design (Pennline & Hoffman, 2000; Srinivasachar, et al., 2014) for large-scale CO₂ capture operation. However, these reactor designs do suffer from higher sorbent attrition in addition to mechanical complexity associated with the equipment involved (Acharya & BeVier, 1985; DOE/NETL, 2012).

Since the adsorber and regenerator steps take place in separate vessels, the design of each unit can be specific to the requirements of that particular process. For instance, the regeneration process may involve elevated temperatures while the adsorber may not need to be designed for such harsh conditions, which adds flexibility to the design of the system (Benson, 2013). Due to the solid sorbent attrition from moving the particles, moving bed systems are considered feasible only in conjunction with attrition-resistant materials (Acharya & BeVier, 1985).

3.3.3. Bubbling and circulating fluidized-bed reactors

Fluidized bed reactors (shown in Figure 3.1(C), both bubbling and circulating, have been used extensively in a wide range of industrial applications, including fluidized catalytic cracking (FCC) and combustion applications (Green, 2008). Fluidized bed reactors operate by passing the gas through the bed of solids at a velocity high enough that the drag forces acting on the solid particles equals or exceeds the force of gravity, referred to as the minimum fluidization velocity. Because of this, the solids act as a “fluid”. Bubbling fluidized beds (BFBs) operate at gas velocities above the minimum fluidization velocity but below the point where all the solids in the bed become entrained by the gas. Compared to fixed and moving beds, BFBs also show comparatively high heat and mass transfer properties, both within the bed and between the bed and heat exchanger surfaces due to the well-mixed behavior of the bed and high degree of contact between gas and solids (Grace, 1986). However, the constant mixing action in the bed can also cause significant attrition of the solid sorbent and erosion of the reactor vessel and internals. Thus, care must be taken when designing a reactor to address these issues.

Circulating fluidized bed (CFB) reactors operate at higher gas velocities, above the point where the solids become entrained in the gas. In these systems, the solids are fully entrained and are carried with the gas as a relatively dispersed mixture. The high gas velocities required to entrain the solids allow CFB reactors to process large amounts of gas in relatively small units; however, gas-solids contacting is not as good as the denser, BFB (DOE/NETL, 2012). Also, as the solids are entrained in the high velocity gas flow, contacting between gas and solids is co-current which reduces efficiency, and the residence

times within even very tall reactors is very short. Circulating fluidized bed reactors also suffer from significant attrition effects, especially near the gas and solids outlet at the top of the reactor (*ibid.*).

The sorbent residence time is an important variable in the fluidized-bed CO₂ capture system and several stages of beds may be used in succession to allow for additional contact time between the solid and gas. The total inventory of solid sorbent required for CO₂ removal is determined by the residence time and initial loading (Tarka & Ciferno, 2005). As the residence time increases, the amount of solid sorbent in the reactor at any given time increases as well, increasing the bed height or number of stages as well as the pressure drop. It is also worth noting that BFBs and CFBs typically has the smallest pressure drop of any of the four vessel types. Like the moving bed system, however, the attrition rate of the solid sorbent will likely increase under highly fluidized conditions, and the area requirement for such a system is likely to be comparatively high given the high gas-to-solid volumetric ratios typical of BFBs/CFBs (DOE/NETL, 2012).

3.3.4. Cascading bed reactors

In the cascading bed design, shown in Figure 3.1(D), solid material is fed through the top of the tower and “cascades” through a series of trays while gas is blown in a counter-current, upward direction through the tower. The trays serve to redistribute the particles and thus achieve better gas-solid contact by preventing large pockets of solid or gas from forming. The geometry of this type of setup could be such that the adsorber and regenerator vessels are stacked, integrating the two steps into a single vertical column and thus resulting in a lower pressure drop and minimizing material handling (SRI International, 2013). This type of design has been chosen for scaling at the 1MW pilot facility constructed at the National Carbon Capture Center (NCCC) in Wilsonville, AL (*ibid.*).

3.4. Process design choice

Choosing a design for the adsorption and regeneration operations is not a simple task. There are complex interactions between the design of the adsorber, regenerator, and the characteristics of the solid that can only be studied using complex modelling tools that are beyond the scope or capability of a reduced order model such as the one presented in this work. Hence, the choice of reactor designs used here is made in deference to the more rigorous modelling work completed by the Carbon Capture Simulation Initiative (CCSI) (DOE/NETL, 2012).

The process flow diagram of the system modelled in this work is shown in Figure 3.6. A bubbling fluidized-bed reactor and a moving-bed reactor are used for the adsorber and regenerator, respectively with other reactor types considered later in Chapter 7. The flue gas stream from the power plant is comprised of nitrogen, water vapor, CO₂, and trace constituents.

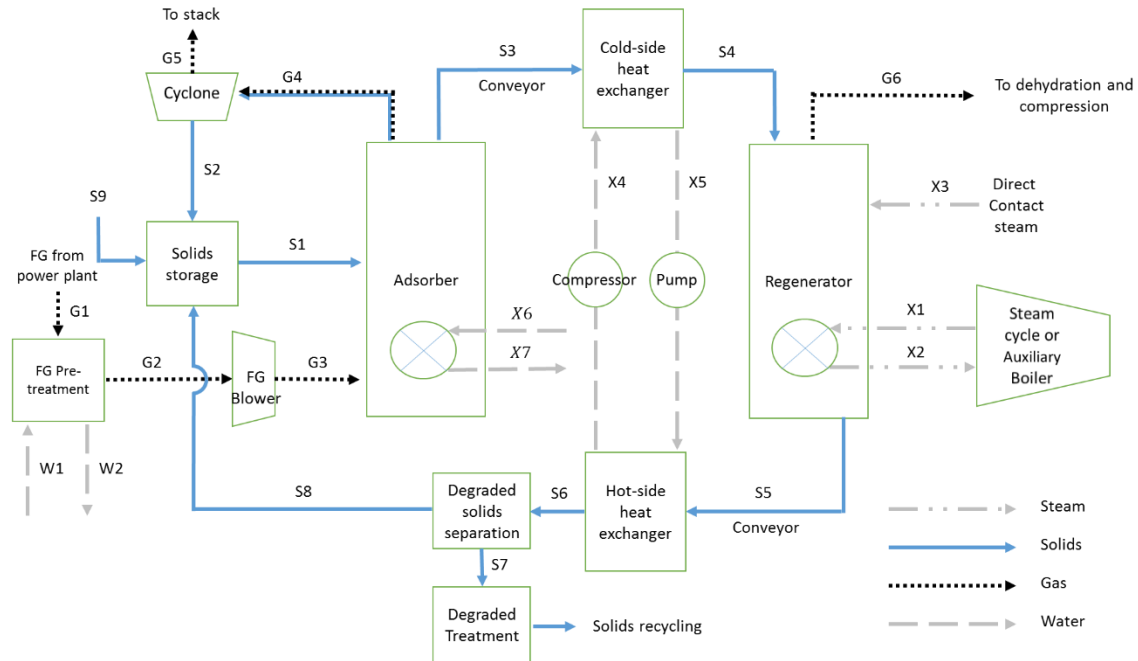


Figure 3.6: Process flow diagram for solid sorbent-based CO₂ capture adapted from the CCSI design (DOE/NETL, 2012).

Flue gas [G1] first enters a pre-treatment step in which the concentration of SO₂ is reduced to 1 ppm using a lime slurry, [W1], whose product, [W2], is mixed with the processed FGD wastewater. The flue gas stream exits pre-treatment, [G2] via a blower used to overcome the pressure drop induced in the pre-treatment unit, adsorber, and flue gas stack. The flue gas stream, [G3], passes into the adsorber where CO₂ is selectively adsorbed on the solid sorbent. A CO₂-depleted flue gas stream, [G4], produced via gas-solid contacting, is sent through a cyclone to remove any entrained solids and then released to the environment [G5]. A small amount of separated solid [S2] is mixed with the incoming solids and recycled back to adsorber from the cyclone.

The solid sorbent stream, [S1], introduced to the adsorber adsorbs CO₂ and other constituents from the flue gas, yielding a CO₂-rich sorbent stream, [S3]. Cooling water [X6] is used to maintain a constant temperature in the adsorber through indirect heat exchange and is directed back to the plant upon exiting the adsorber [X7]. The CO₂-rich solids and any absorbed species are conveyed by a solid moving system, e.g., a bucket elevator, pneumatic conveyor, or some other means, to the cold-side

exchanger. Here, the solids stream is heated indirectly by thermal contact with steam, [X4], which undergoes a phase change to water and is then pumped to the hot-side heat exchanger, [X5]. The water is then heated and converted back to saturated steam by heat recovered from hot solids exiting the regenerator.

The pre-heated solid stream, [S4], enters the regenerator and achieves full regeneration temperature via thermal contact with in-reactor heat exchanging tubes. In the tube side of the regenerator, hot steam, [X1], extracted at the IP/LP crossover in the power plant turbines is used as a heat source. Once used to heat the solids, this steam is then returned to steam cycle for reheating [X2]. Heating the solid causes the CO₂ to be desorbed, yielding a regenerated (CO₂-lean) solid stream. In addition, a mild condition steam, [X3], is also injected into the regenerator as direct contact steam in order to enhance desorption by reducing the mole fraction of gaseous CO₂. The injected steam and desorbed CO₂ (plus any other trace species adsorbed by a particular solid sorbent) are drawn through a gas collector, [G6], and sent to a dehydration and compression stage.

The CO₂-lean solid stream, [S5], exits the regenerator and is conveyed to the hot-side heat exchanger. The solids are cooled via thermal contact with cooling water circulating between the hot- and cold-side heat exchangers. The cooled solids, [S6], are then sent to a degraded solids separation unit where a slipstream, [S7], is removed and for treatment or disposal. The majority of the CO₂-lean solid stream, [S8], is sent to a solid staging area and mixed with make-up solids before being returned to the adsorber where. The returning solid stream is supplemented with fresh solid sorbent [S9] before entering the adsorber to make up for the discarded solid sorbent.

The design described in this section represents one of many possible design configurations of a solid-based CO₂ capture system. This particular design, developed by CCSI, uses a two-stage, multi-vessel adsorption process combined with a multi-vessel regenerator. However, this chapter has also described the variety of reactors currently being evaluated for full scale CCS, and researchers have yet to arrive at a consensus regarding the best-available solid-based CO₂ capture system design. Though the

CCSI process design is used as a “baseline” system, the performance model developed in this work is designed to be flexible and allows for exploration of different vessel types, design conditions, and sorbent materials. The formulation of the performance model is the subject of Chapter 4.

4. Process performance model

This chapter describes the performance model developed for the purpose of quantifying the mass and energy flows for a solid sorbent-based CO₂ capture system. The chapter begins by summarizing the objectives of the performance model followed by a detailed explanation of the assumptions, calculations, and parameters needed in order to describe an operating solid sorbent system. The solid sorbent system described in this chapter is based on the sorbent characteristics and reactor design introduced in Chapters 2 and 3. When needed, this model also calls on the Integrated Environmental Control Model (IECM) for values relating to the functionality of the balance of the plant. The mass balance equations are covered in Section 4.2, followed by CO₂ loading and energy balance equations in Sections 4.3 and 4.4 respectively.

4.1. Model objective

The objective of the performance model is to estimate the mass and energy requirements of a solid sorbent based CO₂ capture process based on the preliminary process design described in Chapter 3. For a desired CO₂ capture efficiency, specific sorbent, and given operating conditions of a specified power plant, the performance model calculates the mass and energy balances of the major process areas which are described in this chapter. Results from this process performance model are used as inputs to the process cost model, which is described in Chapter 6. The process-level performance and cost models are used in conjunction with the IECM to estimate the effect of solid sorbent-based CO₂ capture on the performance and cost of the overall power plant.

4.2. Process mass balance

This section presents the equations used to quantify the solid, liquid, and gas flow rates throughout the system. This section is organized to follow the flow of gases, liquids (e.g. cooling water),

and solids, through the CO₂ capture system defined in Figure 3. Figure 4.1 shows and defines the process mass flows of the CO₂ capture process modelled here.

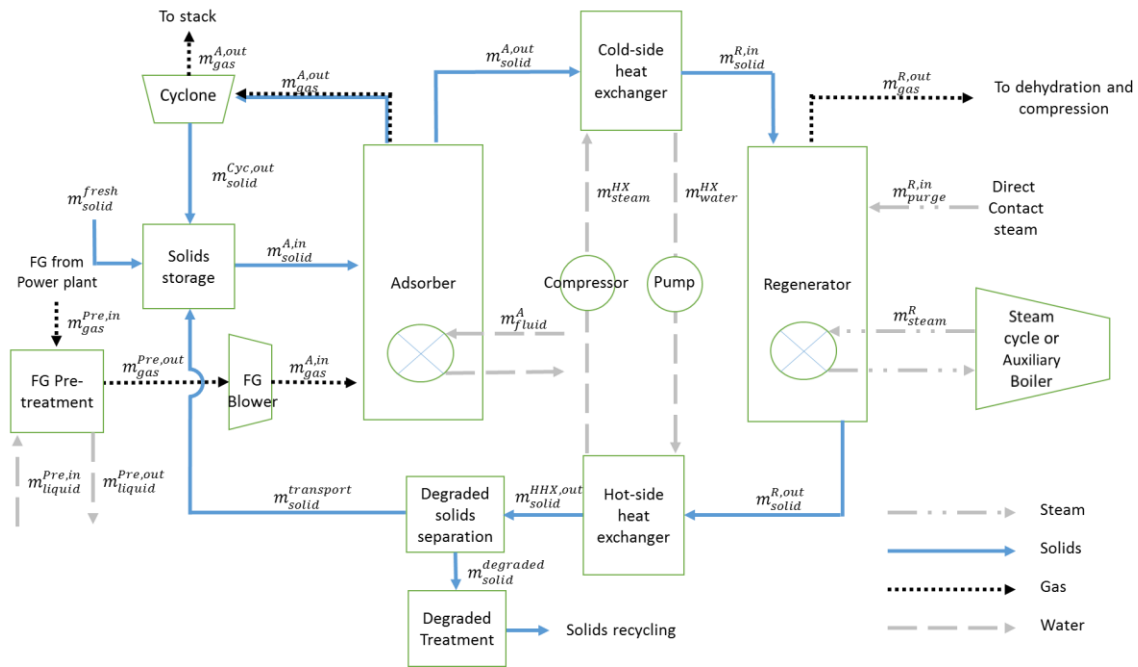


Figure 4.1: Mass flow diagram of a carbon capture system using the nomenclature outlined in this chapter.

There are eleven flue gas constituents passing through the CCS treatment process. Five of these constituents do not react with the solid sorbent and are collectively referred to as “inert”. The remaining constituents may react with the solid sorbent and thereby influence the mass flow rates of the solids and gases flowing throughout the system. Table 4.1 lists the reactive and inert species of flue gas with respect to the carbon capture system.

Table 4.1: Flue gas constituents used as inputs to the solid sorbent model. This table lists the species which potentially undergo physical or chemical interaction in the adsorber (left) and those which are assumed to be unreactive (right).

<u>Influenced by Adsorber (reactive)</u>		<u>Unaffected by Adsorber (inert)</u>	
FG Constituent	Nomenclature	FG Constituent	Nomenclature
Carbon dioxide	M _{CO2}	Carbon monoxide	M _{CO}
Oxygen	M _{O2}		
Nitrogen	M _{N2}	Ammonia	M _{NH3}
Nitrogen oxides (NO + NO ₂)	M _{NOX}	Sulfuric acid equiv.	M _{H2SO4 Equiv.}
Sulfur dioxide	M _{SO2}	Hydrochloric acid	M _{HCl(g)}
Water vapor	M _{H2O}	Argon	M _{Ar}

4.2.1. Flue gas pre-treatment

Upon exiting the base power plant's other pollution control units, flue gas is optionally directed through a pre-treatment step as a means of mitigating the deleterious effects of sulfur dioxide and water. The process modelled in this work is a combined direct contact cooler and SO₂ polisher (DCCSP). Figure 4.2 shows the mass flow streams relating to the pre-treatment and flue gas blower units.

Flue gas enters the pre-treatment vessel with a composition, molar flow rate, temperature and pressure defined by the upstream process areas. For the purposes of this model, these conditions are determined by the settings used in the IECM. The mass of flue gas entering the CO₂ capture process may be described on the basis of the molar flow rates of each constituent multiplied by its molar mass as shown in Equation 4.1.

Equation 4.1:

$$m_{gas}^{Pre,in} = \sum (M_{i(gas)}^{Pre,in} * MW_i)$$

where:

i = Flue gas species, i, as shown in Table 4.1

$m_{gas}^{Pre,in}$ = Mass flow rate of flue gas constituent, i (kg/hr)

$M_{i(gas)}^{Pre,in}$ = Molar flow rate of flue gas constituent, i (kmol/hr)

MW_i = Molecular weight of flue gas species, i (kg/kmol)

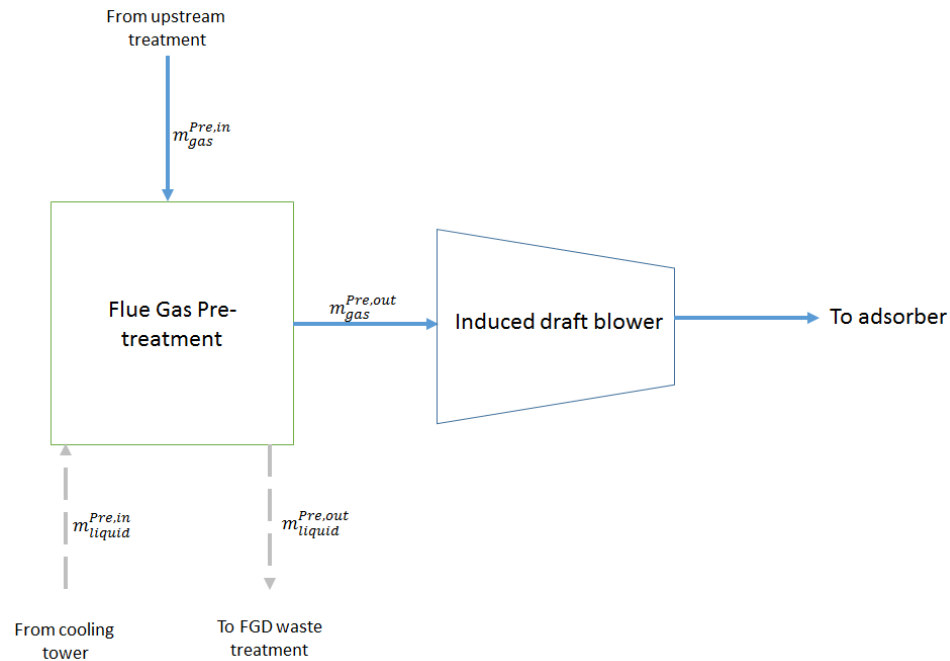


Figure 4.2: A mass flow diagram of the flue gas pre-treatment unit and blower unit. Flue gas enters from the power where it may be treated with a caustic solution in order to remove SO_2 and cool the gas. The treated flue gas exits the pre-treatment unit and enters the induced draft fan before entering the adsorber.

There are two parameters that need to be specified prior to the first calculation for cooling and condensing: an anticipated pressure drop across the contacting column and either a desired temperature for the flue gas exiting the DCCSP or a desired water concentration in the exiting flue gas. If SO_2 polishing is desired, the concentration of sulfur dioxide exiting the DCCSP must also be specified in units of parts per million. Assumptions regarding the performance of this unit are derived from a separate process model developed in a parallel work effort by Kyle Borgert (2015), with details regarding the derivation of the temperature and pressure responses described in Appendix C. The pre-treatment model

calculates the resulting compositions, temperatures, pressures, and mass flow rates of the exiting gas as well as the cooling water inlet and outlet. The flue gas exiting the pre-treatment unit then enters the induced draft blower.

4.2.2. Flue gas blower

The purpose of the flue gas blower is to increase the pressure of the incoming flue gas such that the “clean” gas may be released to the environment at atmospheric pressure. The pressure requirement is determined by the pressure drop across the pre-treatment unit, the adsorber vessel, cyclone vessels, and the flue gas stack. Details regarding the pressure drops, temperature change, and work requirement relating blower are given in the energy requirements section later in this chapter. The composition and flow rates do not change from the blower inlet (which is the same as the pre-treatment outlet if pre-treatment is used or the upstream pollution control equipment if it is not) to the blower outlet. A mass flow diagram of the flue gas blower is included in Figure 4.2.

4.2.3. Adsorber

The purpose of the adsorber vessel is to provide sufficient contact between the solid sorbent and the flue gas such that a desired quantity of CO₂ is removed from the flue gas. Flow rates in and out of the adsorber depend on multiple factors, such as the mass flow rate and composition of flue gas, desired capture efficiency, operating conditions within the reactor, and properties of the solid sorbent. The details of the mass balance model relating to the adsorber are addressed in this section. A mass flow diagram of the adsorber vessel is shown in Figure 4.3. In that figure, the mass flows are defined as follows:

$m_{gas}^{A,in}$ = Mass flow rate of gas at the adsorber inlet (kg/hr)

$m_{solid}^{A,in}$ = Mass flow rate of solids at the adsorber inlet (kg/hr)

$m_{solid}^{Cyc,out}$ = Mass flow rate of solids returning from the cyclone (kg/hr)

$m_{gas}^{A,out}$ = Mass flow rate of gas at the adsorber outlet (kg/hr)

$m_{solid}^{A,out}$ = Mass flow rate of solids at the adsorber outlet (kg/hr)

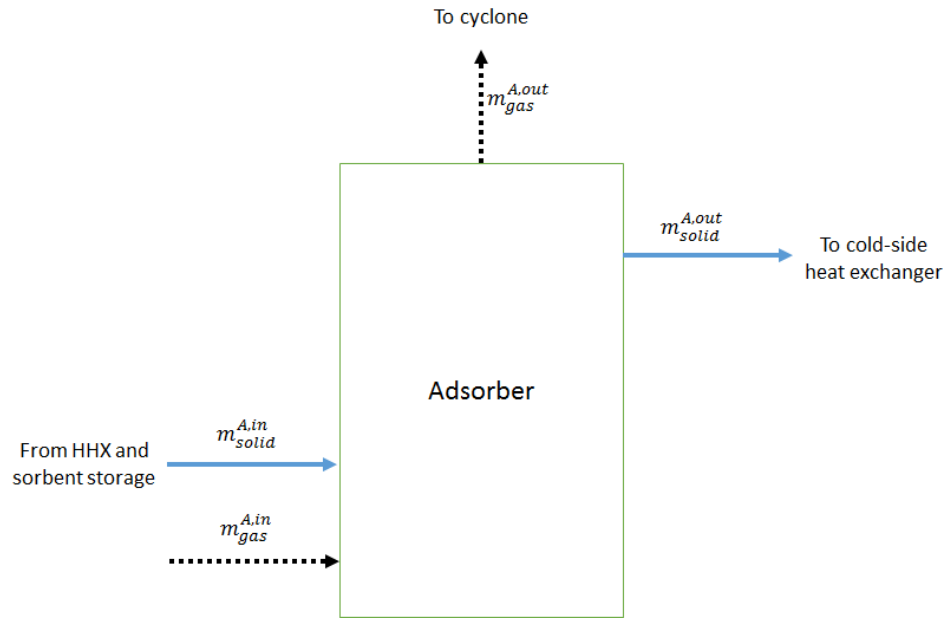


Figure 4.3: Mass balance diagram of a solid sorbent-based adsorber unit. Solids and gas enter the adsorber unit where they are mixed for a time sufficient to ensure the removal of a specified quantity of CO₂.

Inlet flue gas

Flue gas from the induced draft blower enters the adsorber with a well-defined composition, temperature, and pressure. Equation 4.2 calculates the mass flow rate of flue gas at the adsorber inlet based on the molar flow rate of individual flue gas constituents. The mass flow rates of gas constituents at the adsorber inlet are the same as the pre-treatment outlet. If no pre-treatment is required than the constituent mass flow rates are a pre-defined parameter of the model.

Equation 4.2:

$$m_{gas}^{A,in} = \sum (M_{i(gas)}^{A,in} * MW_i)$$

where:

i = Flue gas constituents listed in Table 4.1.

$M_{i(gas)}^{A,in}$ = Molar flow rate of gas constituent, i, existing as a gas at the adsorber inlet (kmol/hr)

MW_i = Molecular weight of flue gas constituent, i (kg/kmol)

Outlet flue gas

Flue gas exits the adsorber with a reduced concentration of reactive species after contacting the solid sorbent. The flow rate of inert species remains constant. As with the inlet flow rate, the outlet flow rate can be expressed as the sum of the flue gas species (Equation 4.3).

Equation 4.3:

$$m_{gas}^{A,out} = \sum (M_{i(gas)}^{A,out} * MW_i)$$

where:

i = represents both reactive and inert species listed in Table 4.1.

$M_{i(gas)}^{A,out}$ = Molar flow rate of species, i, existing as a gas at the adsorber outlet (kmol/hr)

At the adsorber outlet, the flow rate of CO₂, H₂O, SO₂, NO_x, and O₂ is given as a function of the inlet flow rate and the capture efficiency as shown in Equation 4.4.

Equation 4.4:

$$M_{i(gas)}^{A,out} = M_{i(gas)}^{A,in} * (1 - \eta_{C,i})$$

where:

$i = \text{CO}_2, \text{H}_2\text{O}, \text{SO}_2, \text{NO}_x, \text{O}_2$

$\eta_{c,i}$ = Capture efficiency of species, i (fraction)

The capture efficiency ($\eta_{c,i}$) is defined as the difference between the molar flow rate of the reactive species entering the adsorber ($M_{i(\text{gas})}^{A,\text{in}}$) and the molar flow rate exiting as a gas ($M_{i(\text{gas})}^{A,\text{out}}$) divided by the molar flow entering as a gas as shown in Equation 4.5. This parameter may be expressed as a fraction or percentage. Since solid sorbents undergo a wide range of adsorptive interactions with these gases, the capture efficiency for each reactive flue gas species is maintained as a user-defined input parameter of the model.

Equation 4.5:

$$\eta_{c,i} = \frac{M_{i(\text{gas})}^{A,\text{in}} - M_{i(\text{gas})}^{A,\text{out}}}{M_{i(\text{gas})}^{A,\text{in}}}$$

The primary function of solid sorbents for post-combustion application is to separate CO_2 from other flue gas constituents. For conventional air-fired combustion, most of the treated flue gas consists of N_2 . For this reason, the selectivity values, referring to the preferential adsorption of CO_2 over N_2 , for many solid sorbents are known from the literature (refer to Section 2.2). In this model, the quantity of N_2 that is adsorbed by the solid sorbent is estimated using a selectivity value, which is given the symbol, s . At the adsorber outlet, the molar flow rate of nitrogen gas is determined by the flow rate of CO_2 as shown in Equation 4.6.

Equation 4.6:

$$M_{N_2(gas)}^{A,out} = M_{N_2(gas)}^{A,in} - M_{CO_2(gas)}^{A,out} * \frac{1}{s}$$

where:

s = selectivity constant (kmol CO₂/kmol N₂)

In the case of chemisorbents such as amine-based resins, the selectivity factor is assumed to be effectively infinite based on the discussion in Section 2.3.1. Physisorbents such as activated carbon may have lower selectivity constant typically ranging from 10-20. Details regarding the selectivity constant are available in Table 2.2.

The flow rate of inert species at the adsorber outlet is equal to the flow rate at the adsorber inlet. These gas constituents are released into the air as part of the “clean” flue gas. The flow rates of these constituents are collectively represented in Equation 4.7.

Equation 4.7:

$$M_{inert(gas)}^{A,out} = M_{inert(gas)}^{A,in}$$

Inlet solids flow rate

The solids stream entering the adsorber consists of the mass of adsorbed flue gas species entering the adsorber as a solid, $m_{i(solid)}^{A,in}$, plus a larger term representing the mass of solid sorbent, $m_{solid-i}^{A,in}$. The total mass flow rate of solids at the adsorber inlet can be expressed as a sum of these terms as given in Equation 4.8.

Equation 4.8:

$$m_{solid}^{A,in} = \sum m_{i(solid)}^{A,in} + \sum m_{solid-i}^{A,in}$$

where:

i = CO₂, H₂O, SO₂, NO_x, N₂, O₂

$m_{solid}^{A,in}$ = Total mass of solid at the adsorber inlet (kg/hr)

$m_{i(solid)}^{A,in}$ = Mass of reactive flue gas species, i, existing as a solid at the adsorber inlet (kg/hr)

$m_{solid-i}^{A,in}$ = Mass of solid at the adsorber inlet required to capture flue gas constituent, i (kg solid sorbent/hr)

The amount of CO₂ adsorbed on the sorbent at the adsorber inlet is known as “lean loading.” The method used for estimation of lean loading is described in Section 4.3.

Outlet solids flow rate

The flow rate of solids exiting the adsorber is determined by the inlet flow rate and added mass of adsorbed flue gas species. Like the adsorber inlet flow rate, the flow of solids at the adsorber outlet can be expressed as the sum of these two components as shown in Equation 4.9.

Equation 4.9:

$$m_{solid}^{A,out} = \sum m_{solid-i}^{A,out} + \sum m_{i(solid)}^{A,out}$$

where:

i = CO₂, H₂O, SO₂, NO_x, N₂, O₂

$m_{solid}^{A,out}$ = Total mass of solid at the adsorber outlet (kg/hr)

$m_{i(solid)}^{A,out}$ = Mass of adsorber flue gas species, i, at the adsorber outlet (kg/hr)

$m_{solid-i}^{A,out}$ = Mass of solid sorbent at the adsorber outlet required to capture flue gas constituent, i
(kg solid sorbent/hr)

The mass of solid sorbent ($\sum m_{solid-i}$) remains unchanged from the adsorber inlet to the adsorber outlet. However, the quantity of adsorbed species changes based on the reactive properties of the solid sorbent. The second term in Equation 4.9, $\sum m_{i(solid)}^{A,out}$, represents the mass flow rate of adsorbed species. This term is quantified as the summed mass of adsorbed species (CO₂, N₂, H₂O, SO₂, NO_x, and O₂). The mass flow rate of these species must be defined in order to determine the total solid flow rate at the adsorber exit. To begin, the mass flow rate of adsorbed CO₂ is defined using Equation 4.10.

Equation 4.10:

$$m_{CO_2(solid)}^{A,out} = m_{solid-CO_2}^{A,in} * q_{rich} * \frac{1}{1000} * MW_{CO_2}$$

where:

$m_{CO_2(solid)}^{A,out}$ = Mass of adsorbed CO₂ exiting the adsorber (kg CO₂/hr)

$m_{solid-CO_2}^{A,in}$ = Mass of solid sorbent at the adsorber inlet required to the capture of CO₂ (kg solid sorbent/hr)

q_{rich} = Rich loading of CO₂ on the solid sorbent (moles CO₂/kg solid)

1000 = Conversion factor from kilomoles of CO₂ to moles of CO₂

Estimation of rich and lean loadings is explained in Section 4.3.

The mass flow rate of adsorbed nitrogen can be expressed in terms of the selectivity factor and the molar flow rate of CO₂ as shown in Equation 4.11.

Equation 4.11:

$$m_{N_2(solid)}^{A,out} = M_{CO_2(solid)}^{A,out} * \frac{1}{S} * MW_{N_2}$$

The mass flow rates of other adsorbed gases can be quantified using capture efficiencies mentioned earlier in this section as shown in Equation 4.12.

Equation 4.12:

$$m_{i(solid)}^{A,out} = m_{i(solid)}^{A,in} + M_{i(gas)}^{A,in} * \eta_{C,i} * MW_i$$

where:

i = H₂O, SO₂, NO_x, O₂

4.2.4. Flue gas cyclones

Flue gas exiting the adsorber may contain small quantities of entrained solids. The flue gas is therefore sent through a series of cyclone vessels as shown in Figure 4.4 in order to remove larger particles from the flue gas stream. Flue gas and the entrained solids enter the battery of cyclones as a single stream where they are gravimetrically separated. The gas flow is directed to the top of the cyclone and released to the environment via flue gas stack while the solid material is directed to the bottom of the cyclone and transported to the adsorber. This vessel does not influence the solid or gas mass flow rates exiting the adsorber, and the cyclone battery is modelled separately for the purpose of cost estimation. The flow rate of solids exiting the cyclone is therefore assumed negligibly small for the purpose of the mass balance.

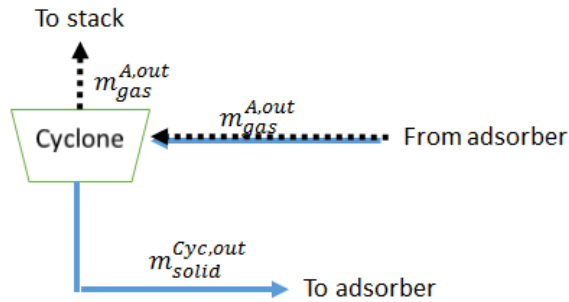


Figure 4.4: Mass flow diagram of the cyclone unit. Flue gas and entrained solids enter the cyclone where the solids are separated from the flue gas. The flue gas is sent to a stack for release to the environment while the solids are diverted back to the adsorber for reuse in the CO₂ capture process. Since there is no change in the composition or thermodynamic conditions of the gas, the nomenclature for the gas exiting the cyclone is the same as that upon exiting the adsorber. The mass flow rate of solids exiting the cyclone is assumed negligible.

4.2.5. Cold-side heat exchanger

In a temperature swing CO₂ capture process, the solids exiting the adsorber must be heated in order to release CO₂. The purpose of the cold- and hot-side heat exchangers (together referred to as the cross-flow heat exchanger) is to reduce the thermal load in the adsorber and regenerator by transferring heat between the cold and hot solids as they exit these respective processes.

The solid stream leaving the adsorber enters the cold-side of the heat exchanger where they are pre-heated by indirect (thermal) contact with steam in a shell-and-tube type vessel. The solids are then loaded on a conveyor and transported to the regenerator. This exit stream is denoted as, $m_{solid}^{R,in}$. Meanwhile, condensing steam passes through the heat exchange tubes and is cooled from 401 K (128°C) to 384 K (111°C) while decreasing in pressure from 150 kPa to 130 kPa. The condensed water exits the cold-side heat exchanger and enters a pump where it is recirculated to the hot-side heat exchanger described in Section 4.2.7. A mass flow diagram and heat transfer profile are shown in Figure 4.5.

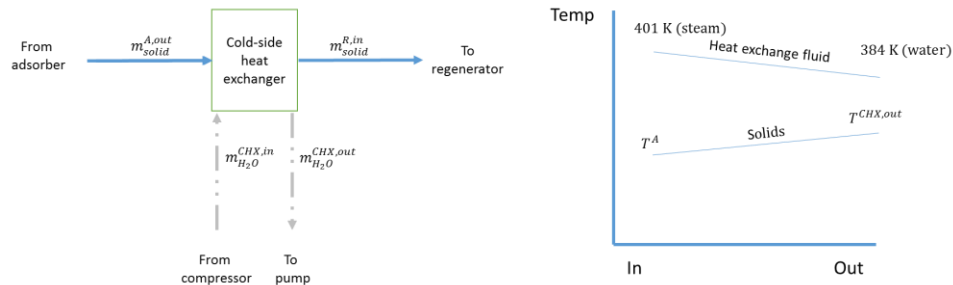


Figure 4.5: A mass flow diagram of the cold-side heat exchanger. Solids from the adsorber enter the heat exchanger and are heated by thermal contact with steam. The temperature diagram on the right shows the relative change in temperature (and phase) occurring in the heat exchanger. No temperatures are shown for the solids since both the inlet and outlet temperatures are variables within the model.

Both the hot- and cold-side solid-gas heat exchangers modelled in this work use the process design and heat exchange fluid properties assumptions published by NETL’s CCSI (Carbon Capture Simulation Initiative) project (DOE/NETL, 2011). As such, the heat exchangers are shell-and-tube type processes. In both processes, a phase change occurs in which the heat exchange fluid is boiled (in the hot-side) or condensed (in the cold-side). More information regarding the design may be found in Sections 4.4 for the energy balance and Appendix E for the original design assumptions from CCSI.

Saturated steam ($m_{H_2O}^{CHX,in}$) enters the heat exchanger through tubes and is cooled by thermal contact with the solids. The water condenses as it cools and is then pumped to the hot-side heat exchanger. The heating duty performed by the condensing steam is determined based on the enthalpy change of the steam and the mass flow rate of steam. The flow rate of steam is calculated using the rate of heat transfer in the hot-side heat exchanger.

4.2.6. Regenerator

The CO₂-rich solid sorbent from the cold-side heat exchanger enters the regenerator where it is heated indirectly with steam. CO₂ and other gases are released in the regenerator, forming a concentrated CO₂ stream. The solid and gas flow rates out of this reactor depend on the properties of the solid sorbent and the vessel’s operating conditions. Under some conditions, a purge gas (steam, in this model) is needed to adjust the CO₂ partial pressure and facilitate desorption of CO₂. The details of the

mass balance model relating to the regenerator are addressed in this section. A mass flow diagram of the regenerator vessel is shown in Figure 4.6.

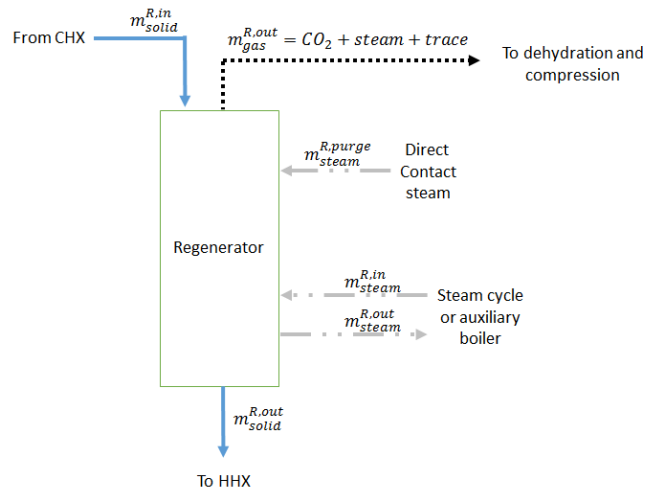


Figure 4.6: Mass flow diagram of the regenerator. Solid material enters the unit and is heated by thermal contact with steam from the steam cycle or auxiliary boiler. The elevated temperature drives off CO₂ and other gases with the assistance of direct contact steam. The released gases are collected and sent for dehydration and compression. Meanwhile, the solids exit the regenerator and are sent to the hot-side heat exchanger.

The mass flow rates shown in Figure 4.6 are defined as:

$$m_{solid}^{R,in} = \text{Mass of solid entering the regenerator (kg solids/hr)}$$

$$m_{solid}^{R,out} = \text{Mass of solid exiting the regenerator (kg solids/hr)}$$

$$m_{gas}^{R,out} = \text{Mass of gas exiting the regenerator (kg gas/hr)}$$

$$m_{steam}^{R,in} = \text{Mass of steam entering the regenerator from the heat source (kg steam/hr)}$$

$$m_{steam}^{R,out} = \text{Mass of steam exiting the regenerator to the heat source (kg steam/hr)}$$

$$m_{steam}^{R,purge} = \text{Mass of purge steam entering the regenerator (kg steam/hr)}$$

Inlet solids

The mass and composition of the solid stream does not change between the solids outlet in the adsorber and the solids inlet in the regenerator. This is shown in Equation 4.13.

Equation 4.13:

$$m_{solid}^{R,in} = m_{solid}^{A,out}$$

The mass of solid sorbent associated with each adsorbate species at the regenerator inlet, $\sum m_{solid-i}^{R,in}$, as well as adsorbed flue gas species exist at the adsorber inlet, $\sum m_{i(solid)}^{R,in}$, remains constant between the adsorber outlet and the regenerator inlet, as shown in Equations 4.14 and 4.15.

Equation 4.14:

$$\sum m_{solid-i}^{R,in} = \sum m_{solid-i}^{A,out}$$

where:

$i = \text{CO}_2, \text{SO}_2, \text{NO}_x, \text{N}_2, \text{O}_2$

and,

Equation 4.15:

$$\sum m_{i(solid)}^{R,in} = \sum m_{i(solid)}^{A,out}$$

where:

$i = \text{CO}_2, \text{H}_2\text{O}, \text{SO}_2, \text{NO}_x, \text{N}_2, \text{O}_2$

Outlet solids

Like the adsorber, the mass of solids at the regenerator outlet is expressed as the sum of the solid sorbent and adsorbed flue gas species as shown in Equation 4.16.

Equation 4.16:

$$m_{solid}^{R,out} = \sum m_{solid-i}^{R,out} + \sum m_{i(solid)}^{R,out}$$

where:

$m_{solid}^{R,out}$ = Total mass of solid at the regenerator outlet (kg/hr)

$m_{i(solid)}^{R,out}$ = Mass of adsorbed reactive flue gas species, i, at the regenerator outlet (kg/hr)

$m_{solid-i}^{R,out}$ = Mass of solid sorbent dedicated to the capture of adsorbate, i, at the regenerator outlet (kg solid sorbent/hr)

The mass flow rate of solid sorbent ($\sum m_{solid-i}^{R,out}$) remains constant between the regenerator and the adsorber. Equation 4.17 expresses this equality.

Equation 4.17:

$$m_{solid-i}^{R,out} = m_{solid-i}^{R,in}$$

where:

i = CO₂, SO₂, NO_x, O₂, N₂

The mass flow rate of the adsorbed species, however, changes as CO₂ and other reactive flue gas species disassociate from the solid sorbent and are collected as a gas exiting the regenerator. The

flow rate of each species that remains as a solid adsorbate at the regenerator outlet is determined individually based on the interaction between the solid sorbent and the reactive species under given the conditions of the regenerator. To begin, the flow rate of adsorbed CO₂ at the regenerator outlet is determined using the mass flow rate of solid sorbent, ($m_{solid(CO_2)}^{R,out}$), and the lean loading as shown in Equation 4.18.

Equation 4.18:

$$m_{CO_2(solid)}^{R,out} = M_{solid-CO_2}^{R,out} * q_{lean} * MW_{CO_2} * \frac{1}{1000}$$

where:

$m_{CO_2(solid)}^{R,out}$ = Mass of adsorbed CO₂ at the regenerator outlet (kg CO₂/hr)

$m_{solid-CO_2}^{R,out}$ = Mass of solid sorbent dedicated to the capture of CO₂ existing at the regenerator outlet (kg/hr)

q_{lean} = Loading of CO₂ on the solid sorbent at the regenerator outlet (moles CO₂/kg solid sorbent)

1000 = Conversion factor from kilograms to grams

The value of q_{lean} is determined using the Langmuir method described in Section 4.3.

The amount of N₂ that remains adsorbed at the regenerator outlet is calculated relative to the lean loading of CO₂, using the selectivity factor, as shown in Equation 4.19.

Equation 4.19:

$$m_{N_2(solid)}^{R,out} = M_{CO_2(solid)}^{R,out} * \frac{1}{S} * MW_{N_2}$$

The mass flow rates of the remaining reactive flue gas species existing as a solid at the regenerator outlet can be quantified using the mass flow rate of solids dedicated to the capture of each species and the regeneration efficiency of each species as shown in Equation 4.20.

Equation 4.20:

$$m_{i(solid)}^{R,out} = M_{i(solid)}^{R,in} * (1 - \eta_{R,i}) * MW_i$$

where:

i = H₂O, SO₂, NO_x, O₂

$\eta_{R,i}$ = Regeneration efficiency of reactive species, i (fraction)

The regeneration efficiency of each reactive flue gas species is calculated in a similar to the adsorption efficiency using the inlet and outlet concentrations of the relevant species existing as a solid as shown in Equation 4.21.

Equation 4.21:

$$\eta_{R,i} = \frac{M_{i(solid)}^{R,in} - M_{i(solid)}^{R,out}}{M_{i(solid)}^{R,in}}$$

where:

i = H₂O, SO₂, NO_x, O₂

For most of the reactive flue gas species (SO₂, NO_x, O₂, and H₂O), the regeneration efficiency is a specified parameter of the model. The solid stream exiting the regenerator next flows to a hot-side heat exchanger.

Outlet product gas

The flue gas species that are disassociated from the solid sorbent in the regenerator are collected as a single gas stream, $m_{gas}^{R,out}$, defined as the sum of the mass flow rates of each species as shown in Equation 4.22.

Equation 4.22:

$$m_{gas}^{R,out} = \sum m_{i(gas)}^{R,out}$$

where:

$i = \text{CO}_2, \text{H}_2\text{O}, \text{SO}_2, \text{NO}_x, \text{O}_2, \text{N}_2$

$m_{i(gas)}^{R,out}$ = Mass flow rate of flue gas constituent, i (kg/hr)

The mass flow rate of CO_2 released in the regenerator can be calculated from the difference between the rich loading and the lean loading of the solid sorbent as shown in Equation 4.23. Further detail regarding the calculation of “rich loading” and “lean loading” as used in this work are discussed in Section 4.3.

Equation 4.23:

$$m_{\text{CO}_2(gas)}^{R,out} = m_{\text{solid-CO}_2}^{R,in} * (q_{rich} - q_{lean}) * \frac{1}{1000} * MW_{\text{CO}_2}$$

where:

q_{rich} = Loading of CO_2 on the solid sorbent at the adsorber outlet (mol CO_2 /kg solid)

q_{lean} = Loading of CO_2 on the solid sorbent at the regenerator outlet (mol CO_2 /kg solid)

The flow rate of nitrogen exiting the regenerator as a gas is calculated using the selectivity constant and the molar flow rate of CO₂ as shown in Equation 4.24.

Equation 4.24:

$$m_{N_2(gas)}^{R,out} = M_{CO_2(solid)}^{R,out} * \frac{1}{S} * MW_{N_2}$$

With the exception of water, the mass flow rates of the remaining reactive species (SO₂, NO_x, and O₂) desorbed from the solid in the regenerator are calculated using the inlet mass flow rate of each species combined with the regeneration efficiency as shown in Equation 4.25.

Equation 4.25:

$$m_{i(gas)}^{R,out} = m_{i(solid)}^{R,in} * \eta_{R,i}$$

where:

i = SO₂, NO_x, O₂

Water vapor exiting the regenerator consists of H₂O desorbed from the solid and the steam used to purge the desorbed gases, as shown in Equation 4.26.

Equation 4.26:

$$m_{H_2O(gas)}^{R,out} = m_{H_2O(solid)}^{R,in} * \eta_{R,H_2O} + m_{steam}^{R,purge}$$

Purge steam

The partial pressure of CO₂ in the regenerator is a parameter of the model used to determine the driving force of the CO₂ desorption reaction. The CO₂ pressure is maintained by adjusting the flow rate of a separate flow stream of water vapor, called “purge gas,” entering the regenerator. If a relatively low CO₂

partial pressure is desired (20-50 kPa), than a positive flow rate of steam purge is added to the regenerator in order to dilute the product CO₂. This is often desirable since a low CO₂ pressure will further drive the desorption reaction and thereby increase the working capacity of the solid sorbent.

Alternatively, a high CO₂ pressure (60-100 kPa) in the regenerator may be desirable in order to decrease the energy and cost requirements during the dehumidification and compression process that happens after regeneration of the solid sorbent. In this case, an initial dewatering process may be used in order to reduce the mass of water evolved from the solid sorbent. It should be noted that dewatering is still considered part of the regeneration process. In terms of the mass balance, the mass flow rate of water removed from the solid sorbent is still considered purge gas for the purposes of this model and assigned a negative flow rate value. The flow rate of purge gas is determined by the ambient pressure (assumed to be atmospheric), the partial pressure of CO₂, and the flow rates of desorbed flue gas species using Equation 4.27.

Equation 4.27:

$$m_{steam}^{R,purge} = \left(\frac{P^{R,out} * M_{CO_2(gas)}^{R,out}}{P_{CO_2}^{R,out}} - \sum M_{i(gas)}^{R,out} - M_{H_2O}^{R,in} * \eta_{CO_2}^R \right) * MW_{H_2O}$$

where:

i = CO₂, SO₂, NO_x, O₂, N₂

$P_{CO_2}^{R,out}$ = Partial pressure of CO₂ at the regenerator outlet (Pa)

$P^{R,out}$ = Total gas pressure at the regenerator outlet (Pa)

The pressure of the gas exiting the regenerator is determined by the ambient air pressure at the location of the process as shown in Equation 4.28.

Equation 4.28:

$$p^{R,out} = p^{ambient}$$

After exiting the regenerator, the gas stream containing CO₂, water vapor, and trace reactive species is sent to a separate processing area for dehumidification and compression. This process has been previously modelled in the IECM, and the performance and cost model described in this work uses the values from IECM in order to calculate the electrical requirements and cost for this equipment. The electrical requirement for the dehumidification and compression process is described in Section 4.4.4 while the costs are addresses in Chapter 6.

4.2.7. Hot-side heat exchanger

The solids exiting the regenerator are sent to the hot-side heat exchanger where they are cooled using an intermediate fluid (water and steam in this model) linking the hot- and cold-side heat exchangers. Heat is transferred from the hot solids to the water by thermal (indirect) contact, which is vaporized and circulated back through a compressor to the cold-side heat exchanger in order to heat the circulating solids. The mass of solids remains constant throughout the hot-side heat exchange process although the solid stream exits at an lower temperature and is designated with the new symbol, $m_{solid}^{(HXX,out)}$. A mass flow diagram and temperature profile of the hot-side heat exchanger is shown in Figure 4.7.

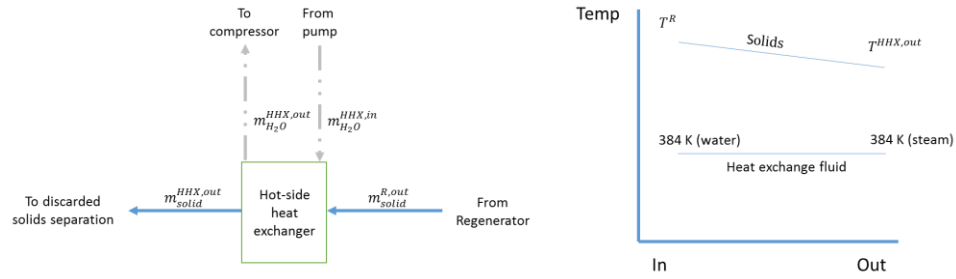


Figure 4.7: Mass flow diagram of the hot-side heat exchanger. Solids enter the hot-side heat exchanger from the regenerator and are cooled by indirect (thermal) contact with water circulating between the hot and cold sides of the heat exchanger. The water is boiled to become steam, which is then compressed and transferred to the cold-side heat exchanger. The temperature diagram on the right shows the relative change in temperature (and phase) occurring in the heat exchanger.

Water passes through the heat exchange tubes where it is boiled by thermal (indirect) contact with the solids. The saturated steam then exits the heat exchanger and into a compressor where it is compressed from 130 kPa to 150 kPa and given the symbol, $m_{H_2O}^{HHX,in}$. The difference in temperature between the steam exiting the hot-side and entering the cold-side heat exchanger occurs in the compressor circulating the fluid between these units. The compression of the gas increases the temperature from 384 K to 401 K in accordance with the CCSI design (DOE/NETL, 2012).

4.2.8. Discarded solids separation

The cooled solids exiting the cross-flow heat exchanger enter a separation step in which a portion of the solids are removed from the recirculating solids stream. The purpose of this step is to counteract losses to the CO₂ removal capacity of the solid flow stream by replacing a portion of the solids with fresh solid sorbent. A mass flow diagram of this process is displayed in Figure 4.8.

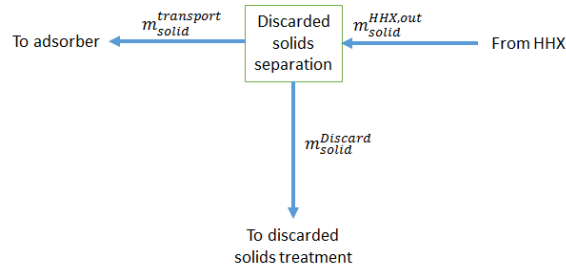


Figure 4.8: Discarded solid separation. Solids enter from the hot-side of the cross-flow heat exchanger. A portion of the solids are separated and diverted to a treatment area where the solids are either refurbished or disposed as needed. The remaining solids are transported to the adsorber.

The mass of solids in the discarded solids flow stream is calculated as a fraction of the incoming solid stream as shown in Equation 4.29.

Equation 4.29:

$$m_{solid}^{discarded} = m_{solid}^{HHX,out} * X_{solid\ purge}$$

where:

$m_{solid}^{discarded}$ = Mass flow rate of solids diverted for treatment of discarded solids (kg/hr)

$X_{solid\ purge}$ = Fraction of solids separated for treatment of degraded solids (fraction)

The solid purge fraction is a parameter of the model with a nominal range of 0.1-40 ppm. Alterations to the purge fraction would depend on economic considerations such as the cost of disposal, solid sorbent cost, and the reduction in solid flow volume resulting from using fresh solid sorbent as opposed to degraded solids.

The remaining solids stream is transported to the adsorber. The mass flow rate of this stream is calculated using Equation 4.30.

Equation 4.30:

$$m_{solid}^{transport} = m_{solid}^{R,out} * (1 - X_{solid\ purge})$$

where:

$m_{solid}^{transport}$ = Mass of solids transported to the adsorber (kg/hr)

4.2.9. Discarded solids treatment

Treatment of discarded (or “spent”) solid sorbent depends on the properties of the solid sorbent. This could entail, for example, a chemical treatment such as emersion in a caustic solution in order to remove acid gas products as is sometimes used for amine solvent reclamation (Versteeg, 2012). If no such treatment is available for the solid sorbent, then the solid stream is sent for disposal. The treatment process is expressed as a flat cost per unit mass of solid as discussed in Chapter 6. A mass flow diagram of the solids treatment unit is shown in Figure 4.9.

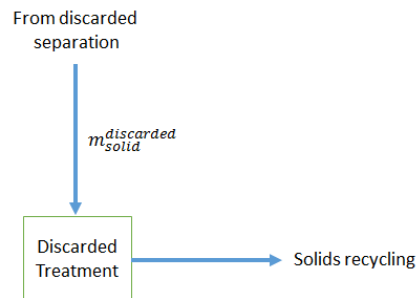


Figure 4.9: The solids diverted from the hot-side heat exchanger for treatment of degradation products is sent to a treatment area where they are processed in order to remove degradation products or sent for disposal or recycling.

4.2.10. Solid sorbent storage and handling area

The solid sorbent storage unit is used as a staging area for solids returning to the adsorber in order to provide operational flexibility for the CO₂ capture system. The unit’s functionality is comparable to

a coal staging area for a pulverized coal boiler unit in addition to serving as a mixing unit for combining fresh and recirculating solids. Fresh solid sorbent is required in order to maintain the adsorption capacity of the solid stream upon entering the adsorber. The mass flow rate of fresh solids is a function of the solid purge fraction and the mass of solid sorbent circulating through the system prior to removal of the discarded solids as shown in Equation 4.31.

Equation 4.31:

$$m_{solid}^{fresh} = \sum (m_{solid-i}^{R,out}) * X_{solid\ purge}$$

where:

$i = \text{CO}_2, \text{SO}_2, \text{NO}_x, \text{O}_2, \text{N}_2$

m_{solid}^{fresh} = Mass flow rate of new solid sorbent introduced to the adsorber (kg/hr)

The mass flow rate of fresh solid sorbent may also be expressed in terms of the flow rate of discarded solid sorbent as shown in Equation 4.32. Note that the mass of discarded solid sorbent, $\sum m_{solid-i}^{discarded}$, is less than the mass of discarded solids defined in Equation 4.29.

Equation 4.32:

$$m_{solid}^{fresh} = \sum m_{solid-i}^{discarded}$$

where:

$i = \text{CO}_2, \text{SO}_2, \text{NO}_x, \text{O}_2, \text{N}_2$

$m_{solid-i}^{discarded}$ = Mass of solid sorbent degraded by reactive flue gas species, i (kg/hr)

Recall from Equation 4.8 that the mass of solids entering the adsorber may be quantified as the sum of the mass of solid sorbent at the adsorber inlet, $\sum m_{solid-i}^{A,in}$, and the mass of adsorbed flue gas species at the adsorber inlet ($\sum m_{i-solid}^{A,in}$). The terms used in Equation 4.8 may now be specified based on the flow rate of transported (i.e. recirculating) and fresh solids. Starting with the flow rate of solid sorbent, ($\sum m_{solid-i}^{A,in}$), the mass of solid sorbent dedicated to the removal of CO₂ is calculated using Equation 4.33.

Equation 4.33:

$$m_{solid-CO_2}^{A,in} = \frac{M_{CO_2(gas)}^{A,in} * 1000 * \eta_{C,CO_2}}{q_{rich} - q_{lean} * (1 - X_{solid\ purge}) + q_{rich} * X_{solid\ purge}}$$

where:

$m_{solid-CO_2}^{A,in}$ = Mass of solid sorbent at the adsorber inlet required to capture CO₂ (kg/hr)

$M_{CO_2(gas)}^{A,in}$ = Molar flow rate of CO₂ existing in the flue gas at the adsorber inlet (kmol/hr)

1000 = Conversion from kilomoles to moles.

Since there are no adsorbed flue gas species in the fresh solids flow stream, all of the adsorbate mass at the adsorber inlet originates from the recirculating solids as part of the “transport” stream. The mass of adsorbed CO₂ at the adsorber inlet is calculated in Equation 4.34 using the mass of solid sorbent dedicated to the capture of CO₂ contained in the transport stream (represented by the first two terms on the right side of Equation 4.34) combined with the lean loading.

Equation 4.34:

$$m_{CO_2(solid)}^{A,in} = m_{solid-CO_2}^{A,in} * (1 - X_{solid\ purge}) * \frac{1}{1000} * q_{lean} * MW_{CO_2}$$

where:

$m_{CO_2(solid)}^{A,in}$ = Mass flow rate of CO₂ existing as a solid at the adsorber inlet (kg/hr)

1000 = Conversion from kilomoles to moles

Recall from Section 2.2.1 that the selectivity factor is used as a means of characterizing the mass of adsorbed N₂ relative to the mass of adsorbed CO₂. Hence, the mass flow rate of solid sorbent at the adsorber inlet that is required for adsorbed N₂ is calculated based on the flow rate of solid sorbent required for CO₂ and the selectivity constant. This is shown in Equation 4.35.

Equation 4.35:

$$m_{Solid-N_2}^{A,in} = m_{Solid-CO_2}^{A,in} * \frac{1}{S}$$

where:

$m_{Solid-N_2}^{A,in}$ = Mass of solid sorbent required to capture N₂ at the adsorber inlet (kg/hr)

The mass of nitrogen existing as a solid at the adsorber inlet is also calculated using the selectivity constant combined with the mass flow rate of CO₂ existing as a solid at the adsorber inlet as shown in Equation 4.36.

Equation 4.36:

$$m_{N_2(solid)}^{A,in} = m_{CO_2(solid)}^{A,in} * \frac{1}{S}$$

where:

$m_{N_2(solid)}^{A,in}$ = Mass of nitrogen existing as a solid at the adsorber inlet (kg/hr)

Ideally, Equations 3.33 and 4.34 would be broadened to include all other reactive flue gas constituents. However, given the dearth of information relating to competitive uptake and release of the

other reactive flue gas species, this model relies on the capture and regeneration efficiencies ($\eta_{C,i}$ and $\eta_{R,i}$) defined as parameters of the model in order to calculate the mass of degraded solid sorbent and adsorbates at the adsorber inlet.

In an ideal scenario in which no solids are removed for the treatment of degradation products (e.g. $X_{solid\ purge} = 0$), the mass of solids required to capture the remaining reactive flue gas species is calculated using in Equation 4.37.

Equation 4.37:

$$m_{i(solid)}^{A,in*} = \frac{\eta_{C,i} - \eta_{C,i} * \eta_{R,i}}{\eta_{R,i}} * M_{i(gas)}^{A,in} * MW_i$$

where:

$i = H_2O, SO_2, NO_x, O_2$

$m_{i(solid)}^{A,in*}$ = Mass flow rate of reactive flue gas species, i , existing as a solid at the adsorber inlet absent a solid purge fraction (kg/hr).

However, Equation 4.37 breaks down mathematically when the regeneration efficiency for any flue gas constituent is zero ($\eta_{R,i} = 0$) since this term is the sole constituent in the denominator. This situation may occur, for example, if an amine based solid sorbent is degraded through a practically irreversible adsorption reaction with SO_2 ($\eta_{R,SO_2} = 0$).

For the non-ideal case, Equation 4.37 may be expanded using the solid purge fraction to account for the removal of discarded solids as replaced by fresh solids. This is shown in Equation 4.38. Derivation of this equation and a more detailed explanation of its utility are available in Appendix F.

Equation 4.38:

$$m_{i(solid)}^{A,in} = \left(\frac{\eta_{C,i} - \eta_{C,i}\eta_{R,i} + \eta_{C,i}\eta_{R,i}X_{solid\ purge} - \eta_{C,i}X_{solid\ purge}}{\eta_{R,i} + X_{solid\ purge} - \eta_{R,i}X_{solid\ purge}} \right) * M_{i(gas)}^{A,in} * MW_i$$

where:

i = H₂O, SO₂, NO_x, O₂

$m_{i(solid)}^{A,in}$ = Mass flow rate of reactive flue gas species, i, existing as a solid at the adsorber inlet (kg/hr)

Equation 4.38 allows for two methods of removing reactive flue gas species products from the a steady-state system. First, the reactive species may be removed in the regenerator as gaseous products when the regeneration efficiency is greater than zero. Second, these species may be removed as part of the solid purge stream when the purge fraction is greater than zero.

The mass of solid sorbent required to capture the reactive flue gas species listed in Equation 4.38 is calculated assuming that the reactions are competitive with CO₂ on a 1:1 molar basis with the solid sorbent and that the solid sorbent's maximum capacity for these species is the same as for CO₂. Using these assumptions, Equation 4.39 is used to quantify the mass of solid sorbent dedicated to the capture of the remaining flue gas constituents.

Equation 4.39:

$$m_{solid-i}^{A,in} = M_{i(solid)}^{A,out} * 1000 * \frac{1}{q_{maximum}}$$

where:

$m_{solid-i}^{A,in}$ = Mass of solid sorbent dedicated to the capture of reactive flue gas species, i, at the adsorber inlet (kg/hr)

$q_{maximum}$ = Maximum CO₂ capacity of the solid sorbent under standard conditions (moles CO₂/kg)

1000 = Conversion from kilomoles to moles

4.2.11. Closing the mass balance

The equations shown in Section 4.2 have outlined a method of quantifying the flow rate of solids, liquids, and gases in a solid sorbent-based CO₂ capture system. However, given the complexity of this method and the similarities among symbols in the provided nomenclature, the reader may find the following equations useful when attempting to reproduce the analysis from this model. These equations are not strictly necessary, but are a useful “debugging” tool for the purposes of model validation.

This model assumes that the CO₂ capture system operates at steady state. Hence, the flow rates of each reactive flue gas species into the adsorber must equal to the flow rate leaving the system as product gas in the regenerator plus the flow rate of discarded solid. This equality is verified using the expression shown in Equation 4.40.

Equation 4.40:

$$m_{i(gas)}^{A,in} = m_{i(solid)}^{discarded} + m_{i(gas)}^{R,out}$$

where:

i = CO₂, SO₂, NO_x, N₂, O₂

This expression is not valid for water given that steam purge steam may be added or removed in the regenerator as a means of meeting the CO₂ pressure requirements as discussed in Section 4.2.6.

Finally, the mass balance is closed by verifying that the total mass of material entering and exiting the adsorber and entering and exiting the regenerator vessels are equal. In the adsorber, this is expressed using Equation 4.41.

Equation 4.41:

$$m_{solid}^{A,in} + m_{gas}^{A,in} = m_{solid}^{A,out} + m_{liquid}^{A,out} + m_{gas}^{A,out}$$

In the regenerator, this equality is expressed using Equation 4.42.

Equation 4.42:

$$m_{solid}^{R,in} + m_{gas}^{R,in} = m_{solid}^{R,out} + m_{gas}^{R,out}$$

This section has outlined the method and equations used in this work in order to calculate the mass flow rates throughout the solid sorbent-based CO₂ capture system. The next section discusses the method used in order to calculate the lean and rich loading of CO₂ on the solid sorbent used throughout the mass balance.

4.3. Quantifying rich and lean CO₂ loading

One of the oldest and most widely practiced methods of characterizing the reaction between solids and gases is the single component Langmuir model. The Langmuir equation expresses the quantity of gas adsorbed on the solid (i.e. loading) as a function of the gas constituent equilibrium partial pressure and temperature. This thesis uses the Langmuir method in order to calculate the lean and rich loading of CO₂ on the solid sorbent under equilibrium conditions and ignoring competitive uptake by other reactive flue gas species. The influence of water and reaction kinetics are added as adjustments to the calculated Langmuir loadings to produce the final lean and rich loading used in the performance model equations outlined in Section 4.2. The actual lean and rich loadings are then calculated by including the influence of other flue gas species.

4.3.1. The Langmuir equations for modelled solid sorbents

According to Langmuir adsorption theory, the loading of a single gas constituent (in this case, CO₂) on the solid sorbent can be expressed as a function of the properties of the solid and the partial pressure and temperature of the gas as shown in Equation 4.43.

Equation 4.43:

$$q_{equilibrium} = q_{maximum} * \frac{(b_{CO_2} * p_{CO_2})}{1 + b_{CO_2} * p_{CO_2}}$$

where:

$q_{equilibrium}$ = Equilibrium loading of CO₂ on the solid sorbent (moles CO₂/kg solid)

$q_{maximum}$ = Maximum loading of CO₂ under standard conditions (moles CO₂/kg solid)

b_{CO_2} = Langmuir loading parameter (1/Pa)

p_{CO_2} = partial pressure of CO₂ (Pa)

When Langmuir data regarding a specific solid sorbents is not available, the maximum capacity and Langmuir parameter may be estimated based on published isotherm and heat of reaction data. This is the method that was used in this work. The maximum solid sorbent loading may be inferred from the highest reported CO₂ capacity. The Microsoft Excel Goalseek function is then used to estimate the Langmuir parameter based on the reported working capacity and the given rich and lean loading conditions.

The maximum adsorption capacity, $q_{maximum}$, is a characteristic of the solid sorbent that describes the saturated CO₂ loading of the solid (see Table 2.1). For amine based solid sorbents, the typical value for the maximum capacity may range from 2-5 moles per kg of solid sorbent under standard temperature and pressure conditions (Choi, et al., 2009). The partial pressure of CO₂, p_{CO_2} , references the gas pressure at the location where the solids and gas reach equilibrium.

The partial pressure in the adsorber is highest at the gas inlet and lowest at the adsorber gas outlet. However, the specific value at which the solid and gas reach equilibrium depends on the reactor

design. The equilibrium pressure is therefore parameterized in this model in order to allow for greater modeling flexibility. The highest CO₂ loading is achieved when the partial pressure of CO₂ is at the highest value and some reactor designs, such as a fixed bed or cascading bed, are modeled in equilibrium at these conditions as shown in Table 4.2.

Table 4.2: Reactor bed designs commonly used for solid-gas reactors and the resulting equilibrium pressures. This work uses variations of a bubbling bed design adsorber and a moving bed regenerator.

Vessel type	Equilibrium pressure
Fluidized bed	Gas outlet
Bubbling- fluidized bed	Variable
Moving bed	Variable
Fixed bed	Gas inlet
Cascading bed	Gas inlet

The adsorber vessel modeled in this work is a bubbling bed. In a single bed design, the lower value for the partial pressure of CO₂ is used. However, there are additional design options which can be used that allow the adsorber design to approach equilibrium at higher CO₂ partial gas pressures. One such option is to use a multi-stage approach in which the solids are introduced to incrementally higher partial pressures of the gas adsorbate. In the final stage, the partial pressure of CO₂ is at or near its maximum value. This multi-stage design is also used by CCSI in their full-scale design model (DOE/NETL, 2012). Hence, the default partial pressure of CO₂ in the adsorber is calculated at the maximum (inlet) value as shown in Equation 4.44.

Equation 4.44:

$$p_{CO_2}^{A,in} = \frac{M_{CO_2(gas)}^{(A,in)}}{\sum M_{i(gas)}^{A,in}} * (P_{atm} + \Delta P^{Cyc} + \Delta P^A)$$

where:

$p_{CO_2}^{A,in}$ = Partial pressure of CO₂ at the adsorber inlet (Pa)

$M_{CO_2(gas)}^{A,in}$ = Molar flow rate of CO₂ at the adsorber inlet (kmol/hr)

$M_{i(gas)}^{A,in}$ = Mass flow rate of flue gas constituent, i, at the adsorber inlet (kmol/hr)

P_{atm} = Atmospheric pressure (Pa)

ΔP^{Cyc} = Pressure drop across the cyclone (Pa)

ΔP^A = Pressure drop across the adsorber (Pa)

The Langmuir loading parameter, b_{CO_2} , is a correction to the maximum loading based on the sorbent properties, temperature, and the heat of reaction. The Langmuir term is quantified using Equation 4.45.

Equation 4.45:

$$b_{CO_2} = b_0 * \exp\left(-\frac{\Delta h}{R * T}\right)$$

where:

b_0 = Langmuir constant (1/Pa)

Δh = Heat of reaction (kJ/kmol CO₂)

R = Universal gas constant (kJ/kmol-K)

T = Temperature (K)

The two equations shown above represent the first principles of the solid-gas interaction needed to calculate the equilibrium loading of CO₂ on a solid sorbent. For a given sorbent material, CO₂ loading in the adsorber and regenerator can be approximated by substituting the temperature and partial pressure of CO₂ into the above equations. This information is often conveyed graphically as a Langmuir isotherm,

and common practice is to present a series of isotherms expressed over discrete temperatures such as those shown in Figures 4.10 and 4.11. The vertical axis for an isotherm represents equilibrium loading and is often expressed in mass or molar units including grams of adsorbate per one hundred (100) grams of dry, fresh solid sorbent; or moles of adsorbate per kilogram of adsorbent. The horizontal axis is the partial pressure of the adsorbate.

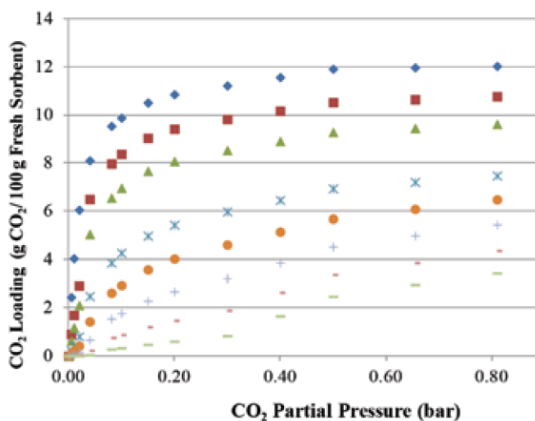


Figure 4.10: A Langmuir isotherm of an ion exchange resin with primary benzyl amine (DOE/NETL, 2013). The primary investigator for this project reports a rich loading of 2.4 moles CO_2/kg fresh solid sorbent and a lean loading of 0.8 moles CO_2/kg solid. To calculate the lean and rich loading, the adsorption conditions are assumed to be 313K (40°C) and $\text{PCO}_2 = 15,000$ Pa (0.15 bar), while the regeneration conditions are assumed to be 393K (120°C) and 81,000 Pa (0.81 bar).

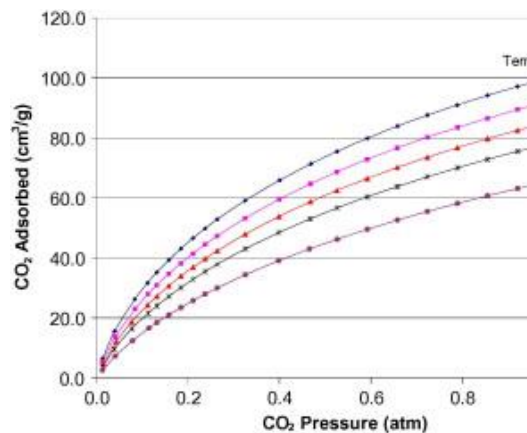


Figure 4.11: A Langmuir isotherm for BrightBlack™, a trademarked activated carbon solid sorbent (Hornbostel, et al., 2013). The reported rich loading of 4.4 moles/kg fresh solid sorbent and a lean loading of 0.01 moles/kg solid (Krishnan, 2013).

The amine-based resin shown in Figure 4.10 is an example of a chemical reaction-based sorbent (chemisorbent). The interaction of CO_2 with amines can be governed by several different mechanisms. Primary and secondary amines can react directly with CO_2 to produce carbamate through the formation of zwitterionic intermediates. The zwitterionic mechanism for the formation of carbamate from the reaction of CO_2 with a primary amine as reported by Caplow (Caplow, 1968) and later summarized, developed, and elaborated by others (Choi, et al., 2009). Tertiary amines react with CO_2 through a different mechanism.

Instead of reacting directly with CO₂, tertiary amines catalyze the formation of bicarbonate. The mechanism involving the base-catalyzed hydration of CO₂ for the reaction of CO₂ with tertiary amines was first reported by Donaldson (Donaldson & Nguyen, 1980) and later reviewed by Kenig (Choi, et al., 2009; Vaidya & Kenig, 2007).

This amine-based solid sorbent has a pronounced change in adsorption at lower pressures which levels off at higher pressures. This sharp change in adsorption occurs over the ranges of pressures appropriate for flue gas adsorption (0-20 kPa) and is an important characteristic for solid sorbents in the temperature swing system. Most chemical solid sorbents have a much lower pressure dependence at higher temperatures making them ideal for the thermal swing process.

In contrast, the carbon-based solid sorbent shown in Figure 4.11 is a physisorbent. Unlike chemisorbents, these materials generally display more gradual increase in loading as adsorbate pressures increase and are less responsive to changes in temperature at lower adsorbate pressures typical of flue gas conditions. The more pronounced influence of adsorbate pressure makes physical adsorbents suitable in situations when the adsorption process is occurring at higher pressures; thus making these types of materials more attractive to pressure-swing operations. The material properties for two solid sorbents considered in this work are shown again for easy reference in Table 4.3.

Table 4.3: Properties of the solid sorbents discussed in this work

Sorbent	Units	Amine Resin Value ¹	Carbon: Value ²	Supported amine ³	Tethered Amine Value ⁴
Heat of reaction	kJ/mol CO ₂	-60	-28	-67	-75
Langmuir constant ⁵	Pa ⁻¹	4.92*10 ⁻¹⁴	6.5*10 ⁻⁹	4.92*10 ⁻¹⁴	1.23*10 ⁻¹³
Manufacturing cost	\$/kg	2.27	2.27	2.27	Not reported
Maximum CO ₂ loading	mol CO ₂ /kg sorbent	2.9	4.5	3.5	15.1
Solid heat capacity ⁶	kJ/kg-K	1.05	1.0	1.0	Not reported

1Values for the amine resin sorbent are from (DOE/NETL, 2013) under project NT-0004343

2Values for the carbon-based sorbent are from (Krishnan, 2013) under project NT-0005578

3Estimated from published data (DOE/NETL, 2012)

4Values for the tethered amine sorbent are from (Qi, et al., 2014)

5Estimated from published data (DOE/NETL, 2013)

6Solid heat capacity measured at standard pressure and temperature (1 atm, 15°C)

Figure 4.12 shows the results of the Langmuir fitting procedure (using the Excel Goalseek function) and the data provided in the amine resin sources referenced in Table 4.3 for several temperatures in the adsorber (303K - 313K or 30°C - 40°C) and regenerator (373K - 393K or 100°C - 120°C). Note that the fitting matches well for the adsorbate pressures described in this work. For the adsorber, the CO₂ pressure ranges between 0 and 20 kPa appropriate for the flue gas inlet and outlet pressures. Regenerator pressures range from 20 to 100 kPa.

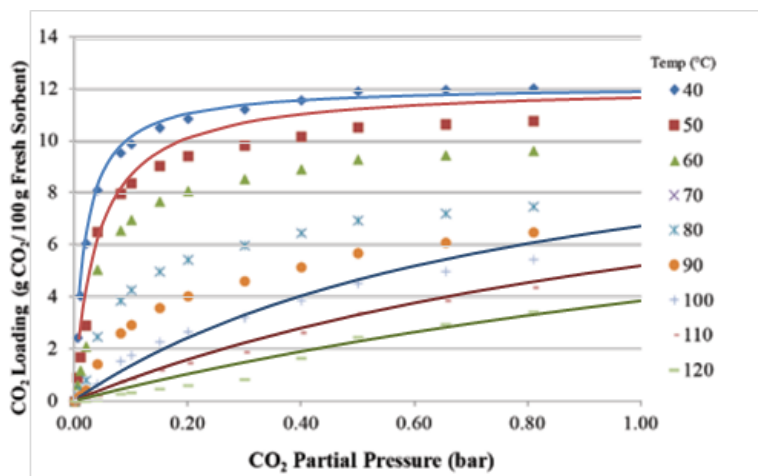


Figure 4.12: Results of the Goalseek data fitting exercise for the amine resin based solid sorbent. The data points represent published values from a publically available data source (DOE/NETL, 2013). The lines represent results of the Goalseek data fitting exercise for the corresponding temperature and pressure conditions.

Data for the physical adsorbent is not shown because the reported temperature ranges, 273K to 303K, are well below the temperature requirements for the process modelled in this work. Such temperatures operate beyond the scope of the equipment modelled in this work although modified processes are under investigation by DOE and others (DOE/NETL, 2013; Ritter, 2013). In general, physisorbents like BrightBlack™ have a much more linear loading response to changes in pressure (for pressures lower than atmospheric, or 101 kPa) and the difference in loading for changing temperatures is much less dramatic over higher temperatures compared to amine sorbents (see Figures 4.10 and 4.11). For this reason, physical adsorbents are generally not considered good candidate for temperature swing adsorption.

Although isotherms are a useful means of characterizing solid materials for flue gas separation, their application is limited in practice by the sterility of a laboratory setting. The loadings are obtained under ideal conditions in which confounding factors such competitive adsorption, attrition, and kinetics are removed for the sake of clarity regarding the solid's capacity to adsorb the constituent of interest. Section 4.2 described how competing flue gas constituents, such as SO₂ and N₂ may decrease the availability of

the solid for CO₂ capture. The next two sections address how the Langmuir method is supplemented in this model in order to account for the presence of water vapor in the flue gas and finite residence time.

4.3.2. Influence of water on solid sorbent capacity

Water is unique among the flue gas species in that its influence on CO₂ uptake is not necessarily negative. Section 2.2 introduced a parameter, $q_{\text{water loss}}$, to indicate the change (increase or decrease) in CO₂ capacity caused by the presence of water vapor in the flue gas stream. A new term, designated the adjusted maximum capacity ($q_{\text{adj.max.}}$) is used to denote the new CO₂ capacity of the solid as influenced by the presence of water vapor in flue gas. This term is calculated using Equation 4.46.

Equation 4.46:

$$q_{\text{adj.max.}} = q_{\text{maximum}} + q_{\text{water loss}}$$

where:

$q_{\text{adj.max.}}$ = Effective maximum CO₂ capacity of the solid including the influence of water (moles/kg)

$q_{\text{water loss}}$ = Change in solid sorbent's CO₂ capacity caused by water vapor (moles/kg)

The $q_{\text{water,loss}}$ term will be positive if the CO₂ adsorption capacity increases and negative if it decreases because of the presence of water vapor at concentrations found in the CO₂ capture process.

The adjusted maximum capacity quantified in Equation 4.46 is used to calculate a new equilibrium capacity, which accounts for the influence of water on CO₂ uptake. The calculation for the adjusted equilibrium capacity is given in Equation 4.47.

Equation 4.47:

$$q_{adj.eq.} = q_{adj.max.} * \frac{(b_{CO_2} * p_{CO_2})}{1 + b_{CO_2} * p_{CO_2}}$$

where:

$q_{adj.eq.}$ = Adjusted equilibrium loading of CO₂ on the solid sorbent (moles/kg)

4.3.3. Kinetics and carbon dioxide loading

Most reactions between CO₂ and the adsorbent require a long time in order to effectively reach equilibrium and reaction times are often measured in tens of seconds or minutes. This is particularly true for porous CO₂ capture materials since gas must diffuse through inter and intra-particle space in order to reach the entirety of possible reaction sites. Longer residence times and consequently larger reactor sizes are therefore required in order to achieve the highest and lowest loading.

The kinetics of sorbent reactions are difficult to model precisely using standard kinetic parameters for several reasons: First, the interactions between the sorbent and flue gas are complex and often poorly understood. These interactions include localized phenomena such as gas diffusion within the particle and those occurring at a larger-scale such as reactor mixing. Second, there is little data regarding the kinetic parameters for many of the more promising solid sorbents. For these reasons, a traditional approach using reaction rate constants for one or more reactions is ill-suited for this reduced-order approach. An alternative method used in this work is to adjust the equilibrium loading from Equations 4.46 and 4.47 based on a working knowledge of the adsorbent and the CO₂ capture system. Two parameters – κ_A and κ_B – for adsorber and regenerator, respectively, are introduced to indicate the extent to which the reaction reaches equilibrium. The value for these parameters, as introduced in Equations 4.48 and 4.49, will always be less than or equal to unity.

The equation for the rich loading is given using Equation 4.48. Note that now rich loading is always less than or equal to the equilibrium value.

Equation 4.48:

$$q_{rich} = q_{adj.eq.}^A * \kappa_A$$

where:

q_{rich} = Loading of CO₂ on the solid exiting the adsorber (moles * kg⁻¹)

$q_{adj.eq.}^A$ = Adjusted equilibrium CO₂ capacity of the solid sorbent in the adsorber (moles * kg⁻¹)

κ_A = kinetic parameter for the adsorber (fraction)

The value for the adsorption kinetic parameter should be expressed by filling in the blank in the phrase, “the rich loading will equal ‘X’% of the equilibrium rich loading.” An adsorption kinetic parameter that approaches unity indicates a higher rich loading that approaches the adjusted equilibrium in the adsorber.

Sensitivity data from a recent version of the CCSI adsorber model (current as of May, 2015) was used to develop a regression equation that calculates the adsorber kinetic parameter based on the inlet CO₂ pressure, inlet solid temperature, and outlet solid temperature. This equation is the default calculation for the adsorber kinetic parameter used in the IECM to denote non-equilibrium conditions. The regression equation is shown in Equation 4.49.

Equation 4.49

$$\kappa_A = \frac{-8.26 + 0.2547 * P_{CO_2}^{A,in} + 4.207 * \eta_{C,CO_2} + 0.2213 * T^A - 0.00906 * (P_{CO_2}^{A,in})^2 - 0.001319 * (T^A)^2 - 0.0653 * \eta_{C,CO_2} * T^A}{q_{adj.eq.}^A} * \frac{q_{maximim}}{3.5}$$

This equation calculates the adsorber kinetic parameter assuming the inlet CO₂ pressure is used to quantify the adjusted equilibrium loading. The data used to develop the regression equation is specific to the adsorber design and sorbent characteristics used in CCSI's model as of May, 2015 and provides a useful means of quantifying adsorption kinetics in the absence of more specific data. Further details regarding this vetting process and derivation of the regression model are available in Appendix G and Appendix H.

The value for the regenerator kinetic parameter should be expressed by filling in the blank in the phrase, "the actual loading will be 'X'% above the equilibrium lean loading." A regeneration kinetic parameter approaching zero signifies that the lean loading is near the adjusted equilibrium loading in the regenerator. The equation for the lean loading is given using equation 4.50. Note that the kinetic parameter for the regenerator appears in the denominator to indicate that a value less than equilibrium increases the concentration of CO₂ on the solid sorbent. Unlike the adsorber, no sensitivity data was available to develop a regression model for the regenerator.

Equation 4.50:

$$q_{lean} = q_{adj.eq.}^R * (1 + \kappa_R)$$

where:

q_{lean} = Actual loading of CO₂ on the solid exiting the regenerator (mol/kg)

$q_{adj.eq.}^R$ = Adjusted equilibrium CO₂ capacity of the solid sorbent in the regenerator (mol/kg)

κ_R = kinetic parameter for the regenerator (fraction)

4.3.4. Actual rich and lean loading

Now that the interactions between the solid sorbent and flue gas are well defined, it is possible to calculate the actual rich and lean loading of CO₂. Recall from Section 4.2 that the equations for calculating the mass of solid at the adsorber and regenerator outlets depend on q_{rich} and q_{lean} respectively in order to quantify the mass of adsorbed CO₂. With these terms now defined, it is possible to quantify the actual rich and lean loading of CO₂ on the solid including the influence of degradation as shown in Equations 4.50 and 4.51 respectively. These equations define CO₂ loading in terms of the molar loading of CO₂ per kilogram of solid sorbent.

Equation 4.51:

$$q_{actual\ rich} = \frac{M_{CO_2(solid)}^{A,out} * 1000}{\sum m_{solid-i}^{A,out}}$$

where:

$q_{actual\ rich}$ = Actual loading of CO₂ on the solid sorbent under rich conditions (mol CO₂/kg solid sorbent)

1000 = Conversion between moles and kilomoles

And,

Equation 4.52:

$$q_{actual\ lean} = \frac{M_{CO_2(solid)}^{R,out} * 1000}{\sum m_{solid-i}^{R,out}}$$

where:

$q_{actual\ lean}$ = Actual loading of CO₂ on the solid sorbent under regenerator conditions (moles CO₂/kg solid sorbent)

1000 = Conversion between moles and kilomoles

This section showed the method to quantify the actual rich and lean loadings of CO₂ on the solid sorbent as a function of the properties of the solid sorbent and operating conditions of the adsorber and regenerator vessels. Water is unique among flue gas constituents in that it does not necessarily compete with CO₂ for reactive sites. Hence, the influence of water must be characterized as having the unique ability to help or hinder the uptake of CO₂. The influence of kinetics is also addressed as a means of adjusting the uptake of CO₂. These kinetic parameters are used to adjust the actual loading of CO₂ on the solid with respect to the completeness of the adsorption and desorption reactions.

4.4. Energy balance

This section quantifies the total energy balance of the CO₂ capture system including the heating and cooling requirements as well as the electrical load of the system. The section begins by describing the heat exchange processes for the relevant units in the system starting with the pre-treatment vessel, followed by the cooling requirement, the heating requirement, and then the auxiliary electrical load. The end of this section summarizes the heat exchange requirements in terms of the total mass flow rate of heat exchange fluids, the steam requirement in the regenerator, and the energy penalty placed on the power plant resulting from the CO₂ capture system.

The overall energy balance may be summarized in terms of the operations requiring heating or cooling. Figure 4.13 shows the process steps falling into these two categories.

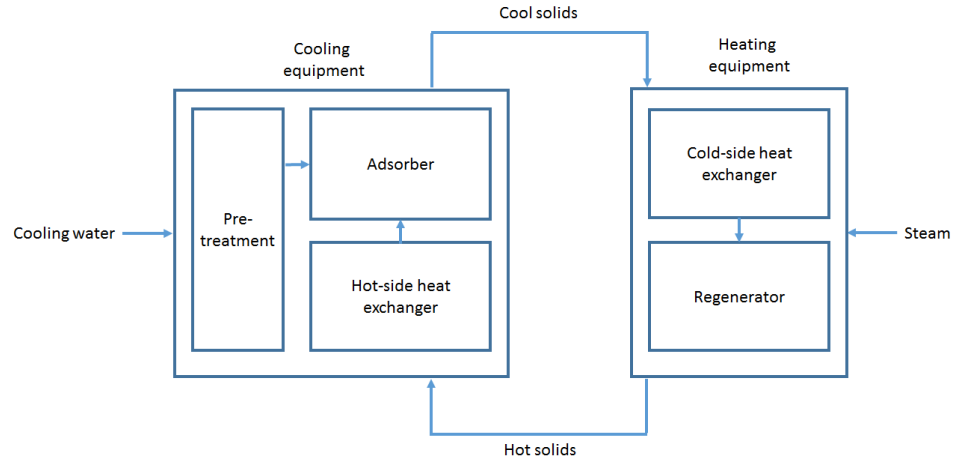


Figure 4.13: Summary of the energy balance for a solid-sorbent CO₂ capture system

In order to ensure the temperature of materials at the adsorber stays at or below the desired level, the solids must be cooled before and during the adsorption process. Two notable studies have incorporated internal or external cooling as part of the adsorber process. The first, published by CCSI, assumes that solids are cooled from 391 K (118°C) to 313 K (40°C) within the adsorber by indirect heat exchange with cooling water (DOE/NETL, 2012). The second study was designed by Stantec, Inc. and incorporated into a solid sorbent screening study conducted by ADA-Environmental Solutions. ADA's early design integrates a rotary contact cooler prior to adsorber entry which partially cools the solids to 331 K (58°C) (ADA-ES, 2011).

In this model, the cooling load is met using two methods: direct contact cooling of the flue gas in the pre-treatment vessel and indirect contact cooling of the solids in the hot-side heat exchanger and adsorber vessel. As discussed in Section 4.2.7, the hot-side heat exchanger serves the dual purpose of partially cooling the solids while simultaneously providing heat used to pre-heat the solids prior to regeneration. Further cooling occurs in the adsorber where the solids are cooled to a temperature specified as a parameter of the model.

Heating of the solids is also accomplished using indirect contact heat exchangers. First, the cold-side heat exchanger pre-heats the solids using low-grade steam recycled from the hot-side heat

exchanger as discussed in Section 4.2.5. The heating process is completed in the regenerator using thermal contact with steam diverted from the steam cycle. Indirect heating is essential for this process in order to avoid contact between water condensate and the solid sorbent, which is known to cause leaching for some supported amine-based sorbents (Hoffman, 2014).

4.4.1. Flue gas pre-treatment and blower

The flue gas pre-treatment process modelled in this work is derived from the latest publically available version of the IECM as of the time of this writing (version 8.0.2). The direct contact cooler and SO₂ polisher (DCCSP) allows IECM users to specify a value for either the outlet flue gas temperature or water vapor concentration, and calculates the quantity of cooling water and alternate variable using these specifications. Details regarding this model may be found in the published IECM literature and are included in Appendix C.

The temperature and pressure of the flue gas leaving the pre-treatment unit are required in order to calculate the cooling load in the adsorber and the compression duty of the flue gas blower. Like the IECM module, this work assumes that the flue gas enters the pre-treatment unit at atmospheric pressure and that the “clean” flue gas exits the cyclone units at atmospheric pressure. Hence, the increase in pressure across the flue gas blower is quantified as the sum of the pressure drop across the DCCSP, adsorber, and cyclone units as shown in Equation 4.53. The pressure drops used in Equation 4.53 are parameters of the model, although the pressure drop across the cyclones are assigned a relatively small value of 7 kPa (or 6 inches of water) to indicate a nominal change.

Equation 4.53:

$$\Delta P^{blower} = \Delta P^A + \Delta P^{Pre} + \Delta P^{Cyc}$$

where:

ΔP^{blower} = Pressure change induced by the flue gas blower (Pa)

ΔP^A = Pressure drop across the adsorber (Pa)

ΔP^{Pre} = Pressure drop across the pre-treatment unit (Pa)

ΔP^{Cyc} = Pressure drop across the cyclone (Pa)

Compression of the flue gas causes a change in flue gas temperature, which must be quantified in order to determine the cooling load in the adsorber. The change in the flue gas temperature across the flue gas blower is calculated as a function of the pressure change using Equation 4.54. The increase in temperature is assumed linear across the narrow range of pressures used in a post-combustion CO₂ capture setting. The linear correlation is based on data published by CCSI (DOE/NETL, 2012) and additional details regarding the CCSI data are provided in Appendix D.

Equation 4.54:

$$\Delta T^{blower} = \Delta P^{Blower} * 1.42 * 10^{-3}$$

where:

ΔT^{blower} = Temperature change caused by compression (K)

$1.42 * 10^{-3}$ = Change in temperature corresponding to a 1 Pascal increase in pressure (K/Pa)

Finally, the temperature of the flue gas entering the adsorber is calculated using Equation 4.55.

Equation 4.55:

$$T_{gas}^{A,in} = T_{gas}^{Pre,out} + \Delta T^{blower}$$

The state and composition of the flue gas are now fully defined at the adsorber inlet.

4.4.2. Cooling duty

Cooling of the solids is accomplished in two stages. First, hot solids enter the hot-side side heat exchanger where heat is transferred via thermal contact to the heat exchange fluid. The partially cooled solids are then transferred to the adsorber where they are further cooled before and/or during contact with flue gas. This energy balance equations for these two cooling mechanisms are described in this section.

Hot-side heat exchanger

The hot-side heat exchanger is used for the dual purpose of cooling the CO₂-lean solids and re-boiling the steam used in the cold-side heat exchanger. The quantity of heat released by the solids is a function of the difference between the inlet and outlet temperature of the solids and entrained water as shown in Equation 4.56.

Equation 4.56:

$$\Delta H^{HHX} = [m_{solid}^{R,out} * c_{p,solid} + m_{H_2O(solid)}^{R,out} * (c_{p,water} - c_{p,solid})] * (T^{R,out} - T_{solid}^{HHX,out})$$

where:

ΔH^{HHX} = Change in heat flow contained within the solid in the hot-side heat exchanger (kJ/hr)

$c_{p,solid}$ = Specific heat of the solid (kJ/kg)

$T_{solid}^{HHX,out}$ = Temperature of the solids at the hot-side heat exchanger outlet (K)

The mass flow rate of solids entering the hot-side heat exchanger is the same as the mass flow rate exiting the regenerator since no solids are diverted elsewhere between these two processes. The heat capacity of the solids, $c_{p,solid}$, is a parameter of the solid sorbent. This term does not include the

thermal mass flow rate of water entrained with the solids, which is calculated separately to reflect the difference in heat content between the solids and water.

Unlike other species, however, water is physically entrained with the solid as opposed to chemically bound to the sorbent. This entrained water is assumed to maintain its original heat capacity of 4.18 kilojoules per kilogram. Thus, the heat capacity of water is used in Equation 4.56 to account for the added heat duty resulting from the difference between the heat capacity of water and the solid.

The hot-side heat exchanger is modelled in this work as a shell and tube reactor in keeping with the design used by CCSI. The temperature and pressure conditions of the heat exchange fluid (water or steam) are needed in order to calculate the mass flow rate of heat exchange fluid and the electrical demands of the compressor and pump used in the cross-flow heat exchange process. These conditions are shown in Table 4.4.

Table 4.4: Thermodynamic properties of the heat exchanger fluid circulating through the cold-side heat exchangers. This information may be found in the Appendix of the NETL ARRA Milestone Report (DOE/NETL, 2012).

Mass flow nomenclature	Specific Enthalpy (kJ/kg)	Temperature (K)	Pressure (kPa)
$m_{water}^{HHX,in}$	467	384	150
$m_{steam}^{HHX,out}$	2,687	384	130

The mass flow rate of heat exchange fluid is calculated using the enthalpy conditions from the above table combined with the cooling load calculated in Equation 4.56. The mass flow rate of cooling water is calculated using the flow rate of exchanged heat (ΔH^{HHX}) and the enthalpy change of the fluid as shown in Equation 4.57.

Equation 4.57:

$$m_{fluid}^{HX} = \frac{\Delta H^{HHX}}{\Delta H_{fluid}}$$

where:

m_{fluid}^{HX} = Mass of heat exchange fluid moving through the hot-side heat exchange system (kg/hr)

ΔH_{fluid}^{HHX} = Change in specific enthalpy of the heat exchange fluid across the hot-side heat exchanger (2,244 kJ/kg)

Additional information regarding sizing of the heat exchanger is found in Chapter 6. The total heat transfer quantified in this section is used later to calculate the heat exchange area, which is the basis for the sizing calculation.

Adsorber

In the adsorber, cooling is required to maintain a constant temperature inside the vessel. Cooling water is used to meet the cooling load and the quantity of cooling load is calculated using Equation 4.58

Equation 4.58:

$$m_{cooling\ water}^A = \frac{H_{cooling}^A}{c_{p,water} * (T_{cooling}^{A,in} - T_{cooling}^{A,out})}$$

where:

$m_{cooling\ water}^A$ = Mass flow rate of cooling water required by the adsorber (kg/hr)

$H_{cooling}^A$ = Total cooling load in the adsorber (kJ/hr)

$T_{cooling}^{A,out}$ = Temperature of cooling water at the adsorber outlet (K)

$T_{cooling}^{A,in}$ = Temperature of cooling water at the adsorber inlet (K)

The cooling load is generated from three sources: reaction heat, sensible heat, and environmental losses. In this model, the adsorption process is assumed adiabatic and environmental losses are therefore zero. The total cooling load in the adsorber is expressed using Equation 4.59.

Equation 4.59:

$$H_{cooling}^A = H_{reaction}^A + H_{sensible}^A + H_{equipment}^A$$

where:

$H_{reaction}^A$ = Total heat of reaction in the adsorber (kJ/hr)

$H_{sensible}^A$ = Sensible heat load of flue gas (kJ/hr)

$H_{equipment}^A$ = Heat additions to the adsorber caused by non-ideal conditions (kJ/hr)

The reaction between CO₂ and the solid sorbent is the dominant source of reaction heat in the adsorber vessel due to the much larger rate of adsorption compared to other flue gas constituents. Rates of reaction between the sorbent and other constituents are at least an order of magnitude smaller. The heats of reaction between other gas constituents and the sorbent are therefore considered negligible in the adsorber energy balance. One possible exception to this order of magnitude assumption is the uptake of water. In this model, reactions between the solid sorbent and water are assumed to occur through physical uptake and the heat consumed by this interaction is equal to the latent heat of condensation. The total heat of reaction is therefore estimated based on the CO₂ adsorption reaction and heat of condensation as shown in Equation 4.60.

Equation 4.60:

$$H_{reaction}^A = h_{rxn} * M_{CO_2}^{A,in} * \eta_{c,CO_2} + (M_{water(gas)}^{A,out} - M_{water(gas)}^{A,in}) * -h_{vaporization}$$

where:

h_{rxn} = Specific heat of reaction between CO₂ and the solid sorbent (kJ/kmol CO₂)

$h_{vaporization}$ = Latent heat of vaporization of water (40,680 kJ/kmol water)

The sensible heat load in the adsorber results from differences in the temperature of the flue gas, transported solids, and fresh solids entering the adsorber compared the specified adsorber temperature. This is expressed using Equation 4.61.

Equation 4.61:

$$H_{sensible}^A = m_{gas}^{A,in} * c_{p,gas} * (T_{gas}^{A,in} - T^A) + [m_{solid}^{transport} * c_{p,solid} + m_{H_2O(solid)}^{A,in} * (c_{p,water} - c_{p,solid})] * (T_{solid}^{HHX,out} - T^A) + m_{solid}^{fresh} * c_{p,solid} * (T^{ambient} - T^A)$$

where:

T^A = Adsorber temperature (K)

$T^{ambient}$ = Ambient temperature (K)

$T_{gas}^{A,in}$ = Temperature of the gas at the adsorber inlet (K)

$c_{p,gas}$ = Heat capacity of the flue gas (kJ/kg)

$c_{p,solid}$ = Heat capacity of the solid sorbent (kJ/kg)

4.4.3. Heating duty

The solid temperature increase in the CO₂ capture process is accomplished in two stages. First, solids are pre-heated in the cold-side heat exchanger as steam condenses in the heat exchange tubes. The solids are then fully heated in the regenerator using high quality steam. The energy balance equations for these two heating mechanisms are described in this section.

Cold-side heat exchanger

The cold-side heat exchanger uses low quality steam to heat the solids between the adsorber and regenerator, thereby reducing the quantity of high quality steam required to heat the solids. The solids enter the cold-side heat exchanger at the same temperature at which they exited the adsorber and are heated by thermal contact with condensing steam. The heat exchangers are modelled after the system developed by CCSI and the conditions of the heat exchange fluid (steam/water) are the same as their model. Table 4.5 shows the conditions of the heat exchange fluid as specified by CCSI's process design report (DOE/NETL, 2012).

Table 4.5: Thermodynamic properties of the heat exchanger fluid circulating through the cold-side heat exchangers. This information may be found in the Appendix of the NETL ARRA Milestone Report (DOE/NETL, 2012).

Mass flow nomenclature	Specific heat (kJ/kg)	Temperature (K)	Pressure (kPa)
$m_{steam}^{CHX,in}$	2693	401	150
$m_{water}^{CHX,out}$	449	384	130

The heat flow rate transferred to the solids and entrained water is calculated using the change in thermal mass of the heat exchange fluid. The enthalpy change of the condensing steam is equal to the heat recovered in the hot-side heat exchanger and a small (>10 kJ/kg) additional enthalpy gain caused by a 20 kPa pressure increase in the compressor. Using these conditions, the temperature of the solids and entrained water exiting the cold-side heat exchanger may be calculated using Equation 4.62.

Equation 4.62:

$$T_{solid}^{CHX,out} = T^A + \frac{m_{fluid}^{HX} * \Delta h_{steam}^{CHX}}{m_{solid}^{A,out} * c_{p,solid} + m_{H_2O(solid)}^{A,out} * (c_{p,water} - c_{p,solid})}$$

where:

$T_{solid}^{CHX,out}$ = Temperature of the solids and entrained water exiting the cold-side heat exchanger (K)

Δh_{steam}^{CHX} = Change in specific heat of the steam/water across the cold-side heat exchanger
(kJ/*kg)

$c_{p,solid}$ = Heat capacity of the solid sorbent (kJ/kg)

$c_{p,water}$ = Heat capacity of water (kJ/kg)

Since the heat exchanger is a closed system, the mass flow rate of heat exchange fluid (steam/water) flowing through the cold-side heat exchanger is the same as the mass flow rate through the hot-side heat exchanger as previously calculated in Section 4.4.2.

Regenerator

The total heat requirement in the regenerator is the sum of the sensible heat, reaction heat, and losses to the environment resulting from non-ideal conditions as shown in Equation 4.63. This last term is assumed to be zero for the purposes of this model. Note that the temperature of the solids at the regenerator outlet is a parameter of the model.

Equation 4.63:

$$H_{heating}^R = H_{sensible}^R + H_{reaction}^R + H_{vaporization}^R + H_{environment}^R$$

where:

$H_{heating}^R$ = Heating requirement in the regenerator (kJ/hr)

$H_{sensible}^R$ = Increase in sensible heat flow rate of the solids within the regenerator (kJ/hr)

$H_{reaction}^R$ = Heat of reaction in the regenerator (kJ/hr)

$H_{vaporization}^R$ = Latent heat of vaporization of water (kJ/hr)

$H_{environment}^R$ = Heat loss to the environment (kJ/hr)

The sensible heat load is generated by the heating of solids and entrained water is quantified using Equation 4.64.

Equation 4.64:

$$H_{sensible}^R = [m_{solid}^{A,out} * c_{p,solid} + m_{H_2O(solid)}^{A,out} * (c_{p,water} - c_{p,solid})] * (T_{solid}^{R,out} - T_{solid}^{CHX,out})$$

where:

$T_{solid}^{R,out}$ = Temperature of solids at the regenerator outlet (K)

As in the adsorber, the dominant heat of reaction is caused by the evolution of CO₂. Hence, the heat of reaction in the regenerator is equal in magnitude and opposite in direction as the heat of reaction in the adsorber. The heat of reaction in the regenerator is calculated using Equation 4.65.

Equation 4.65

$$H_{reaction}^R = M_{CO_2(gas)}^{R,out} * h_{rxn}$$

The latent heat of vaporization is calculated based on the mass of vaporized water entering the regenerator as shown in Equation 4.66. The heat of vaporization is assumed to be a constant of 40,680 kJ/kmol water which is the heat of vaporization at 373K (100°C).

Equation 4.656:

$$H_{vaporization}^R = M_{H_2O(solid)}^{A,out} * \eta_{R,H_2O} * h_{vaporization}$$

The steam flow rate required to heat the solids is a function of the heating requirement of the system and the steam enthalpy change from the regenerator to the outlet as shown in Equation 4.67.

Equation 4.67:

$$m_{steam}^R = \frac{H_{heating}^R}{h_{steam}^{R,in} - h_{steam}^{R,exit}}$$

where:

$H_{heating}^R$ = Total heating requirement in the regenerator (kJ)

$h_{steam}^{R,in}$ = Enthalpy of the steam at the regenerator inlet (kJ/kg)

$h_{steam}^{R,exit}$ = Enthalpy of the steam at the regenerator outlet (kJ/kg)

The steam is extracted from the IP/LP interchange in the steam cycle or an alternative source such as a dedicated steam generator. The default initial enthalpy of the steam represents a supercritical PC power and has a value of 3,249 kJ/kg of steam. This value is comparable to the system modeled in the 2010 NETL baseline report (DOE/NETL, 2010). This steam is then desuperheated to a temperature tolerable by the solid sorbent (nominally 408K or 135°C) and sent to the regenerator to heat the solid sorbent. The energy penalty caused by the diversion of steam from the power cycle to the regenerator is discussed in Section 4.5.2.

The enthalpy of the steam exiting the regenerator depends upon the state conditions of the steam. This model assumes that steam condensate exits the regenerator at a temperature that is 20 K above the initial temperature of the solids entering the regenerator. The exiting steam enthalpy is derived using a regression curve fit to a Mollier diagram for steam at atmospheric conditions. The resulting regression is used to calculate the enthalpy of the exiting steam within the temperature range expected (323K - 363K or 60°C - 90°C) shown in Equation 4.68. This value optimistically assumes that the latent heat of vaporization from the steam has been used to heat the solids.

Equation 4.668:

$$h_{steam}^{R,exit} = 4.17 * (T_{solid}^{CHX,out} + T_{steam}^{R,approach}) - 1137.7$$

where:

$T_{steam}^{R,approach}$ = Temperature approach of the heating steam to the solids at the regenerator inlet (K).

4.4.4. Auxiliary electrical load

The solid sorbent CO₂ capture system employs a combination of compressors, conveyors, and other secondary equipment in order to move materials throughout the system. The auxiliary equipment adding to the electrical demand of the CO₂ capture system includes:

- Induced draft flue gas blower
- Conveyor systems (4)
- Heat exchange fluid pump
- Heat exchange compressor
- Product gas dryer and compressor

Wherever possible, the equipment modeled in this work utilizes specifications for similar equipment from other technologies previously incorporated into the IECM (version 8.0.2) in order to maintain consistency with models of other IECM-based CO₂ capture models. Otherwise, the reference electrical demand for these units use values from various sources including NETL Baseline reports (DOE/NETL, August, 2007; DOE/NETL, 2010), published CCSI work on solid sorbent systems (DOE/NETL, 2012), and existing amine models (Carnegie Mellon University, 2014). Reference values for this equipment and associated source are shown in Table 4.6.

Table 4.6: Reference values and assumptions for the solid sorbent-based CO₂ capture system. These values are mostly taken from the code of the most recent IECM release.

Reference term	Value	Reference
Conveyor system		
$n_{conveyor}$	4	
$Conveyor\ MW_{e,ref}$	0.15 MW _e	(DOE/NETL, 2013)
$m_{solid,ref}$	2.268*10 ⁶ kg/hr	(DOE/NETL, 2010)
Heat exchanger fluid pump		
$n_{HXpumps}$	2	
$HX\ Pump\ MW_{e,ref}$	2.0 MW _e	(Carnegie Mellon University, 2014)
$M_{liquid,ref}^{HX}$	3.03*10 ⁶ kg/hr	(Carnegie Mellon University, 2014)
Product gas dryer and compressor		
$e_{compressor}$	118 kWh/tonne CO ₂	(Rao, 2003)

The electricity demand equations for this equipment are shown in the rest of this section.

Induced draft flue gas blower

The electrical load required by the induced draft blower depends on the molar flow rate and temperature of flue gas, the pressure increase across the blower, and the blower efficiency. The electrical load is calculated using Equation 4.69. This equation is the same as that used in previous IECM models relating to liquid amine-based capture (Rao, 2003).

Equation 4.679:

$$FG\ Blower\ MW_e = \frac{M_{gas}^{Pre,out} * R * T^{Pre,out} * \Delta P^{blower}}{\eta_{blower} * P^{Pre,out}} * 2.81 * 10^{-10}$$

where:

$FG\ Blower\ MW_e$ = Electrical demand of the flue gas blower (MW_e)

$M_{gas}^{Pre,out}$ = Molar flow rate of flue gas at the pre-treatment outlet (kmol/hr)

R = Universal gas constant (8,314 m³*Pa/kmol-K)

ΔP^{blower} = Calculated pressure increase across the flue gas blower (Pa)

$T^{Pre,out}$ = Temperature of the flue gas at the pre-treatment outlet (K)

η_{blower} = Flue gas blower efficiency (fraction)

$m_{gas,ref}^{blower}$ = Reference flue gas mass flow rate (kg/hr)

$p^{Pre,out}$ = Pressure of the flue gas at the pre-treatment outlet (Pa)

$2.81 * 10^{-10}$ = Empirical correlation factor

Conveyor systems

The electrical requirement of the conveyor systems is a function of the solids flow rate. Coal handling equipment is used as a proxy for the conveyor system electrical demand within the CO₂ capture process, and reference values are taken from Case 11, Acct. 1 (Supercritical PC plant without CCS) of the NETL 2010 Baseline report (DOE/NETL, 2010, p. 394). This system was chosen because it is similar in size and complexity to the flow rates of the CO₂ capture system, and four major conveyor systems are required in the solid sorbent process in order to transfer solids to each of the following units:

- Adsorber
- Cold-side heat exchanger
- Regenerator
- Hot-side heat exchanger

Solid flow rates for the four process areas are equal in magnitude when the fresh fraction is under ~10 percent. Since the nominal fresh fraction is well below this value (1 to 40 ppm), the flow rate of a

single stream ($m_{solid}^{transport}$) is used to represent all four streams in order to simplify the electrical usage calculation shown in Equation 4.70.

Equation 4.70:

$$Transport\ return\ conveyor\ MW_e = n_{conveyor} * Conveyor\ MW_{e,ref} * \frac{m_{solid}^{transport}}{m_{solid,ref}}$$

where:

Transport return conveyor MW_e = Total electrical demand of the conveyor systems (MW_e)

Conveyor Usage MW_{e,ref} = Reference conveyor power usage (MW_e)

n_{conveyor} = number of conveyor systems

m_{solid,ref} = Mass flow rate of solids in the reference system (kg/hr)

Heat exchange fluid circulation pump

The auxiliary electrical load required by the heat exchanger fluid pump is calculated using Equation 4.71. Heat exchange fluid pump equipment is required for water exiting the cold-side heat exchanger.

Equation 4.71:

$$HX\ Pump\ MW_e = HX\ Pump\ MW_{e,ref} * \frac{m_{fluid}^{HX}}{m_{liquid,ref}^{HX}} * \frac{1}{\eta_{HXpump}}$$

where:

HX Pump MW_e = Electrical load required by the heat exchanger fluid pump (MW_e)

$HX Pump MW_{e,ref}$ = Reference electrical requirement used to circulate solvent in the reference liquid amine system of the IECM (MW_e)

m_{fluid}^{HX} = Mass of cooling water circulating through the heat exchanger system (kg/hr)

$m_{liquid,ref}^{HX}$ = Reference mass flow rate of heat exchange fluid (kg/hr)

η_{HXpump} = Heat exchange fluid pump efficiency (%)

The reference system used in order to calculate the electrical load for the heat exchange circulation pumps system is derived from the adsorber circulation cooling water circulating rate in the reference amine system in the IECM (Carnegie Mellon University, 2014).

Cross-flow heat exchange fluid compressor

Like the induced draft blower, the electrical load required by the heat exchange fluid compressor depends on the molar flow rate and temperature of the flue gas, the pressure drop across the compressor, and the compressor efficiency. The electrical load is calculated using Equation 4.72. The values for the pressure drop and temperature change are referenced in Table 4.4.

Equation 4.682:

$$HX \text{ Compressor } MW_e = \frac{m^{HX \text{ fluid}} * R * T_{steam}^{HHX,out} * \Delta P^{HX \text{ Comp.}}}{MW_{H_2O} * \eta_{compressor} * P_{steam}^{HHX,out}} * 2.81 * 10^{-10}$$

where:

HX Compressor MW_e = Electrical load required by the heat exchange compressor (MW_e)

$T_{steam}^{HHX,out}$ = Temperature of the saturated steam exiting the hot-side cross-flow heat exchanger (K)

$\Delta P^{HX \text{ Comp}}$ = Change in pressure across the compressor (Pa)

$\eta_{compressor}$ = Efficiency of the compressor (%)

$P_{steam}^{HHX,out}$ = Pressure of the steam at the hot-side heat exchanger outlet

$2.81 * 10^{-10}$ = Empirical correlation factor

The electrical usage of the compressor system is relatively small compared to the usage by the induced draft blower because of the smaller flow rate and lower pressure change. The efficiency of the compressor is assumed to be equal to the flue gas blower because of the similar function of these systems.

Product gas dryer and compressor

The total compression work and associated electrical requirement is dependent upon the mass flow rate of CO₂ that goes to the compressor and the unit energy requirement for CO₂ compression. The auxiliary electrical load required by the CO₂ compressors is calculated using Equation 4.73.

Equation 4.73:

$$CO_2 \text{ compressor } MW_e = e_{compressor} * m_{CO_2(gas)}^{R,out} * 10^{-6}$$

where:

$CO_2 \text{ compressor } MW_e$ = Electrical demand of the product gas compressor (MW_e)

$e_{compressor}$ = Unit energy requirement for CO₂ compression (kWh/tonne CO₂)

$m_{CO_2(gas)}^{R,out}$ = mass flow rate of CO₂ in the product gas at the regenerator exit (kg/hr)

The unit energy requirement for CO₂ compression term is a user set parameter. The default value of 117.95 kWh/tonne CO₂ is determined by the compressor efficiency and final CO₂ pressure. Derivation of this term is explained in previous IECM modelling work (Rao, 2003, p. 43).

4.5. Performance estimators

There are several metrics used to evaluate the performance of the CCS systems described in this work, and the calculation procedure for these estimators is described in this section. Several of these metrics are used to evaluate the solid sorbent-based CO₂ capture system while others are required in to calculate the overall performance of the power plant. This section begins by describing the solid sorbent metrics that are important for estimating the thermal and mass flows of the CO₂ capture process. For the plant level data, this work relies on the IECM as a means of estimating plant performance outside the boundaries of the CO₂ capture system.

4.5.1. Total CCS electricity requirements

The total CCS electricity requirement is a parameter used to convey the loss to net electrical output of the power plant induced by the addition of a carbon capture and storage system. This term is relative to the size, efficiency, and base plant configuration and must therefore be viewed in the given context. The total CCS electricity requirement is calculated using Equation 4.74.

Equation 4.74:

$$\textit{Total electricity requirement} = \textit{EEL} + \sum \textit{Auxiliary electrical load}$$

where:

Total electricity requirement = Electrical demand attributed to the CCS system (MW)

EEL = Electrical equivalent loss (MW)

Auxiliary electrical load = Sum of the electrical load outlined in Section 4.4.4 (MW)

The carbon capture process employs steam in the regenerator to heat the solids and provide the conditions necessary to desorb CO₂. In most cases, this steam is provided by the power plant itself through an access port located at the last crossover between steam turbines. Absent a CCS system, the diverted steam would have instead produced additional electricity. The lost electricity output is quantified in terms of the electrical equivalent loss (EEL) and is calculated using Equation 4.75.

Equation 4.695:

$$EEL = (HEE) * m_{steam}^R * h_{steam}^{R,initial} * (2.78 * 10^{-7})$$

where:

EEL = Equivalent Electricity Loss (MW)

HEE = Heat to electricity conversion efficiency (dimensionless)

m_{steam}^R = Mass of steam required by the regenerator (kg/hr)

$h_{steam}^{R,initial}$ = Energy content of the steam at the regenerator inlet (kJ/kg)

$2.78 * 10^{-7}$ = Conversion for Btu to MW_e [MW/(kJ/hr)]

The heat to electricity conversion efficiency is a factor which has been calculated previously to determine the efficiency by which a coal fired power plant can convert steam to electricity in turbine system that has an added steam extractor used for the purpose of supplying steam to a CCS system. The Integrated Environmental Control Model (IECM) uses a value of 22% as the steam-to-electricity conversion efficiency after CO₂ capture has been added based on data obtained from the NETL 2007 baseline report (DOE/NETL, August, 2007). The calculation of the conversion efficiency is found in the 2009 IECM update report (Berkenpas, et al., 2009).

4.5.2. Energy penalty

The energy penalty of the system is a useful metric for evaluating the performance of the carbon capture system because it takes into account the reduction in net generation capacity caused by diverting steam from the power block and the electrical demand of the CCS equipment. The energy penalty associated with a CCS system may be calculated using Equation 4.76.

Equation 4.70:

$$\text{Energy Penalty (\%)} = \frac{\text{Equivalent Electricity Loss}}{\text{Net Generation Capacity without CCS}} * 100$$

4.5.3. Specific solid requirement

The specific solid requirement is a useful means of evaluating the performance of the solid sorbent. This metric looks at the ratio between the mass of solids entering the adsorber normalized by the quantity of captured CO₂. The specific solid requirement is calculated using Equation 4.77.

Equation 4.77:

$$R = \frac{m_{solid}^{A,in}}{M_{CO_2(gas)}^{R,out}}$$

where:

R = Ratio of the solids mass flow rate at the adsorber inlet to the molar flow rate of captured CO₂
(kg solid/kmol CO₂)

4.5.4. Net plant efficiency

The final performance metric used throughout this work is the net plant efficiency. This value reports the net power output of the plant compared to the initial heat content of the fuel as delivered to the plant and is measured at a percentage of the higher heating value (%HHV) as shown in Equation 4.78.

Equation 4.78:

$$\text{Plant efficiency (\%HHV)} = \frac{\text{Net electrical output}}{\text{fuel flow rate} * \text{fuel heating value as received}} * 3.6 * 10^5$$

Both the net and gross electrical output of the power plant without CCS are determined using the latest public model of the IECM (v8.0.2) as of August, 2015. These outputs coincide with a specific power plant configuration, fuel type, and other plant-specific conditions. In most of the scenarios shown in this work, the net electrical output is maintained at a constant 550 MW_{net} and the size of the base plant is modified in order to meet this constraint. The fuel flow rate and higher heating value are determined using the IECM (v8.0.2). Finally, a unit conversion term is required in order to reach equivalent units.

4.6. Performance calculation procedure

Several of the equations in the performance model are dependent upon one another, and so they are calculated in a particular order that generally follows the process flow of the system. For example, the mass of solid at the adsorber inlet depends on the rich and lean loading of the solid sorbent. The order of the overall calculation is outlined below.

1. Calculate pre-treatment stream conditions
 - a. Pre-treatment outlet composition
 - b. Pre-treatment outlet temperature and pressure
 - c. Pre-treatment cooling water requirement
 - d. Pre-treatment caustic requirement
2. Calculate flue gas blower stream conditions
 - a. Flue gas flow rate into adsorber

- b. Pressure change across flue gas blower
 - c. Change in temperature through flue gas blower
 - d. Temperature of flue gas at adsorber inlet
3. Calculate the rich loading
- a. CO₂ pressure at adsorber inlet
 - b. Adjusted maximum loading
 - c. Langmuir loading parameter for adsorber
 - d. Adjusted adsorber equilibrium loading
 - e. Rich loading
4. Calculate lean loading
- a. Langmuir loading parameter for regenerator
 - b. Adjusted regenerator equilibrium loading
 - c. Lean loading
5. Calculate adsorber flow rates
- a. Mass flow rate of gas at adsorber outlet
 - b. Mass flow rate of solids at adsorber inlet
 - c. Mass flow rate of solids at adsorber outlet
6. Calculate regenerator flow rates
- a. Mass flow rate of solids at regenerator inlet
 - b. Mass flow rate of purge gas
 - c. Mass flow rate of gas at regenerator outlet
 - d. Mass flow rate of solids at regenerator outlet
7. Calculate transport, discarded, and fresh solid flow rates
8. Calculate cooling requirement
- a. Hot-side heat exchanger cooling requirement
 - b. Heat exchange fluid flow rate
 - c. Adsorber cooling requirement

- d. Adsorber cooling water requirement
- 9. Calculate heating requirement
 - a. Temperature of solids at regenerator inlet
 - b. Heating requirement in the regenerator
 - c. Steam enthalpy at the regenerator outlet
 - d. Steam requirement in regenerator
- 10. Calculate performance metrics
 - a. Actual rich loading
 - b. Actual lean loading
 - c. Specific solid requirement
 - d. Auxiliary electrical load
 - e. Electrical equivalent loss
 - f. Total electrical loss
 - g. Plant efficiency

4.7. Chapter conclusion

This chapter outlined the performance model developed in order to estimate the mass and energy flow rates within the solid sorbent-based CO₂ capture system. The model is parameterized with respect to key input variables relating to the materials and operation of the system and demonstrates the reliance of this model on an external model, the IECM, in order to quantify the overall performance of a pulverized coal power plant equipped with solid sorbent-based CO₂ capture. The result is a generalized model capable of evaluating multiple sorbent types such as the amine-based solid sorbents identified in Chapter 2. The performance model from this chapter is used in subsequent chapters to evaluate the performance and cost of a full-scale solid sorbent system for CO₂ capture.

5. Performance model case studies for a full-scale system

This chapter presents a series of case studies detailing the CO₂ capture system performance model presented in Chapter 4 and integrating this system into a larger framework describing the overall performance of a coal-fired power plant. First, this chapter sets the context by defining the power plant at which the CO₂ capture system in this thesis is implemented. Next, case studies are presented in order to demonstrate the performance method outlined in chapter 4. These case studies are intended to function as a starting point for estimating the performance of solid sorbent-based CO₂ capture in a general process, and the technical details are used in later chapters to illustrate the differences in the system's performance and cost when assumptions about the sorbent and process are changed.

5.1. Baseline assumptions about the power plant

The baseline power plant configuration used throughout this work is based on a widely used set of plant characteristics specified by the U.S. Department of Energy (DOE/NETL, 2010). Additional plant characteristics such as the flue gas composition, incoming and outgoing cooling water temperature, and steam quality extracted from the steam cycle power block are simulated based on the latest version of the IECM code available at the time of this writing (Carnegie Mellon University, 2014). Table 5.1 lists the assumptions used in this chapter relating to the configuration and operating conditions of the baseline power plant.

Table 5.1: Configuration parameters for the baseline power plant used to evaluate the solid sorbent-based CO₂ capture system

Power plant parameters	Value
Ambient air pressure (kPa)	101
Ambient air temperature (K)	298
Cooling	Wet cooling tower
Environmental controls	SCR, fabric filter, wet FGD
Flue gas heat capacity constant (kJ/kmol)	0.036
Fuel type	Illinois No. 6
Fuel heating value as received (HHV, kJ/kg)	30,840
Fuel flow rate (tonnes/hr)	217
Nominal net power plant output (MWe)	550
Steam cycle	Supercritical

In Chapter 4, several assumptions were required regarding the operating conditions of the base plant and the capture system. These parameters are constant throughout the forthcoming case studies unless otherwise stated, and a summary of these assumed values is available in Table 5.2. The values are presented based on their order of appearance in the calculation procedure outlined in Section 4.6.

Table 5.2: Summary table of constant values relating to the performance model shown in Chapter 4.
 These values are constant throughout all of the case studies.

Parameter	Assumed Value	Units
Adsorber cooling water inlet temperature	283	K
Adsorber cooling water outlet temperature	308	K
CHX fluid pressure	150	kPa
CHX fluid temperature at inlet	401	K
CHX fluid temperature at outlet	384	K
Cyclone and stack pressure drop	1.5	kPa
Heat capacity of water	4.18	kJ/kg-K
HHX fluid temperature at inlet	384	K
HHX fluid temperature at outlet	401	K
HHX fluid pressure	130	kPa
Latent heat of water vaporization	2260	kJ/kg
Pre-treatment flue gas pressure at inlet	101	kPa
Pre-treatment flue gas temperature at inlet	327	K
Product CO ₂ gas pressure at compressor outlet	15.2	MPa
Regenerator pressure	101	kPa
Regenerator steam inlet temperature	408	K
Regenerator steam-solid temperature approach	20	K
Stack flue gas outlet	101	kPa
Steam extractor steam temperature	773	K
Steam extractor steam enthalpy	3,249	kJ/kg
$\Delta T/\Delta P$ caused by FG blower	$1.42 \cdot 10^{-3}$	K/Pa

5.2. Case Study #1: The “ideal sorbent” performance model

This first case study examines an “ideal” solid sorbent in which chemical degradation and physical attrition of the solid sorbent are non-existent and the adsorption reaction between CO₂ and the sorbent reaches equilibrium at the adsorber inlet. CO₂ concentration assumptions were chosen for this first case study to provide a “best achievable” benchmark for comparison with future iterations. Later case studies and sensitivity analyses will relax these assumptions to provide alternative variations of the material and process performance.

This first case is presented in a level of detail meant to clarify the performance model calculations and exercise the required order of calculation outlined in Section 4.6. To begin, the initial conditions of the flue gas at the entrance to the CO₂ capture process are defined. The molar flow rates, shown in Table 5.3, are from the latest publically available version of the IECM (Carnegie Mellon University, 2014) and are iteratively calculated such that the net electrical output of the plant (with CO₂ capture) is 550 MW.

Table 5.3: Flue gas conditions and molar composition upon entering the CO₂ capture system. The flue gas composition and maximum flow rates shown here represent Illinois No. 6 coal burned in a supercritical PC power plant (550 MW_{net}) and capable of meeting new source performance standards (Carnegie Mellon University, 2014).

Flue gas composition	Flow rate (kmol/hr)	% Mole
Nitrogen (N ₂)	76,000	67
Oxygen (O ₂)	4,700	4
Water Vapor (H ₂ O)	17,500	15
Carbon Dioxide (CO ₂)	13,400	12
Carbon Monoxide (CO)	<1	0
Hydrochloric Acid (HCl)	<1	0
Sulfur Dioxide (SO ₂)	27	0
Sulfuric Acid (equivalent SO ₃)	<1	0
Nitric Oxide (NO)	9	0
Nitrogen Dioxide (NO ₂)	<1	0
Ammonia (NH ₃)	<1	0
Argon (Ar)	910	1

Total	113,000	100
-------	---------	-----

The inlet flue gas flow rates will vary in other scenarios as changes are made to the performance parameters reflecting different assumptions about the materials and processes. These changes influence the electrical and steam demands of the CCS system, and the size of the base plant must vary in order to meet the design requirement of 550 MW of net electrical output.

Table 5.4 lists the parameter values used in the “ideal system” case study regarding the performance of the solid sorbent system. In this initial system, pre-treatment of the flue gas using a direct contact cooler or SO₂ polisher is not required and the flue gas is piped from the wet FGD unit to the flue gas blower. In addition, the adsorber pressure at which the solid sorbent and CO₂ reach equilibrium is equal to the adsorber inlet CO₂ pressure. This assumption is made in order to show the best achievable system since the rich loading is highest when achieving equilibrium with the inlet CO₂ pressure. The equilibrium CO₂ temperature and pressure in the regenerator are set to 81 kPa and 393 K (120°C) respectively in keeping with the lean loading conditions specified by ADA-ES for their work regarding the amine resin (DOE/NETL, 2013). Finally, degradation and attrition are assumed to be non-existent and so the quantity of fresh solids introduced to the system is effectively zero.

Table 5.4: Baseline configuration for the solid sorbent-based CO₂ capture system for Case Study #1.

Input variable	Value	Units
Configuration		
Adsorber CO ₂ removal efficiency	90	%
CO ₂ product compressor used?	Yes	
Solid sorbent material	Amine-based resin	
Flue gas pre-treatment		
Direct contact cooler used?	No	
Pressure drop across the pre-treat unit	0	Pa
SO ₂ polisher used?	No	
SO ₂ polisher outlet concentration	237	ppmv
Temperature exiting DCC	327	K
Water vapor mole fraction at adsorber inlet	0.155	
Sorbent properties		
Solid sorbent name	Primary amine resin	
Heat capacity	1	kJ/kg dry solid-K
Heat of reaction	-60	kJ/mol CO ₂
Langmuir isotherm parameter (b ₀)	4.92*10 ⁻¹⁴	1/Pa
Maximum CO ₂ loading	2.9	moles CO ₂ /kg dry solid
CO₂ capture system		
<u>Adsorber</u>		
Adsorber operating temperature	313	K
Adsorber pressure drop	29	kPa
CO ₂ equilibrium pressure*	15.7	kPa
Effective adsorption kinetics (% equilib. capacity)	100	%
Overall heat transfer coefficient	300	W/m ² -K
<u>Regenerator</u>		
CO ₂ pressure in product gas stream	81	kPa
Effective desorption kinetics	0	%
Overall heat transfer coefficient	60	W/m ² -K
Regenerator operating temperature	393	K
Steam inlet temperature	408	K
Steam temperature approach	20	K
Cross-flow heat exchanger		
Overall heat transfer coefficient	60	W/m ² -K

Temperature of solids at hot-side HX outlet	353	K
		<u>Auxiliary</u>
Flue gas blower efficiency	75	%
System-wide constants and variables		
Ambient air pressure	101,325	Pa
Ambient air temperature	298	K
Coal heat value	30840	kJ/kg
Cooling water temp. in	283	K
Cooling water temp. out	308	K
Cost of caustic	507.5	\$/tonne
Cost of water	0.3033	\$/tonne
FG Heat capacity	0.036	kJ/kmol
FG pressure entering CCS system	101,325	Pa
FG temp. entering CCS system	326.5	°C
Latent heat of vaporization of water	2260	kJ/kg
Plant capacity factor	0.75	fraction
Steam temperature	773	K
Universal gas constant	8,314	m ³ -Pa/kmol-K
Water heat capacity	4.18	kJ/kg-K

* Calculated value equal to $P_{A,in} * M_{CO_2}^{A,in} / \sum M_i^{A,in}$ where i=all flue gas constituents at the adsorber inlet

5.2.1. Case Study #1 calculation

The following sections show the calculations required to derive the loadings and flow rates in the CO₂ capture system. The calculations shown below are in the same order as shown in Section 4.6 and use the parameter values listed in Tables 5.1-5.4.

Calculate pre-treatment flow rates

In this case, no pre-treatment unit is used and the flue gas enters the induced draft blower directly from the flue gas desulfurization unit. The mass flow rate of flue gas at the pre-treatment outlet is therefore identical to the inlet flow rate. Likewise, the temperature and pressure of the flue gas are

unchanged. In this case, the temperature of the flue gas is 327.5 K (54.5°C) and the pressure is 101.3 kPa (1 atm).

Calculate flue gas blower stream conditions

a. Flue gas flow rate into the adsorber

The flow rate of the flue gas does not change in the flue gas blower. Hence, the mass flow rate of flue gas at the adsorber inlet is 3,300,000 kg/hr.

b. Pressure change across the flue gas blower

A flue gas blower is used in order to overcome the pressure drop across the pre-treatment unit (when required), adsorber, and subsequent flue gas processing (i.e. the cyclones, ductwork, and stack). The pressure change in the flue gas blower is calculated using Equation 4.53.

$$\Delta P^{blower} = \Delta P^A + \Delta P^{Pre} + \Delta P^{Cyc}$$

The nominal pressure drop across the adsorber is 29 kPa in keeping with the pressure drop estimation for the adsorber process reported by CCSI (DOE/NETL, 2012). Since no flue gas pre-treatment is used in this case study, its pressure drop is zero. The pressure drop through the cyclone bank, duct work, and flue gas stack is 1.5 kPa (6 inches of water) based on a similar process model developed for a liquid amine system (Versteeg, 2012).

Dependent variable	Value	Independent variable	Unit	Calc.
ΔP^{blower}	30,500		Pa	=
	29,000	ΔP^A	Pa	+
	0	ΔP^{Pre}	Pa	+
	1,500	ΔP^{Cyc}	Pa	

c. Change in temperature through flue gas blower (K)

The temperature of the flue gas increases as the gas is slightly compressed in the flue gas blower. The temperature increase is based on the pressure change in the adsorber and a linear correlation over the narrow temperature and pressure ranges used for this application as discussed in Section 4.4.1. This temperature change of the flue gas across the flue gas blower is calculated using Equation 4.54.

$$\Delta T^{blower} = \Delta P^{Blower} * 1.42 * 10^{-3}$$

This calculation is shown below:

Dependent variable	Value	Independent variable	Unit	Calc.
ΔT^{blower}	43		K	=
	30,500	ΔP^{Blower}	Pa	*
	$1.42 * 10^{-3}$	Constant	K/Pa	

d. Temperature of flue gas at adsorber inlet (K)

Now that the temperature change is estimated across the flue gas blower, the temperature of the flue gas at the adsorber inlet can be calculated. The temperature of the flue gas at the adsorber inlet is calculated using Equation 4.55.

$$T_{gas}^{A,in} = T_{gas}^{Pre,out} + \Delta T^{blower}$$

This calculation is shown below.

Dependent variable	Value	Independent variable	Unit	Calc.
$T_{gas}^{A,in}$	370		K	=
	327	$T_{gas}^{Pre,out}$	K	+
	43	ΔT^{blower}	K	

For the initial flue gas temperature of 40°C (313 K) specified for the ideal loading scenario, the flue gas will require cooling when contacting the solids in the adsorber.

Calculate the rich loading

a. CO₂ pressure at adsorber inlet (Pa)

The equilibrium partial pressure of CO₂ is a calculated parameter of the model needed in order to determine the rich loading of the solid sorbent. For this case study in which equilibrium is achieved at the adsorber inlet pressure, the equilibrium CO₂ pressure is a function of the inlet gas pressure and the inlet concentration of CO₂. The equilibrium CO₂ pressure is then calculated using Equation 4.44.

$$p_{CO_2}^{A,in} = \frac{M_{CO_2(gas)}^{(A,in)}}{\sum M_{i(gas)}^{A,in}} * (P_{atm} + \Delta P^{Cyc} + \Delta P^A)$$

This calculation is shown below.

Dependent variable	Value	Independent variable	Unit	Calc.
$p_{CO_2}^{A,in}$	15,700		Pa	
	13,733	$M_{CO_2(gas)}^{(A,in)}$	kmol/hr	/
	115,000	$M_{gas}^{A,in}$	Kmol/hr	*
	132,000	$P_{atm} + \Delta P^{Cyc} + \Delta P^A$	Pa	

b. Adjusted maximum loading (moles CO₂/kg)

The adjusted maximum loading of the solid sorbent is used to describe the influence of water on the solid sorbent's capacity to adsorb CO₂ (see Section 4.3 for more details). The adjusted maximum loading is calculated using Equation 4.46. However, since this case study assumes that water exerts no positive or negative influence on the solid sorbent. The adjusted maximum capacity is therefore equal to the maximum CO₂ capacity.

Dependent variable	Value	Independent variable	Unit	Calc.
$q_{adj,max}$	2.9		moles CO ₂ /kg solid sorbent	=
	2.9	$q_{maximum}$	moles CO/kg solid sorbent	+

c. Langmuir loading parameter for adsorber

The Langmuir loading term is a calculated value required in order to determine the rich loading of CO₂ on the solid sorbent. This term is a function of characteristics of the solid sorbent and the equilibrium temperature in the adsorber. Its value is calculated using Equation 4.45.

$$b_{CO_2} = b_0 * \exp\left(-\frac{\Delta h}{R * T}\right)$$

This calculation is shown below.

Dependent variable	Value	Independent variable	Unit	Calc.
$b_{CO_2}^A$	$5.07 * 10^{-4}$		1/Pa	=
	$4.92 * 10^{-14}$	b_0		*
	$1.03 * 10^{10}$	$\exp\left(-\frac{\Delta h}{R * T}\right)$		

d. Adjusted adsorber equilibrium loading (moles CO₂/kg)

Recall that the adjusted maximum loading is used to describe how the presence of water influences the uptake of CO₂ in an operating CCS system. Water exerts no positive or negative influence on maximum loading in this initial case study and so the adjusted maximum CO₂ loading is the same as equal to the maximum value ($q_{maximum}$). This term and the calculated Langmuir loading term are needed in order to determine the equilibrium CO₂ loading in the adsorber (called the “adjusted equilibrium loading”) using the Langmuir equation (Equation 4.47).

$$q_{adj.eq.} = q_{adj.max.} * \frac{(b_{CO_2} * p_{CO_2})}{1 + b_{CO_2} * p_{CO_2}}$$

This calculation is shown below.

Dependent variable	Value	Independent variable	Unit	Calc.
$q_{adj.eq.}^A$	2.58		moles CO ₂ /kg solid sorbent	=
	2.9	$q_{adj.max.}$	moles CO ₂ /kg solid sorbent	*
	7.96	$(b_{CO_2}^A * p_{CO_2})$		/
	8.96	$(1 + b_{CO_2}^A * p_{CO_2})$		

Note that the equilibrium loading has dropped approximately 10% from the maximum value of 2.9 specified as a property of the solid material. This departure from the maximum loading is a function of the Langmuir parameter and heat of reaction properties of the solid sorbent as well as the pressure and temperature of the system.

e. Rich loading (moles CO₂/kg solid sorbent)

The next step required to calculate the rich loading is to incorporate the influence of kinetics into the equilibrium loading described in the previous calculation step. In this ideal case, the adsorption reaction is assumed to reach equilibrium ($\kappa_A=1$). The rich CO₂ loading calculated using Equation 4.48.

$$q_{rich} = q_{adj.eq.}^A * \kappa_A$$

This calculation is shown below.

Dependent variable	Value	Independent variable	Unit	Calc.
q_{rich}	2.58		moles CO ₂ /kg solid sorbent	=
	2.58	$q_{adj.eq.}^A$	moles CO ₂ /kg solid sorbent	*
	1	κ_A		

Note that no degradation terms have yet to appear in the calculation of the rich loading. The next case study, presented in Section 5.3, will use the term “actual rich loading” in an additional calculation step to describe how the uptake of SO₂, NO_x, and other flue gas constituents influence the actual composition of the solid sorbent. The actual rich loading is the concentration of CO₂ on the solid sorbent (measured in moles CO₂/kg solid) at the solid outlet of the adsorber.

Calculate lean loading

The calculation steps involved in determining the lean loading in the regenerator are very similar to the procedure required in order to calculate the rich loading in the adsorber. These steps are reviewed below.

a. Langmuir loading parameter for regenerator

The Langmuir loading parameter for the regenerator is calculated using Equation 4.45.

$$b_{CO_2}^R = b_0 * \exp\left(-\frac{\Delta h}{R * T}\right)$$

This equation combines the Langmuir parameter and heat of reaction (properties of the solid sorbent) with the regenerator conditions listed in Table 5.4.

Dependent variable	Value	Independent variable	Unit	Calc.
$b_{CO_2}^R$	$4.64 * 10^{-6}$		1/Pa	=
	$4.03 * 10^{-14}$	b_0	1/Pa	*
	$9.44 * 10^7$	$\exp\left(-\frac{\Delta h}{R * T}\right)$		

b. Adjusted regenerator equilibrium loading

The adjusted equilibrium loading in the regenerator is calculated using Equation 4.47.

$$q_{adj.eq.} = q_{adj.max.} * \frac{(b_{CO_2}^R * p_{CO_2})}{1 + b_{CO_2} * p_{CO_2}}$$

This calculation is shown below.

Dependent variable	Value	Independent variable	Unit	Calc.
$q_{adj.eq.}^R$	0.79		moles CO ₂ /kg solid sorbent	=
	2.9	$q_{adj.max.}$	moles CO ₂ /kg solid sorbent	*

$$\frac{0.38 (b_{CO_2}^R * p_{CO_2})}{1.38 (1 + b_{CO_2}^R * p_{CO_2})} /$$

c. Lean loading (moles CO₂/kg solid sorbent)

The lean loading is calculated using Equation 4.50.

$$q_{lean} = q_{adj.eq.}^R * (1 + \kappa_R)$$

As with the rich loading in the adsorber, the lean loading adjusts the equilibrium value based on the influence of kinetics. However, this initial case study assumes that the reaction achieves equilibrium ($\kappa_R=0$).

Dependent variable	Value	Independent variable	Unit	Calc.
q_{lean}	0.79		moles CO ₂ /kg solid sorbent	=
	0.79	$q_{adj.eq.}^R$	moles CO ₂ /kg solid sorbent	*
	1	$(1 + \kappa_R)$		

It is worth noting that degradation is not included in the lean loading calculation as of yet. Additional case studies require an additional calculation step will be needed in order to calculate the actual lean loading ($q_{actual\ lean}$) which describes the concentration of CO₂ (moles CO₂/kg) on the solid pellet at the regenerator solid outlet.

Calculate adsorber flow rates

This calculation step describes how the solid and gas flow rates are quantified.

a. Mass flow rate of gas at the adsorber outlet

The mass flow rate of flue gas at the adsorber outlet is quantified using equation 4.3.

$$m_{gas}^{A,out} = \sum (M_{i(gas)}^{A,out} * MW_i)$$

The total quantity of gas is calculated as the sum of the individual flue gas constituents exiting the adsorber. In this first case study, the mass flow rate of each flue gas constituent exiting the adsorber is the same as the inlet flow rate with the exception of CO₂. The mass flow rate of CO₂ is equal to the inlet CO₂ gas flow rate ($m_{CO_2(gas)}^{A,in}$) multiplied by the capture efficiency (90%).

Dependent variable	Value	Independent variable	Unit	Calc.
$m_{gas}^{A,out}$	2,700,000		kg/hr	=
	60,000	$m_{CO_2(gas)}^{A,out}$	kg/hr	+
	2,000	$m_{SO_2(gas)}^{A,out}$	kg/hr	+
	0	$m_{NO_x(gas)}^{A,out}$	kg/hr	+
	150,000	$m_{O_2(gas)}^{A,out}$	kg/hr	+
	2,140,000	$m_{N_2(gas)}^{A,out}$	kg/hr	+
	315,000	$m_{H_2O(gas)}^{A,out}$	kg/hr	+
	37,000	$m_{inert(gas)}^{A,out}$	kg/hr	

b. Mass flow rate of solids at the adsorber inlet

The mass flow rate of solids at the adsorber inlet is calculated using Equation 4.8.

$$m_{solid}^{A,in} = \sum m_{i(solid)}^{A,in} + \sum m_{solid-i}^{A,in}$$

The total mass of solids at the adsorber inlet is equal to the sum of the adsorbate and the adsorbent. Note that the flow rate of each adsorbate is calculated individually as is the flow rate of the associated adsorbent.

Dependent variable	Value	Independent variable	Unit	Calc.
$m_{solid}^{A,in}$	7,020,000		kg/hr	=
	240,000	$m_{CO_2(solid)}^{A,in}$	kg/hr	+
	0	$m_{SO_2(solid)}^{A,in}$	kg/hr	+
	0	$m_{H_2O(solid)}^{A,in}$	kg/hr	+
	6,790,000	$m_{solid-CO_2}^{A,in}$	kg/hr	+
	0	$m_{solid-SO_2}^{A,in}$	kg/hr	

c. Mass of solids at the adsorber outlet

The mass of solids at the adsorber outlet is calculated using Equation 4.9.

$$m_{solid}^{A,out} = \sum m_{solid-i}^{A,out} + \sum m_{i(solid)}^{A,out}$$

In this initial case study in which CO₂ is the only gas constituent reacting with the solid sorbent, only the mass of CO₂ adsorbate increases between the adsorber inlet and outlet. The mass of solid sorbent is constant. Note that the mass of adsorbed CO₂, 769,000 kg/hr, is the sum of the adsorbed CO₂ entering the adsorber (~240,000 kg/hr) plus the mass of CO₂ removed from the flue gas (~529,000 kg/hr).

Dependent variable	Value	Independent variable	Unit	Calc.
$m_{solid}^{A,out}$	7,560,000		kg/hr	=
	769,000	$m_{CO_2(solid)}^{A,out}$	kg/hr	+
	0	$m_{SO_2(solid)}^{A,out}$	kg/hr	+
	0	$m_{H_2O(solid)}^{A,out}$	kg/hr	+
	6,790,000	$m_{solid-CO_2}^{A,out}$	kg/hr	+
	0	$m_{solid-SO_2}^{A,out}$	kg/hr	

Calculate the regenerator mass flow rates

a. Mass flow rate of solids at the regenerator inlet

Solids exit the adsorber and pass through the cross-flow heat exchanger where they are heated to an intermediate temperature before entering the regenerator. The mass flow rate of the solids, however, does not change in this process. The solids therefore enter the regenerator with the same composition (including water content) as existed at the adsorber outlet.

b. Mass flow rate of purge steam

As the solids are heated in the regenerator by thermal contact with steam, CO₂ and possibly other adsorbates are released. The partial pressure of CO₂ in the regenerator is maintained at a pre-determined level by adjusting the flow rate of an additional process stream consisting of low quality steam. The quantity of steam entering the vessel is calculated using Equation 4.27.

$$m_{steam}^{R,purge} = \left(\frac{P^{R,out} * M_{CO_2(gas)}^{R,out}}{P_{CO_2}^{R,out}} - \sum M_{i(gas)}^{R,out} - M_{H_2O}^{R,in} * \eta_{CO_2}^R \right) * MW_{H_2O}$$

This calculation is shown below.

Dependent variable	Value	Independent variable	Unit	Calc.
$m_{steam}^{R,purge}$	54,000		kg H ₂ O/hr	=
	3,000	$\left(\frac{101 * 12,000}{81} \right) - 12,000 - 12,000 * 0$	kmol H ₂ O/hr	*
	18		g*mol ⁻¹	

Note that this process stream is assumed to have no heating effect on the solid stream. Instead, heating is only provided by indirect (thermal) contact with heating steam provided by the steam cycle or an external steam source.

c. Mass flow rates of gas at the regenerator outlet

The purge steam and the adsorbate gases released from the solid sorbent are collected in a single product stream at the regenerator outlet. The total mass flow rate of this gas stream is calculated as the sum of its individual components using Equation 4.22.

$$m_{gas}^{R,out} = \sum m_{i(gas)}^{R,out}$$

This calculation is shown below.

Dependent variable	Value	Independent variable	Unit	Calc.
$m_{gas}^{R,out}$	586,000		kg/hr	=
	532,000	$m_{CO_2(gas)}^{R,out}$	kg/hr	+
	0	$m_{SO_2(gas)}^{R,out}$	kg/hr	+
	54,000	$m_{H_2O(gas)}^{R,out}$	kg/hr	

Note that the flow rate of steam exiting the regenerator combines the flow rate of purge steam and any water vapor released from the solid sorbent. However, since no water is transferred to the regenerator from the adsorber in this first case study, the flow rate of steam exiting the regenerator is equal to the flow rate of purge steam.

d. Mass flow rate of solids at the regenerator outlet

The mass flow rate of solids at the regenerator outlet is calculated using Equation 4.16.

$$m_{solid}^{R,out} = \sum m_{solid-i}^{R,out} + \sum m_{i(solid)}^{R,out}$$

This calculation is shown below.

Dependent variable	Value	Independent variable	Unit	Calc.
$m_{solid}^{R,out}$	7,020,000		kg/hr	=
	237,000	$m_{CO_2(solid)}^{R,out}$	kg/hr	+
	0	$m_{SO_2(solid)}^{R,out}$	kg/hr	+
	0	$m_{H_2O(solid)}^{R,out}$	kg/hr	+
	6,790,000	$m_{solid-CO_2}^{R,out}$	kg/hr	+
	0	$m_{solid-SO_2}^{R,out}$	kg/hr	

This term is the sum of the mass flow rates of the adsorbent and adsorbate not released in the regenerator.

Calculate transport, discarded, and fresh solid flow rates

a. Discarded solids

The flow rate of discarded solids is calculated as a percentage of the solids exiting the regenerator. In this case study in which no degradation is occurring, the flow rate is zero.

b. Transport solids

The mass flow rate of solids transported back to the adsorber is calculated using Equation 4.30.

$$m_{solid}^{transport} = m_{solid}^{R,out} * (1 - X_{solid\ purge})$$

This calculation is shown below.

Dependent variable	Value	Independent variable	Unit	Calc.
$m_{solid}^{transport}$	7,020,000		kg/hr	=
	7,020,000	$m_{solid}^{R,out}$	kg/hr	*
	1.0	$(1 - X_{solid\ purge})$		

Because the solid purge fraction in this case is zero, the flow rate of solids transported back to the adsorber is nearly identical to the flow rate exiting the regenerator.

c. Fresh solids

The flow rate of fresh solid sorbent added to the transported stream at the adsorber inlet is calculated using Equation 4.31.

$$m_{solid}^{fresh} = \sum (m_{solid-i}^{R,out}) * X_{solid\ purge}$$

This calculation is shown below.

Dependent variable	Value	Independent variable	Unit	Calc.
m_{solid}^{fresh}	0		kg/hr	=
	6,790,000	$\sum m_{solid-i}^{R,out}$	kg/hr	*
	0	$X_{solid\ purge}$		

The fresh solid stream serves as “make-up” for the lost capacity exiting the system in the discarded solid stream. In this example, the fresh solid stream is zero. However, in other steady-state scenarios which consider degradation, the fresh solid stream is critical to prevent the build-up of degradation products in the system.

Calculate cooling requirements

a. Cooling requirement of the hot-side heat exchanger

The solids exiting the regenerator are transferred to the hot-side heat exchanger and are cooled by thermal contact with water (or steam when exiting the cold-side heat exchanger) circulating between the cross-flow heat exchangers. The heat transferred to the water is then used in the hot-side heat exchanger to pre-heat the solids. The heat transferred to the water in the cold-side heat exchanger is calculated using Equation 4.56.

$$\Delta H^{HHX} = [m_{solid}^{R,out} * c_{p,solid} + m_{H_2O(solid)}^{R,out} * (c_{p,water} - c_{p,solid})] * (T^{R,out} - T_{solid}^{HHX,out})$$

This calculation is shown below.

Dependent variable	Value	Independent variable	Unit	Calc.
ΔH^{HHX}	302,000,000		kJ/hr	=
	7,020,000	$(m_{solid}^{R,out})$	kg/hr	*
	1.00	$c_{p,solid}$	kJ/kg	+
	0	$m_{H_2O(solid)}^{R,out}$	kg/hr	*
	3.18	$(c_{p,liquid} - c_{p,solid})$	kJ/kg	*
	40	$(T^{R,out} - T_{solid}^{HHX,out})$	K	

b. Heat exchange fluid flow rate

The flow rate of fluid flowing through the hot- and cold-side heat exchange system is calculated using the rate of heat transfer (shown above) combined with the change in enthalpy (ΔH_{fluid}) of the heat exchange fluid. Equation 4.57 calculates the flow rate of the water or steam.

$$m_{fluid}^{HX} = \frac{\Delta H^{HHX}}{\Delta H_{fluid}}$$

This calculation is shown below.

Dependent variable	Value	Independent variable	Unit	Calc.
m_{fluid}^{HX}	136,000		kg/hr	=
	302,000,000	ΔH^{HHX}	Kg/hr	/
	2220	ΔH_{fluid}	kJ/kg	

The change in specific enthalpy of the steam/water used as the heat exchange fluid is the same value used by CCSI for their cross-flow heat exchange process (DOE/NETL, 2012). More details are available regarding the specific enthalpy assumptions used in this work by referring to Section 4.4.2.1.

c. Adsorber cooling requirement

After exiting the hot-side heat exchanger, the solids must still be cooled in the adsorber. Cooling is also required in order to overcome the exothermic reaction between the sorbent and CO₂. The remaining cooling requirement completed in the adsorber is calculated using Equation 4.59.

$$H_{cooling}^A = H_{reaction}^A + H_{sensible}^A + H_{equipment}^A$$

This calculation is shown below.

Dependent variable	Value	Independent variable	Unit	Calc.
$H_{cooling}^A$	1,010,000,000		kJ/hr	=
	726,000,000	$H_{reaction}^A$	kJ/hr	+
	281,000,000	$H_{sensible}^A$	kJ/hr	+
	0	$H_{equipment}^A$	kJ/hr	

The individual components of this equation are described in further detail in Section 4.4.2. Note that this particular formulation of the heating requirement includes a single term for the heat of reaction which includes both the heat generated by the exothermic CO₂ adsorption reaction and the heat of condensation which cools the solids as water condenses.

d. Calculate the adsorber cooling water requirement

The adsorber cooling requirement calculated above is used to determine the cooling water flow rate in the adsorber. The cooling water conditions are pre-defined values described in Table 5.2. The flow rate of cooling water in the adsorber is calculated using Equation 4.58.

$$m_{cooling\ water}^A = \frac{H_{cooling}^A}{c_{p,water} * (T_{cooling}^{A,in} - T_{cooling}^{A,out})}$$

This calculation is shown below. Note that the cooling water temperatures (283 K and 308 K) are listed in the system-wide constants and variables section of Table 5.4.

Dependent variable	Value	Independent variable	Unit	Calc.
$m_{cooling\ water}^A$	9,640,000		kg/hr	=
	1,020,000,000	$H_{cooling}^A$	kJ/hr	/
	4.18	$c_{p,water}$	kJ/kg	/
	25	$T_{cooling\ water}^{A,in} - T_{cooling\ water}^{A,out}$	K	

Calculate heating requirement

- a. Temperature of the solids at the regenerator inlet

Heat is transferred to the solids in the cold-side heat exchanger prior to entering the regenerator as a means of reducing the steam requirement in the regenerator. This heat is supplied by indirect contact with condensing steam which captures heat from the hot solids exiting the regenerator. The quantity of heat available to pre-heat the solids is determined by the rate of heat transfer in the hot-side heat exchanger. Thus, the temperature of the solids at the regenerator inlet is dependent upon the specific enthalpy of the steam entering the cold-side heat exchanger as calculated in Equation 4.62.

$$T_{solid}^{CHX,out} = T^A + \frac{\Delta H^{HHX}}{m_{solid}^{A,out} * c_{p,solid} + m_{H_2O(solid)}^{A,out} * (c_{p,water} - c_{p,solid})}$$

This calculation is shown below.

Dependent variable	Value	Independent variable	Unit	Calc.
$T_{solid}^{CHX,out}$	353		K	=
	313	T^A	K	+
	40	$\frac{302,000,000}{7,560,000 * 1.0 + 0 * (4.18 - 1.0)}$	K	

- b. Heat requirement in the regenerator

After exiting the cold side of the cross-flow heat exchanger, the solids then enter the regenerator. The remaining heating requirement is calculated using Equation 4.63.

$$H_{heating}^R = H_{sensible}^R + H_{reaction}^R + H_{vaporization}^R + H_{environment}^R$$

This calculation is shown below. More details regarding the specific components of this equation may be found in Section 4.4.3.2.

Dependent variable	Value	Independent variable	Unit	Calc.
$H_{heating}^R$	1,030,000,000		kJ/hr	=
	302,000,000	$H_{sensible}^R$	kJ/hr	+
	726,000,000	$H_{reaction}^R$	kJ/hr	+
	0	$H_{vaporization}^R$	kJ/hr	+
	0	$H_{environment}^R$	kJ/hr	

c. Steam enthalpy at the regenerator outlet

Steam extracted from the power plant steam cycle (or an external source such as an auxiliary boiler) is used to heat the solids in the regenerator. The initial temperature of steam at the regenerator inlet is set so as not to cause thermal degradation of the solid sorbent. In this case, the temperature of the steam is set to 408 K (135°C). The final enthalpy of the steam upon exiting the regenerator is determined by the temperature of the incoming solids and the approach temperature. The enthalpy of steam at the regenerator outlet is calculated using Equation 4.68.

$$h_{steam}^{R,exit} = 4.17 * (T_{solid}^{CHX,out} + T_{steam}^{R,approach}) - 1137.7$$

This calculation is shown below.

Dependent variable	Value	Independent variable	Unit	Calc.
$h_{steam}^{R,out}$	418		kJ/kg	=
	418	$4.17 * (353 + 20) - 1137.7$	kJ/kg	

d. Steam requirement in the regenerator

Using the initial and final conditions of the heating steam used in the regenerator, the total steam requirement is calculated using Equation 4.67.

$$m_{steam}^R = \frac{H_{heating}^R}{h_{steam}^{R,in} - h_{steam}^{R,exit}}$$

This calculation is shown below.

Dependent variable	Value	Independent variable	Unit	Calc.
m_{steam}^R	363,000		kg/hr	=
	1,030,000,000	$H_{heating}^R$	kJ/hr	/
	2,831	3,249 – 418	kJ/kg	

Note that an assumption is made that heat loss occurring in the steam extractor as steam is desuperheated from the initial conditions to those at the inlet of the regenerator is included in the steam-to-electricity conversion factor. This factor is used to calculate the energy penalty caused by steam withdrawal from the turbine in order to conform with newer releases of the NETL Baseline studies regarding CCS applications to supercritical power plants. More discussion regarding the heat-to-electricity conversion factor can be found in Section 4.5.2 or the original IECM documentation (Berkenpas, et al., 2009).

Calculate performance metrics

There are several metrics used to measure the performance of the solid sorbent system. The actual rich loading, actual lean loading, and specific solid requirement refer to the uptake and working capacity of the solid for CO₂ and are shown first. The next three performance estimators measure the electrical requirements for CO₂ capture and include the auxiliary electrical load, equivalent electrical loss for thermal energy, and the total electrical loss. Finally, the net power plant efficiency and fuel usage are reported.

a. Actual rich loading

The actual rich loading is calculated using Equation 4.51.

$$q_{actual\ rich} = \frac{M_{CO_2(solid)}^{A,out} * 1000}{\sum m_{solid-i}^{A,out}}$$

This calculation is shown below.

Dependent variable	Value	Independent variable	Unit	Calc.
$q_{actual\ rich}$	2.58			=
	17,500	$M_{CO_2(solid)}^{A,out}$		*
	1000	Conversion	mol/kmol	/
	6,790,000	$\sum m_{solid-i}^{A,out}$	kg/hr	

This actual rich loading term differs from the rich loading previously calculated by including the flow rate of degraded solid sorbent. The influence of the solid sorbent characteristics and kinetics are also included since these characteristics influence the molar flow rate of adsorbed CO₂ at the adsorber outlet. In a real system, the actual rich loading is the loading that would be observed at the adsorber solid outlet.

b. Actual lean loading

This term represents the CO₂ loading at the regenerator solids outlet. The actual lean loading is calculated using Equation 4.52.

$$q_{actual\ lean} = \frac{M_{CO_2(solid)}^{R,out} * 1000}{\sum m_{solid-i}^{R,out}}$$

This equation is shown below.

Dependent variable	Value	Independent variable	Unit	Calc.
$q_{actual\ lean}$	0.79		mol/kg	=
	5,380	$M_{CO_2(solid)}^{R,out}$	mol/hr	*
	6,790,000	$\sum m_{solid-i}^{R,out}$	Kg/hr	/
	1000	Conversion	mol/kmol	

c. Specific solid requirement

The specific solid requirement is calculated using Equation 4.77. This term describes the mass flow rate of solids per mole of captured CO₂ as described in Section 4.5.3.

$$R = \frac{m_{solid}^{A,in}}{M_{CO_2(gas)}^{R,out}}$$

This equation is shown below.

Dependent variable	Value	Independent variable	Unit	Calc.
R	580		kg/kmol	=
	7,020,000	$m_{solid}^{A,in}$	kg/hr	/
	12,100	$M_{CO_2(gas)}^{R,out}$	kmol/hr	

d. Auxiliary electrical load

The auxiliary electrical load is calculated as the sum of the electrical requirements for the individual system components using Equation 4.74.

$$Total\ electriciy\ loss = EEL + \sum Auxiliary\ electrical\ load$$

This calculation is shown below.

Dependent variable	Value	Independent variable	Unit	Calc.
$\sum MW_e$	101		MW _e	=
	35	<i>FG Blower MW_e</i>	MW _e	+
	2	<i>Transport return conveyor MW_e</i>	MW _e	+
	0	<i>HX Pump MW_e</i>	MW _e	+
	1	HX Compressor	MW _e	+
	63	<i>CO₂ compressor MW_e</i>	MW _e	

The five components shown in this calculation are defined in Equations 4.67 through 4.71.

e. Electric equivalent loss

In addition to the electrical requirements incurred by the system components listed above, additional losses result from the reduction of steam available for electricity generation. The electric equivalent loss is calculated using Equation 4.75. More details regarding the electricity equivalent loss and its component can be found in Section 4.5.2.

$$EEL = (HEE) * m_{steam}^R * h_{steam}^{R,initial} * (2.78 * 10^{-7})$$

This calculation is shown below.

Dependent variable	Value	Independent variable	Unit	Calc.
<i>EEL</i>	73			=
	0.222	HHE		*
	363,000	m_{steam}^R	Kg/hr	*
	3,249	$h_{steam}^{R,initial}$	kJ/kg	*
	$2.78 * 10^{-7}$	Conversion	MW _e *hr/kJ	

f. Total electrical loss

The total electricity loss is calculated using Equation 4.74.

$$Total\ electricity\ loss = EEL + \sum Auxiliary\ electrical\ load$$

This calculation is shown below.

Dependent variable	Value	Independent variable	Unit	Calc.
<i>TEL</i>	174		MW _e	=
	73	EEL	MW _e	+
	101	Total auxiliary load	MW _e	

In this idealized case study, the auxiliary load is the larger component of the total electricity loss (TEL) accounting for about 60% of the electrical load while the electrical loss due to the regenerator steam requirement is 40% of the TEL. These terms are similar in magnitude indicating that neither the electrical nor steam requirement dominated the energy demand of the system.

g. Plant efficiency

The efficiency of the power plant is calculated using Equation 4.78.

$$Plant\ efficiency\ (\%HHV) = \frac{Net\ electrical\ output}{fuel\ flow\ rate * fuel\ heating\ value\ as\ received} * 3.6 * 10^5$$

This calculation is shown below.

Dependent variable	Value	Independent variable	Unit	Calc.
<i>Plant efficiency</i>	29.6		%HHV	=
	550	MW	MW _e	/
	217,000	Fuel flow rate	kg/hr	/
	30,840	Fuel HHV as received	kJ/kg	*
	3.6*10 ⁵	Conversion		

5.2.2. Case Study #1 discussion

The calculations shown in this section serve to clarify the model's framework and serve as an introduction to the methods used in this and later chapters to address more complex issues regarding degradation, kinetics, and vessel design. The "Ideal System" is a benchmark for the "best achievable" CO₂ capture system for this particular amine resin-based solid sorbent represented by favorable performance parameters given this solid sorbent and the current state of technology development. This system achieves a favorable "working capacity" of about 1.8 moles of CO₂ per kilogram of solid sorbent as a result of the equilibrium adsorber and regenerator vessel conditions and circulates approximately 580 kg of solids for every kmol of CO₂ captured at 90% CO₂ capture. The electrical equivalent loss from steam is 73 MW and the electrical usage by the CCS system is 101 MW for a total energy penalty of 174 MW. As a result of this high energy penalty, this power plant designed to produce 550 MW_{net} of power has a gross size of 724 MW with a net thermal efficiency of 30% compared to the no-CCS case of 39% at a gross size of 588 MW.

5.3. Performance model sensitivity studies

This section uses the performance model to examine the sensitivity of key performance metrics to changes in solid sorbent and process parameters. The results from this exercise reveal several important insights regarding the materials and process design utilized in the carbon capture system as discussed at the conclusion of this chapter.

First, to help identify the parameters that most affect the overall system performance, the process model parameters are subjected to a uniform $\pm 10\%$ change from the baseline value (unless bound to an upper or lower limit). A total of 50 parameters were investigated in this manner, including the reference plant values (Tables 5.1 and 5.2) and process-specific values (Table 5.4) used in the ideal sorbent analysis. In the performance model, the influence of these parameters is measured in terms of changes to the specific solid requirement and net plant efficiency, which represent the mass and energy flow rates required by the CO₂ capture system. Figure 5.1 shows the effect of the eight most important variables

identified in this exercise on the specific solid requirement in the solid sorbent system when all other input variables are at their nominal values.

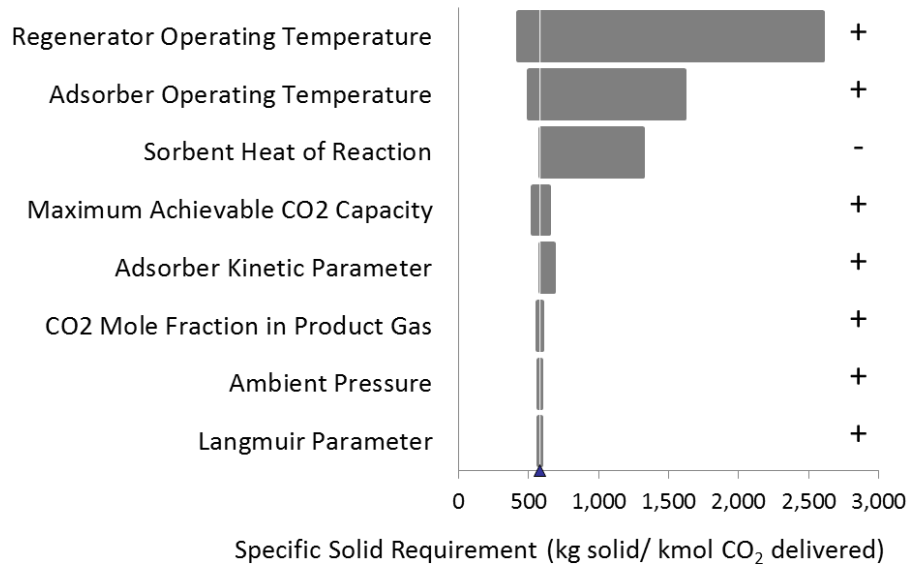


Figure 5.1: Tornado diagram showing the parameters demonstrating the largest influence on the specific solid requirement for the CCS system. The +/- signs represent whether an increase or decrease resulted in the higher specific solid requirement.

One of the most important insights from this figure is the skewness of the results towards a less efficient system with higher flow rates of solids per unit of CO₂ captured relative to the nominal finding of 580 kg of solid per kmol of captured CO₂. The regenerator and adsorber temperatures play an important role in determining the efficiency of the system. Nominally, these vessels operate at 393 K (120°C) and 313 K (40°C) respectively, but a 10% deviation in both cases causes a large increase in the mass flow rate of solids. These results also suggest that the solid sorbent characteristics and adsorber design are also important including the heat of reaction, maximum CO₂ capacity, and adsorption kinetics.

A similar exercise was applied to determine the effects of a uniform ±10% change in the parameter values on the plant efficiency. Recall that the efficiency of the reference plant without CO₂ capture was 39%. With the “ideal” solid sorbent CCS system installed on new PC plant, the system drops to a 29% plant efficiency. Figure 5.2 shows a tornado diagram of the plant efficiency and the key

parameters influencing the efficiency value. These results indicate that changes in the fuel heating value, the heat of reaction (between CO₂ and the solid sorbent), and the maximum temperatures of the solids in the hot side of the cross-flow heat exchanger dominate the plant efficiency calculation for equal changes in all variables. Significant changes are also driven by the CO₂ capture efficiency, adsorber operating temperature, and the compressor efficiency.

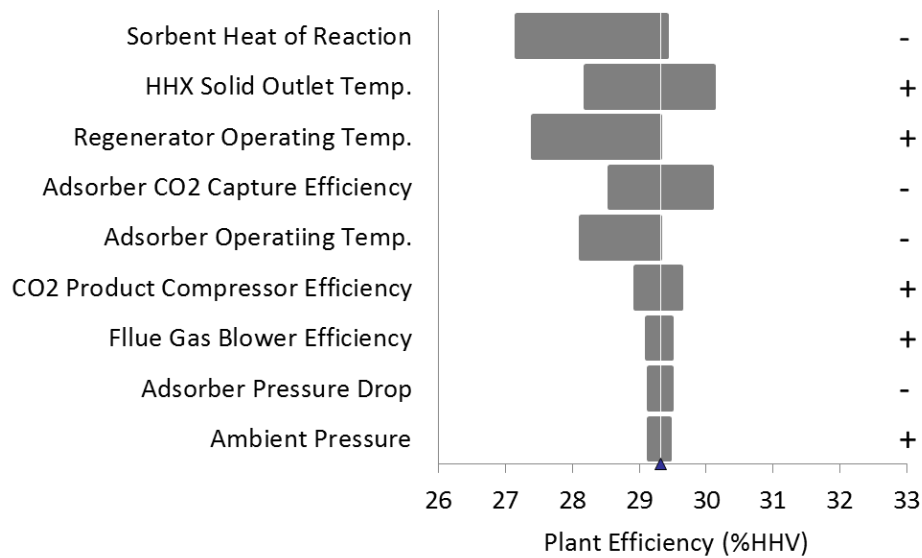


Figure 5.2: A tornado graph indicating the change in the plant efficiency for a +/-10% change in the input of ten important variables. The +/- signs indicate whether an increase or decrease resulted in the higher net plant efficiency.

These sensitivity analyses are useful because they reveal which parameters most affect key results. In practice, of course, some parameters are more uncertain or variable than others. The next section explores the impact of these variables over more complete ranges of potential values.

5.3.1. Solid sorbent variables

This section provides more detail regarding the solid sorbent properties and their influence on the flow rates and energy requirements of the system. Recall from Chapter 2 that five parameters were used in order to define the basic characteristics of the solid sorbent. These include the maximum loading, the Langmuir parameter, activation energy, heat capacity, and the material cost. The first four properties are

examined in this section in order to discover how these properties influence the overall performance of the system. The material cost is discussed in the next chapter relating to the capital and operating costs of CO₂ capture.

Maximum CO₂ loading

Figure 5.3 shows how the maximum CO₂ loading potential of the solid sorbent influences the rich and lean CO₂ loadings for the ideal sorbent case study. This diagram shows that the equilibrium rich and lean loadings are proportional to the maximum loading. However, the lean loading increases more slowly with maximum capacity resulting in a direct correlation between working capacity and maximum capacity. Note that other parameters are assumed to be constant.

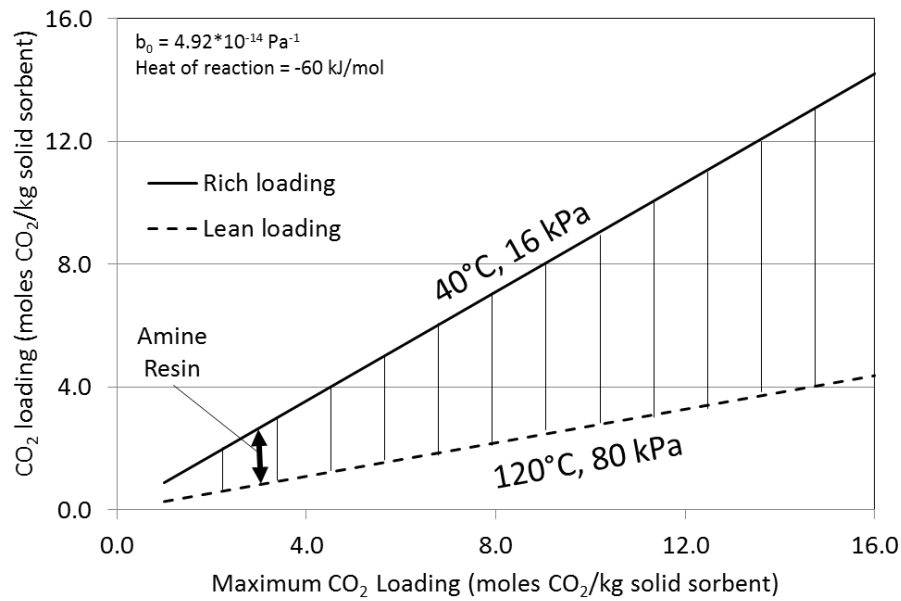


Figure 5.3: The solid sorbent loading for the amine resin solid sorbent increases as a function of the maximum CO₂ capacity. All other parameters are fixed at their nominal values. The nominal maximum capacity for the amine resin solid sorbent (2.9 moles CO₂/kg) and subsequent working capacity (1.8 moles CO₂) are shown. The highest recorded solid sorbent capacity is 16 moles/kg for an amine-based solid sorbent (Qi, et al., 2014).

The direct proportionality between the working and maximum capacities is significant because improvements to the working capacity result in an overall smaller CCS system and improves the efficiency of the power plant. These results suggest that one method of improving the performance of the solid sorbent system is to increase the maximum capacity of the solid sorbent. The extent to which the maximum capacity can be improved is a subject for material developers. The range of potential changes in maximum capacity were obtained through expert elicitation and are discussed in a later chapter addressing uncertainty (Chapter 7).

Sorbent Langmuir parameter

Recall from Section 4.3.1 that CO₂ solid sorbents exhibit their highest loading at low temperatures. The Langmuir parameter expresses the material's loading response to changes in adsorbate pressure (in this case, CO₂). Generally, a higher adsorbate pressure increases loading and the magnitude of this increase is determined by the Langmuir parameter. In a CO₂ capture system, a higher CO₂ pressure is desirable in the adsorber in order to increase rich loading. Conversely, a lower CO₂ pressure is favourable in the regenerator in order to reduce lean loading. In this manner, the Langmuir parameter helps determine the CO₂ working capacity (the difference between the rich and lean loading).

The CO₂ pressures characteristic of this process, however, are greater in the regenerator compared to the adsorber (20 to 80 kPa in the regenerator compared to 1-16 kPa in the adsorber). Consequently, a lower pressure response (*i.e.* smaller Langmuir parameter) would seem desirable for this application. A value that is too small, however, will cause the loading under both rich and lean conditions to drop to zero. The optimal sorbent, therefore, is one with a Langmuir parameter that will maximize the difference between the rich and lean loadings thereby improving the working capacity of the solid sorbent.

Figure 5.4 shows how the Langmuir parameter influences the equilibrium CO₂ loading at the nominal adsorber and regenerator conditions for the ideal sorbent case study. For the conditions shown, A Langmuir value of 10⁻¹² to 10⁻¹⁴ Pa⁻¹ is optimal. This is close to the calculated values of 4.92*10⁻¹⁴ and 1.23*10⁻¹³ Pa⁻¹ for the amine resin and tethered amine solid sorbents, respectively. For contrast, consider the activated carbon discussed in Chapter 2. This material exerts a much stronger response to differences in pressure at a value of 6.5*10⁻⁹ Pa⁻¹. At this pressure sensitivity, the difference in loading at rich and lean conditions is equal to or less than zero, which renders this particular solid sorbent useless given the process design and operating conditions.

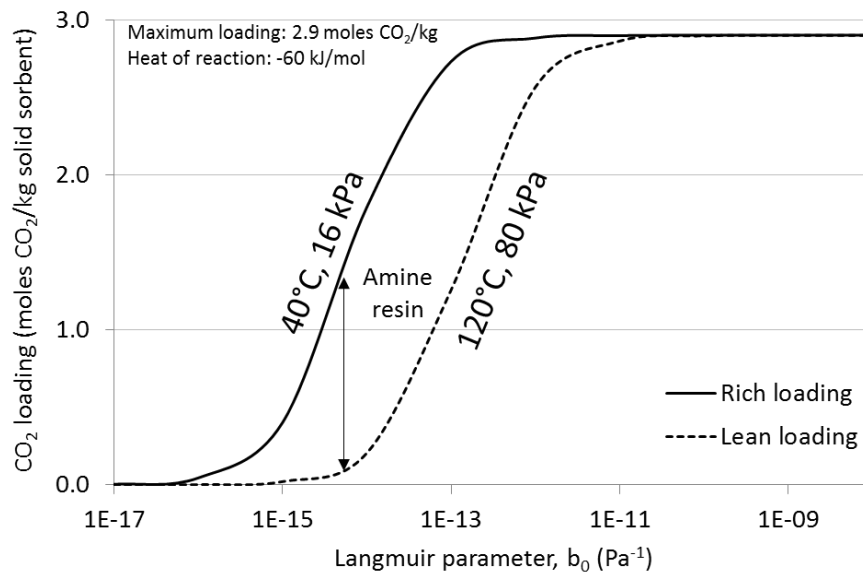


Figure 5.4: Influence of the Langmuir parameter on rich and lean loadings at the default conditions used for the adsorber and regenerator. The Langmuir term for the amine-based resin shown here is estimated based on loadings reported in the literature.

Sorbent heat of reaction

A third characteristic of the solid sorbent is the heat of reaction between CO₂ and the solid sorbent. This parameter is important for determining the sorbent's loading response to differences in temperature. Figure 5.5 shows how the heat of reaction influences the rich and lean loading for a solid

sorbent. The rich loading begins increasing when the heat of reaction is approximately -40 kJ/mol CO₂ and stabilizes at a maximum value between -60 to -65 kJ/mol CO₂. The lean loading is unchanged over the same range of reaction energies. Thus, for the nominal conditions considered in this work, one may conclude that the highest working capacities are achieved at heats of reaction between -60 and -65 kJ/mol CO₂. Sorbents with a heat of reaction above this narrow range only add to the heating and cooling requirements of the system without realizing returns in the form of higher working capacity.

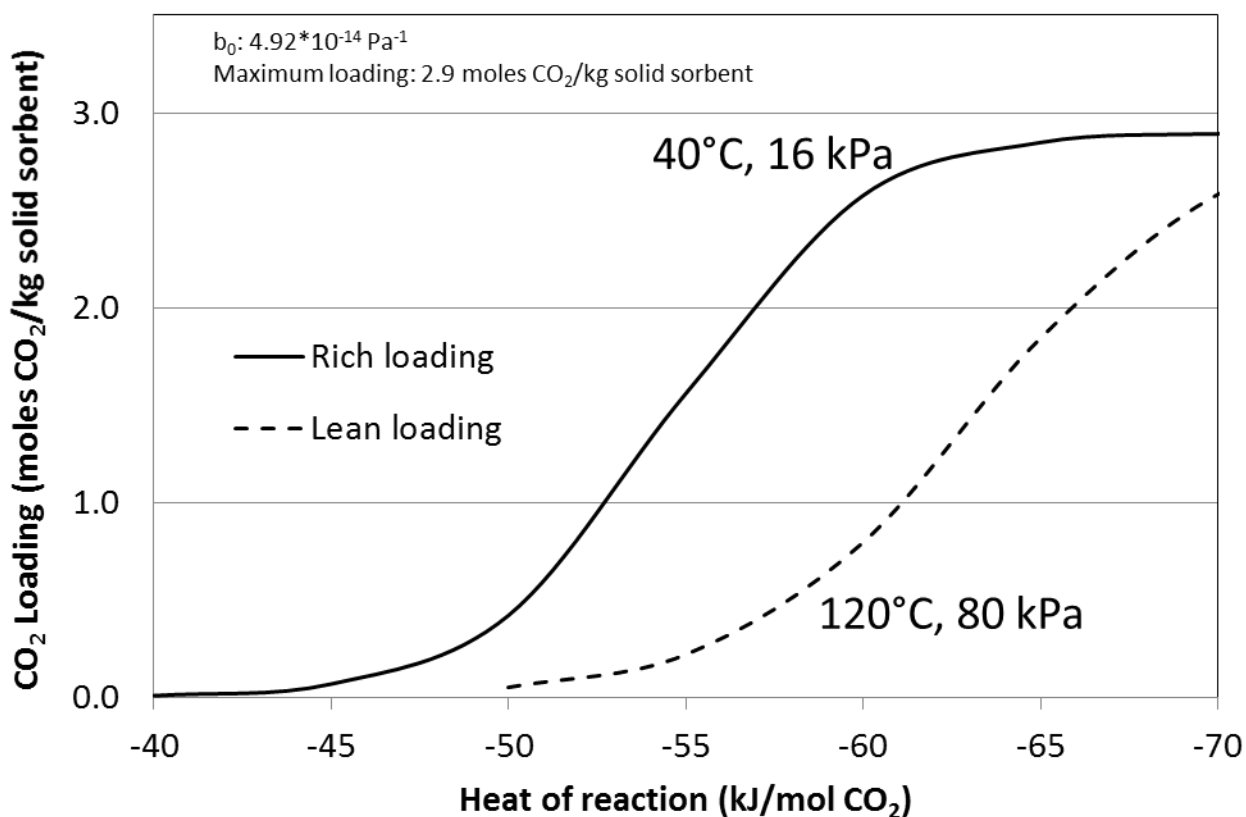


Figure 5.5: The influence of the heat of reaction between CO₂ and the sorbent on CO₂ loading in the adsorber (rich) and regenerator (lean) using the nominal ideal case study process conditions. The working capacity increases with the heat of reaction to a value of -60 kJ/mol CO₂. Higher heats of reaction result in no gain in working capacity but add additional heating and cooling loads to the system.

One means of determining the efficacy of solid sorbents is to the ratio between the material's working capacity and the maximum CO₂ capacity. Figure 5.6 compares the amine resin and tethered

amine solid sorbents based on this metric. This graph shows how the Langmuir parameter influences utilization of the solid sorbent's maximum capacity for several heats of reaction. The two curves represent the heats of reaction of the amine resin (-60 kJ/mol CO₂) and tethered amine (-75 kJ/mol CO₂) materials.

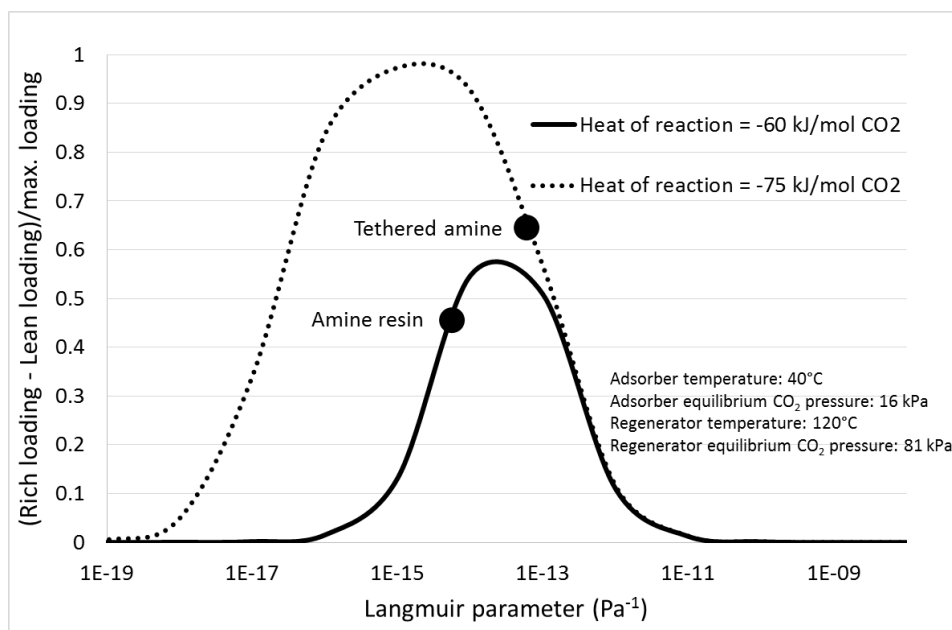


Figure 5.6: Ratio of the working capacity versus the maximum capacity for the two amine solid sorbents considered in this work. The tethered amine-based solid sorbent has a higher utilization factor due to the a pronounced response to temperature change (heat of reaction) despite displaying a pressure change response (larger b_0 term) that is higher than optimal under the specified conditions

The amine resin solid sorbent has a lower utilization factor compared to the tethered amine solid sorbent due, in part, to a sub-optimal pressure response (b_0). These results are consistent with those shown in Figure 5.2 which suggests that a higher rich loading and working capacity could be achieved for the amine resin material if the material could be designed with a with a larger pressure response (*i.e.* higher Langmuir parameter). Conversely, the tethered amine solid sorbent would require a less pronounced pressure response (lower Langmuir parameter) in order to achieve optimal loading. It is also worth noting that the higher activation energy for the tethered amine (-75 kJ/mol CO₂) could enable the material to utilize a greater proportion of the maximum capacity. Thus, greater utilization of sorbent material's maximum capacity by adjusting the material's loading response to adsorbate pressure changes is one of the more promising areas of future materials research.

The results of these sensitivity studies emphasize the significant variation in the working capacity of the solid sorbent as a function of the properties of the material. These findings indicate that certain traits and material property values are more suitable for a given set of adsorber and regenerator operating conditions. However, the adsorber and regenerator operating conditions presented here are only one set of a possible range of conditions, and changes to these parameters will also influence the performance of the solid sorbent-based CO₂ capture process. The following sections examine the effects of changes to several of the adsorber and regenerator conditions.

5.3.2. Adsorber design variables

This section and the next provide more detail regarding the equilibrium adsorbate pressure and solid temperature conditions in the adsorber and regenerator. Consider how the adsorber design influences CO₂ adsorption equilibrium. The design and operating conditions of the reactor cause the solid-gas reaction to progress towards equilibrium over a range of CO₂ pressures determined by the total gas pressure, the composition of the flue gas, and the design of the adsorber. In the ideal case study, the adsorber performs as a counter-current, fluidized bed and equilibrium is achieved at the flue gas inlet. This scenario serves as the upper bound for the equilibrium rich loading and in this case, the CO₂ pressure is 15.7 kPa (or 11.9% by volume of an inlet total pressure of 1.32 kPa). At the other extreme, for adsorber designs with well-mixed solid-gas phases, the equilibrium CO₂ partial pressure is the outlet pressure of the flue gas reflecting the depleted CO₂ concentration. Figure 5.7 shows how the equilibrium CO₂ pressure influences the rich loading for the range of possible pressures in the ideal case study scenario.

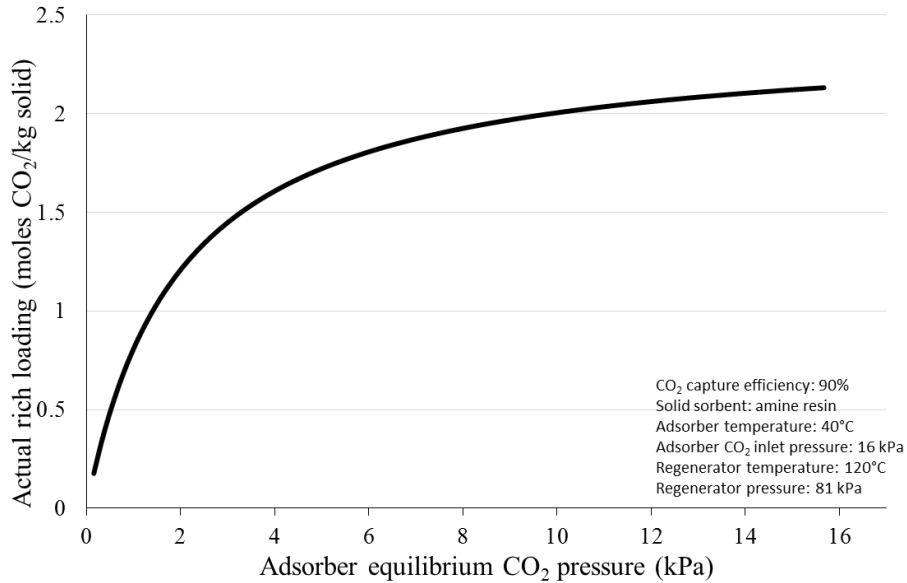


Figure 5.7: Influence of the equilibrium pressure on rich loading. The rich loading increases with pressure and a higher equilibrium CO₂ pressure is therefore desirable in the adsorber.

In an actual system, the loading is also influenced by other design considerations such as the number of adsorber stages, solid and gas flow regime, internal components, and the extent of turbulence and back-mixing of the solids and gases. As a result, the most representative CO₂ pressure for equilibrium calculations is likely to be an intermediate pressure falling between these bounding conditions.

5.3.3. Regenerator design variables

Similar to the adsorber process described in the previous section, a relationship exists between the lean loading of the solid and the CO₂ pressure in the regenerator. Figure 5.8 shows how the CO₂ pressure in the regenerator influences the equilibrium lean loading at different temperatures. Although the lean loading in the regenerator is less sensitive to changes in adsorbate pressure compared to the rich loading in the adsorber, higher regeneration temperatures result in significantly lower lean loadings. For the default partial CO₂ regenerator pressure (80 kPa), a 10°C change in temperature from the nominal value of 120°C results in a 0.2 to 0.3 mole CO₂ per kilogram change in lean loading, which represents a 11 to

17 percent change in the working capacity of the solid sorbent. Higher regeneration temperatures are therefore desirable in order to decrease the lean loading and improve the working capacity of the solid.

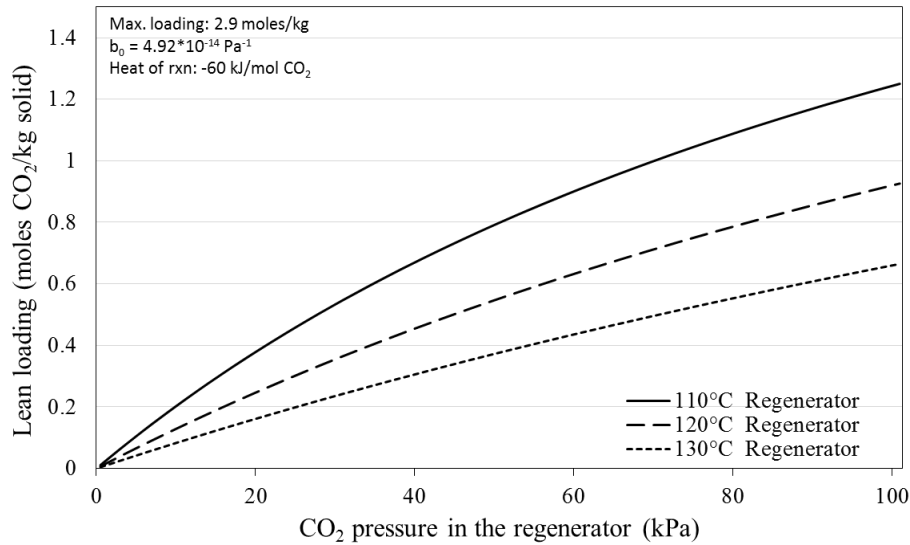


Figure 5.8: Performance model results for the lean CO₂ loading as a function of CO₂ pressure and temperature.

5.3.4. CO₂ capture efficiency

In the ideal sorbent case study, equilibrium is achieved at the inlet pressure of 15.5 kPa. However, CO₂ capture efficiency plays a key role in determining the rich loading when equilibrium is not achieved at the inlet CO₂ pressure. Using the system conditions specified in the ideal sorbent case study, Figure 5.9 shows the bounding cases in which the equilibrium rich loading is reached at either the inlet or outlet CO₂ partial pressure. If equilibrium is reached at the inlet CO₂ pressure, then the rich loading is not sensitive to the CO₂ capture efficiency. However, the rich loading falls off drastically with higher capture efficiencies when equilibrium is reached at the flue gas adsorber outlet.

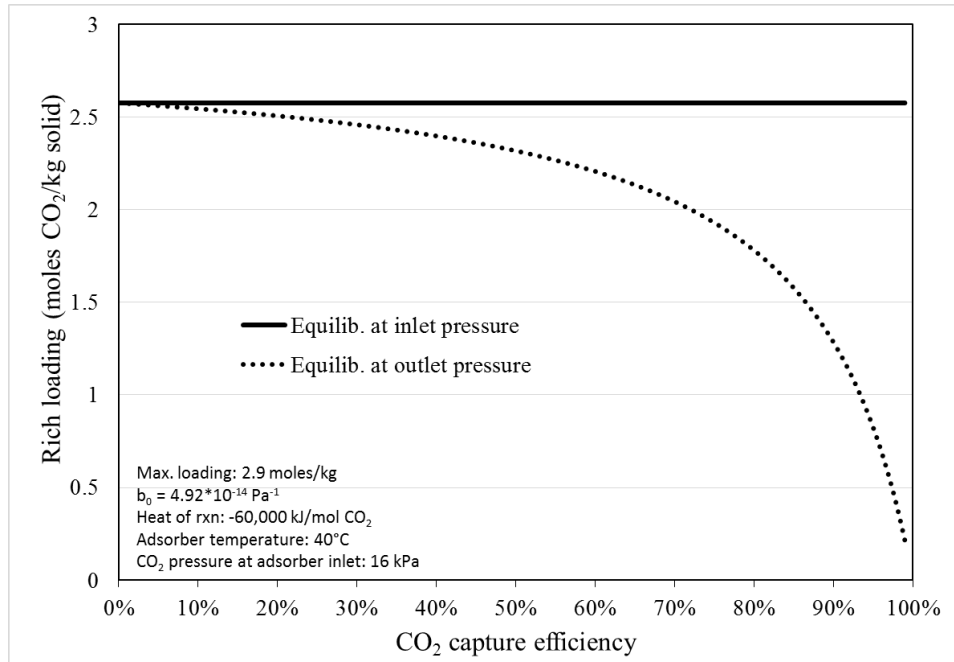


Figure 5.9: Influence of CO₂ capture efficiency on the rich loading in the adsorber vessel for the bounding conditions of the inlet and outlet CO₂ pressures.

One of the performance metrics used in this work is the specific solid requirement. This metric is used to measure the influence of rich and lean loading by quantifying the mass of solids required in order to capture a mole of CO₂. Figure 5.10 shows how the CO₂ capture efficiency influences the specific solid requirement. In the ideal case, the specific solid requirement is 580 kg solid sorbent per kilomole of captured CO₂. Additional solid sorbent is required as the equilibrium pressure departs from the inlet pressure. The dotted line shown in Figure 5.10 assumes that adsorption equilibrium is instead achieved at the outlet concentration as would occur in a fluidized bed or well-mixed bubbling bed.

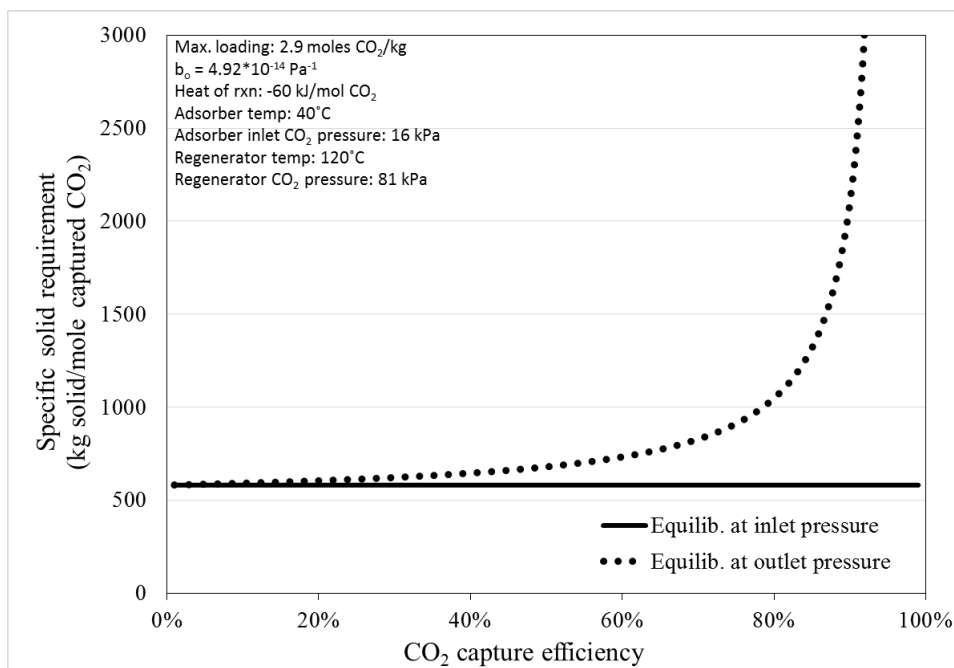


Figure 5.10: Specific solid requirement as a function of the CO₂ capture efficiency. Additional solid sorbent is required as the equilibrium pressure departs from the ideal case.

The contrast between these bounding equilibrium pressure assumptions is important given that most systems assume a 90% CO₂ capture efficiency. In Figure 5-10, for example, achieving 90% capture requires four times more solid sorbent based on outlet CO₂ pressure compared to the inlet pressure. Hence, for a given adsorber design, determining the effective equilibrium pressure is vital to determining the specific solid requirement of a real system.

5.4. Case Study #2: Effects of SO₂ impurities

This case study incorporates the influence of SO₂ in the performance of the CO₂ capture system. Excluding the degradation parameters and pre-treatment requirements shown in Table 5.5, the performance parameters and conditions are the same as those used in the first case study. The degradation effects shown in this case study serve as an example of how SO₂ could influence the performance of the CCS system. In this case study, it is assumed that all of the SO₂ entering the system is irreversibly adsorbed by the solid sorbent.

Table 5.5: Changes in the input parameters for case Study #2 as different from those used in Case Study #1. These changes reflect the influence of sulfur dioxide on the performance of the solid sorbent.

Input variable	Value	Units
Flue Gas Pre-treatment		
SO ₂ polisher used?	Yes	
SO ₂ polisher outlet concentration	1	ppmv
Drop in pressure across the pre-treatment unit	6,894	Pa
Water vapor mole fraction at pre-treat outlet	10	%
Degradation		
Solids purge fraction	0.004	%
Degradation parameters		
SO ₂	Yes	
SO ₂ capture efficiency (moles in - moles out)/moles in	100	%
SO ₂ gas release in regenerator (moles in -moles out as gas)/moles in	0	%

This case study follows the same calculation method used in the first case study. Additional steps are required, however, in order to quantify the influence of SO₂ on the solid sorbent. These steps are shown in detail while the calculation steps identical to those in the previous case study are summarized.

5.4.1. Case study #2 calculation

This section shows the calculations required to derive the loadings and flow rates in the CO₂ capture system. The calculations shown below are in the same order as shown in Section 4.6.

Pre-treatment flow rates

In this case, a pre-treatment step is used which acts as both a SO₂ polisher and direct contact cooler. The initial temperature and pressure of the flue gas are unchanged. However, the flue gas flow rates are higher in this system in order maintain a constant net electrical output of 550 MW. The flue gas flow rates are shown in Table 5.6.

Table 5.6: Flue gas conditions and molar composition upon entering the CO₂ capture system for Case Study #2. Flue gas flow rates at the pre-treatment inlet are iteratively calculated such that the net electrical output of the system is 550 MW.

Flue gas conditions	Pre-treatment inlet	Pre-treatment outlet
Flue gas temperature (K)	327	317
Flue gas pressure (kPa)	101.3	94.4
Flue gas composition		kmol/hr
Nitrogen (N ₂)	78,000	78,000
Oxygen (O ₂)	4,700	4,700
Water Vapor (H ₂ O)	18,000	11,000
Carbon Dioxide (CO ₂)	14,000	14,000
Carbon Monoxide (CO)	<1	<1
Hydrochloric Acid (HCl)	<1	<1
Sulfur Dioxide (SO ₂)	<1	<1
Sulfuric Acid (equivalent SO ₃)	<1	<1
Nitric Oxide (NO)	9	9
Nitrogen Dioxide (NO ₂)	1	1
Ammonia (NH ₃)	<1	<1
Argon (Ar)	930	930
Total	115,000	108,000

At the pre-treatment outlet, the flue gas has an SO₂ concentration of 1 ppm and a temperature of 318 K (45°C), which is 10 K less than the initial temperature. Also note that the total flue gas flow rate is slightly higher than in the first case study (approximately 2000 kmol/hr) because of larger electrical demands from the balance of the plant and CO₂ capture system.

Calculate flue gas blower stream conditions

The flue gas stream conditions are calculated using the same method shown in Case 1. These results are summarized below. Note that the pressure change is higher in the blower due to the pressure drop across the pre-treatment unit.

Calculation step	Dependent variable	Value	Units
a	$m_{gas}^{A,in}$	3,200,000	Kg/hr
b	ΔP^{blower}	37,400	Pa
c	ΔT^{blower}	53	K
d	$T_{gas}^{A,in}$	370	K

Calculate the rich loading

The results for the rich loading calculations are summarized below. The adjusted maximum loading in the adsorber is same as the ideal case.

Calculation step	Dependent variable	Value	Units
a	$P_{CO_2}^{A,in}$	15,700	Pa
b	$q_{adj,max}$	2.9	mol CO ₂ /kg
c	$b_{CO_2}^A$	$5.07 \cdot 10^{-4}$	1/Pa
d	$q_{adj,eq}^A$	2.58	mol CO ₂ /kg
e	q_{rich}	2.58	mol CO ₂ /kg

Calculate lean loading

A summary of the lean loading calculations are shown below. Like the rich loading calculation, the lean loading in the regenerator is the same as the ideal case.

Calculation step	Dependent variable	Value	Units
a	$b_{CO_2}^R$	$4.65 \cdot 10^{-6}$	1/Pa
b	$q_{adj,eq}^R$	0.79	mol CO ₂ /kg
c	q_{lean}	0.79	mol CO ₂ /kg

Calculate adsorber flow rates

- a. Mass flow rate of gas at the adsorber outlet

The mass flow rate flue gas at the adsorber outlet is quantified using equation 4.3. The calculations shown here are the same as those used in the ideal sorbent case study. Note that the clean flue gas is free of SO₂ due to adsorption by the solid sorbent.

Dependent variable	Value	Independent variable	Unit	Calc.
$m_{gas}^{A,out}$	2,630,000		kg/hr	=
	60,000	$m_{CO_2(gas)}^{A,out}$	kg/hr	+
	0	$m_{SO_2(gas)}^{A,out}$	kg/hr	+
	300	$m_{NO_X(gas)}^{A,out}$	kg/hr	+
	150,000	$m_{O_2(gas)}^{A,out}$	kg/hr	+
	2,200,000	$m_{N_2(gas)}^{A,out}$	kg/hr	+
	190,000	$m_{H_2O(gas)}^{A,out}$	kg/hr	+
	38,000	$m_{inert(gas)}^{A,out}$	kg/hr	

b. Mass flow rate of solids at the adsorber inlet

The mass flow rate of solids at the adsorber inlet is calculated using Equation 4.8. The mass flow rate of adsorbed SO₂ ($m_{SO_2(solid)}^{A,in}$) is calculated using Equation 4.38 and the mass flow rate of solid sorbent degraded by SO₂ ($m_{solid-SO_2}^{A,in}$) is calculated using Equation 4.39.

Dependent variable	Value	Independent variable	Unit	Calc.
$m_{solid}^{A,in}$	8,300,000		kg/hr	=
	242,000	$m_{CO_2(solid)}^{A,in}$	kg/hr	+
	184,000	$m_{SO_2(solid)}^{A,in}$	kg/hr	+
	0	$m_{H_2O(solid)}^{A,in}$	kg/hr	+
	6,900,000	$m_{solid-CO_2}^{A,in}$	kg/hr	+
	990,000	$m_{solid-SO_2}^{A,in}$	kg/hr	+

The solid flow rate is higher than in the ideal case because of the uptake of SO₂. Unlike the ideal case, degraded solid sorbent and adsorbed SO₂ now circulates through the system causing the solids flow rate to be significantly higher (19%) compared to the ideal case study presented previously.

c. Mass of solids at the adsorber outlet

The mass flow rate of solids at the adsorber outlet is calculated using Equation 4.9. The mass flow rate of adsorbed SO₂ is calculated using Equation 4.10 and the mass flow rate of degraded solid remains unchanged from the adsorber inlet to the adsorber outlet.

Dependent variable	Value	Independent variable	Unit	Calc.
$m_{solid}^{A,out}$	8,900,000		kg/hr	=
	780,000	$m_{CO_2(solid)}^{A,out}$	kg/hr	+
	180,000	$m_{SO_2(solid)}^{A,out}$	kg/hr	+
	0	$m_{H_2O(solid)}^{A,out}$	kg/hr	+
	6,970,000	$m_{solid-CO_2}^{A,out}$	kg/hr	+
	990,000	$m_{solid-SO_2}^{A,out}$	kg/hr	+

Calculate the regenerator mass flow rates

a. Mass flow rate of solids at the regenerator inlet

The mass flow rate of solids at the regenerator inlet is the same as the mass flow rate of solids at the adsorber outlet.

b. Mass flow rate of regenerator purge gas

The mass flow rate of purge gas in the regenerator is calculated using Equation 4.27. Like the first case study, steam must be removed from the regenerator in order to ensure that the outlet flow of CO₂ reaches a specified pressure (nominally set at 81 kPa).

Dependent variable	Value	Independent variable	Unit	Calc.
$m_{steam}^{R,purge}$	55,000		kg H ₂ O/hr	=
	3,100	$\left(\frac{101,325 * 12,000}{81,000} - 12,000 - 0 * 0 \right)$	kmol H ₂ O/hr	*
	18	MW_{H_2O}	g/mol	

c. Mass flow rates of gas at the regenerator outlet

The mass flow rate of gas at the regenerator outlet is calculated using Equation 4.22. Here, water entrained with the solid sorbent is released along with CO₂ in order to produce the 81 kPa of CO₂ pressure specified as the nominal parameter value of the model. The pressure of the gas stream is 101.3 kPa (atmospheric).

Dependent variable	Value	Independent variable	Unit	Calc.
$m_{gas}^{R,out}$	600,000		kg/hr	=
	540,000	$m_{CO_2(gas)}^{R,out}$	kg/hr	+
	0	$m_{SO_2(gas)}^{R,out}$	kg/hr	+
	56,000	$m_{H_2O(gas)}^{R,out}$	kg/hr	

d. Mass flow rate of solids at the regenerator outlet

The mass flow rate of solids at the regenerator outlet is calculated using Equation 4.16. Since sulfur dioxide is not regenerated, there is a sizable flowrate of solid sorbent degraded by SO₂ ($m_{solid-SO_2}^{R,out}$) which accounts for about 14% of the solids exiting the regenerator.

Dependent variable	Value	Independent variable	Unit	Calc.
$m_{solid}^{R,out}$	8,300,000		kg/hr	=
	240,000	$m_{CO_2(solid)}^{R,out}$	kg/hr	+
	180,000	$m_{SO_2(solid)}^{R,out}$	kg/hr	+
	0	$m_{H_2O(solid)}^{R,out}$	kg/hr	+
	6,900,000	$m_{solid-CO_2}^{R,out}$	kg/hr	+
	990,000	$m_{solid-SO_2}^{R,out}$	kg/hr	

Calculate transport, discarded, and fresh solid flow rates

a. Discarded solids

The mass flow rate of discarded solids is calculated using Equation 4.29. Solid purge is needed in order to prevent the accumulation of degraded solids and maintain a constant solid flow rate. The composition of this flow stream is the same as that exiting the regenerator and thereby consists of approximately 14% degraded solid sorbent. Increasing the discarded solid flow rate by increasing the solid purge fraction would reduce the percentage of degraded solids. However, there is an operating cost associated with replacing the discarded solids with fresh solid sorbent and thus, selection of a proper solid purge fraction requires a trade-off between performance and cost. Note that the nominal value of the purge fraction is relatively small compared to the flow rate of solid transported back the adsorber as a result of this trade-off which is discussed in Appendix I.

Dependent variable	Value	Independent variable	Unit	Calc.
$m_{solid}^{discarded}$	330		kg/hr	=
	8,300,000	$m_{solid}^{R,out}$	kg/hr	*
	0.00004	$X_{solid\ purge}$	fraction	

b. Transport solids

The mass flow rate of returning solids transported to the regenerator is calculated using Equation 4.30. This flow rate is nearly identical to the solid flow rate exiting the regenerator

Dependent variable	Value	Independent variable	Unit	Calc.
$m_{solid}^{transport}$	8,300,000		kg/hr	=
	8,300,000	$m_{solid}^{R,out}$	kg/hr	*
	0.99996	$(1 - X_{solid\ purge})$	fraction	

c. Fresh solids

The flow rate of fresh solid sorbent added to the transported stream at the adsorber inlet is calculated using Equation 4.31. This flow rate is required to replace the sorbent capacity lost to the discarded solid stream.

Dependent variable	Value	Independent variable	Unit	Calc.
m_{solid}^{fresh}	320		kg/hr	=
	8,300,000	$\sum m_{solid-i}^{R,out}$	kg/hr	*
	0.00004	$X_{solid\ purge}$		

Calculate cooling requirement

The cooling requirement calculations are summarized in below based on the method outlined in the previous case study. The cooling requirement is 6% higher in this scenario than in the first case study for several compounding reasons. Principal among these reasons is the increase in sensible heat caused by a higher solid flow rate. In the adsorber, for example, the sensible heat of the solids increases to 330 GJ/hr in this case from 302 GJ/hr in the ideal case. The larger plant size also increases the heat generated by the exothermic CO₂ adsorption reaction to 740 GJ/hr from 702/hr GJ.

Dependent variable	Value	Unit
ΔH^{HHX}	355,000,000	kJ/hr
m_{fluid}^{HX}	160,000	kg/hr
$H_{cooling}^A$	1,070,000,000	kJ/hr
$m_{cooling\ water}^A$	10,300,000	kg/hr

For comparison, consider that the cooling water flow rate required in the ideal case is 9,600 tonnes per hour. Hence, the addition of SO₂ degradation results in a 7% increase in the mass flow rate of cooling water.

Calculate heating requirement

The heating requirement calculations are summarized below based on the method outlined in the previous case study. The heating requirement is higher than the previous section principally because of the higher solid requirement. For comparison, the steam requirement (m_{steam}^R) for the ideal case is 440 tonnes per hour. Thus, the addition of SO₂ degradation results in a 7% increase in the steam requirement.

Dependent variable	Value	Unit
$T_{solid}^{CHX,out}$	355	K
$H_{heating}^R$	1,100,000,000	kJ/hr
$h_{steam}^{R,out}$	418	kJ/kg
m_{steam}^R	390,000	kg/hr

Performance estimators

a.) Actual rich loading

The actual rich loading is calculated using Equation 4.51. The rich loading is 0.33 moles CO₂/kg solid lower than in the ideal case due to degradation from SO₂.

Dependent variable	Value	Independent variable	Unit	Calc.
$q_{actual\ rich}$	2.25			=
	17,800	$M_{CO_2(solid)}^{A,out}$	kmol/hr	*
	1000	Conversion	mol/kmol	/
	7,910,000	$\sum m_{solid-i}^{A,out}$	Kg/hr	

b.) Actual lean loading

The actual lean loading is calculated using Equation 4.52. The lean loading is approximately 0.1 moles CO₂/kg lower than in the ideal case.

Dependent variable	Value	Independent variable	Unit	Calc.
$q_{actual\ lean}$	0.69		mol/kg	=
	5,490	$M_{CO_2(solid)}^{R,out}$	kmol/hr	*
	1000	Conversion	mol/kmol	/
	7,910,000	$\sum m_{solid-i}^{R,out}$	kg/hr	

c.) Specific solid requirement

The specific solid requirement is calculated using Equation 4.77. This value is 17% higher than the 580 kg solid per kilomole CO₂ due to SO₂ degradation (which accounts for 10% of the solid sorbent) and the higher flow rate of flue gas which results in higher sorbent requirement to capture 90% of the CO₂ entering the CCS system.

Dependent variable	Value	Independent variable	Unit	Calc.
R	676		kg/kmol	=
	8,300,000	$m_{solid}^{A,in}$	kg/hr	/
	12,300	$M_{CO_2(gas)}^{R,out}$	kmol/hr	

d.) Auxiliary electrical load

The auxiliary electrical load is calculated as the sum of the electrical requirements defined in Equations 4.67 through 4.70. The electrical requirements of the systems are approximately 16 MW higher compared with the ideal case due to the higher solid flow rates.

Dependent variable	Value	Independent variable	Unit	Calc.
$\sum MW_e$	110		MW _e	=
	42	$FG\ Blower\ MW_e$	MW _e	+
	2	$Transport\ return\ conveyor\ MW_e$	MW _e	+
	0	$HX\ Pump\ MW_e$	MW _e	+
	2	HX Compressor	MW _e	+
	64	$CO_2\ compressor\ MW_e$	MW _e	

e.) Electric equivalent loss

The electric equivalent loss is calculated using Equation 4.75. The steam requirement in this scenario is 13 MW higher than the ideal case (which was 80 MW_{equivalent}) due to the higher heating requirement.

Dependent variable	Value	Independent variable	Unit	Calc.
<i>EEL</i>	78			=
	0.222	HHE		*
	390,000	m_{steam}^R	Kg/hr	*
	3,249	$h_{steam}^{R,initial}$	kJ/kg	*
	$(2.78 * 10^{-7})$	Conversion	MW _e *hr/kJ	

f.) Total electrical loss

The total electricity loss is calculated using Equation 4.74. The electrical loss for this system is about 41 MW above the ideal case.

Dependent variable	Value	Independent variable	Unit	Calc.
<i>ToL</i>	188		MW _e	=
	78	EEL	MW _e	+
	110	Total auxiliary load	MW _e	

g.) Plant efficiency

The efficiency of the power plant is calculated using Equation 4.76. This calculation is shown below.

Dependent variable	Value	Independent variable	Unit	Calc.
<i>Plant efficiency</i>	29.0		%HHV	=
	550	MW	MW _e	/
	221,000	Fuel flow rate	kg/hr	/
	30,840	Fuel HHV as received	kJ/kg	*
	$3.6 * 10^5$	Conversion		

5.4.2. Case study #2 discussion

The calculations shown in this section build upon the framework discussed for the ideal case study and introduce the effects of SO₂ degradation. The actual working capacity of the solid sorbent drops from 1.8 to 1.6 moles per kilogram. As a result, the system circulates approximately 680 kg per kilomole of CO₂ captures, which is 17% more than the ideal sorbent case study. The regeneration step of the CO₂ capture process also requires an additional 27 tonnes of steam per hour (a 7% increase over the ideal sorbent system). The resulting system has a gross size of 788 MW with a net thermal efficiency of 29%. This may be compared to the ideal sorbent system efficiency of 30% and the no-CCS case of 39%.

5.5. Case study #3: Effect of water vapor impurities

This case study incorporates the influence of flue gas water vapor in the performance of the CO₂ capture system. Excluding the flue gas pre-treatment requirements and water-based interactions shown in Table 5.7, the performance parameters and conditions are the same as those used in the first case study. The degradation effects shown in this case study serve as an example of how water could influence the performance of the CCS system. In this case, it is assumed that 30% of the flue gas water entering the adsorber is captured by the solid sorbent and 30% is released in the regenerator. These values were chosen based on assumptions about the solid sorbent process outlined by a DOE patent regarding the solid sorbent process (Pennline, et al., 2011). In this case, the uptake of water has net effect of reducing the maximum capacity of the solid by 0.5 moles of CO₂ per kilogram of solid sorbent based on values reported in the literature for amine-based solid sorbents. It should be noted that assumptions regarding the decrease in maximum CO₂ capacity caused by water are generalized for amine-based solid sorbents and are not necessarily indicative of the performance of the solid sorbent used for this case study.

Table 5.7: Changes in the input parameters for Case Study #3 as different from those used in Case Study #1. These changes reflect the influence of water on the performance of the solid sorbent.

Input variable	Value	Units
Flue Gas Pre-treatment		
SO ₂ Polisher Used?	Yes	
SO ₂ Polisher Outlet Concentration	1	ppmv
Drop in pressure across the Pre-treatment unit	6894	Pa
Water vapor mole fraction at pre-treat outlet	.10	fraction
Degradation		
Water adsorption	Yes	
Water uptake (% removed from flue gas)	30	%
Water regeneration efficiency (%)	30	%
Competitively adsorbed water (Influence on CO ₂ capacity)	-0.5	mole/kg solid sorbent

This case study follows the same calculation method used in the first case study. Additional steps are required, however, in order to quantify the influence of water on the solid sorbent. These steps are shown in detail while the calculation steps identical to those in the previous case study are summarized.

5.5.1. Case study #3 calculation

This section shows the calculations required to derive the loadings and flow rates in the CO₂ capture system. The calculations shown below are in the same order as shown in Section 4.6.

Pre-treatment flow rates

In this case, a pre-treatment step is used which acts as both a SO₂ polisher and direct contact cooler. The initial temperature and pressure of the flue gas are unchanged. However, the flue gas flow rates are higher in this system in order maintain a constant net electrical output of 550 MW. The flow rate as are shown in Table 5.8. Like the previous case studies, the flue gas flow rates are iteratively calculated in order to achieve the desired net electrical output.

Table 5.8: Flue gas conditions and molar composition upon entering the CO₂ capture system for Case Study #3.

Flue gas conditions	Pre-treatment inlet	Pre-treatment outlet
Flue gas temperature (K)	327	317
Flue gas pressure (kPa)	101.3	94.4
<u>Flue gas composition</u>		<u>kmol/hr</u>
Nitrogen (N ₂)	79,300	79,300
Oxygen (O ₂)	4,800	4,800
Water Vapor (H ₂ O)	18,200	11,000
Carbon Dioxide (CO ₂)	13,900	13,900
Carbon Monoxide (CO)	<1	<1
Hydrochloric Acid (HCl)	<1	<1
Sulfur Dioxide (SO ₂)	28	28
Sulfuric Acid (equivalent SO ₃)	<1	<1
Nitric Oxide (NO)	9	9
Nitrogen Dioxide (NO ₂)	<1	1
Ammonia (NH ₃)	<1	<1
Argon (Ar)	900	900
Total	117,000	110,000

At the pre-treatment outlet, the flue gas has an SO₂ concentration of 1 ppm and a temperature of 318 K (45°C), which is 10 K less than the initial temperature. Note that the flue gas flow rates are slightly higher in this case compared to either of the previous cases due to the larger plant size and higher fuel consumption. For reference, the flue gas flow rates in the first and second cases were 113,000 and 115,000 kmol/hr respectively.

Calculate flue gas blower stream conditions

The flue gas stream conditions are calculated using the same method shown in Case 1. These results are summarized below. Note that the pressure change is higher in the blower due to the pressure drop across the pre-treatment unit.

Calculation step	Dependent variable	Value	Units
a	$m_{gas}^{A,in}$	3,200,000	kg/hr
b	ΔP^{blower}	37,400	Pa
c	ΔT^{blower}	53	K
d	$T_{gas}^{A,in}$	370	K

Calculate the rich loading

The results for the rich loading calculations are summarized below. The adjusted maximum loading in the adsorber is lower than in the ideal case due to the influence of water. The lower maximum loading results in a lower rich loading as well.

Calculation step	Dependent variable	Value	Units
a	$p_{CO_2}^{A,in}$	15,700	Pa
b	$q_{adj,max}$	2.4	mol CO ₂ /kg
c	$b_{CO_2}^A$	$5.07 \cdot 10^{-4}$	1/Pa
d	$q_{adj,eq.}^A$	2.13	mol CO ₂ /kg
e	q_{rich}	2.13	mol CO ₂ /kg

Calculate lean loading

A summary of the lean loading calculations are shown below. Like the rich loading calculation, the lean loading in the regenerator is lower than in the ideal case due to the lower adjusted maximum capacity of the solid sorbent.

Calculation step	Dependent variable	Value	Units
a	$b_{CO_2}^R$	$4.65 \cdot 10^{-6}$	Pa ⁻¹
b	$q_{adj,eq.}^R$	0.66	mol CO ₂ /kg
c	q_{lean}	0.66	mol CO ₂ /kg

Calculate adsorber flow rates

d. Mass flow rate of gas at the adsorber outlet

The mass flow rate flue gas at the adsorber outlet is quantified using equation 4.3. The calculations shown here are the same as those used in the ideal sorbent case study. Note that the gas flow rate of water is proportionately lower than in the ideal case because of the interaction between water the solid.

Dependent variable	Value	Independent variable	Unit	Calc.
$m_{gas}^{A,out}$	2,600,000		kg/hr	=
	61,000	$m_{CO_2(gas)}^{A,out}$	kg/hr	+
	1,800	$m_{SO_2(gas)}^{A,out}$	kg/hr	+
	300	$m_{NO_x(gas)}^{A,out}$	kg/hr	+
	150,000	$m_{O_2(gas)}^{A,out}$	kg/hr	+
	2,200,000	$m_{N_2(gas)}^{A,out}$	kg/hr	+
	139,000	$m_{H_2O(gas)}^{A,out}$	kg/hr	+
	38,000	$m_{inert(gas)}^{A,out}$	kg/hr	

e. Mass flow rate of solids at the adsorber inlet

The mass flow rate of solids at the adsorber inlet is calculated using Equation 4.8. The solid flow rate is higher than in the ideal case because of the reduced working capacity of the solid.

Dependent variable	Value	Independent variable	Unit	Calc.
$m_{solid}^{A,in}$	8,900,000		kg/hr	=
	250,000	$m_{CO_2(solid)}^{A,in}$	kg/hr	+
	0	$m_{SO_2(solid)}^{A,in}$	kg/hr	+
	140,000	$m_{H_2O(solid)}^{A,in}$	kg/hr	+
	8,500,000	$m_{solid-CO_2}^{A,in}$	kg/hr	+
	0	$m_{solid-SO_2}^{A,in}$	kg/hr	

f. Mass of solids at the adsorber outlet

The mass flow rate of solids at the adsorber outlet is calculated using Equation 4.9. The mass flow rate of adsorbed SO₂ is calculated using Equation 4.10 and the mass flow rate of degraded solid remains unchanged from the adsorber inlet to the adsorber outlet.

Dependent variable	Value	Independent variable	Unit	Calc.
$m_{solid}^{A,out}$	9,500,000		kg/hr	=
	800,000	$m_{CO_2(solid)}^{A,out}$	kg/hr	+
	0	$m_{SO_2(solid)}^{A,out}$	kg/hr	+
	200,000	$m_{H_2O(solid)}^{A,out}$	kg/hr	+
	8,500,000	$m_{solid-CO_2}^{A,out}$	kg/hr	+
	0	$m_{solid-SO_2}^{A,out}$	kg/hr	

Calculate the regenerator mass flow rates

e. Mass flow rate of solids at the regenerator inlet

The mass flow rate of solids at the regenerator inlet is the same as the mass flow rate of solids at the adsorber outlet.

f. Mass flow rate of regenerator purge gas

The mass flow rate of purge gas in the regenerator is calculated using Equation 4.27. In this case, a small flow rate of water must be removed from the regenerator in order to ensure that the outlet flow of CO₂ reaches a specified pressure (nominally set at 81 kPa). The mass flow rate of purge steam is negative to indicate that water is removed from the regenerator.

Dependent variable	Value	Independent variable	Unit	Calc.
$m_{steam}^{R,purge}$	-3,000		kg H ₂ O/hr	=
	-160	$\left(\frac{101,325 * 13,000}{81,000} - 16,000 - 11,000 * 0.3 \right)$	kmol H ₂ O/hr	*

Removing water as a separate flow stream is required in some process configurations in which the evaporation of water in the regenerator would lower the partial pressure of CO₂ below the specified value. The specific method used to remove water from the solid stream, however, would depend upon multiple factors including the solid's degree of water saturation, water tolerance, and resistance to attrition among others. Detailed modeling of this process, however, are beyond the scope of this work and mentioned here simply in recognition of the potential need of such a process under certain process conditions.

g. Mass flow rates of gas at the regenerator outlet

The mass flow rate of gas at the regenerator outlet is calculated using Equation 4.22. Here, water entrained with the solid sorbent is released along with CO₂ in order to produce the 81 kPa of CO₂ pressure specified as the nominal parameter value of the model. The pressure of the gas stream is 101.3 kPa (atmospheric).

Dependent variable	Value	Independent variable	Unit	Calc.
$m_{gas}^{R,out}$	610,000		kg/hr	=
	550,000	$m_{CO_2(gas)}^{R,out}$	kg/hr	+
	0	$m_{SO_2(gas)}^{R,out}$	kg/hr	+
	56,000	$m_{H_2O(gas)}^{R,out}$	kg/hr	

h. Mass flow rate of solids at the regenerator outlet

The mass flow rate of solids at the regenerator outlet is calculated using Equation 4.16. Note that some water remains entrained by the solid sorbent. In this case study, only 30% of the water is vaporized in the regenerator as specified in Table 5.8. This value as chosen in keeping with a 2011 NETL patent regarding the uptake and removal of water in a solid sorbent-based CO₂ capture system and subsequent conversations with the patent's authors (Pennline, et al., 2011). This water is physically entrained within

the solid flow stream and does not chemically degrade the solid. Hence, there is not a term listed below for adsorbent degraded by the solid ($m_{solid-H_2O}^{R,out}$).

Dependent variable	Value	Independent variable	Unit	Calc.
$m_{solid}^{R,out}$	8,900,000		kg/hr	=
	250,000	$m_{CO_2(solid)}^{R,out}$	kg/hr	+
	0	$m_{SO_2(solid)}^{R,out}$	kg/hr	+
	140,000	$m_{H_2O(solid)}^{R,out}$	kg/hr	+
	8,500,000	$m_{solid-CO_2}^{R,out}$	kg/hr	+
	0	$m_{solid-SO_2}^{R,out}$	kg/hr	

Calculate transport, discarded, and fresh solid flow rates

a. Discarded solids

The mass flow rate of discarded solids is calculated using Equation 4.29. However, since water is not degrading the solid sorbent, the flow rate of discarded solids is effectively zero as is the case with the first case study ($X_{solid\ purge} = 0.00001\%$).

Dependent variable	Value	Independent variable	Unit	Calc.
$m_{solid}^{discarded}$	0		kg/hr	=
	8,900,000	$m_{solid}^{R,out}$	kg/hr	*
	0	$X_{solid\ purge}$	fraction	

b. Transport solids

The mass flow rate of returning solids transported to the regenerator is calculated using Equation 4.30. This flow rate is identical to the solid flow rate exiting the regenerator

Dependent variable	Value	Independent variable	Unit	Calc.
$m_{solid}^{transport}$	8,900,000		kg/hr	=
	8,900,000	$m_{solid}^{R,out}$	kg/hr	*

0	$(1 - X_{solid\ purge})$	fraction
---	--------------------------	----------

c. Fresh solids

The flow rate of fresh solid sorbent added to the transported stream at the adsorber inlet is calculated using Equation 4.31. However, no make-up stream is required in this case study.

Dependent variable	Value	Independent variable	Unit	Calc.
m_{solid}^{fresh}	0		kg/hr	=
	8,900,000	$\sum m_{solid-i}^{R,out}$	kg/hr	*
	0	$X_{solid\ purge}$		

Calculate cooling requirement

The cooling requirement calculations are summarized in below based on the method outlined in the first and second case studies. The cooling requirement is slightly (1%) lower in this case compared to the first case study despite the increase in sensible heat as a result of water condensation and 8% lower than the SO₂ degradation case study.

Dependent variable	Value	Unit
ΔH^{HHX}	400,000,000	kJ/hr
m_{fluid}^{HX}	180,000	kg/hr
$H_{cooling}^A$	990,000,000	kJ/hr
$m_{cooling\ water}^A$	9,500,000	kg/hr

Calculate heating requirement

The heating requirement calculations are summarized below based on the method outlined in the previous case study. The heating requirement is higher than the previous cases principally because of the higher solid requirement. For reference, the steam requirement (m_{steam}^R) for the ideal and SO₂

degradation scenarios shown in the previous sections were 363,000 and 387,000 kilograms per hour respectively. Thus, the solid sorbent's interaction with water discussed in this case study represents a 21% increase in the steam requirement compared to the ideal case and 14% higher than the water degradation case study.

Dependent variable	Value	Unit
$T_{solid}^{CHX,out}$	355	K
$H_{heating}^R$	1,200,000,000	kJ/hr
$h_{steam}^{R,out}$	418	kJ/kg
m_{steam}^R	440,000	kg/hr

Performance estimators

d. Actual rich loading

The actual rich loading is calculated using Equation 4.51. The rich loading is 0.45 moles CO₂/kg solid lower than in the ideal case due to degradation (from water) and loss of available sorbent caused by pore blockage. This reduction to the rich loading assumes that uptake inhibiting phenomena such as pore blockage that may occur at flue gas conditions predominate water uptake interactions.

Dependent variable	Value	Independent variable	Unit	Calc.
$q_{actual\ rich}$	2.13			=
	18,000	$M_{CO_2(solid)}^{A,out}$	kmol/hr	*
	1000	Conversion	mol/kmol	/
	8,500,000	$\sum m_{solid-i}^{A,out}$	Kg/hr	

e. Actual lean loading

The actual lean loading is calculated using Equation 4.52. The lean loading is approximately 0.1 moles CO₂/kg lower than in the ideal case.

Dependent variable	Value	Independent variable	Unit	Calc.
$q_{actual\ lean}$	0.66		mol/kg	=
	5,600	$M_{CO_2(solid)}^{R,out}$	kmol/hr	*
	1000	Conversion	mol/kmol	/
	8,500,000	$\sum m_{solid-i}^{R,out}$	kg/hr	

h.) Specific solid requirement

The specific solid requirement is calculated using Equation 4.77. This value is almost 40% higher than the 580 kg solid per kilomole CO₂ due both to degradation (which accounts for 10% of the solid sorbent) and the higher flow rate of flue gas which results in higher sorbent requirement to capture 90% of the CO₂ entering the CCS system.

Dependent variable	Value	Independent variable	Unit	Calc.
R	710		kg/kmol	=
	8,900,000	$m_{solid}^{A,in}$	kg/hr	/
	12,600	$M_{CO_2(gas)}^{R,out}$	kmol/hr	

i.) Auxiliary electrical load

The auxiliary electrical load is calculated as the sum of the electrical requirements defined in Equations 4.67 through 4.70. The electrical requirements of the systems are approximately 20 MW higher due to the higher solid flow rates.

Dependent variable	Value	Independent variable	Unit	Calc.
$\sum MW_e$	113		MW _e	=
	43	<i>FG Blower MW_e</i>	MW _e	+
	2	<i>Transport return conveyer MW_e</i>	MW _e	+
	0	<i>HX Pump MW_e</i>	MW _e	+
	2	HX Compressor	MW _e	+
	65	<i>CO₂ compressor MW_e</i>	MW _e	

j.) Electric equivalent loss

The electric equivalent loss is calculated using Equation 4.75. The steam requirement in this scenario is 13 MW higher than the ideal case (which was 80 MW_{equivalent}) due to the higher heating requirement.

Dependent variable	Value	Independent variable	Unit	Calc.
<i>EEL</i>	89			=
	0.222	HHE		*
	440,000	m_{steam}^R	Kg/hr	*
	3,249	$h_{steam}^{R,initial}$	kJ/kg	*
	$(2.78 * 10^{-7})$	Conversion	MW _e *hr/kJ	

k.) Total electrical loss

The total electricity loss is calculated using Equation 4.74. The electrical loss for this system is about 41 MW above the ideal case.

Dependent variable	Value	Independent variable	Unit	Calc.
<i>ToL</i>	201		MW _e	=
	89	EEL	MW _e	+
	113	Total auxiliary load	MW _e	

l.) Plant efficiency

The efficiency of the power plant is calculated using Equation 4.76. This calculation is shown below.

Dependent variable	Value	Independent variable	Unit	Calc.
<i>Plant efficiency</i>	28.5		%HHV	=
	550	MW	MW _e	/
	225,000	Fuel flow rate	kg/hr	/
	30,840	Fuel HHV as received	kJ/kg	*
	3.6*10 ⁵	Conversion		

5.5.2. Case study #3 discussion

The calculations shown in this section discuss the method used to quantify the effects of flue gas water vapor on the CO₂ capture system. In this case study, water causes a 0.5 mole decrease in the maximum CO₂ capacity of the solid resulting in a working capacity of 1.5 moles CO₂ per kilogram of solid sorbent compared to 1.8 moles in the ideal case and 1.6 moles CO₂ per kilogram in the SO₂ degradation case. The system circulates approximately 710 kg per mole of CO₂ captured, which is 22% more than the ideal sorbent system and 5% more than the SO₂ degradation case study. The additional steam required in the regenerator also results in a higher energy penalty, resulting in a gross plant size of 802 MW and a net thermal efficiency of 29%.

5.6. Case study #4: Effects of water and SO₂ impurities

This case study incorporates the influence of water and SO₂ in the performance of the CO₂ capture system. Excluding the degradation parameters and pre-treatment requirements shown in Table 5.9, the performance parameters and conditions are the same as those used in the first case study. The degradation effects shown in this case study serve as an example of how water and SO₂ could influence the performance of the CCS system. In this case, all of the SO₂ entering the system is irreversibly adsorbed by the solid sorbent and a small percentage of the solids are removed as purge in order to

prevent the accumulation of degradation products. Adsorption and desorption of water is also included in this study.

Table 5.9: Changes in the input parameters different from those used in Case Study #1. These changes reflect the influence of water and sulfur dioxide on the performance of the solid sorbent.

Input variable	Value	Units
Flue gas pre-treatment		
SO ₂ polisher used?	Yes	
SO ₂ polisher outlet concentration	1	ppmv
Drop in pressure across the pre-treatment unit	6,894	Pa
Water vapor mole fraction at pre-treat outlet	10	%
Degradation		
Solids purge fraction	0.004	%
Degradation parameters	Yes	
	<u>SO₂</u>	Yes
SO ₂ capture efficiency (moles in - moles out)/moles in	100	%
SO ₂ gas release in regenerator (moles in -moles out as gas)/moles in	0	%
	<u>Water adsorption</u>	Yes
Water uptake (% removed from flue gas)	30	%
Water regeneration efficiency (%)	30	%
Competitively adsorbed water (influence on CO ₂ capacity)	-0.5	moles/kg solid

This case study follows the same calculation method used in the first case study. Additional steps are required, however, in order to quantify the influence of water and SO₂ on the solid sorbent. These steps are shown in detail while the calculation steps identical to those in the previous case study are summarized.

5.6.1. Case study #4 calculation

This section shows the calculations required to derive the loadings and flow rates in the CO₂ capture system. The calculations shown below are in the same order as shown in Section 4.6.

Pre-treatment flow rates

In this case, a pre-treatment step is used which acts as both a SO₂ polisher and direct contact cooler. The initial temperature and pressure of the flue gas are unchanged. However, the flue gas flow rates are higher in this system in order maintain a constant net electrical output of 550 MW. The flow rates as are shown in Table 5.6. The flue gas flow rates, shown in Table 5.7, are iteratively calculated in order to achieve the desired net electrical output.

Table 5.10: Flue gas conditions and molar composition upon entering the CO₂ capture system for Case Study #4.

Flue gas conditions	Pre-treatment inlet	Pre-treatment outlet
Flue gas temperature (K)	327	317
Flue gas pressure (kPa)	101.3	94.4
<u>Flue gas composition</u>		<u>kmol/hr</u>
Nitrogen (N ₂)	79,900	80,884
Oxygen (O ₂)	4,900	4,929
Water Vapor (H ₂ O)	18,300	11,100
Carbon Dioxide (CO ₂)	14,100	14,100
Carbon Monoxide (CO)	<1	<1
Hydrochloric Acid (HCl)	<1	<1
Sulfur Dioxide (SO ₂)	28	<1
Sulfuric Acid (equivalent SO ₃)	<1	<1
Nitric Oxide (NO)	9	9
Nitrogen Dioxide (NO ₂)	<1	1
Ammonia (NH ₃)	<1	<1
Argon (Ar)	900	900
Total	118,100	110,900

At the pre-treatment outlet, the flue gas has an SO₂ concentration of 1 ppm and a temperature of 318 K (45°C), which is 10 K less than the initial temperature. Note that the flue gas flow rates are approximately 5% higher than the ideal (no degradation case) due to the larger plant size and higher fuel consumption.

Calculate flue gas blower stream conditions

The flue gas stream conditions are calculated using the same method shown in Case 1. These results are summarized below. Note that the pressure change is higher in the blower due to the pressure drop across the pre-treatment unit.

Calculation step	Dependent variable	Value	Units
a	$m_{gas}^{A,in}$	3,250,000	Kg/hr
b	ΔP^{blower}	37,400	Pa
c	ΔT^{blower}	53	K
d	$T_{gas}^{A,in}$	370	K

Calculate the rich loading

The results for the rich loading calculations are summarized below. The adjusted maximum loading in the adsorber is lower than in the ideal case due to the influence of water. The lower maximum loading results in a lower rich loading as well.

Calculation step	Dependent variable	Value	Units
a	$p_{CO_2}^{A,in}$	15,700	Pa
b	$q_{adj,max}$	2.4	mol CO ₂ /kg
c	$b_{CO_2}^A$	$5.07 \cdot 10^{-4}$	1/Pa
d	$q_{adj,eq.}^A$	2.13	mol CO ₂ /kg
e	q_{rich}	2.13	mol CO ₂ /kg

Calculate lean loading

A summary of the lean loading calculations are shown below. Like the rich loading calculation, the lean loading in the regenerator is lower than in the ideal case due to the lower adjusted maximum capacity of the solid sorbent.

Calculation step	Dependent variable	Value	Units
a	$b_{CO_2}^R$	$4.65 \cdot 10^{-6}$	1/Pa
b	$q_{adj.eq.}^R$	0.66	mol CO ₂ /kg
c	q_{lean}	0.66	mol CO ₂ /kg

Calculate adsorber flow rates

a. Mass flow rate of gas at the adsorber outlet

The mass flow rate of flue gas at the adsorber outlet is quantified using equation 4.3. The calculations shown here are the same as those used in the previous solid sorbent case studies. Note that the gas flow rates of water and SO₂ are proportionately lower than in the ideal case because of the interaction between the solid and these constituents.

Dependent variable	Value	Independent variable	Unit	Calc.
$m_{gas}^{A,out}$	2,630,000		kg/hr	=
	62,000	$m_{CO_2(gas)}^{A,out}$	kg/hr	+
	0	$m_{SO_2(gas)}^{A,out}$	kg/hr	+
	300	$m_{NO_X(gas)}^{A,out}$	kg/hr	+
	156,000	$m_{O_2(gas)}^{A,out}$	kg/hr	+
	2,240,000	$m_{N_2(gas)}^{A,out}$	kg/hr	+
	140,000	$m_{H_2O(gas)}^{A,out}$	kg/hr	+
	38,000	$m_{inert(gas)}^{A,out}$	kg/hr	

b. Mass flow rate of solids at the adsorber inlet

The mass flow rate of solids at the adsorber inlet is calculated using Equation 4.8. The mass flow rate of adsorbed SO₂ ($m_{SO_2(solid)}^{A,in}$) is calculated using Equation 4.38 and the mass flow rate of solid sorbent degraded by SO₂ ($m_{solid-SO_2}^{A,in}$) is calculated using Equation 4.39. The solid flow rate is higher than in the ideal case because of the reduced working capacity of the solid and the uptake of SO₂. Unlike the ideal case, degraded solid sorbent and adsorbed SO₂ now circulates through the system.

Dependent variable	Value	Independent variable	Unit	Calc.
$m_{solid}^{A,in}$	10,200,000		kg/hr	=
	248,000	$m_{CO_2(solid)}^{A,in}$	kg/hr	+
	189,000	$m_{SO_2(solid)}^{A,in}$	kg/hr	+
	0	$m_{NO_X(solid)}^{A,in}$	kg/hr	+
	0	$m_{O_2(solid)}^{A,in}$	kg/hr	+
	0	$m_{N_2(solid)}^{A,in}$	kg/hr	+
	140,000	$m_{H_2O(solid)}^{A,in}$	kg/hr	+
	8,570,000	$m_{solid-CO_2}^{A,in}$	kg/hr	+
	1,020,000	$m_{solid-SO_2}^{A,in}$	kg/hr	+
	0	$m_{solid-NO_X}^{A,in}$	kg/hr	+
	0	$m_{solid-O_2}^{A,in}$	kg/hr	+
	0	$m_{solid-N_2}^{A,in}$	kg/hr	

c. Mass of solids at the adsorber outlet

The mass flow rate of solids at the adsorber outlet is calculated using Equation 4.9. The mass flow rate of adsorbed SO_2 is calculated using Equation 4.10 and the mass flow rate of degraded solid remains unchanged from the adsorber inlet to the adsorber outlet.

Dependent variable	Value	Independent variable	Unit	Calc.
$m_{solid}^{A,out}$	10,800,000		kg/hr	=
	84,000	$m_{CO_2(solid)}^{A,out}$	kg/hr	+
	189,000	$m_{SO_2(solid)}^{A,out}$	kg/hr	+
	200,000	$m_{H_2O(solid)}^{A,out}$	kg/hr	+
	8,570,000	$m_{solid-CO_2}^{A,out}$	kg/hr	+
	1,020,000	$m_{solid-SO_2}^{A,out}$	kg/hr	

Calculate the regenerator mass flow rates

m.) Mass flow rate of solids at the regenerator inlet

The mass flow rate of solids at the regenerator inlet is the same as the mass flow rate of solids at the adsorber outlet.

n.) Mass flow rate of regenerator purge gas

In this scenario, water is removed from the regenerator at a rate of 3000 kilograms per hour, which is comparable to the flow rate of steam purge removed from the water degradation only case study. However, these values are very different from the no degradation and SO₂ degradation case studies, which require 54 and 56 tonnes of added purge steam per hour respectively.

Dependent variable	Value	Independent variable	Unit	Calc.
$m_{steam}^{R,purge}$	-		kg	=
	3,000		H2O/hr	
	-164	$\frac{M_{CO_2(gas)}^{R,out} * P^{R,out} - P_{CO_2} (M_{CO_2}^{R,out} + M_{H_2O(solid)}^{R,in} + \sum M_{i(gas)}^{R,out})}{P_{CO_2}}$	kmol H2O/hr	*
	18	MW_{H_2O}	g/mo1	

o.) Mass flow rates of gas at the regenerator outlet

The mass flow rate of gas at the regenerator outlet is 27 tonnes per hour higher than the ideal (no degradation) case study representing a 5% increase. This value is only 3 tonnes per hour higher than the water degradation case study and 5 tonnes higher than the SO₂ only degradation case (less than 1%).

Dependent variable	Value	Independent variable	Unit	Calc.
$m_{gas}^{R,out}$	613,000		kg/hr	=
	556,000	$m_{CO_2(gas)}^{R,out}$	kg/hr	+
	0	$m_{SO_2(gas)}^{R,out}$	kg/hr	+
	57,000	$m_{H_2O(gas)}^{R,out}$	kg/hr	

p.) Mass flow rate of solids at the regenerator outlet

Like the previous case study, this study assumes that only 30% of the water is vaporized in the regenerator in keeping with a 2011 NETL patent regarding the uptake and removal of water in a solid sorbent-based CO₂ capture (Pennline, et al., 2011). There is, however, a sizable mass flow rate of solid sorbent degraded by SO₂ ($m_{solid-SO_2}^{R,out}$) which accounts for about 10% of the solids exiting the regenerator. Overall, the flow rate of solids exiting the regenerator is approximately 45% higher than the ideal study without degradation, 22% higher than the SO₂ degradation case, and 8% higher than the water degradation case. These results indicate that the detrimental effects of water and SO₂ together can contribute very significantly to the mass flow rate of material flowing through the system.

Dependent variable	Value	Independent variable	Unit	Calc.
$m_{solid}^{R,out}$	10,200,000		kg/hr	=
	248,000	$m_{CO_2(solid)}^{R,out}$	kg/hr	+
	189,000	$m_{SO_2(solid)}^{R,out}$	kg/hr	+
	0	$m_{NO_X(solid)}^{R,out}$	kg/hr	+
	0	$m_{O_2(solid)}^{R,out}$	kg/hr	+
	0	$m_{N_2(solid)}^{R,out}$	kg/hr	+
	140,000	$m_{H_2O(solid)}^{R,out}$	kg/hr	+
	8,570,000	$m_{solid-CO_2}^{R,out}$	kg/hr	+
	1,020,000	$m_{solid-SO_2}^{R,out}$	kg/hr	+
	0	$m_{solid-NO_X}^{R,out}$	kg/hr	+
	0	$m_{solid-O_2}^{R,out}$	kg/hr	+
	0	$m_{solid-N_2}^{R,out}$	kg/hr	

Calculate transport, discarded, and fresh solid flow rates

d. Discarded solids

The composition of this flow stream is the same as that exiting the regenerator and thereby consists of approximately 10% degraded solid sorbent compared to 14% degraded solids in the SO₂ degradation case study. The influence of the solid purge fraction on the performance of the system is discussed in Section 5.7. Recall from Section 5.5, however, that the selection of a proper solid purge fraction requires a trade-off between working capacity and cost, which is addressed in Chapter 6.

Dependent variable	Value	Independent variable	Unit	Calc.
$m_{solid}^{discarded}$	407		kg/hr	=
	10,200,000	$m_{solid}^{R,out}$	kg/hr	*
	0.00004	$X_{solid\ purge}$	fraction	

e. Transport solids

The mass flow rate of returning solids transported to the regenerator is comparable to the flow rate exiting the regenerator and is similarly higher than the flow rates for the previous case studies.

Dependent variable	Value	Independent variable	Unit	Calc.
$m_{solid}^{transport}$	10,200,000		kg/hr	=
	10,200,000	$m_{solid}^{R,out}$	kg/hr	*
	0.99996	$(1 - X_{solid\ purge})$	fraction	

f. Fresh solids

The flow rate of fresh solid sorbent added to the recirculating solids are 21% higher compared to the SO₂ degradation case study proving that the increase in mass flow rate is constant for the solid flow rates throughout the system. In contrast, recall that case studies #1 and #3 do not use fresh solid sorbent to maintain the working capacity of the solid sorbent.

Dependent variable	Value	Independent variable	Unit	Calc.
m_{solid}^{fresh}	384		kg/hr	=
	9,590,000	$\sum m_{solid-i}^{R,out}$	kg/hr	*
	0.00004	$X_{solid\ purge}$		

Calculate cooling requirement

The mass flow rate of cooling water in the adsorber is about 4% higher than first case study (without degradation). Although one would expect the cooling requirement to be much higher because of the higher solids flow rate, condensation of the water vapor in the flue gas offsets the higher thermal load of the solids and reduces the cooling water requirement. Given this context, it is less surprising that the cooling water flow rate for this case study is slightly (2%) lower than the SO₂ degradation case study and 6% higher than the water degradation only case study.

Dependent variable	Value	Unit
ΔH^{HHX}	455,000,000	kJ/hr
m_{fluid}^{HX}	205,000	kg/hr
$H_{cooling}^A$	1,050,000,000	kJ/hr
$m_{cooling\ water}^A$	10,000,000	kg/hr

Calculate heating requirement

The steam required in the regenerator is 32% higher than the ideal case study due to the higher thermal mass of the solids in addition to the added energy required to vaporize water entrained with the solids. Vaporization of water is an important component of this system shown by the contrast between this scenario and the single-component (SO₂ and water) degradation scenarios. The steam requirement for this case study is 19% higher than the SO₂ degradation scenario, but represents only a 5% increase over theater degradation scenario.

Dependent variable	Value	Unit
$T_{solid}^{CHX,out}$	355	K
$H_{heating}^R$	1,300,000,000	kJ/hr
$h_{steam}^{R,out}$	418	kJ/kg
m_{steam}^R	460,000	kg/hr

Performance estimators

f. Actual rich loading

The actual rich loading for the water and SO₂ degradation case is 0.45 moles CO₂/kg solid lower than in the ideal case due to degradation (from SO₂) and loss of available sorbent caused by pore blockage.

Dependent variable	Value	Independent variable	Unit	Calc.
$q_{actual\ rich}$	1.91			=
	18,300	$M_{CO_2(solid)}^{A,out}$	kmol/hr	*
	1000	Conversion	mol/kmol	/
	9,590,000	$\sum m_{solid-i}^{A,out}$	kg/hr	

g. Actual lean loading

The actual lean loading is approximately 0.2 moles CO₂ per kilogram lower than in the ideal case and 0.1 moles per kilogram lower than the water and SO₂ degradation cases.

Dependent variable	Value	Independent variable	Unit	Calc.
$q_{actual\ lean}$	0.59		mol/kg	=
	5,630	$M_{CO_2(solid)}^{R,out}$	kmol/hr	*
	1000	Conversion	mol/kmol	/
	9,590,000	$\sum m_{solid-i}^{R,out}$	kg/hr	

h. Specific solid requirement

The specific solid requirement is calculated using Equation 4.77. This value is almost 40% higher than the 580 kg solid per mole CO₂ due both to degradation (which accounts for 10% of the solid sorbent) and the higher flow rate of flue gas which results in higher sorbent requirement to capture 90% of the CO₂ entering the CCS system.

Dependent variable	Value	Independent variable	Unit	Calc.
R	804		kg/kmol	=
	10,200,000	$m_{solid}^{A,in}$	kg/hr	/
	12,600	$M_{CO_2(gas)}^{R,out}$	kmol/hr	

i. Auxiliary electrical load

The auxiliary electrical load for the water and SO₂ degradation case is shown below. Note that the electrical requirements of the systems are approximately 20 MW higher than Case study #1 (no degradation) due to the higher solid and gas flow rates.

Dependent variable	Value	Independent variable	Unit	Calc.
$\sum MW_e$	114		MW _e	=
	43	<i>FG Blower MW_e</i>	MW _e	+
	3	<i>Transport return conveyor MW_e</i>	MW _e	+
	0	<i>HX Pump MW_e</i>	MW _e	+
	2	HX Compressor	MW _e	+
	66	<i>CO₂ compressor MW_e</i>	MW _e	

j. Electric equivalent loss

The electric equivalent loss in Case study #4 is 13 MW higher than the first case study (which was 80 MW_{equivalent}) due to the higher heating requirement.

Dependent variable	Value	Independent variable	Unit	Calc.
<i>EEL</i>	93			=
	0.222	HHE		*
	460,000	m_{steam}^R	Kg/hr	*
	3,249	$h_{steam}^{R,initial}$	kJ/kg	*
	$(2.78 * 10^{-7})$	Conversion	MW _e *hr/kJ	

k. Total electrical loss

The total electricity loss for Case study #4 is about 41 MW above the ideal case.

Dependent variable	Value	Independent variable	Unit	Calc.
<i>ToL</i>	207		MW _e	=
	93	EEL	MW _e	+
	114	Total auxiliary load	MW _e	

l. Plant efficiency

The efficiency of the power plant is approximately 1.3% lower than Case study #1 because of the added electrical load and electrical equivalent losses of the CO₂ capture process. Note that these results are compared to other case study scenario in Chapter 7 as part of a larger discussion regarding the performance and cost of full-scale power plants equipped with solid sorbent-based CO₂ capture.

Dependent variable	Value	Independent variable	Unit	Calc.
<i>Plant efficiency</i>	28.3		%HHV	=
	550	MW	MW _e	/
	227,000	Fuel flow rate	kg/hr	/
	30,840	Fuel HHV as received	kJ/kg	*
	$3.6 * 10^5$	Conversion		

5.6.2. Case study #4 discussion

The system described in this degradation case study is larger, more complex, and less efficient than the three previous cases. Perhaps the most distinguishing characteristic of this systems is the larger

total electrical loss. The CCS system described in this section requires 207 MW in order to operate compared to 174 MW in the ideal case. This is caused by several compounding factors. First, the addition of degradation products and water interactions to the system increases the amount of solids circulating through the system. This has the effect of raising the heating load in the system and the subsequent steam requirement in the regenerator. Since less steam is then available to produce electricity, the base power plant must be larger in order to produce 550 MW of electricity. A larger plant increases the flow rate of flue gas, thereby raising the quantity of solid sorbent required in order to capture 90% of CO₂. Thus, the system is burdened by not only by the influence of degraded products circulating through the system but also the need to capture additional CO₂ in order to meet the 90% capture requirement and produce 550 MW of electricity.

Although the pre-treatment unit removes the vast majority of the SO₂ entering the system (down to 1 ppm), approximately 10% of the total flow rate of solids in the system is comprised of solid sorbent degraded by SO₂ at steady state conditions. The accumulation of degraded products reduces the working capacity of the solid sorbent resulting in a higher specific solid requirement (804 kilograms per kilomole CO₂ compared to 580 kg per kilomole CO₂). However, it is important that these values are sensitive to assumptions regarding the solid purge fraction, which is discussed in the Section 5.8.

The circulation of a large fraction of degradation products is one of the disadvantages of solid sorbent-based CCS compared to the liquid solvent system counterpart. In a liquid-based CCS system, the degraded products may be separated from the functioning solvent which may then be removed through mechanical or chemical processing. Solid-based systems, however, must cope with a much larger fraction of degraded products because degraded and non-degraded sorbent cannot be separated. Instead, the active and degraded sites are bound to the surface of substrate particles and therefore inseparable. The inability to separate and treat degraded sorbent results in a higher solid requirement, higher energy penalty, and greater cooling water requirements. The economic implications of the higher mass and energy requirements caused by degradation are discussed in Chapter 7.

Figure 5.11 shows the influence of CO₂ capture efficiency and equilibrium pressure on the mass flow rate of solids for case studies #1 (no degradation) and #4 (water and SO₂ degradation). Here, the equilibrium pressure is expressed at the flue gas inlet and outlet conditions of the adsorber vessel representing the two extremes for CO₂ adsorption. In both cases, the solid flow rate increases with CO₂ capture efficiency, but the contrast between these two scenarios is more pronounced at higher CO₂ capture efficiencies because of the growing difference in the driving force (CO₂ partial pressure) at higher capture efficiencies. Note that in both the inlet and outlet equilibrium scenarios, the flow rate of solid sorbent is always higher when accounting for degradation.

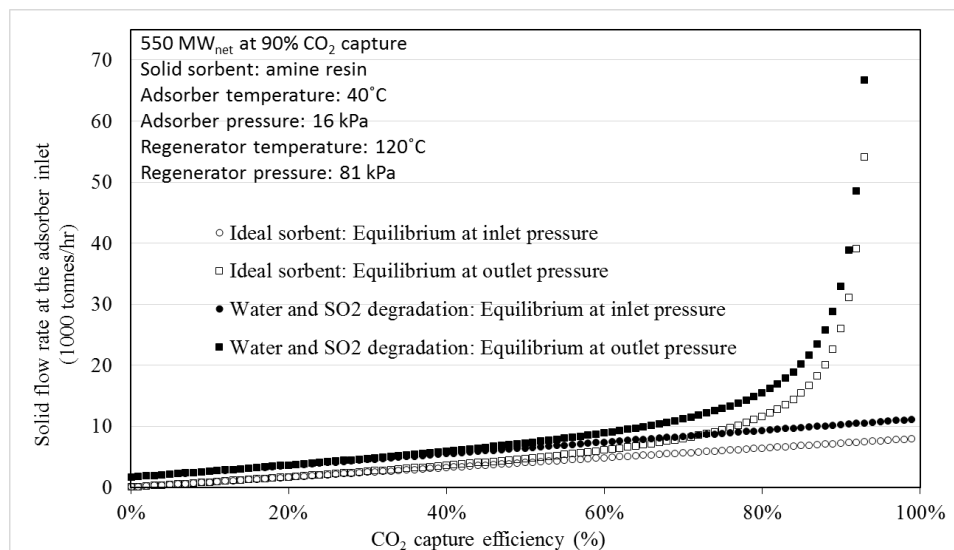


Figure 5.11: Mass flow rate of solids at the adsorber inlet as a function of the CO₂ capture efficiency. Assumptions about the equilibrium CO₂ pressure are varied for both the ideal (Case study #1) and water and SO₂ degradation case study (Case study #4).

It is important to stress that these cases do not reflect the current state-of-the-technology. Rather, these results are included here to demonstrate the utility of the model, and reflect the performance of a hypothetical solid sorbent material. Later sections will estimate the performance of other adsorbents based on theoretical models produced by CCSI and currently available materials.

5.7. Summary results for Case Studies #1 through #4

A summary comparison of these idealized case studies is presented in Table 5.12. These studies show that interactions between the solid and water and/or SO₂ can have a significant influence on the size and performance of the CO₂ capture system due to the higher flow rates of solid sorbent required in order to capture 90% of the CO₂ emissions from the base plant. In these cases, the best achievable system has a thermal efficiency of 29.6%, and degradation reduces the thermal efficiency of the plant by 0.6 to 1.3 percentage points for the nominal conditions described in these four case studies.

Table 5.11: Performance results for solid sorbent system using performance parameters informed by deterministic CCSI model results. The case study plants shown below have a net electrical output of 550 MW and capture 90% of the CO₂ from the flue gas.

Performance estimator	Units	#1: Ideal without degradation	#2: Ideal with SO₂ degradation	#3: Ideal with water degradation	#4: Ideal with SO₂ and water degradation
Actual rich loading	moles CO ₂ /kg solid	2.58	2.25	2.13	1.91
Actual lean loading	moles CO ₂ /kg solid	0.79	0.69	0.66	0.59
Specific solid requirement	kg solid/kmol captured CO ₂	580	676	708	804
Gross plant output	MW _g	700	710	713	715
Net plant output	MW _e	550	550	550	550
CO ₂ compress.	MW _e	63	64	65	66
Conveyors	MW _e	2	2	2	3
FG blower	MW _e	35	42	43	43
HX Compress.	MW _e	1	2	2	2
HX Pump	MW _e	0	0	0	0
Total Auxiliary electrical load	MW _e	101	110	113	114
Electrical equivalent loss (steam use)	MW _e	73	78	89	93
Total electrical loss	MW _e	174	189	201	207
Plant efficiency	%HHV	29.6	29.0	28.5	28.3

5.8. Effect of solid purge fraction

The specific solid requirement can be reduced by decreasing the quantity of degraded material circulating throughout the system. This is accomplished by increasing the solid purge fraction and replacing the discarded solids with fresh solid sorbent. Figure 5.12 shows how the solid purge rate influences the specific solid requirement for 90% CO₂ capture.

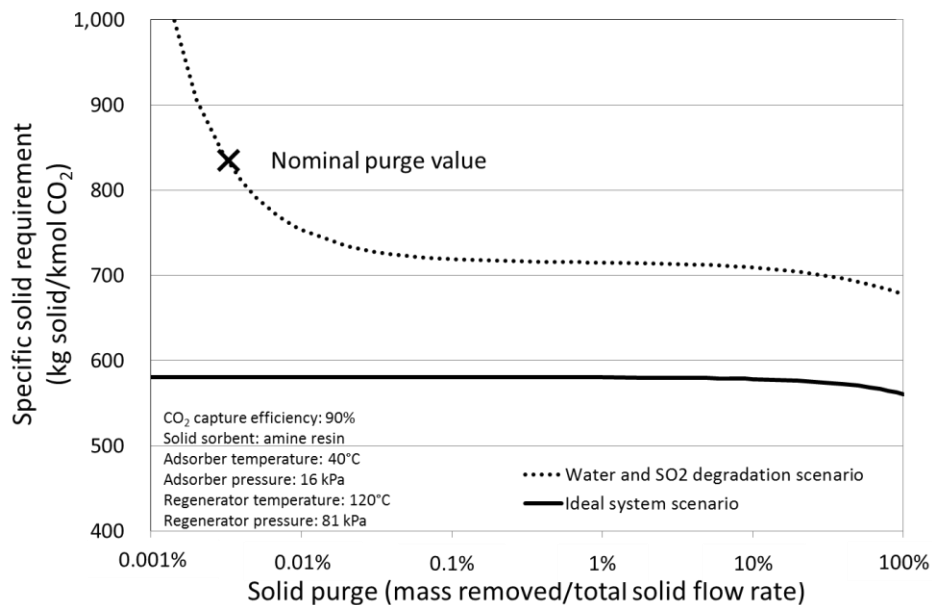


Figure 5.12: Specific solid requirement as a function of the solid purge fraction. The ideal sorbent system (Case study #1) always requires less solid material per mole of CO₂ captured than Case study #4 in which water and SO₂ hinder CO₂ uptake. Selection of the nominal solid purge value is based on reducing the levelized cost of electricity and not reducing the mass flow rate of solids.

For the nominal conditions and values shown in these two cases, Case study #4 consistently requires a larger mass flow rate of solids compared to the ideal case (Case study #1) due to the solid sorbent's reduced working capacity. This is true even in a "once-through" system in which the purge fraction is 100%, which is shown to the far right of Figure 5.12 because water is reducing the solid sorbent's capacity for CO₂.

The influence of SO₂ degradation is shown by the difference in the slope of these curves, especially at lower purge fractions (the left side of Figure 5.12). In the ideal case, the system sorbent experiences no change in efficiency even as the purge fraction approaches zero because there is no lost capacity caused by SO₂ degradation. In contrast, the degraded solid sorbent from the second scenario experiences a decrease in CO₂ capacity and thus, the system requires much more solid sorbent to achieve the same proportion of CO₂ capture. Thus, lower purge fractions result in higher disparities between the efficiency of the solid sorbent for the ideal and non-ideal cases.

The nominal value used for cases that consider degradation is 0.004% as indicated in Figure 5.12. Note that the selection of this value is not made on the basis of reducing the mass flow rate of solids in the system. If this were true, Figure 5.12 indicated that the best choice would be to use a solid purge value of 100%. Instead, the chosen value approximates the lowest overall cost of this system as measured by the levelized cost of electricity. However, the economics of this system are a topic addressed in later chapters of this work (see Chapters 6 and 7).

The solid purge fraction also influences the heat exchange fluid flow rate (i.e. cooling water in the adsorber, steam in the regenerator, and a combination of steam and water in the cross-flow heat exchanger) as shown in Figure 5.13. Notice that the mass flow rates increase at lower purge values due to higher solid flow rates.

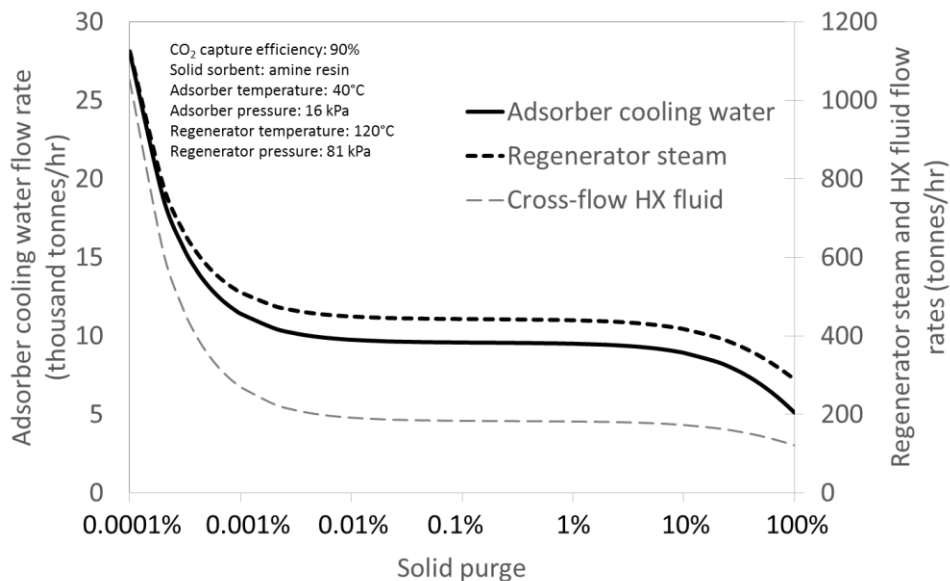


Figure 5.13: Flow rates of heat exchange fluids in the adsorber, regenerator, and cross-flow heat exchangers as a function of the solid purge fraction for Case study #4. (water and SO₂ degradation).

A larger flow rate of solid sorbent also increases the energy penalty of the CO₂ capture process. In Case study #1, the energy penalty is 174 MW_{equiv.} compared to 207 MW_{equiv.} in Case study #4. The cause of this increase is several-fold: More steam is required in the regenerator to overcome the larger thermal mass of the solids. This steam is diverted from the base power plant. Hence, a larger power plant must be constructed in order to provide the same flow rate of steam for electricity production. The larger plant produces greater quantities of flue gas, and so the CO₂ capture equipment requires more electricity in order to operate.

5.9. Case Studies #5 and #6: Systems informed by CCSI's model

This section introduces two additional case studies that use performance data developed by NETL under the Carbon Capture Simulation Initiative (CCSI). These case studies differ from the previous series of case studies in several respects including the plant's efficiency at converting steam to electricity, regeneration steam temperature, and solid sorbent characteristics among others. Thus, the results reflect the performance results from CCSI's models and are unique to their multi-stage adsorber and moving bed

regenerator designs (Cozad, et al., 2010; Lee, et al., 2011). The changes to the plant operation and performance parameters values that differ from Case study #1 are shown in Table 5.12.

Although most of the parameter values used to represent the CCSI model are derived from and vetted using the results and assumptions developed by CCSI (DOE/NETL, 2012), sensitivity data from a more recent iteration of the CCSI model is used to calculate the rich loading using a response surface model. The response model assumes the adsorption reaction would reach equilibrium with gaseous CO₂ at the adsorber inlet and calculates an adsorber kinetic parameter value that achieves a rich loading value consistent with CCSI's analysis (Equation 4.49). Information regarding the sensitivity analysis and response surface model derivation is available in Section 4.3.3, Appendix G, and Appendix H.

Three constants are altered from the original model formulation in order to better match CCSI's design. These values include the temperature of the solids in the regenerator, the temperature of the heating steam at the regenerator inlet, and the temperature of the steam at the regenerator outlet. In the previous case studies (i.e. Case Studies #1 through #4), the upper temperature limit for the heating steam is 408K (135°C) in order to limit the denaturing effects of high temperatures on amine-based solid sorbents. This constraint is relaxed for both the solid sorbent and the steam in order to allow temperatures of 408 K (135°C) for the solids and 438 (165°C) for the heating steam. The enthalpy of the steam exiting the regenerator was adjusted as well in keeping with the values from CCSI's report (DOE/NETL, 2012). Other notable changes to the system include alteration of the kinetic parameters, water adsorption, and water regeneration parameter values.

Table 5.12: Changes to the performance parameter values used for the CCSI case studies.

Parameter	Assumed Value	Units
Reference values		
CCS heating steam exiting enthalpy	1,082	kJ/kg
Steam-solid temperature approach in regenerator	85	K
Temperature of steam at the regenerator inlet	438	K
System configuration		
Direct contact cooler?	Yes	
Pressure drop across pre-treatment unit	6,894	Pa
Temperature exiting DCC	317	K
Water vapor mole fraction at adsorber inlet	10	%
Sorbent properties		
Solid sorbent name	32D	
Heat of reaction	-67	kJ/mol CO ₂
Maximum CO ₂ loading	3.5	moles CO ₂ /kg dry solid
Capture		
Adsorber		
Adsorber Operating Temperature	327	K
Cooling water temperature	32	
Effective Adsorption Kinetics (% Equilib. Capacity)*	65	%
Regenerator		
Effective Desorption Kinetics	11	%
CO ₂ Pressure in Product Gas Stream	42	kPa
Regenerator Operating Temperature	408	K
Cross-flow heat exchanger		
Overall heat transfer coefficient	300	W/m ² -K
Temperature of solids at hot-side HX outlet	391	K
Degradation		
Water adsorption	Yes	
Water regeneration efficiency	79	%
Water uptake (% removed from flue gas)	92	%

*Value is calculated using Equation 4.49.

Like the previous series of case studies, this work uses separate cases to show the performance of the CO₂ capture system with and without the influence of SO₂. When the influence of SO₂ is included,

the system is modified to include SO₂ polishing and a higher solid purge fraction as was shown for Case Study #2 (see Table 5.5). The influence of water, however, is not modelled separately since the chemical uptake and regeneration of water is already included in the deterministic results published by CCSI (DOE/NETL, 2012).

For the sake of clarity and brevity, this section will not repeat the model walkthrough exercise used in the previous section. The performance results, however, for the two CCSI case studies are presented in Table 5.13. A complete listing of the parameter values used in these case studies is available in Appendix J should the reader wish to reproduce the results on their own.

Table 5.13: Performance results for solid sorbent system using performance parameters informed by deterministic CCSI model results. The plants shown below have a net electrical output of 550 MW and capture 90% of the CO₂ from the flue gas.

Performance estimator	Units	Case study #5: CCSI without degradation	Case study #6: CCSI with SO₂ degradation
Actual rich loading	moles CO ₂ /kg solid	2.22	1.98
Actual lean loading	moles CO ₂ /kg solid	0.35	0.31
Specific solid requirement	kg solid/kmol captured CO ₂	546	628
Gross plant output	MW _g	747	751
Net plant output	MW _e	550	550
CO ₂ compressor	MW _e	76	77
Conveyors	MW _e	2	2
FG blower	MW _e	50	51
HX Compressor	MW _e	7	7
HX Pump	MW _e	2	2
Total Auxiliary electrical load	MW _e	137	140
Electrical equivalent loss (steam use)	MW _e	190	200
Total electrical loss	MW _e	327	340
Plant efficiency	%HHV	24.4	24.0

The results summarized in Table 5.13 show that the specific solid requirement for Case Study #5 is lower than the ideal case shown in Case Study #1 by 6%. The cause for this improvement is two-fold: First, the solid sorbent simulated by CCSI is different than the solid sorbent modelled in the first series of case studies. This solid sorbent has a higher maximum capacity than the amine resin shown previously (3.5 moles CO₂/kg solid sorbent compared to 2.9 moles CO₂/kg solid sorbent). Second, CCSI assumes higher operating temperatures in the regenerator, which lowers the lean loading and improves the working capacity of the solid.

It is also worth noting that while the solid sorbent system excluding degradation produces the same net electrical output as the plant that includes degradation, it has a slightly higher net plant efficiency, lower electrical requirement, and lower steam use in the regenerator. The drop in net plant efficiency for the plant with degradation is caused by the poorer performance of the solid sorbent, which increases the required solid flow rate and subsequent steam and electrical requirements of the system.

5.10. Performance case studies based on expert elicitation

The case studies described in this section combine lessons learned from the previous case studies with estimated parameter values elicited from experts for . The new performance parameter values address the limitations of both the CO₂ capture process and solid sorbent materials to estimate the performance of a CO₂ capture system. These cases, labelled the “Present case” and “Future case,” describe the expected results if a full-scale system were built using today’s technology, versus a system built ten years in the future given steady and moderately increasing levels of funding. Like the four “ideal sorbent” cases, case studies #7 through #10 represent the present scenario with increasing levels of degradation, while case studies #11 through #14 represent the future scenario. Appendix B includes the questionnaire used in the elicitation exercise while the detailed results and distributions are included in Appendix I. Details regarding the specific treatment of water and SO₂ are discussed later in this section.

The performance parameters values for the Present and Future cases are shown in Table 5.14 with references to the information source. These values show the configuration absent the influence of degradation.

Case studies #7 through #14 differ from the previous in several in several ways. First, the maximum CO₂ capacity is expected to increase from 2.9 (the same as the previous cases) to 3.9 moles per kilogram as better materials are developed. The influence of water may also improve as the chemistry and design of the materials become available. The heat transfer properties of the adsorber, regenerator, and cross-flow heat exchangers are similar to Case Studies #1 through #4, although the values for the cross-flow heat exchanger resemble the moving bed design rather than the fluidized bed.

Table 5.14: Performance parameter values for the elicited performance scenarios

Input variable	Present Elicitation	Future Elicitation	Units	References and notes
Configuration				
Flue Gas Pre-treatment				
Direct contact cooler used?	Yes	Yes		(DOE/NETL, 2012)
Pressure drop across the pre-treat unit	7	7	kPa	(Versteeg, 2012)
SO ₂ polisher outlet concentration	24	24	ppmv	(Carnegie Mellon University, 2014)
SO ₂ polisher used?	No	No		
Temperature exiting DCC	317	317	K	(Borgert, 2015)
Water vapor mole fraction at adsorber inlet	0.10	0.10	fraction	(Borgert, 2015)
Sorbent Properties				
Heat capacity	1.0	1.0	kJ/kg dry solid-K	This work
Heat of reaction	-60	-60	kJ/mol CO ₂	This work
Langmuir isotherm parameter (b ₀)	4.92*10 ⁻¹⁴	4.92*10 ⁻¹⁴	Pa ⁻¹	This work
Maximum CO ₂ loading*	2.9	3.9	moles CO ₂ /kg dry solid	This work
CO₂ Capture System				

Adsorber				
Adsorber operating temperature	327	327	K	(DOE/NETL, 2012)
Adsorber overall heat transfer coefficient*	300	385	W/m ² -K	This work
Adsorber pressure drop	29	29	kPa	(DOE/NETL, 2012)
CO ₂ equilibrium pressure	15.7	15.7	kPa	This work
Effective adsorption kinetics*	83	90	% equilib. capacity	This work
Regenerator				
CO ₂ pressure in product gas stream	42	42	kPa	(DOE/NETL, 2012)
Effective desorption kinetics*	11	10	%	This work
Regenerator operating temperature	383	383	K	This work
Regenerator overall heat transfer coefficient*	55	73	W/m ² -K	This work
Cross-flow heat exchanger				
Cross-flow heat exchanger overall heat transfer coefficient*	55	73	W/m ² -K	This work
Temperature of solids at hot-side HX outlet	355	355	K	(DOE/NETL, 2012)

*Values derived from the expert elicitation exercise. Details are available in Appendices I and J

The Present and Future cases both use a flue gas pre-treatment system in order to reduce the water vapor concentration prior to entering the adsorber in order to match the process described by CCSI. The pressure drop across the flue gas pre-treatment unit, flue gas temperature change, and gas composition resulting from pre-treatment, however, are derived from the process used in the IECM.

The properties of the solid sorbent used in these cases are the same as the amine resin described in Chapter 2 of this work. An exception, however, is the maximum loading of the solid sorbent determined by the expert elicitation exercise. The nominal values for the Present and Future cases are the averages of the “best estimate” reported by expert respondents.

The CO₂ capture system parameters are derived from the CCSI design. Exceptions are based upon responses from the expert elicitation exercise and thermal restrictions in the regenerator as described in the previous section. The equilibrium CO₂ pressure in the adsorber is based on the inlet conditions in order to create an easily understood anchoring data point during the expert elicitation process. Experts were asked to estimate the kinetic parameter based on this assumption in order to determine the rich loading. More details regarding the expert elicitation exercise are available in Appendix B.

Degradation is modelled for both the Present and Future case scenarios. The parameters used to describe degradation are shown in Table 5.15 below. The water adsorption and regeneration efficiencies are derived from the CCSI process described in (DOE/NETL, 2012). Parameter values describing the influence of water on CO₂ uptake, however, are from the expert elicitation exercise. Scenarios describing SO₂ degradation assume that 100% of the SO₂ is irreversibly adsorbed from the flue gas.

Table 5.15: Degradation parameter values used in the elicited performance scenarios. Like the previous case studies, the solid purge fraction is adjusted to this higher value (0.004%) when SO₂ degradation occurs. Otherwise, the value is negligibly small (0.00001%).

Input variable	Present Elicitation (Case studies #7 through #10)	Future Elicitation (Case studies #11 through #14)	Units	References and notes
Degradation				
SO ₂ capture efficiency (moles in - moles out)/moles in	100	100	%	This work
SO ₂ gas release in regenerator (moles in - moles out as gas)/moles in	0	0	%	This work
Solids purge fraction	0.004	0.004	%	This work
Water influence on CO ₂ capacity*	-0.02	0.6	mol/kg	This work
Water regeneration efficiency	79	79	%	(DOE/NETL, 2012)
Water uptake (removed from flue gas)	92	92	%	(DOE/NETL, 2012)

*Values derived from the expert elicitation exercise. Details are available in Appendices I and J.

Results for the four cases that are based on the Present case study are shown in Table 5.16. Case study #7 shows the performance of the system without degradation as informed by the results of the expert elicitation exercise. This system circulates just over a tonne of solid per kilomole of captured CO₂ compared to the 580 kg of solid in the ideal scenario shown in Case study #1. This decrease in performance is caused by a reduction in the working capacity of the solid. The working capacity is lower than the ideal case because of kinetic limitations to the adsorption and desorption reactions.

The degradation scenarios suggest a significant reduction in plant performance. Case study #8 shows that SO₂ reduces the uptake of CO₂ and increases the flow rate of solids in the CO₂ capture system thereby increasing the overall steam and electrical demands of the process. Case study #9 suggests that water does not exert a strong influence on the working capacity of the solid, but greatly increases the steam requirement in order to overcome the sensible and latent heat requirements of water during regeneration. Case study #10 suggests a significant reduction in performance measured by both solid flow rate and plant efficiency caused by the combined effects of water and SO₂ degradation.

Table 5.16: Results for the Present case scenarios.

Performance estimator	Units	Case study #7: Present without degradation	Case study #8: Present w/ SO ₂ degradation	Case study #9: Present w/ water degradation	Case study #10: Present w/ SO ₂ & water degradation
Actual rich loading	moles CO ₂ /kg solid	1.80	1.66	1.79	1.65
Actual lean loading	moles CO ₂ /kg solid	0.77	0.71	0.77	0.71
Specific solid requirement	kg solid/kmol captured CO ₂	1,005	1,101	1,016	1,111
Gross plant output	MW _g	703	714	721	723
Net plant output	MW _e	550	550	550	550
CO ₂ Compress.	MW _e	63	65	68	68
Conveyors	MW _e	3	4	4	4
FG blower	MW _e	35	43	45	45
HX Compress.	MW _e	2	2	2	2
HX Pump	MW _e	0	0	0	0
Auxiliary electrical load	MW _e	103	113	118	119
Electrical equivalent loss	MW _e	78	81	115	117
Total electrical loss	MW _e	181	194	233	236
Plant efficiency	%HHV	29.3	28.8	27.4	27.2

The results of the present case scenarios suggest that the performance of the solid sorbent system using today's available materials and technology are significantly hindered by degradation and kinetic limitations as apparent by the increase in the specific solid requirement and decrease in the plant efficiency.

Similar results for the future scenarios are shown in table 5.17. Case studies #11 through #14 benefit from improvements to the maximum CO₂ capacity and interactions with water as well as better adsorption and desorption kinetics. For example, results for the future case without degradation experiences a near doubling of the working capacity to 1.0 mole CO₂ per kilogram compared to the 0.6 moles in the Present case (Case #7). The better working capacity results in a 40% reduction to the specific solid requirement and a subsequent increase the plant efficiency.

The degradation case studies offer similar improvements to the system performance compared to the Present case scenarios. The added adsorption capacity caused by favorable interactions with water are particularly beneficial as evidenced by the increased loadings and working capacity shown in in Cases #13 and #14. In these cases, the working capacity and specific solid are lower than the case study excluding degradation. Although these improvements are notable, the CO₂ capture process still circulates nearly a ton of solids per mole of CO₂ captured. The implications of this large circulation volume are the subject of later discussions concerning the size and cost of the solid sorbent system.

Table 5.17: Results for the Future case scenarios.

Performance estimator	Units	Case study #11: Future without degradation	Case study #12: Future w/ SO ₂ degradation	Case study #13: Future w/ water degradation	Case study #14: Future w/ SO ₂ & water degradation
Actual rich loading	moles CO ₂ /kg solid	2.62	2.40	3.03	2.73
Actual lean loading	moles CO ₂ /kg solid	1.02	0.94	1.19	1.07
Specific solid requirement	kg solid/mol captured CO ₂	655	729	575	650
Gross plant output	MW _g	699	709	715	716
Net plant output	MW _e	550	550	550	550
CO ₂ Compress.	MW _e	62	63	66	66
Conveyors	MW _e	2	2	2	2
FG blower	MW _e	34	42	44	44
HX Compress.	MW _e	1	1	1	1
HX Pump	MW _e	0	0	0	0
Auxiliary electrical load	MW _e	100	109	113	114
Electrical equivalent loss	MW _e	68	71	100	102
Total electrical loss	MW _e	168	179	213	216
Plant efficiency	%HHV	29.8	29.3	28.1	27.9

5.11. Characterization of performance uncertainty and variability

Any techno-economic analysis, and especially that of new energy and environmental control technologies that are still in the research phase, involves uncertainties regarding performance and costs. These uncertainties come from incomplete information available and numerous assumptions and approximations built into simulations. Some parameters, especially the cost parameters, are influenced

by a larger set of factors outside the scope of the particular study (such as changes in commodity prices that influence construction costs), and fluctuations in these quantities may be seen as “inherent randomness” when viewed within this limited focus area. In addition, there may be significant variability in plant or process design assumptions across different studies or organizations.

One of the distinguishing features of this modelling effort is a probabilistic capability that allows model inputs to be represented by probability distributions rather than single deterministic values. Probability distributions for these parameters reflect the ranges of values reported in the literature, the evolving nature of the technology, and practical considerations in running such plants. In addition, it is possible to use probability distributions for more than one parameter (or all the parameters together) simultaneously.

Table 5.18 lists the uncertainty distributions developed for performance model parameters based on the current literature on solid sorbent-based systems. These distributions reflect both uncertainty and variability in system designs. Details are presented in Appendix A and Appendix I. The data sources from which the parameter values were obtained also included peer-reviewed journal articles, conference papers, books, technical reports, and technical judgments given by experts (Belmabkhout, et al., 2011; Carnegie Mellon University, 2014; Choi, et al., 2009; DOE/NETL, 2011; Drage, et al., 2012).

Almost all the sources reported a CO₂ capture efficiency of 90%. Hence, this value has been used as the default nominal value without any default probability distribution. Also note that the equilibrium CO₂ pressure and adsorber kinetic parameter are not included in Table 5.18. Instead, the rich loading is based on the regression model described earlier in Equation 4.49.

Table 5.18: Solid sorbent system performance model parameters and uncertainties for system which would be built using today’s state-of-the-art solid sorbent system.

Performance parameter	Units	Data (range)	Nominal value	Unc. Representation (Distribution function)	Source
Ads. heat transfer coeff.	W/m ² -K	250 - 600	300	Uniform(250,390)	This work

Ads. pressure drop	kPa	4 - 37	29	Triangular(4,29,37)	(DOE/NETL, 2012)
Ads. temp	K	313 -343	327	Triangular(313,327,343)	(DOE/NETL, 2012)
CO ₂ capture efficiency	%	Mostly 90	90	-	(Rao, 2003)
CO ₂ compressor efficiency	%	75 - 88	80	Uniform(75,88)	(Rao, 2003)
CO ₂ outlet pressure	kPa	20 - 101	42	Triangular(20,42,101)	(DOE/NETL, 2012)
Cross-flow HX solid temp. at hot-side outlet	K	391	355	-	This work
Cross-flow HX overall heat transfer coeff.	W/m ² -K	55-60	55	Uniform(40,80)	(DOE/NETL, 2012)
Final CO ₂ product pressure	MPa	7.58 - 15.16	13.79	Triangular(7.58,13.79,15.16)	(Rao, 2003)
Flue gas blower efficiency	%	70 - 80	75	Uniform(70,80)	(Rao, 2003)
Heat of reaction	kJ/mol CO ₂	-40 - -80	-60	Triangular(-40,-,60,-80)	(Yang, 2003)
Maximum CO ₂ loading	mol CO ₂ /kg dry solid	1.5 – 12.4	2.81	Uniform(2.4,3.4)	(Choi, et al., 2009; Hicks, et al., 2008; Qi, et al., 2014)
Regen. kinetics	%	5 – 20	11	Uniform(4,17)	This work
Regen. overall heat transfer coeff.	W/m ² -K	40 – 80	55	Uniform(40,80)	This work
Regen. temperature	K	378 - 393	383	Uniform(378,393)	This work
SO ₂ capture efficiency (in CO ₂ capture system)	%	99 - 100	100	Uniform(99,100)	(Rao, 2003)
Solid sorbent heat capacity	kJ/kg-K	0.7 - 1.5	1.0	Normal(1.0,0.1)	(DOE/NETL, 2013)
Solids purge fraction	%	0.0 - 0.004	0.004	Uniform(0.002,0.005)	This work
Water influence on CO ₂ capacity	mol CO ₂ /kg solid sorbent	-1 – 1.5	-0.02	Uniform(-.4,.4)	This work

Water regeneration efficiency	%	79	79	Triangular (71,87)	(DOE/NETL, 2012)
Water uptake (% removed from flue gas)	%	92	92	Uniform(83,100)	(DOE/NETL, 2012)

The uncertainty distributions shown in Table 5.18 represent a solid sorbent system built using the materials and process design available as of the time of this writing. Hence, the system assumes the use of an amine-based solid sorbent and reactor designs comparable to the simulated beds assumed in NETL’s 2012 report (DOE/NETL, 2012) with some alteration to accommodate temperature limitations of the solid. These probability distributions are used in Chapter 7 to produce uncertainty estimates regarding the performance and cost of CO₂ capture systems.

5.12. Chapter conclusion

This chapter has demonstrated the function and execution of a performance model for a post-combustion solid sorbent-based CO₂ capture system. The plant-level IECM is used to provide inlet conditions of the flue gas and provide values for variables common throughout the power plant model such as flue gas composition, steam quality and cooling water temperature. These conditions are combined with a default set of performance variables for the CO₂ capture system in order to provide a complete listing of key parameters needed to estimate the mass and energy flows in the CO₂ capture model. Case studies are used as examples to show how the model handles increasingly complex situations in which performance degradation due to flue gas impurities is treated within the capture system model.

The main conclusions from this chapter are as follows: First, solid sorbent systems in the absence of degradation effects show the potential for performance comparable to or better than current liquid amine-based CO₂ capture systems in terms of the net plant efficiency under similar operating conditions. This is evident in three of the four no-degradation case studies (Case studies #1, #7, and #11), which have relatively high plant efficiencies ranging from 29.3% to 29.8%. These values are similar

to the 28-35 % plant efficiency estimates for liquid systems described earlier in Table 1.4. However, the limits imposed on the system by time-dependent solid-gas interactions, water-inhibited CO₂ adsorption, and SO₂ impurities cause substantial reductions in the working capacity of the solid sorbent. These reductions increase the solid flow rate and thermal load needed to achieve a desired CO₂ capture efficiency. This, in turn, results in increased cooling water and steam use in the adsorber and regenerator respectively, resulting in lower plant efficiencies and larger cooling water requirements. The performance of the CO₂ capture system is also sensitive to changes in assumptions such as the CO₂ capture efficiency, solid purge fraction, and interactions with water.

The next chapter demonstrates how the output values from the performance model are used to evaluate the cost of CO₂ capture as well as CO₂ transport and storage costs in a fully integrated pulverized coal-fired power plant.

6. Process cost model

This chapter describes how the performance model described in the previous two chapters can be used to estimate the capital and operating costs of the entire plant. Cost estimation is important in order to determine whether solid sorbent-based CO₂ capture is commercially viable under a given set of circumstances. This chapter describes the method developed to estimate the cost of a coal-fired power plant equipped with solid sorbent-based CO₂ capture.

6.1. Cost estimation method

The procedure used in this this work follows the Electric Power Research Institute's (EPRI) Technical Assessment Guide (TAG) guidelines for cost estimation of power plants. The total capital requirement (TCR) of a solid sorbent-based CO₂ capture system takes into account the direct costs of purchasing and installing all process equipment (denoted as the process facilities capital, PFC), plus a number of indirect costs such as the general facilities cost, engineering and home office fees, contingency costs, and several categories of owner's costs. These costs are added to those of the entire power plant in order to determine the overall cost of the plant. Figure 6.1 outlines the TAG method developed by EPRI.

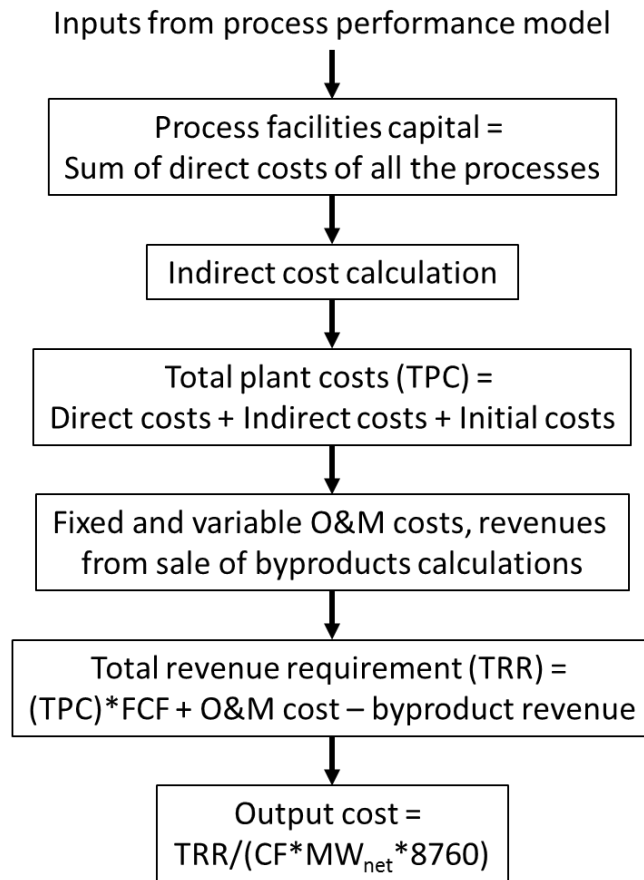


Figure 6.1: Method of cost assessment (EPRI, 1986)

The calculation methods and associated equations for each of the cost components shown in Figure 6.1 are provided in the following sections. Where costs in the literature are given different year-dollars the costs are scaled in the IECM to a given year specified by the user using the Chemical Engineering Plant Cost index or a similar index. These costs as well as the parameters used to determine these costs are shown below.

6.2. Process facilities capital (PFC)

The PFC of a component refers to the capital required to purchase a particular piece of equipment or process area and install it at the plant. Ideally, these costs are known from the equipment manufacturer and then scaled based on well-documented cost correlations (Tribe & Alpine, 1986). The

scaling of most equipment is non-linear because the value to be scaled is assumed to benefit from economies of scale as the size of the equipment increases. The form of the equation for much of the cost scaling is similar to the one shown below.

Equation 6.1:

$$X = X_{ref} * \left(\frac{Y}{Y_{Ref}} \right)^n$$

where:

X = Estimated direct cost of a given piece of equipment or process area

X_{Ref} = Reference cost of a similar piece of equipment that may be larger or smaller

Y = A process parameter used as the basis for cost scaling (such as a mass flow or surface area)

Y_{Ref} = Process parameter value of the reference equipment

n = Scaling coefficient

The cost savings for larger equipment sizes is the result of the growing difference between the external surface area (i.e. the construction material) and volume of the equipment vessel. Tribe and Alpine published a paper in 1986 which gave popularity to the “0.6 Rule” regarding the relation between changes in material throughput and the scaling of capital cost. This rule results from the fact that many equipment devices can be roughly described as cylindrical or cubic combined with the geometric relationship between surface area and volume, which is used to determine cost scales by a corresponding exponent of 0.6-0.7. Thus, vessels that scale based on the external surface area tend to benefit from the economies of scale principle since a doubling of the volume will result in less than double the cost.

Although benefits from economies of scale apply to many types of equipment, exceptions to this rule do exist. For example, Tribe and Alpine cite two examples in their study of twelve equipment areas

relating to sugar cane processing in which the scaling coefficient was greater than 1.0 (Tribe & Alpine, 1986). For solid sorbents systems, indirect contact heat exchangers are the notable exception to the economies of scale rule. This is caused by the demand for construction materials (often carbon steel or stainless steel) for the internal heat exchange surface area in addition to the materials used for the exterior area of the vessel. At larger vessel sizes, the cost of the interior heat exchange materials dominate the cost of the vessel. The size at which the cost of the vessel is more a function of the internal versus external surface area materials depends on the specific design of the vessel and the types of construction materials required for the process (Seider, 2014).

Literature regarding the construction of indirect contact heat exchangers suggests that the internal materials become the dominant cost component when the internal surface area is between 1,000 m² and 10,000 m² (Seider, 2014; Viguri-Fuente, n.d.). This range is quite broad because it encompasses a wide variety of designs and includes heat transfer between two liquids as well as between liquids and solids. Evidence suggests that liquid-solid heat exchangers tend to fall toward the lower end of this range (Green, 2008; Viguri-Fuente, n.d.). Because of this, heat exchange vessels for the solid sorbent-based CO₂ capture system may be expected to have an internal exchange surface area limited to a value closer to 1000 m² rather than 10,000 m².

The concept of a size-constrained heat exchange vessel is supported by the solid sorbent-based CO₂ capture system design published by CCSI (DOE/NETL, 2012). In this report, the solid-liquid heat exchanger designs use an upper bound for their internal surface area that falls between 208 m² and 1,744 m² per unit for their adsorber, regenerator, and cross-flow heat exchanger vessels. Moreover, the solid sorbent process requires several-fold more heat exchange surface area than can be provided by a single unit in order to meet the large heating and cooling demands of the system. For this reason, the adsorber and regenerator units modelled in their work employ 14 and 10 units, respectively, operating in series (ibid). Details regarding the number of cross-flow heat exchangers used in the CCSI design are somewhat more ambiguous.

The low internal surface area per vessel combined with the high number of process vessels suggests that the upper bound for the heat exchange surface area is relatively low for solid sorbent-based CO₂ capture applications before multiple units are required and economies of scale no longer apply. For these reason, the heat exchanger costs modelled in this work scale linearly with internal heat exchange surface area requirements.

Table 6.1 reviews the list of major equipment or process areas of the solid sorbent system for which capital and O&M costs are estimated. The reference equipment and associated costs are taken from NETL Baseline reports (DOE/NETL, August, 2007), (DOE/NETL, 2010) or from existing equipment models in the IECM (Carnegie Mellon University, 2014). The “0.6 Rule” is applied in this work according to the values used in the reference source or in accordance with the guidelines given by Tribe and Alpine when the scaling coefficient is not available in the source data (Tribe & Alpine, 1986). Cost estimates that are already available in the IECM are used when applicable to the solid sorbent model in order to maintain consistency between comparable technologies in the IECM modeling framework. Under these circumstances, this work refers to a “reference model” which denotes that the cost data is derived from pre-existing IECM models.

Table 6.1: List of equipment and process areas and the reference source used for cost data.

Equipment or process area	Reference cost source
Adsorber	(DOE/NETL, 2012)
CO ₂ transport and storage	(Carnegie Mellon University, 2014)
Cold-side heat exchanger	(DOE/NETL, 2012)
Conveyor systems	(DOE/NETL, 2010)
Cyclone bank	(DOE/NETL, 2013)
Flue gas blower	(Carnegie Mellon University, 2014)
Flue gas pre-treatment	(Carnegie Mellon University, 2014)
Heat exchange circulation pumps	(Carnegie Mellon University, 2014)
Hot-side heat exchanger	(DOE/NETL, 2012)
Product gas drying and compression	(Carnegie Mellon University, 2014)
Regenerator	(DOE/NETL, 2012)
Solid sorbent storage and staging	(DOE/NETL, 2010)
Steam extractor	(Carnegie Mellon University, 2014)

The following equations are used to calculate direct costs of components in the CO₂ process. In all the equations, $N_{o,i}$ refers to the number of operating trains and $N_{T,i}$ refers to the total number of trains for component 'i'. All costs are reported in constant 2011 U.S. dollars.

6.2.1. Flue gas pre-treatment system

The total cost for the pre-treatment unit is based on the volumetric flow rate entering the pre-treatment unit. The volumetric flow rate is nominally calculated by the IECM based on the power plant and upstream treatment process specifications or may be input separately if using the CO₂ process as a stand-alone model. In the later case, the molar flow rate is a reasonable substitute for the volumetric flow rate since the temperature and pressure conditions are known. The cost of the system is calculated according to Equation 6.2.

Equation 6.2:

$$FG \text{ pretreatment cost } (\$) = N_{T,pre} * Reference \text{ cost } * \left(\frac{Pretreat \text{ inlet } FG \text{ flow rate}}{N_{O,pre}} \right)^{0.6}$$

Where the reference cost is equal to \$35.64M (2011) and the maximum train size for the pre-treatment unit is 1,145,000 kmol/hr. Both values are derived from the IECM reference model. No spare trains are assumed for flue gas pre-treatment.

6.2.2. Flue gas blower

The total cost for the flue gas blower is based on the volumetric flow rate exiting the flue gas pre-treatment unit. The pre-treatment outlet FG flow rate (kmol/hr) is a function of the base plant assumptions and the quantity of water removed in the pre-treatment unit. The amount of water removed from the flue gas is estimated using the flue gas pre-treatment model described in Appendix C. Its cost is calculated according to Equation 6.3.

Equation 6.3:

$$FG \text{ blower cost } (\$) = N_{T,pre} * Reference \text{ cost } * \left(\frac{Pretreat \text{ outlet } FG \text{ flow rate}}{N_{O,pre}} * \frac{\Delta P_{blower}}{\Delta P_{blower,ref}} \right)^{0.6}$$

Where the reference cost (\$) is calculated in the IECM reference and is equal to \$7.319M (2011). The maximum train size is derived from the IECM reference model and is equal to 1,145,000 (kmol/hr). The reference pressure drop across the flue gas blower is 6,894 Pa (psi). No spare trains are assumed for the flue gas blower.

6.2.3. CO₂ adsorber

The total cost of the adsorber is assumed to scale with the heat exchanger surface area according to Equation 6.4.

Equation 6.4:

$$\text{Adsorber system cost (\$)} = N_{T,A} * \text{Reference cost (\$)} * \frac{\text{Adsorber HX surface area}}{N_{O,A}}$$

Where the reference system cost (\$) is \$254,000 per train (2011) and the reference adsorber surface per train area is 2,675 m² (DOE/NETL, 2012). The reference adsorber heat exchange surface area represents one of fourteen adsorber trains in the CCSI process. No spare trains are assumed for the adsorber process.

The adsorber heat exchange surface area is calculated based on the total cooling requirement and the heat exchange properties of the system as shown in Equation 6.5.

Equation 6.5:

$$\text{Adsorber HX surface area} = H_{Cooling}^A * \frac{1000}{3600 * LMTD^A * U^A}$$

where:

$H_{Cooling}^A$ = Total adsorber cooling duty calculated using Equation 4.58 (kJ/hr)

1000 = Conversion from kilojoules to joules

3600 = Conversions from seconds to hours

$LMTD^A$ = Logarithmic mean temperature difference in the adsorber (K)

U^A = Overall heat exchange coefficient (W/m²-K)

The overall heat exchange coefficient is a parameter of the model. The nominal value is 300 W/m²-K, which is the value reported by CCSI (DOE/NETL, 2012). The inlet cooling water temperature used to determine the LMTD is a called variable common among all processes in the IECM and equal 283 K at the inlet. The outlet temperature for the cooling process is 293 K in order to maintain consistency with the temperature increase reported by CCSI.

6.2.4. Cyclone bank

The total cost of the cyclone bank is based on the total volumetric flue gas flow rate exiting the adsorber and is calculated according to Equation 6.6.

Equation 6.6:

$$\text{Cyclone bank cost (\$)} = N_{T,CB} * \text{Reference cost} * \frac{\text{Molar flow rate exiting adsorber}}{N_{O,CB}}$$

Where the reference cost is given by the ADA solid sorbent evaluation study (Sjostrom, et al., 2011) and equal to \$1.81M (2011) for a single cyclone bank with a maximum capacity of 73,100 kmol/hr at atmospheric pressure and a temperature of 313 K. The molar flow rate exiting the adsorber is calculated using Equation 4.3. No spare cyclone bank trains are assumed.

6.2.5. Cold-side heat exchanger

The total cost of the cold-side heat exchanger is based on the heat exchanger surface area and is calculated according to Equation 6.7:

Equation 6.7:

$$\text{CHX cost(\$)} = N_{T,CHX} * \text{Reference cost (\$)} * \frac{\text{CHX surface area}}{N_{O,CHX}}$$

Where the reference cost is given by the CCSI process model report (DOE/NETL, 2012) and equal to \$1.91M (2011). The heat exchange surface area per train is given by the same report and equal to 1,573 m². Note that the reference cost and reference surface area are the same as the regenerator and no spare trains are assumed. The cold-side heat exchanger surface area is determined using Equation 6.8.

Equation 6.8:

$$CHX \text{ surface area} = \Delta H^{HHX} * \frac{1000}{3600 * LMTD^{CHX} * U^{HX}}$$

where:

ΔH^{HHX} = Heat transfer (kJ/hr) between the heat exchange fluid flowing through the cross-flow heat exchanger and the solid flowing from the adsorber as quantified using Equation 4.56.

1000 = Conversion from kilojoules to Joules

3600 = Conversion from hours to seconds

$LMTD^{CHX}$ = Logarithmic mean temperature difference in the cold-side heat exchanger (K)

U^{HX} = Overall heat exchange coefficient for the cross-flow heat exchangers (W/m²-K)

The hot-side heat exchanger rate of heat transfer (ΔH^{HHX}) is calculated as a performance value using the method described in Section 4.4.2, and this value is also used to quantify the heat exchange surface area for the cold-side heat exchanger.

The temperature gradient parameter, $LMTD^{CHX}$, is calculated using the values shown in Table 6.2.

Table 6.2: Nomenclature and temperature values used to calculate the logarithmic mean temperature difference in the cold-side heat exchanger

Parameter	Mass symbol (kg/hr)	Temperature symbol (K)	Temperature value (K)
HX fluid at CHX inlet	$m_{H_2O}^{HHX,out}$	$T_{H_2O}^{HHX,out}$	401 (128°C)
HX fluid at CHX outlet	$m_{H_2O}^{HHX,in}$	$T_{H_2O}^{HHX,in}$	384 (111°C)
Solids at inlet	$m_{solid}^{A,out}$	T^A	Model parameter
Solids at outlet	$m_{solid}^{CHX,out}$	$T_{solids}^{CHX,out}$	Equation 4.62

The overall heat transfer coefficient for the cold- and hot-side the heat exchangers depends on the design. For this work, the cross-flow heat exchangers are modelled after the regenerator due to their shared shell-and-tube design combined with the low solid-gas mixing requirement. This assumption is a deviation from CCSI's process model, which assumes that the cross-flow heat exchangers have an overall heat transfer coefficient comparable to a fully fluidized bed. However, CCSI's heat exchanger process does not include fluidizing equipment in order to overcome the significant (29 kPa) pressure drops included in CCSI's fluidized bed adsorber model. For these reasons, the reference cost and overall heat transfer coefficient are derived from CCSI's regenerator model.

6.2.6. Regenerator

The total cost for the regenerator process is calculated according to Equation 6.9.

Equation 6.9:

$$Regenerator\ cost\ (\$) = N_{T,R} * Reference\ cost * \frac{Regenerator\ HX\ surface\ area}{N_{O,R}}$$

Where the reference cost is given by the CCSI process model report (DOE/NETL, 2012) and equal to \$1.91M (2011) per train. The surface area per unit is given in the same report and has a value of 1,573 m². No spare trains are assumed for the regenerator.

The regenerator heat exchange surface area is calculated based on the heat exchange characteristics of the regeneration process using Equation 6.10.

Equation 6.10:

$$\text{Regenerator HX surface area} = H_{\text{heating}}^R * \frac{1000}{3600 * LMTD^R * U^R}$$

where:

H_{heating}^R = Heat transfer (kJ/hr) between the heat exchange fluid flowing through the cross-flow heat exchanger and the solid flowing from the adsorber as quantified using Equation 4.63

1000 = Conversion from kilojoules to Joules

3600 = Conversion from hours to seconds

$LMTD^R$ = Logarithmic mean temperature difference between the solids and heat exchange steam the regenerator (K)

U^R = Overall heat exchange coefficient between the solids and heat exchange steam in the regenerator (W/m²-K)

The value for the heat transfer coefficient is a parameter of the model. The nominal value is 60 W/m²-K based on CCSI's data for a moving bed reactor (DOE/NETL, 2012). Table 6.3 shows the data source for the solid flow rate variables required to calculate the heat exchange surface area in the regenerator.

Table 6.3: Derivation of the temperatures for the solid and steam used to calculate the heat exchange surface area and steam requirements for the regenerator.

Parameter	Mass symbol (kg/hr)	Temperature symbol (K)	Temperature value (K)
Solids at inlet	$m_{solid}^{CHX,out}$	$T^{CHX,out}$	Equation 4.62
Solids at outlet	$m_{solid}^{R,out}$	T^R	Model parameter
Steam inlet	$m_{H_2O}^{HHX,out}$	$T_{steam}^{HHX,out}$	408 K (135°C)
Steam outlet	$m_{H_2O}^{HHX,in}$	$T_{water}^{HHX,in}$	$T_{solid}^{R,out} + T_{steam}^{R,approach}$

It is important to remember that the sorbent materials used in a CO₂ capture system can restrict the solid and steam temperature profiles used in the regenerator since the sorbent may oxidize when exposed to high temperatures (see Section 2.2.3 for more details). In this work, the nominal assumption is that the solids are heated to 120°C through thermal (indirect) contact with steam based on solid screening tests performed by ADA-ES (Starns, et al., 2012). The steam used to heat the solids enters the regenerator at a maximum value of 135°C and cools to a minimum temperature that is 20°C higher than the solids at the regenerator inlet.

Although CCSI's process design is the basis for many of the base case design assumptions simulated in this work, there is an important discrepancy in their design regarding the maximum temperatures allowed for amine-based solid sorbents. The material studies conducted by NETL regarding the adsorption kinetics of the solid sorbent, 32D, limit the maximum reported temperature to 108°C (Lee, et al., 2011). In the design studies using the same material, however, the solids are exposed to heat exchange surfaces at temperatures greater than 165°C. This discrepancy is the reason why the regenerator solids and steam temperatures are modified in the other case studies. Moreover, these differences are among the most important assumptions in the model as discussed in Section 6.7.2.

6.2.7. Hot-side heat exchanger

The total cost of the hot-side heat exchanger is based on the heat exchanger surface area and is calculated according to Equation 6.11.

Equation 6.11:

$$HHX \text{ cost } (\$) = N_{T,HHX} * \text{Reference cost} * \frac{HHX \text{ surface area}}{N_{O,HHX}}$$

Where the reference cost is equal to \$1.91M (2011) and the maximum train size is 1,573 m². No spare trains are assumed for the hot-side heat exchanger. Note that the reference cost and surface area values are the same as the regenerator. This assumption is based on the similar design and function of the two vessels since both the cross-flow heat exchangers and regenerator use a moving bed design coupled with indirect heat exchange between the solids and steam.

The hot-side heat exchanger surface area is determined using Equation 6.12.

Equation 6.12:

$$HHX \text{ surface area} = \Delta H^{HHX} * \frac{1000}{3600 * LMTD^{HHX} * U^{HX}}$$

where:

ΔH^{HHX} = Heat transfer (kJ/hr) between the heat exchange fluid flowing through the cross-flow heat exchanger and the solid flowing from the regenerator as quantified using Equation 4.56

1000 = Conversion from kilojoules to Joules

3600 = Conversion from hours to seconds

$LMTD^{HHX}$ = Logarithmic mean temperature difference in the hot-side heat exchanger (K)

U^{HX} = Overall heat exchange coefficient for the cross-flow heat exchangers (W/m²-K¹)

Note that the total heat transfer between the heat exchange fluid and the solids in the hot-side system is equal to that in the cold-side. Since the hot-side heat transfer is calculated in Chapter 4, this

value is also used to quantify the heat exchange surface area for the cold-side heat exchanger. The temperature gradient parameter, $LMTD^{HHX}$, is calculated using the values shown in the Table 6.4.

Table 6.4: Nomenclature and temperature values used to calculate the logarithmic mean temperature difference in the hot-side heat exchanger

Parameter	Mass symbol (kg/hr)	Temperature symbol (K)	Value (K)
HX fluid at HHX inlet	$m_{H_2O}^{HHX,out}$	$T_{water}^{HHX,in}$	384 (111°C)
HX fluid at HHX outlet	$m_{H_2O}^{HHX,in}$	$T_{steam}^{HHX,out}$	384
Solids at inlet	$m_{solid}^{A,out}$	T^A	Parameter
Solids at outlet	$m_{solid}^{HHX,out}$	$T_{solids}^{HHX,out}$	Parameter

6.2.8. Product gas drying and compression

The total compression work and therefore electrical use required is dependent upon the flow rate of product CO₂ through the compressor as well as the initial and final stream pressures and temperatures. The costs of the compressors are assumed proportional to the MW_e usage (Versteeg, 2012) and the total cost for the drying and compression unit is calculated according to Equation 6.13.

Equation 6.13:

$$\begin{aligned}
 & \text{Drying and compression unit cost}(\$) \\
 & = \text{Reference cost} * \left(\frac{\text{Auxiliary electrical load for CO}_2 \text{ compressor}}{\text{Reference electrical use for CO}_2 \text{ compressor}} \right)^{0.7}
 \end{aligned}$$

Where the reference cost is based on the drying and compression unit cost in the IECM reference model and is equal to \$18.28M (2011). The reference electrical use per train for the product compressor is based on the IECM reference model and is equal to 38.53 MW_e as derived from the IECM reference model. The auxiliary electrical load for the CO₂ compressor is calculated as previously described using Equation 4.71.

6.2.9. Solid sorbent storage and staging

The cost for the solid sorbent storage and staging area is calculated according to Equation 6.14.

Equation 6.14:

$$\text{Solid storage area cost (\$)} = N_{T,stage} * \text{Reference cost} * \left(\frac{m_{solid}^{transport}}{N_{O,stage}} \right)^{0.6}$$

Where the reference cost is \$1.15M (2011) based on the cost of auxiliary coal handling systems used in the NETL baseline studies (DOE/NETL, 2010, p. 404). The maximum train size is based on the flow rate of coal used in the staging area and equal to 2,268 tonnes per hour for two staging systems (DOE/NETL, 2010, p. 394). No spare staging areas are assumed.

6.2.10. Conveyor systems

Belt conveyors are required to transport solids between the adsorber, cross-flow heat exchangers, and regenerator. The total cost for all conveyor systems is calculated according to Equation 6.15.

Equation 6.15:

$$\text{Conveyor systems cost (\$)} = 4 * N_{T,conveyor} * \text{Reference system cost (\$)} * \left(\frac{m_{solid}^{transport}}{N_{O,conveyor}} \right)^{0.6}$$

Where four conveyor areas are required to transport solids between various process areas and $N_{T,conveyor}$ represents the number of conveyors per area. The reference system cost is \$0.51M (2011) based on the coal conveyor line item referenced in Case Study 11, Account number 1.7 of the NETL Bituminous Coal Report (DOE/NETL, 2010, p. 404). The reference mass flow rate is the same as the reference flow rate for the solid sorbent storage and staging area (2,268 tonnes per hour). No spare conveyor systems are assumed.

6.2.11. Heat exchange circulation pump

The total cost for the heat exchanger circulation pump is calculated according to Equation 6.16.

Equation 6.16:

$$\text{Heat exchange circulation pump (\$)} = N_{T,HXpump} * \text{Reference cost} * \left(\frac{m_{H_2O}^{HHX,in}}{N_{O,HXpump}} \right)^{0.6}$$

Where the reference cost is derived from the water circulation pump used within the IECM reference model and has a value of \$1.23M (2011). The maximum fluid flow rate for these systems is 3,030,000 kg/hr. No spare heat exchange circulation pumps are assumed.

6.2.12. Heat exchange circulation compressor

The total cost for the heat exchange circulation compressor is calculated according to Equation 6.17.

Equation 6.17:

$$\text{Heat exchange circulation compressor (\$)} = N_{T,HXcomp} * \text{Reference cost} * \left(\frac{M_{H_2O}^{HHX,in}}{N_{O,HXcomp}} * \frac{\Delta P_{HXcomp}}{\Delta P_{ref}} \right)^{0.6}$$

Where the reference compressor cost is \$7.329M (2011) and the maximum train size is 114,500 kmol/hr. The reference pressure change is 6,894 Pa. These values are derived from the IECM reference model (Carnegie Mellon University, 2014). No spare compressor trains are assumed.

6.2.13. Steam extractor

The steam extractor is used to divert steam from the IP/LP crossover and desuperheat the steam to a suitable temperature for use in the regenerator system. The total cost for the steam extractor is taken

from the IECM reference model and equal to \$3.6M (2011). This value is assumed constant regardless of the size of the plant based on the IECM code (Carnegie Mellon University, 2014; Rao, 2003).

6.3. Total plant cost (TPC)

Besides the process facilities cost, there are a number of other capital cost items (often referred to as indirect costs) that need to be applied. Usually, these are estimated as percentages of total PFC.

These additional costs are divided into the following categories:

- Engineering and home office fees (EHO)
- General facilities capital (GFC)
- Process contingency
- Project contingency
- Royalty charges

The sum of these costs, called the total plant cost (TPC), is developed on the basis of overnight construction. These items are discussed in this section.

General facilities capital (GFC) is the capital required for the construction of general facilities such as buildings, roads, shops, etc. This cost is usually estimated to be between 5 and 20% of PFC.

Engineering and home office overhead is included if the cost estimates for the general facilities capital do not include these fees as part of the equipment costs. For these fees, 7 and 15% of PFC is typical.

Royalty charges are included as indirect capital costs and typically range from 1-10% of PFC.

The EPRI TAG™ method uses two types of contingencies: the process contingency and the project contingency. The process contingency is a capital cost contingency factor applied to a new technology in an effort to quantify the uncertainty in the technical performance and cost of commercial-scale equipment (EPRI, 1986). Therefore, a higher process contingency factor is used for more basic cost

estimates. Table 6.5 shows the how the maturity of the technical design influences the process contingency.

Table 6.5: Process contingency cost guidelines (EPRI, 2011)

Technology status	Process contingency cost (%PFC)
New concept with limited data	40+
Concept with bench-scale data	30-70
Small pilot plant data	20-35
Full-sized modules have been operated	5-20
Process is used commercially	0-10

EPRI recommends that separate process contingency be given for each major plant section. This work used the default contingency factors provided by the IECM for all major non-CCS sections of the plant. For the CO₂ capture section, this thesis uses a default process contingency of 55% based on the average value for a technology concept with bench-scale data, reflecting the current (2015) state of fully integrated solid sorbent CO₂ capture systems.

The project contingency is a capital cost contingency factor that is intended to cover the cost of additional equipment or other costs that would result from a more detailed design of a definitive project specific to the actual site (EPRI, 1986). Specifically, the project contingency addresses the need for additional equipment, structural support, and miscellaneous equipment required when the actual plant is built. Table 6.6 lists the project contingency cost guidelines as suggested by the Electric Power Research Institute (EPRI). This work uses a simplified design intended to be applicable for a range of equipment options.

Table 6.6: Project contingency costs (EPRI, 2011)

EPRI cost classification	Design effort	Project contingency
Class I (~AACE Class 5/4)	Simplified	30-50
Class II (~AACE Class 3)	Preliminary	15-30
Class III (~AACE Class 3/2)	Detailed	10-20
Class IV (~AACE Class 1)	Finalized	5-10

Like the process contingency, EPRI recommends that project contingencies be applied for each plant section and this work uses the default IECM values for each major plant section excluding the CCS process. In regards to the solid sorbent-based CO₂ capture system, a contingency factor of 40% is used as the default value. This contingency was selected based on the limited availability of solid-based CCS system design data combined with the difficulty of managing large volumes of solid material. Moreover, the flexibility inherent in this model means that the process design detail is necessarily preliminary or simplified in order to accommodate a wide range of design variability.

We note that process and project contingency cost values used here are intended to yield the “bottom up” cost of a plant built today based on the current state of knowledge. Later in Chapter 7, we discuss and employ a method to estimate the future cost of a mature plant technology.

6.4. Total capital requirement (TCR)

The total capital requirement (TCR) includes all of the capital necessary to complete the entire project. These items include:

- Total plant cost (TPC)
- Allowance for funds used during construction (AFUDC)
- Prepaid royalties
- Inventory capital
- Pre-production costs

In this study, the AFUDC is calculated as 0.5% of the process facilities capital based on assumptions about the time required for construction and cost of borrowed funds. Pre-production costs account for operator training and costs accrued during the start-up of the plant. Typically, these are taken as equivalent to one month of fixed operating costs. Pre-production cost is taken as equivalent to one month of variable operating costs. Inventory capital is the cost of inventories such as fuels and other consumables. This is taken as 0.5% of TPC.

Initial costs of catalysts and chemicals account for the initial loading of these materials in certain equipment. For example, a certain quantity of solid sorbent is loaded into the staging area or adsorber prior to its start-up. Wherever possible, these costs are estimated from open literature.

Table 6.5 summarizes the steps required in order to calculate the total capital requirement.

Table 6.7: Solid sorbent capital cost model parameters and nominal values

	Capital cost elements	Nominal value
A	Process area costs	A1, A2, A3,... An
B	Process facilities capital (PFC)	ΣA_i
C	Engineering and home office fees	7% PFC
D	General facilities	10% PFC
E	Project contingency	40% PFC
F	Process contingency	55% PFC
G	Total plant cost (TPC) = sum of above	B+C+D+E+F
H	AFUDC (Interest during construction)	Calculated
I	Royalty fees	0.5% PFC
J	Pre-production	1 month fixed O&M
K	Pre-production	1 month variable O&M
L	Inventory capital	0.5% TPC
M	Total capital requirement (TCR)	G+H+I+J+K+L

In addition to the capital requirement for the CO₂ capture process, this work also assumes that a dedicated CO₂ pipeline is required in order to transport product CO₂ to an off-site storage facility. The costs associated with this pipeline are the subject of previous modeling efforts (McCoy, 2009) and the estimates in this work use an empirical correlation between the transport and storage (T&S) TCR and the gross plant output of a similar plant equipped with a liquid amine-based CO₂.

6.5. Operation and maintenance costs

The operating and maintenance (O&M) costs are usually estimated for one year of operation. These can be divided into fixed O&M and variable O&M costs. These costs are discussed in this section.

6.5.1. Fixed O&M costs

The fixed O&M (FOM) costs in the model include the costs of maintenance (materials and labor) and labor (operating labor, administrative and support labor). These are estimated on an annual basis (\$M/yr) using the Equations 6.18-6.21.

Equation 6.18

$$FOM = FOM_{labor} + FOM_{maint} + FOM_{admin} + FOM_{T\&S}$$

Equation 6.19

$$FOM_{labor} = N_{labor} * N_{shifts} * \frac{8 \text{ hrs}}{\text{shift}} * rate * 365 \frac{\text{days}}{\text{yr}}$$

Equation 6.20

$$FOM_{maint} = TPC * f_{maint}$$

Equation 6.21

$$FOM_{admin} = f_{admin} * (FOM_{labor} + f_{maintlab} * FOM_{maint})$$

where:

N_{labor} = number of operating positions per shift (jobs/shift)

N_{shifts} = number of shifts per day (shifts/day)

$rate$ = the hourly wages to the labor (\$/hr)

f_{maint} = total annual maintenance cost expressed as a fraction of the total plant cost (TPC) (%)

f_{admin} = the administrative labor cost expressed as the fraction of the total labor cost (%)

There is also an annual fixed cost associated with the CO₂ transport and storage system. This cost is equal to \$0.31 M (2011) in keeping with the upkeep costs reported by the latest publically available version of the IECM (Carnegie Mellon University, 2014).

6.5.2. Variable O&M

The variable O&M (VOM) costs include the cost of materials consumed (solid sorbent, caustic, etc.), utilities (water, steam, etc.), fuel (natural gas in the case of an auxiliary boiler), and services used (waste disposal, CO₂ transport and storage). These quantities are determined in the performance model. The unit cost of each item (e.g., dollars per tonne of solid sorbent or dollars per tonne of CO₂ stored) is a parameter specified as a cost input to the model. The total annual cost of each item is then calculated by multiplying the unit cost by the total annual quantity used or consumed. Total annual quantities are strongly dependent upon the plant capacity factor. The individual components of variable O&M costs are explained in more detail below. Note that the unit costs for all of the consumables excluding solid sorbent are based on the default values used in the IECM.

Cost of solid sorbent

The makeup solid sorbent requirement estimated in the performance model is transformed into a dollar amount by using the unit cost of solid sorbent, which is a user-defined cost input variable. The cost of solid sorbent is calculated using Equation 6.22.

Equation 6.22:

$$VOM_{solid\ sorbent} = m_{solid}^{fresh} * \frac{1}{1000} * UC_{solid\ sorbent} * HPY$$

where:

$VOM_{solid\ sorbent}$ = Variable O&M cost of solid sorbent (\$/yr)

m_{solid}^{fresh} = Mass flow rate of discarded solid sorbent (kg/hr)

$\frac{1}{1000}$ = conversion from kilograms to tonnes

$UC_{solid\ sorbent}$ = Unit cost of solid sorbent (\$/tonne)

HPY = Equivalent annual hours per year of plant operation at full capacity (CF*8760)

The default value for the cost of solid sorbent is based on CCSI's estimate \$2,270 per tonne (i.e. \$5/pound). However, this value is somewhat controversial and responses from experts interviewed as part of this work returned cost estimates ranging from \$1,000 to \$15,000 per tonne of solid sorbent with an average "best guess" of \$4,300 per tonne (see Appendix B). This variation is dealt with in the uncertainty analysis in Section 7.3.

Cost of Caustic

Caustic (NaOH) is used in the pre-treatment unit in order to reduce the concentration of SO₂ to a user-defined level. Caustic reacts at a 1:1 molar ratio with SO₂ and the reactants and products are dissolved in the direct contact cooling water in the pre-treatment unit. As a default, the concentration of SO₂ is reduced from 25ppm (the lower limit of the New Source Performance Standards) to 1 ppm. The cost of caustic is a parameter common to several IECM process models. The cost of caustic required for the CO₂ capture system is calculated using Equation 6.23.

Equation 6.23:

$$VOM_{caustic} = m_{caustic} * \frac{1}{1000} * UC_{caustic} * HPY$$

where:

$VOM_{caustic}$ = Variable O& cost of caustic (\$/yr)

$m_{caustic}$ = Mass flow rate of caustic (kg/hr)

$\frac{1}{1000}$ = Conversion from kilograms to tonnes

$UC_{caustic}$ = Unit cost of caustic (\$/tonne)

The flow rate of caustic is estimated based on rate of SO₂ removal in the pre-treatment unit. Generally, the annual cost of caustic is negligible given the low cost of caustic and the flow rate of SO₂ through the CCS process. The unit cost of caustic used in this work is \$508 per tonne in order to maintain consistency with the IECM (v8.0.2).

Cost of waste disposal

Another important variable operating cost item is the cost incurred from disposal or treatment of the discarded solid stream. The cost is estimated from using the mass flow rate of discarded solids as shown in the equation below. The cost of disposing of the discarded solids is calculated using Equation 6.24.

Equation 6.24:

$$VOM_{discard} = m_{solid}^{discarded} * \frac{1}{1000} * UC_{discard} * HPY$$

where:

$VOM_{discard}$ = Variable O&M cost of solid waste disposal (\$/yr)

$m_{solid}^{discarded}$ = Mass flow rate of discarded solid (kg/hr)

$\frac{1}{1000}$ = Conversion from kilograms to tonnes

$UC_{discard}$ = Unit cost of disposal or treatment of the discarded solid stream (\$/tonne)

The unit cost of disposal (\$19.11/tonne) is the same used by the IECM (v.8.0.2) for disposal of particulate matter collected in the electrostatic precipitator.

Cost of CO₂ transport

Transportation of CO₂ product is assumed to take place via pipeline. The cost of CO₂ transport is estimated based on the transportation distance (TD, in km), the unit cost of transport, and the CO₂ product flow rate (calculated result from the performance model). By default, the cost of transport is \$0.02/tonne CO₂-km and the transport distance is 100 km as determined by the IECM reference model. The cost of transporting the product CO₂ stream is calculated using Equation 6.25.

Equation 6.25:

$$VOM_{transport} = m_{CO_2}^{R,out} * \frac{1}{1000} * UC_{transport} * TD * HPY$$

where:

$VOM_{transport}$ = Variable O&M cost of transporting the product CO₂ to the storage site (\$/yr)

$m_{CO_2}^{R,out}$ = Mass flow rate of product CO₂ exiting the CO₂ capture process (kg/hr)

$\frac{1}{1000}$ = Conversion from kilograms to tonnes

TD = transport distance (km)

$UC_{transport}$ = Unit cost of transporting CO₂ (\$/tonne-km)

Cost of CO₂ storage

Depending upon the method of CO₂ storage, there may be revenue generated (as in enhanced oil recovery) or additional cost (as in most other storage methods) associated with CO₂ storage. The total revenue or cost of CO₂ storage is estimated from the unit cost and CO₂ product flow rate ($UC_{storage}$). The storage costs are set nominally to \$5 per tonne representing injection into a deep saline aquifer. This is the default setting in IECM. The cost of CO₂ storage is calculated using Equation 6.26.

Equation 6.26

$$VOM_{storage} = m_{CO_2}^{R,out} * UC_{storage} * HPY$$

where:

$VOM_{storage}$ = Variable O&M of CO₂ storage (\$/yr)

$UC_{storage}$ = Unit cost of storing CO₂ (\$/tonne)

Cost of steam and power

By default, all energy costs for CO₂ capture and storage are handled internally in the model by decreasing the overall electricity output of the plant based on the calculated power requirements for CCS, and the equipment power loss for steam is taken from within the plant. The CO₂ capture system is charged for the total electricity production foregone because of CO₂ capture and compression.

Cost of auxiliary energy

When regeneration steam and/or additional electricity are provided by an auxiliary natural gas boiler, the cost of energy is estimated from the total annualized cost of the new boiler and secondary

steam turbine, which takes into account their capital cost and the cost of natural gas fuel (Berkenpas, et al., 2009).

Cost of water

Water is required mainly for process cooling in the adsorber and pre-treatment unit. Generally, this is a minor cost item in the overall plant operation, but it is included for the sake of completeness. The cost of water required for the CO₂ capture system is calculated using Equation 6.27.

Equation 6.27:

$$VOM_{water} = (m_{cooling\ water}^A + m_{cooling\ water}^{Pre}) * \frac{1}{1000} * UC_{water} * HPY$$

where:

VOM_{water} = Variable O&M cost of water (\$/yr)

$m_{cooling\ water}^A$ = Mass flow rate of cooling water in the adsorber (kg/hr)

$m_{cooling\ water}^{Pre}$ = Mass flow rate of cooling water (or caustic slurry) in the pre-treatment unit (kg/hr)

$\frac{1}{1000}$ = Conversion from kilograms to tonnes

UC_{water} = Unit cost of water (\$/tonne)

The unit cost of water is 0.3033 per tonne of water to maintain consistency with the cost of water used in the IECM (v.8.0.2). Note that this cost includes the treatment of recirculating water as well as withdrawal of makeup water.

Variable O&M cost summary

The total variable O&M cost (VOM, \$/yr) is obtained by adding all of these costs:

$$VOM = VOM_{solid\ sorbent} + VOM_{caustic} + VOM_{discard} + VOM_{transport} + VOM_{storage} + VOM_{energy} \\ + VOM_{water}$$

6.5.3. Total O&M cost summary

Finally, the total annual O&M cost (TOM, \$/yr) is calculated using Equation 6.28.

Equation 6.28:

$$TOM = FOM + VOM$$

The nominal (default) values of all major operating and maintenance (O&M) costs in the solid sorbent process model are summarized in Table 6.8. Note that the cost of solid sorbent is maintained at \$2,270 per tonne for all deterministic case studies, but the expert elicitation values are used in the probabilistic analyses.

Table 6.8: Solid sorbent O&M cost model parameters and nominal values. All costs are on 2011 dollars.

O&M cost elements	Typical value
Fixed O&M costs	
Admin. & support labor cost (f_{admin})	30% of total labor cost
Maintenance cost allocated to labor (f_{maintlab})	40% of total maint. cost
Number of operating shifts (N_{shifts})	4.75/day
Operating labor (N_{labor})	2 jobs/shift
Operating labor rate (rate)	\$34.65/hr
Total maintenance cost (f_{maint})	2.5% TPC
Variable O&M costs*	
Caustic (NaOH) cost	\$460/tonne
CO ₂ storage cost	\$5/tonne
CO ₂ transport	\$0.02/tonne-km
Purge steam	\$0.3/kg
Solid sorbent	\$2,270 /tonne
Solid waste disposal cost	\$19/tonne
Water cost	\$0.3/tonne

*All values are IECM (v8.0.2) defaults from except solid sorbent cost.

6.6. Overall cost metrics

There are a variety of metrics used in the literature to report the total cost of CO₂ capture and storage systems. Among the most common metrics are the cost of CO₂ avoided; cost of CO₂ captured; cost of CO₂ abated (or reduced); and the increased cost of electricity (IPCC, 2005). The first three of these metrics have very different meanings, but because all three are reported in similar units of “dollars (or other currency) per tonne CO₂” there is significant potential for misinterpretation. The increased cost of electricity is often used in studies related to power plant and is similarly subject to misunderstanding (Rubin, 2012). In an effort to bring consistency and uniformity to power plant and CCS cost estimates, Rubin (2012) suggests that a standard for defining these terms. The method used in this work to calculate these terms is outlined in this section and the values reported may be reasonably compared to others following these definitions.

6.6.1. Cost of electricity generation

The most robust way to evaluate the cost of energy-intensive processes such as CO₂ capture systems is to compare the cost of electricity generation for power plants with and without CCS (the difference being the cost of CCS) (Rubin, 2012). The levelized cost of electricity (LCOE) represents the income that the plant would need to receive from the sale of electricity in order to fully recover all capital and operating costs, while earning a specified rate of return over the plant life. The cost of electricity is calculated by first quantifying the annual revenue requirement and normalizing its value by the total annual electricity generation. Total annual revenue requirement shown in Equation 6.29.

Equation 6.29:

$$\begin{aligned} \text{Total annual revenue requirement} \left(\frac{\$}{\text{yr}} \right) \\ = TCR * FCF + \text{Fixed O\&M} + \text{Variable O\&M} + \text{Byproduct credits} \end{aligned}$$

Like most engineering-economic studies of CCS, this model uses a fixed set of cost parameter values in order to calculate the annual revenue requirement. Thus, the reported value represents the “levelized” annual revenue stream, defined as the uniform yearly revenue stream that a power plant must realize from the sale of electricity in order to produce the same net present value as a stream of variable year-to-year costs over the life of the plant. The annual rate of return, plant life, and other plant assumptions are embedded in the fixed charge factor (FCF) described in greater detail in Appendix K.

The LCOE is calculated by normalizing the total annual revenue requirement using the average annual electrical output of the plant (Rao, 2003). This value is calculated using Equation 6.30.

Equation 6.30:

$$\text{Levelized cost of electricity} \left(\frac{\$}{\text{MWh}} \right) = \frac{\text{Total annual revenue requirement}}{8760 * \text{capacity factor} * \text{MW of net plant efficiency}}$$

Note that the LCOE includes the cost of all environmental controls. Thus, by running two scenarios of the power plant model, one without CCS (reference plant) and one with CCS, the incremental capital costs, O&M costs, and total annualized costs attributed to the CCS system are obtained. The addition of a CO₂ capture and storage system increases the LCOE for the plant; this incremental cost of electricity is attributed to CO₂ mitigation.

6.6.2. Cost of CO₂ avoidance

Since the purpose of adding the CCS process is to reduce the CO₂ emissions per net MWh delivered, the “cost of CO₂ avoided” is the economic indicator that is most widely used in this field (Rubin, 2012). For a power plant, this value can be calculated using Equation 6.31 (IPCC, 2005).

Equation 6.31:

$$\text{Cost of CO}_2 \text{ Avoided} \left(\frac{\$}{\text{tonne CO}_2} \right) = \frac{(LCOE)_{\text{withCCS}} - (LCOE)_{\text{withoutCCS}}}{(tCO_2/MWh)_{\text{withoutCCS}} - (tCO_2/MWh)_{\text{withCCS}}}$$

Where LCOE is the levelized cost of electricity generation (\$/MWh), tCO₂/MWh is the mass emission rate to the atmosphere in tonnes per MWh (based on the net generation capacity of each plant). Because emissions to the atmosphere are avoided if and only if the captured CO₂ is sequestered, the cost of CO₂ avoided necessarily included the cost of transport and storage.

6.7. Illustrative cost model results

This section revisits several of the capital cost models for key system components to illustrate the model behaviour as a function of key process or design variables. We begin with a discussion of adsorber costs.

6.7.1. Adsorber costs

Recall from Section 6.2 that the heat exchange surface area is used as the basis for calculating the direct capital cost of the adsorber, regenerator, and cross-flow heat exchange process areas. Because of this, the heat transfer properties of these processes have significant influence on the overall cost of the system. Figure 6.2 shows how the overall heat transfer coefficient and the adsorber temperature influence the direct capital cost of the adsorber for the ideal sorbent scenario. In this figure, the overall heat transfer coefficient between the cooling water flowing through the heat exchanger tubes and the solids and gasses in the shell impact the direct capital cost of the vessel. This coefficient depends on the process design. General ranges for these vessels are indicated in the margin above the cost curves. The nominal heat transfer coefficient for the adsorber ($300 \text{ W/m}^2\text{-K}$) and temperature (313 K or 40°C) result in a nominal direct capital cost of the adsorber of \$33M (2011) for the ideal sorbent case (Case study #1).

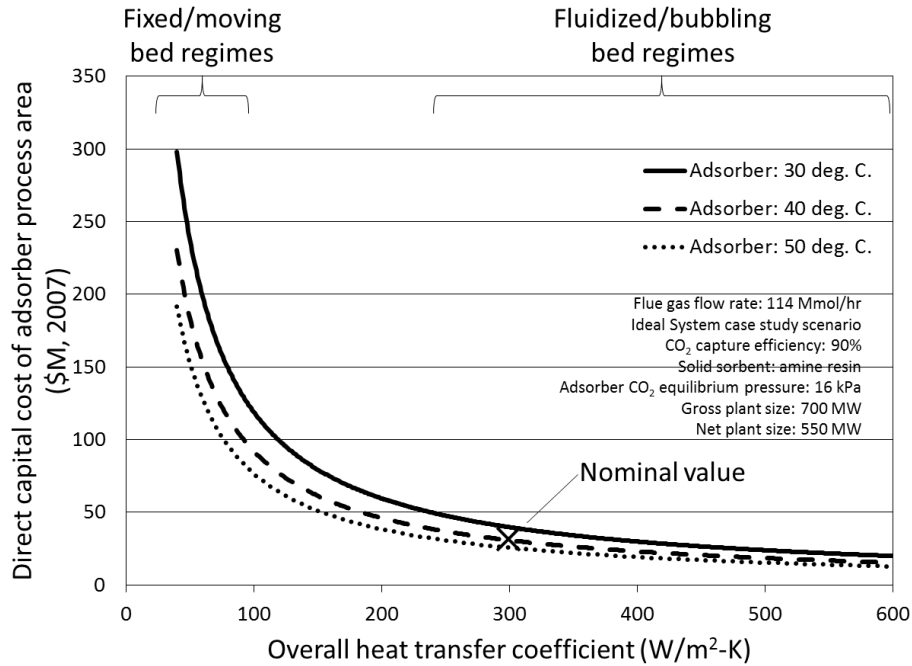


Figure 6.2: Direct capital cost of the adsorber as a function of the overall heat transfer coefficient and adsorber temperature for Case study #1. The capital cost is estimated as a function of the internal the heat exchange surface area. The nominal overall heat transfer coefficient for the adsorber is 300 W/m²-K at 40°C resulting in a capital cost of \$33 Million (2011).

The important trends in this figure are the decreasing cost of the adsorber process with increasing heat transfer coefficient and increasing temperature. The favorability of higher temperatures is due to complex (and non-intuitive) trade-offs among adsorber temperature, LMTD, specific cooling requirements, and total solid sorbent requirements for 90% capture. An example of how the specific cooling requirement and LMTD are sensitive to the adsorber temperature is shown in Figure 6.3 using performance values for the ideal sorbent case scenario. A higher final temperature in the shell side increases the LMTD, thereby lowering the heat exchange surface area. The adsorber cooling requirement, however, initially decreases with rising temperature since the solids do not need to be cooled as much, but then begins to increase at around 40°C as the rich loading dwindles and additional solids are required in order to capture CO₂.

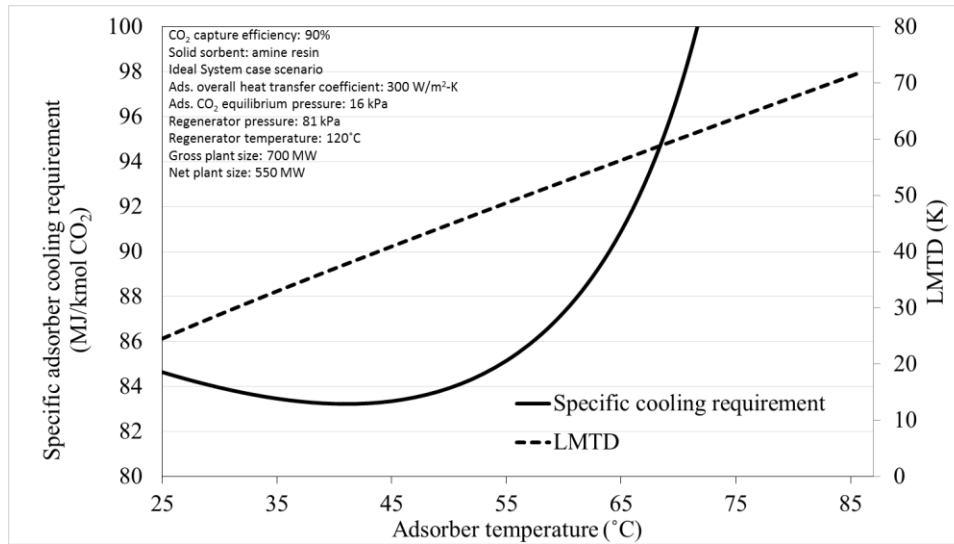


Figure 6.3: Log mean temperature difference and cooling requirement as a function of the outlet solid temperature. The nominal temperature for the in the adsorption process is 40°C and the solids are cooled from an initial temperature of 80°C.

When these terms are combined to calculate the adsorber heat exchange surface area as a function of the adsorber temperature, the resulting trend is an initial decline in the specific heat transfer surface area with rising temperature (25°C to 75°C) due to the benefits of an increasing LMTD. This is followed by a sharp rise in surface area as the specific cooling requirement overtakes the benefits of a higher LMTD caused by the thermal mass of larger solid flow rates. This occurs as the working capacity of the solid decreases from 1.8 moles per kilogram to zero and more solid sorbent is required to capture CO₂.

Figure 6.4 shows the adsorber heat exchange surface area (normalized by the rate of CO₂ capture) as a function of adsorber temperature. This trend, in which the surface area initially decreases with temperature followed by a sharp increase, is the result of the trade-off between LMTD and cooling requirement shown in the previous graph. This trade-off explains how temperature influences the adsorber heat exchange requirement and why higher temperatures in the adsorber may reduce the cost of the adsorber vessel. This result is calls into question the common practice of reporting rich loadings based on lower and more favorable adsorption temperatures (typically 40°C). This trade-off between material performance and operating cost is examined in more detail in Chapter 7.

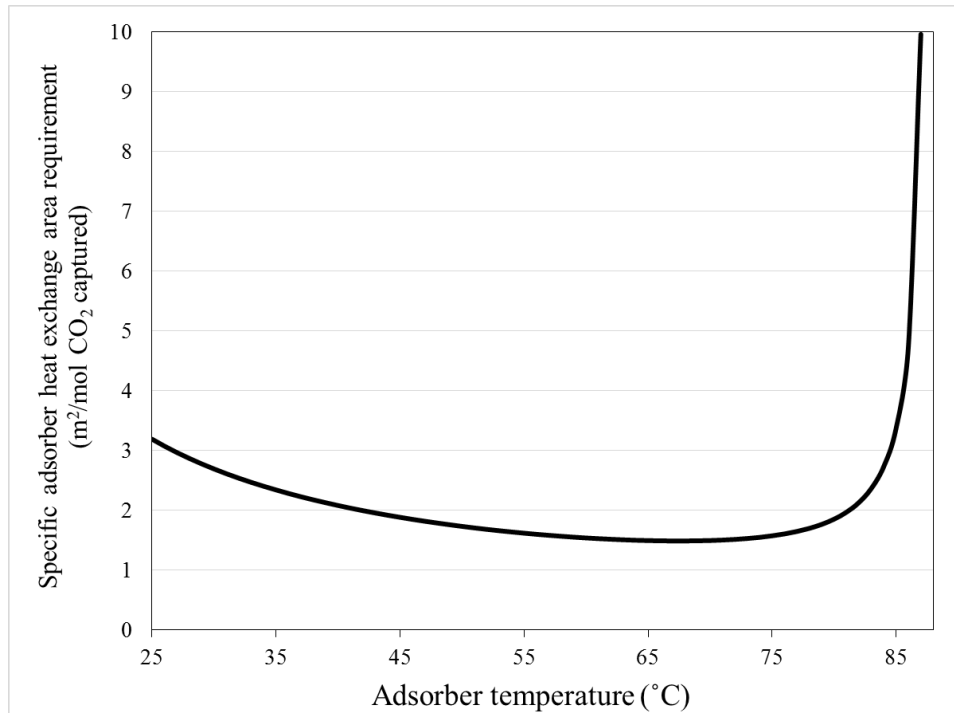


Figure 6.4: The adsorber heat exchange surface area requirement normalized by the quantity of CO₂ and expressed as a function of the adsorber temperature. Higher solid outlet temperatures initially reduce the specific surface area requirement but this trend is reversed as the working capacity of the solid falls to zero and increases the sensible heating requirement of the solid flow rate. The nominal solid outlet temperature is 40°C.

6.7.2. Regenerator cost

The steep decline in adsorber cost observed in Figure 6.2 also occurs in the regenerator as the overall heat transfer coefficient increases from a lower value (typical of fixed and moving beds) to a higher value (typical of more fluidized bed designs). Unlike the adsorber, however, the regenerator is nominally a moving bed design and so the direct capital cost is located at the higher end of the available curve. Figure 6.5 shows how the overall heat transfer coefficient influences the regenerator cost for several solid temperatures. For the initial conditions of 60 W/m²-K and 120°C, the direct capital cost of the regenerator is \$332 million (expressed in 2011 U.S. dollars).

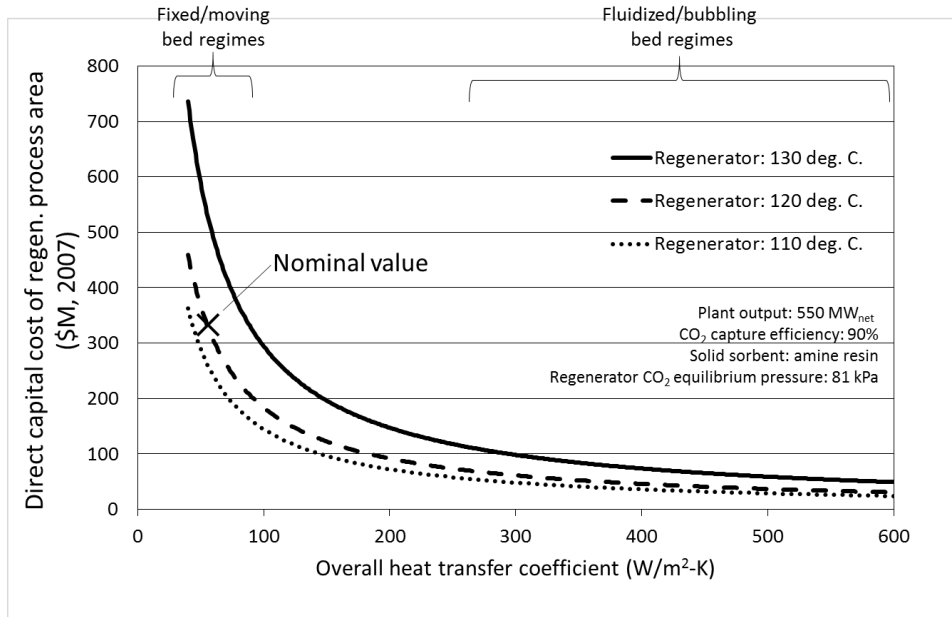


Figure 6.5: Direct capital cost of the regenerator as a function of the overall heat transfer coefficient and regenerator temperature for Case study #1. The capital cost is a function of the heat exchange surface area. The nominal overall heat transfer coefficient for the regenerator is 60 W/m²-K at 120°C resulting in a capital cost of \$332 Million (2011). Results are for a 700 MW_{gross} (550 MW_{net}) plant.

As with the adsorber, the correlation between temperature and direct capital cost in the regenerator is the result of non-intuitive trade-offs. In this case, lower solid temperatures and higher steam temperatures result in lower capital costs. Figure 6.5 demonstrates the relationship between the regenerator heat exchange surface area and the temperature of the solids and steam using Case study #1 as an example.

The horizontal axis in Figure 6.5 shows the maximum temperature of the solids in the regenerator. As the solid temperature increases toward an upper bound at the steam temperature (nominally 135°C shown in the middle curve), the log mean temperature difference (LMTD) decreases. This results in a higher heat exchange surface area and higher capital costs. For the same steam temperature, lower solid temperatures increase the LMTD resulting in lower capital costs.

The steam temperature can be varied as well. Figure 6.5 shows three curves representing three regenerator steam temperatures including the nominal value of 135°C, a lower value of 120°C and a

higher value of 165°C. For a given solid temperature in the regenerator, a higher steam temperature allows for a larger LMTD, which results in lower heat exchange surface area requirements and lower capital cost.

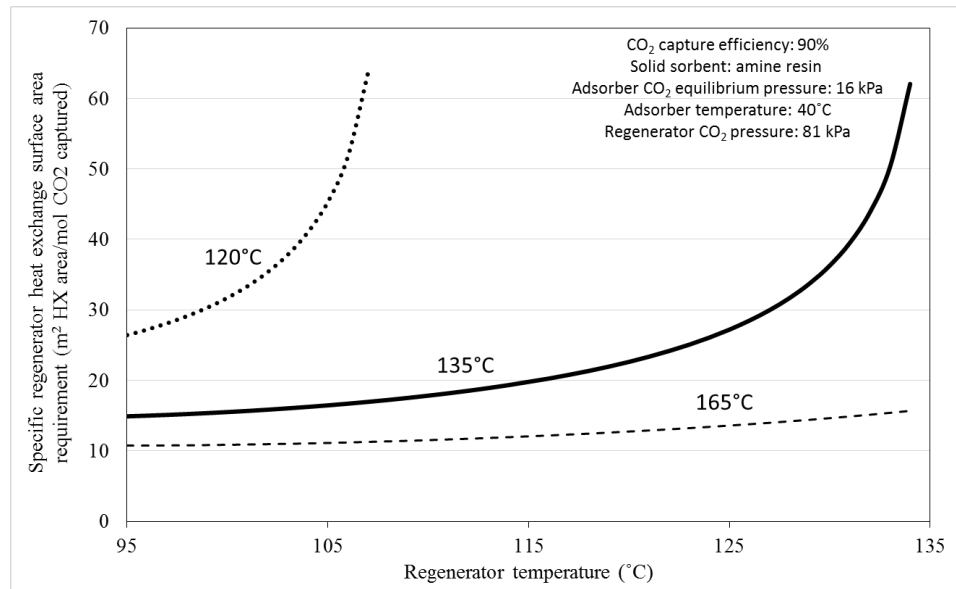


Figure 6.6: The regenerator surface area requirement as a function of the maximum solids temperature (shown on the x-axis) and the maximum steam temperature (represented by the three curves). These two values are used to determine the regenerator LMTD. Assumptions regarding the solid sorbent's tolerance of higher temperatures are very important in terms of the heat exchange surface area and resulting capital cost.

It is important to remember that the type of sorbent materials used in a CO₂ capture system can impose limitations on the maximum temperatures of the solid and steam since the solid material may be denatured by exposure to oxygen at high temperatures. Case study #1 assumes that the amine-based solid sorbent will not be oxidized when heated to 120°C nor when thermally contacted by steam at 135°C. The steam temperature is a compromise between regeneration temperature (120°C) reported in the literature (DOE/NETL, 2013) for the amine-based solid sorbent during laboratory testing and the maximum steam temperature (165°C) used in CCSI process model (DOE/NETL, 2012). However, the temperature limits of the solid sorbent are uncertain at this stage of development nor is it clear that solid sorbents may use the same corrosion inhibitors used in liquid systems. Thus, the three curves shown in

Figure 6.6 are needed to represent potential temperature limits that may be imposed on the regenerator depending on the thermal stability of the solid sorbent.

These results show that the temperature regime in the regenerator can have substantial influence on the heat exchange area of the regenerator. Since the capital cost of these vessels is determined by the heat exchange surface area, these values are an important source of uncertainty that exert a large influence the cost of the regenerator process.

6.7.3. Solid purge fraction

Recall from earlier discussions that a value of 0.004% is used for the solid purge fraction in case studies that include SO₂ degradation. This section discusses the rationale for using this as the nominal value in these cases. First, Figure 6.7 displays the levelized cost of electricity and solids flow rate as a function of the solid purge fraction for Case study #4 (the ideal case with degradation due to water and SO₂). Note that the lowest LCOE does not occur at the lowest solids flow rate, which would be the highest solid purge fraction, but rather at a value between 0.001% and 0.01%.

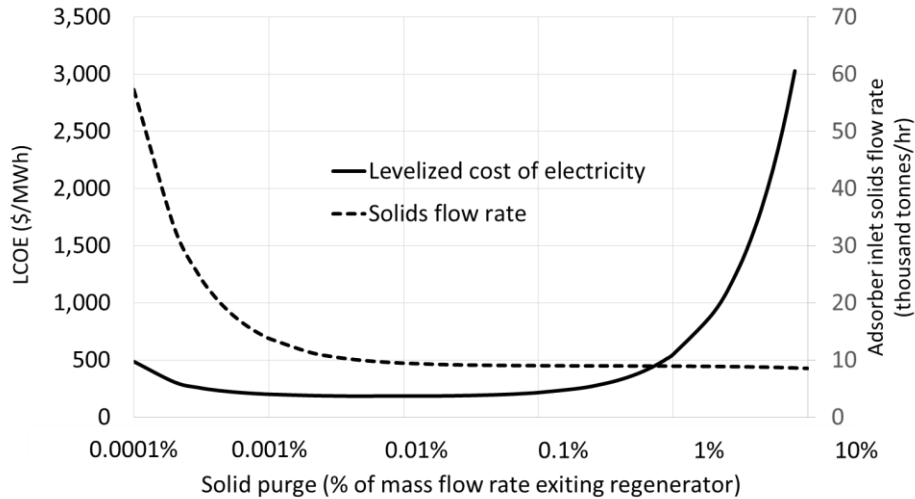
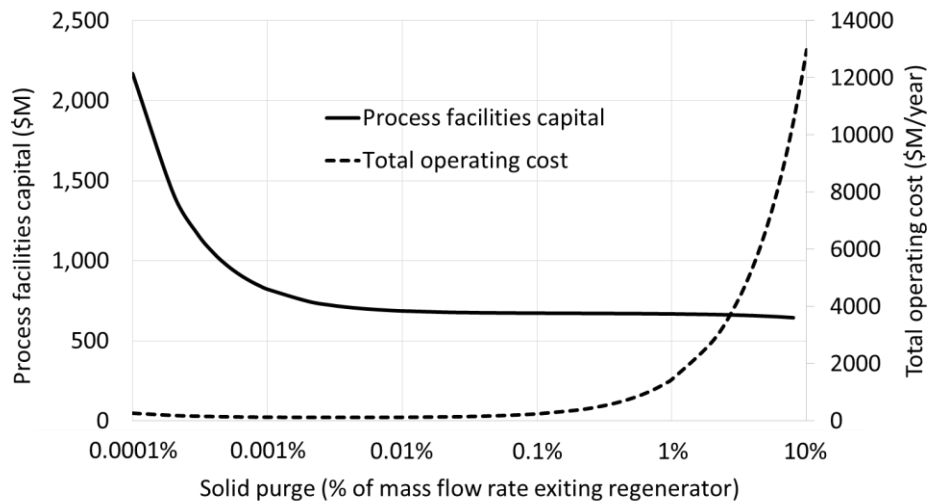


Figure 6.7: Levelized cost of electricity and solid flow rate as a function of the solid purge fraction. Note that the lowest LCOE does not occur at the lowest solid flow rates.

In order to understand why the LCOE is lowest in this particular range of solid purge fraction, consider the influence of the solid purge fraction on the size of the equipment. At high solid purge rates, the solid flow rate is lower due to the higher working capacity of fresh solid sorbent, thus resulting in lower capital costs for the solids handling equipment. However, higher purge rates also result in higher demands for fresh solids, which increase the operating cost of the system. Conversely, lower purge fractions result in lower working capacities and higher capital costs, but require less solid sorbent and have lower operating costs. The optimal solid purge rate strikes a balance between the total process facilities capital and the total operating cost as shown in Figure 6.8.



6.8. Characterization of parameter uncertainty and variability

The model developed in this thesis allows a user to easily look at the performance of the system for many different assumptions. In this respect, it is also possible to expand this model beyond its deterministic capabilities. As mentioned earlier, the IECM modelling framework (for which this model was developed) has probabilistic capabilities that allow model inputs to be represented by distributions rather than deterministic values. In addition to uncertainties or variability in performance model parameters, there is also uncertainty and variability in cost model parameters to which distributions may be applied.

Table 6.8 lists the uncertainty distributions developed for the cost model parameters based on the current literature on solid sorbent-based systems and views elicited from experts working in this field via interviews conducted as part of this research. These distributions reflect both uncertainty and/or variability in the model parameters for indirect costs. Additional information and justification for these values and distributions is available in Appendix A and Appendix I. The direct cost estimates for each major component of the process (*i.e.* adsorber, regenerator, cross-flow heat exchangers, etc.) contribute to the overall uncertainty of cost estimates for this technology. Data about the variability or uncertainty for direct capital costs are unavailable and a range of +/- 25% of the deterministic value is used. This amount of uncertainty is common for estimating equipment costs (DOE/NETL, August, 2007).

Table 6.9: Solid sorbent system cost model parameters and uncertainties for system that would be built using today's state-of-the-art solid sorbent system. These values are used in the Present Case scenarios and uncertainty analysis discussed in Chapter 7.

Cost Parameter	Units	Nominal Value	Unc. Representation (Distribution function)	Reference
CO ₂ storage/disposal cost	S/tonne CO ₂	5	-	
CO ₂ transport cost	\$/tonne CO ₂ /km	0.02	-	
Direct capital costs	% of reference cost	Variable	Triangular(-25%, reference cost, +25%)	This work
Engineering & home office fees	%PFC	7	Triangular (5,7,10)	(Versteeg, 2012)
General facilities capital	%PFC	10	Triangular (5,10,15)	(Versteeg, 2012)
Inventory capital (AFUDC)	%TPC	0.5	Triangular (0.4,0.5,0.6)	(Versteeg, 2012)
Inventory cost	Months VOM	1	Triangular (0.5,1,1)	(Versteeg, 2012)
Operating labor	Jobs/shift	2	Triangular (1,2,3)	(Versteeg, 2012)
Project contingency cost	%PFC	40	Triangular (30,40,50)	(EPRI, 2011)
Process contingency cost	%PFC	55	Triangular (30,55,70)	(EPRI, 2011)
Royalty fees	%PFC	0.5	Triangular (0,0.5,0.5)	(Versteeg, 2012)
Purge steam	\$/tonne	0.30	Triangular (0.20,0.30,0.40)	(Versteeg, 2012)
Solid sorbent cost	\$/kg	4.29	Uniform (3.05,5.78)	This work
Start-up cost	Month of TOM	1	Triangular (0.5,1,1)	(Versteeg, 2012)
Total maintenance cost	% TPC	2.5	Triangular (1,2.5,5)	(Versteeg, 2012)
Waste disposal cost	\$/tonne	19.11	Normal (1.0,0.1)	(Carnegie Mellon University, 2014)

A host of other characteristics of the facility as a whole also influence the cost of the CO₂ capture process as discussed in Chapter 7.

6.9. Chapter conclusion

This chapter reviewed the cost method and equations used to estimate the capital and operating costs of a solid sorbent-based CO₂ capture system and the method used to integrate these system costs with plant-level IECM models to estimate the total cost of a new PC power plant equipped with solid sorbent-based CO₂ capture. Several sensitivity studies were used to illustrate the effects of performance and design variables on the cost of process components using the characteristics of the adsorber and regenerator process areas. The sensitivity studies suggest that improving the overall heat transfer coefficients of the regenerator and developing solid sorbents capable of resisting oxidation at higher temperatures would reduce the capital cost of the CO₂ capture system.

This chapter also reviewed the trade-offs between capital and operating costs when selecting a solid purge fraction. However, these results are sensitive to the parameter values used in the performance model, and the optimal values for the temperatures and purge depend on the characteristics of the solid sorbent and achievable design specifications for the process equipment.

Finally, this chapter presented uncertainty distributions for the cost parameters used in the CO₂ capture system. In the next chapter, the integrated performance and cost models are also used to estimate the cost of a new coal-fired power plant equipped with solid sorbent-based CO₂ capture for the deterministic case studies presented in Chapter 5. The model also considers performance and cost uncertainty for implementing the current generation of solid sorbent technology.

7. Model applications

One of the major objectives behind building the performance and cost models described earlier is to provide an assessment of solid sorbent technology as an option for controlling CO₂ emissions from a variety of fossil-fuel power plants. Such assessments are useful indications of the technology's range of potential costs as well as the performance improvements which would yield the greatest return in terms of the technology's cost. This type of model is also useful for determining where there exists a void in performance data that, if filled, would reduce uncertainty about the performance and cost of an integrated, full-scale solid sorbent-based CCS system. In this sense, these types of models are useful for determining research and development objectives and priorities. Analysis of options for controlling CO₂ emissions from power plants might include questions such as:

- If a new coal-fired power plant were built today, how does solid sorbent-based CO₂ capture affect the overall performance and cost of the power plant?
- How much would it cost in terms of capital requirement, levelized cost, and cost per unit of CO₂ avoided? What are the uncertainties associated with these costs?
- What are the key factors that affect these costs?
- What is the scope for improvement in solid sorbent-based CO₂ capture through targeted R&D efforts?
- How might the costs change between a first-of-a-kind plant versus a future mature system?

These questions address issues relating to the technical, economic, and environmental feasibility of CO₂ capture and storage. This chapter will address these questions using a combination of specific case studies and sensitivity analyses for new plant applications of solid sorbent-based CCS technology while maintaining transparency regarding the performance and cost assumptions. This transparency is one of the major advantages of this work compared to more complex modelling approaches.

There are other sets of questions related to the deployment of large-scale CCS technology such as the technical feasibility of storing large quantities of CO₂ in deep reservoirs, long-term risks, public perceptions, and the feasibility of enacting legislation that would result in large-scale CCS deployment. While important to the success of CCS as a CO₂-reduction strategy, these questions are beyond the scope of this study.

7.1. Baseline plant characteristics

The baseline plant configuration, performance, and financial assumptions used for the power plants throughout this chapter are based on a commonly-used set of “baseline” plant characteristics specified by the U.S. Department of Energy (DOE/NETL, August, 2007), (DOE/NETL, 2010) as shown in Table 7.1. All costs are evaluated in 2011 constant dollars.

Table 7.1: Baseline PC power plant assumptions for the reference (no CO₂ capture) case and CCS-equipped cases. Reference values are derived from previous IECM work (Rubin & Zhai, 2011; Versteeg, 2012).

Plant specification	PC Power Plant w/o CCS	PC Power Plant w/ CCS
Power plant specifications		
Ambient air pressure (kPa)	101.3	101.3
Ambient air temperature (K)	298	298
Capacity factor (%)	75%	75%
Constant flue gas heat capacity (kJ/kmol)	0.036	0.036
Cooling	Wet cooling tower	Wet cooling tower
Environmental controls	SCR, fabric filter, wet FGD	SCR, fabric filter, wet FGD
Fuel cost (2011\$/GJ)	\$2.1	\$2.1
Fuel type	Illinois No. 6	Illinois No. 6
Fuel cost nominal escalation (real escalation plus inflation %)	0%	0%
Fuel heating value as received (HHV, kJ/kg)	30,840	30,840
Nominal net power plant output (MWe)	550	550
Steam cycle	Supercritical	Supercritical
Financial assumptions		

Annual inflation rate	N/A	N/A
Cost year and type	2011 constant dollars	2011 constant dollars
Fixed charge factor*	0.113	0.143
Percentage debt	50%	45%
Percentage equity	50%	55%
Real bond interest rate	4.5%	5.5%
Real escalation rate	0%	0%
Real stock return	12%	12%
Plant book life	30	30
Weighted cost of capital before taxes	8.25%	9.075%
Years of construction	5	5
Tax rates		
Federal tax rate (%)	36%	36%
State tax rate (%)	6%	6%
Property tax rate	0%	0%
CO₂ capture and storage system specifications		
CO ₂ product pressure (MPa)	N/A	13.79
CO ₂ storage cost (\$/tonne)	N/A	5
CO ₂ transportation distance (km)	N/A	100
Flue gas CO ₂ capture requirement	N/A	90%
Flue gas CO ₂ concentration into CO ₂ capture system	N/A	13.5%
Project contingency (%)**	N/A	55%
Process contingency (%)**	N/A	40%

*The fixed charge factor is calculated based on the year end carrying charges and a present worth factor according to the equation: $FCF = [CC_1(1+i)^{-1} + CC_2(1+i)^{-2} + \dots + CC_n(1+i)^{-n}] / a_n$ where n is the book life of the plant, i is the interest rate, CC is the year by year carrying charges of the plant and a_n is the present worth factor for a uniform series. The year by year carrying charges are the sum of: (the return on debt, the return on equity, the payable income taxes, book depreciation, property tax, and insurance)/the total plant cost (TPC). The value of a_n is calculated according to the following equation $a_n = [(1+i)^n - 1] / [i(1+i)^n]$ (EPRI, 1986). A value of 0.113 represents financing assumptions for a mature system while 0.143 represents a first-of-a-kind plant (FOAK). See (Borgert, 2015; Versteeg, 2012) for details.

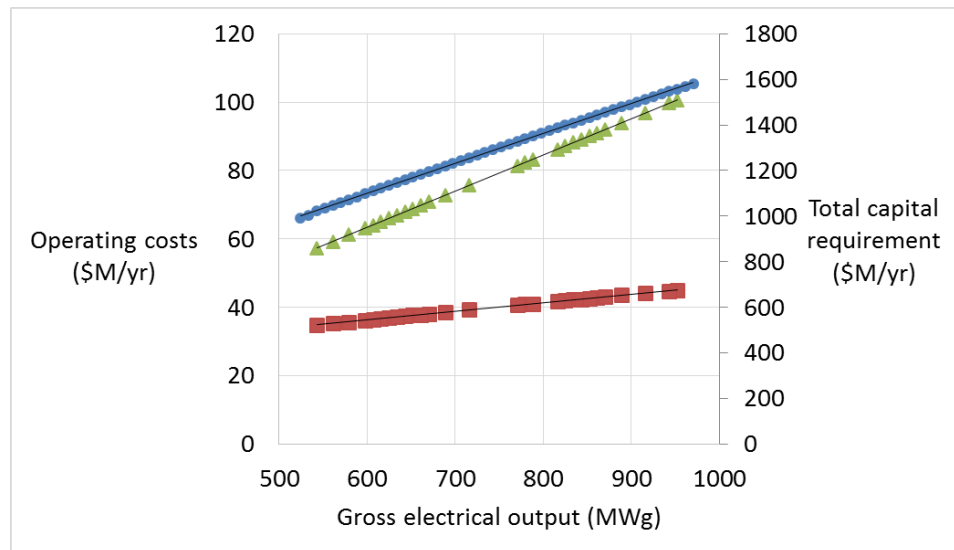
**Contingency values follow EPRI TAG™ guidelines. See Section 6.1 for details.

A more detailed breakdown of owner's costs typically includes a site-specific and comprehensive financial analysis that is not included in this work for simplicity and clarity. Much of this detail is specific to the fixed charge factor, which reflects whether a plant process is financially considered high risk. A higher (0.143) fixed charge factor is used for the power plant that includes the solid sorbent CCS process owing

to the high financial risk of owning and operating a first-of-a-kind (FOAK) facility. A lower (0.113) fixed charge factor is used for processes not related to CO₂ capture. Later sections in this chapter will discuss the method used to derive Nth-of-a-kind (NOAK) estimates using the cost estimates provided in proceeding section. More details regarding the power plant specifications and financial assumptions are available in Appendix K.

Changes to the configuration and financial assumptions of a plant can cause large changes to the final costs of the plant. However, there exists no standard set of assumptions used by analysts nor entities that perform these types of analyses, and costs for power plants can vary widely depending on the person and/or organization performing the analysis. Moreover, cost methods often vary over time as an individual/organization's understanding of best practices evolve. Therefore, the cases presented in this thesis are most usefully compared to other plants in this thesis and not to costs presented in other studies that use different assumptions.

The capital and operating costs for the rest of the power plant excluding CO₂ capture (commonly called the “balance of plant” (BOP)) are estimated based on the gross output of the plant. When CO₂ capture is applied, the costs for the balance of plant are scaled using the gross capacity of the plant before steam withdrawal for the CO₂ capture system. For example, if a power plant with CO₂ capture produces 650 MW gross and requires 150 MW equivalent of steam in the CO₂ capture system, then the gross plant capacity used to estimate the BOP costs is 800 MW_{gross}. These cost correlations are based on the cost estimates produced by the IECM using the assumptions from Table 7.1. Figure 7.1 shows the scaling of total capital requirement and operating costs of the plant with gross output. This relationship is used in all case studies to quantify the TRR of the balance of the plant.



Cost component	Symbol	Regression	R ² value
Total capital requirement	Circle	$y = 1.308x + 317$	>0.99
Fixed O&M	Triangle	$y = 0.0251x + 21.3$	0.99
Variable O&M	Square	$y = 0.1057x + 0.0085$	0.99

Figure 7.1: Scaling functions for the total capital and operating costs for the PC power plant without CO₂ capture as a function of the gross electrical output. These cost functions are also used to calculate the costs of the balance of the plant (BOP) when CO₂ capture is applied.

The cost correlations defined in Table 7.1 are based on specific plant setup serving as the default system for post-combustion capture in the IECM. This plant is based on a supercritical PC plant burning Illinois #6 coal meeting the U.S. New Source Performance Standards.

The reference power plant (Case 0) does not include CO₂ capture and storage. Such a plant would have a higher efficiency and therefore produce electricity with greater efficiency in terms of the capital and operating costs. This case therefore requires a separate estimation of costs and efficiency. The IECM (version 8.0.2) provides an estimate for a similar plant without CO₂ capture of \$61 per megawatt hour. A summary of the results for the reference power plant without CO₂ capture is shown in Table 7.2. This power plant has the standard suite of environmental controls as explained earlier in this document and this plant follows the assumptions outlined in Table 7.1.

Table 7.2: Summary of IECM results for the reference supercritical power plant without CO₂ capture. All costs are in constant 2011\$.

Case Study	Gross Output (MW _g)	Plant Efficiency (%HHV)	CO ₂ Emissions (tonnes/hr)	Total Capital Requirement (\$Million)	LCOE (\$/MWh)
Case 0: Reference System (No CCS)	588	38.9	450	1084	61

These costs represent a 550 MW_{net} power plant that would be constructed in the absence of CO₂ control technology. In this sense, these estimates provide a baseline estimate used to evaluate the impacts of CO₂ capture.

7.2. Case studies with solid sorbent-based CO₂ capture

This section presents the nominal results for several case studies using the performance and cost models described in Chapters 4, 5, and 6 along with the baseline plant assumptions in Table 7.1. These case studies represent a wide gamut of CO₂ capture systems ranging from an idealized system to the currently available system built using available materials and process design. A summary of the initial 14 case studies modelled in this Chapter is available in [Table 7.3](#). A more thorough description is available in Chapter 5 and complete details for reproducing these results using the performance and cost models are given in Appendix J. Again, it should be noted that the costs shown in these studies represent a first-of-a-kind (FOAK) plant reflected in the high contingency cost and fixed charge factors. As a reminder, all costs in the following tables are labeled FOAK.

Table 7.3: Differences in parameter values for the initial 14 case studies.

Case	Adsorber HX		Regen HX		X Flow HX		Sorbent				Degradation			
	300	Other	60	Other	Moving	Fluid	ADA	CCSI	2015	2025	None	H ₂ O	SO ₂	Both
1	✓		✓		✓		✓				✓			
2	✓		✓		✓		✓					✓		
3	✓		✓		✓		✓						✓	
4	✓		✓		✓		✓							✓
5	✓		✓			✓		✓				✓		
6	✓		✓			✓		✓						✓
7	✓		✓		✓				✓		✓			
8	✓		✓		✓				✓			✓		
9	✓		✓		✓				✓				✓	
10	✓		✓		✓				✓					✓
11		✓		✓	✓					✓	✓			
12		✓		✓	✓					✓		✓		
13		✓		✓	✓					✓			✓	
14		✓		✓	✓					✓				✓

7.2.1. Power plants with idealistic CO₂ capture (Case Studies 1-4)

This section presents the first four case studies that represent a benchmark goal for power plants with solid sorbent-based CO₂ capture. The first case study is an idealistic process previously described in Section 5.2 using a mixed amine ion exchange resin demonstrated at the National Carbon Capture Center (NCCC) demonstration plant. This is an idealized study seeking to maximize the working capacity of a typical mixed amine-based sorbent by assuming gas inlet adsorption equilibrium conditions and a large (80 K) temperature change between the adsorber and regenerator. Case #2 characterizes the same system while including degradation of the material caused by SO₂. Case #3 considers the ideal sorbent system with only the influence of flue gas water uptake. Case #4 includes the effects of both SO₂ and water on an idealized process.

A summary of the performance and cost results for the plants is given below in Table 7.4. The ideal sorbent system plant has the highest net efficiency, lowest CO₂ emissions, and lowest revenue required of the three plants with ideal capture. The added influence of SO₂ and water cause noticeable reductions in the performance of the power plant leading to a larger gross plant size and higher costs. Degradation causes higher solid flow rates, which increase the regenerator steam requirement and lower the plant efficiency. The higher solid flow rates also require larger equipment leading to higher capital costs as seen in the higher TCR when degradation is included.

Table 7.4: Summary of case study supercritical PC plants with idealized solid sorbent-based CO₂ capture. Plants produce 550 MW_{net} and burn Illinois #6 coal. All costs are in constant \$Millions (2011).

Case study	Gross Output (MW _g)	Plant Efficiency (%HHV)	CO ₂ Emissions (tonnes/hr)	Total FOAK Capital Req'ment (\$M)	FOAK LCOE (\$/MWh)
Case #1: Ideal solid sorbent	700	29.6	59	2,570	161
Case #2: SO ₂ degradation only	710	29.0	60	2,698	170
Case #3: Water degradation only	713	28.5	61	2,857	176
Case #4: SO ₂ and water degradation	715	28.3	62	2,956	184

7.2.2. Power plants with CCSI response surface model (Cases 5 and 6)

This section presents two case studies for power plants with solid sorbent-based CO₂ capture compliant with the performance and cost parameter values developed by the NETL-led Carbon Capture Simulation Initiative (CCSI) and unique to NETL's solid sorbent, 32D. Case #5 shows results using the nominal performance and cost assumptions used by CCSI in which no SO₂ degradation is considered. Case #6 shows the added effect of SO₂ degradation.

A summary of the performance and cost results for the CCSI-based systems is given in Table 7.5. The system that does not include degradation (Case# 5) has a higher net efficiency, lower CO₂ emissions, and lower revenue required than the scenario with SO₂ degradation.

Table 7.5: Summary of case study results for supercritical PC plants with CO₂ capture using CCSI's response surface models. Plants produce 550 MW_{net} and burn Illinois #6 coal. All costs are in constant \$Millions (2011).

Case study	Gross Output (MW _g)	Plant Efficiency (%HHV)	CO ₂ Emissions (tonnes/hr)	Total FOAK Capital Req'ment (\$M)	FOAK LCOE (\$/MWh)
Case #5: CCSI ideal sorbent	747	24.4	72	2,323	160
Case #6: CCSI with SO ₂ Degradation	751	24.0	73	2,381	165

7.2.3. Power plants with present-case elicitation results (Cases 7-10)

Four case studies were modelled based on the present-case scenario described in Section 5.9. Case #7 examines the present-case scenario when no degradation of the solid sorbent occurs. Case #8 shows results for the same scenario with the added influence of SO₂ degradation. Case #9 shows the present-case results with the added effect of water uptake. Finally, Case #10 considers the influence of both SO₂ and water degradation.

A summary of the performance and cost results for the present-case systems is given in Table 7.6. As seen with the ideal cases shown previously, degradation causes significant deterioration to the performance and cost of the power plant.

Table 7.6: Summary of case study results for supercritical PC plants with CO₂ capture using the present case performance and cost models. Plants produce 550 MW_{net} and burn Illinois #6 coal. All costs are in constant \$Millions (2011).

Case study	Gross Output (MWg)	Plant Efficiency (%HHV)	CO₂ Emissions (tonnes/hr)	Total FOAK Capital Req'ment (\$M)	FOAK LCOE (\$/MWh)
Case #7: Ideal present elicitation	703	29.3	60	2,899	178
Case #8: Present case with SO ₂ degradation	714	28.8	61	3,030	188
Case #9: Present case with H ₂ O degradation	721	27.4	64	3,230	199
Case #10: Present case with SO ₂ and water degradation	723	27.2	64	3,435	210

7.2.4. Power plants with future-case elicitation results (Cases 11-14)

This section examines four case studies on the future-case scenario. Like the present-case study, the parameters used in section are described in Section 5.9. Case #11 examines the idealized future-case scenario in which no degradation of the solid sorbent occurs. Case #12 shows results when the influence of SO₂ is included. Case #13 shows the results for when water degradation is occurring and Case #14 considers the influence of both SO₂ and water degradation.

A summary of the results for the future-case systems is given in Table 7.7. As seen with the ideal cases shown previously, degradation causes significant deterioration to the performance and cost results although these losses are somewhat offset by advancements in material and process development.

Table 7.7: Summary of case study results for supercritical PC plants with CO₂ capture using the future case performance and cost models. Plants produce 550 MW_{net} and burn Illinois #6 coal. All costs are in constant \$Millions (2011).

Case study	Gross Output (MW _g)	Plant Efficiency (%HHV)	CO ₂ Emissions (tonnes/hr)	Total FOAK Capital Req'ment (\$M)	FOAK LCOE (\$/MWh)
Case #11: Ideal future elicitation	699	29.8	59	2,303	147
Case #12: Future case with SO ₂ degradation	709	29.3	60	2,86	154
Case #13: Future case with H ₂ O degradation	715	28.1	62	2,550	158
Case #14: Future case with SO ₂ and water degradation	716	27.9	63	2,610	164

7.2.5. Case study discussion

A breakdown of the CO₂ capture system direct capital costs for a selection of case studies is shown in Table 7.8. The most expensive equipment for the CO₂ capture system is the regenerator followed by the hot-side heat exchanger. In each case, these vessels combine to make up more than half of the total process facilities capital. In order to understand why these vessels are so expensive, it is helpful to recall from Section 6.2 that the cost of these vessels scale with heat exchange surface area. The high costs shown in these case studies are the result of the high thermal mass of circulating solids, which is caused by a low working capacity, combined with the low overall heat transfer coefficient of these vessels and the low temperature gradient between the solids and heat transfer fluid.

The lowest capital costs are realized by the CCSI case studies (Cases #5 and #6) at \$332 and \$350 million respectively because of lower heat exchange surface areas for the regenerator and hot-side cross-flow heat exchangers vessel. The lower heat exchange surface areas for these vessels is the result of higher temperatures in the regenerator (165°C for the steam and 135°C for the solids) which allow for a large temperature gradient between the solids and heat exchange. The other systems use lower

temperatures (110°C to 135°C) due to concerns regarding oxidation of the amine sorbent at temperatures in excess of 100°C (Ahmadalinezhad, et al., 2013; Drage, et al., 2009).

Table 7.8: CO₂ capture system direct capital cost estimates for select cases. Results are for supercritical PC plants producing 550 MW_{net}, capturing 90% CO₂ emissions, and burning Illinois #6 coal. All costs are in constant \$Millions (2011).

CO₂ Capture System	Case							
Direct Capital Costs	#1	#4	#5	#6	#7	#10	#11	#14
Adsorber	33	35	29	32	29	21	20	12
Cold-side heat exchanger	29	44	3	3	43	52	21	24
Conveyors	4	5	4	5	6	6	4	4
Cyclones	9	8	9	9	9	8	9	8
Drying and Compression Unit	16	16	18	18	16	17	16	16
Flue gas blower	18	20	22	22	18	20	18	20
Flue gas pre-treatment	9	9	10	10	9	9	9	9
Heat exchange fluid pump	0	0	0	0	0	0	0	0
Heat exchange fluid compressor	3	4	2	2	3	4	3	3
Hot-side heat exchanger	95	143	13	14	264	320	130	144
Regenerator	331	419	217	229	298	448	196	295
Sorbent storage	2	3	2	3	3	4	2	3
Steam extractor	4	4	4	4	4	4	4	4
Process Facilities Capital	552	709	332	350	700	913	430	541

Another important result is the contrast in direct capital cost between cases that exclude and include solid sorbent degradation. When included, the influence of water and SO₂ increases the overall capital cost by 25% to 30% in the ideal, present, and future scenarios. This is the result of the additional degraded solid material circulating through the system. The added material requires larger and thus more costly equipment. The added capital costs are particularly high for the regenerator and cross-flow heat exchangers tasked with transferring heat to or from the solids.

The total capital requirement (TCR) and its components for the same case studies are shown in Table 7.9. The indirect costs for the CO₂ capture system are quantified based on the direct capital costs

and the resulting TCR is roughly twice the direct capital costs for each case. The lower direct capital costs realized in the cases shown previously therefore result in a lower capital requirement.

Table 7.9: Breakdown of CO₂ capture and storage system total capital requirement (TCR) by cost component for FOAK systems. Results are for supercritical PC plants producing 550 MW_{net}, capturing 90% CO₂ emissions, and burning Illinois #6 coal. All costs are in constant \$Millions (2011).

Cost component	Case #1	Case #4	Case #5	Case #6	Case #7	Case #10	Case #11	Case #14
Process Facilities Capital	552	709	332	350	700	913	430	541
General Facilities Capital	55	71	33	35	70	91	43	54
Eng. & Home Office Fees	39	50	23	24	49	64	30	38
Project Contingency Cost	221	284	133	140	280	365	172	217
Process Contingency Cost	303	390	183	193	335	502	237	298
Interest Charges (AFUDC)	3	4	2	2	4	5	2	3
Royalty Fees	3	4	2	2	4	5	2	3
Preproduction (Startup) Cost	4	5	2	2	5	6	3	4
Inventory (Working) Capital	4	5	6	7	4	5	4	4
Capture System Total Capital Requirement (TCR)	1,182	1520	716	755	1,499	1,956	922	1,161
T&S system TCR	61	62	65	65	62	63	61	62
Effective TCR	1,244	1,582	780	819	1,560	2,018	983	1,223

The levelized cost of electricity for the all case studies are shown in Figure 7.2. The diagram shows the breakdown of the plant costs in terms of the annualized capital and operating costs for the CO₂ capture system and the balance of the plant (BOP). For reference, the case without CO₂ capture had an LCOE of \$61 per MWh. The BOP costs for the CO₂ capture cases range between \$80 and \$100 per MWh due to the larger gross plant size for the same electrical output. The annualized cost of a solid sorbent-based CO₂ capture system is approximately equal to the balance of the plant. A summary of the results for the initial 14 case studies discussed in Section 7.2 is available in Table 7.10.

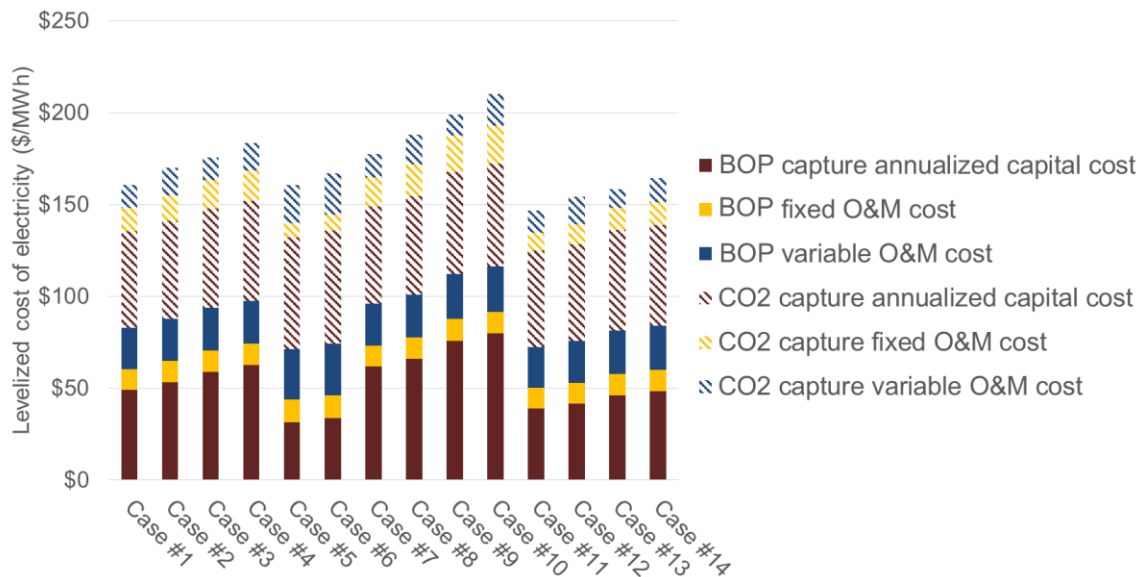


Figure 7.2: Breakdown of the levelized cost of electricity separated by the costs associated with the CO₂ capture system and the balance of the plant (BOP). Costs for these FOAK cost estimates are reported in \$/MWh (2011).

The predominant cost of the CO₂ capture system is high process facilities capital (PFC) requirement, the value of which is approximately equal to the PFC for the balance of the power plant. The insights discussed in this section suggest that the underlying cause of the high capital cost is the high internal surface area required by the solid heat exchangers (e.g. the adsorber, regenerator, and cross-flow heat exchangers). Given the significant economic penalties associated with the currently available solid sorbent-based CO₂ capture technology, these results indicate that step-change improvements to these vessels and/or reductions in their unit cost will be required to achieve DOE's development goals for second-generation post-combustion CCS technologies. Furthermore, degradation and temperature tolerance together play a nuanced but vital role in determining the capital cost of a solid-based CO₂ capture system as well as the levelized cost of electricity produced by a power plant equipped with this technology.

Table 7.10: Summary of results for the initial 14 case studies. All costs are reported in 2011 constant dollars.

Case	TCR (\$M)	Plant Efficiency (% HHV)	LCOE (\$/MWh)	Case	TCR (\$M)	Plant Efficiency (% HHV)	LCOE (\$/MWh)
1	2,572	29.6	161	8	2,020	28.8	188
2	2,697	29.0	170	9	3,330	27.4	199
3	2,857	28.5	176	10	3,435	27.2	210
4	2,956	28.3	184	11	2,303	29.8	147
5	2,323	24.4	160	12	2,386	29.3	154
6	2,380	24.0	165	13	2,550	28.1	158
7	2,899	29.3	178	14	2,610	27.9	164

7.3. Cost uncertainty for solid sorbent systems

Many parameter values need to be defined for this system. If a single value is used for each parameter the results represent a unique system configuration with well-defined design and operating conditions. This was the objective of the deterministic exercise in the previous section. However, if one considers the population of potential parameter values for this process, than most of the parameters are better represented as ranges of values (or probability distributions) in lieu of deterministic values. Various combinations of these parameter values then represent a set of possible configurations for the solid sorbent-based CO₂ capture process.

Figure 7.3 first shows the effect on the levelized cost of electricity of a uniform $\pm 10\%$ change from the baseline value of the most influential variables for the present case technology with water and SO₂ degradation scenario (Case #10). This figure shows that the performance parameters, particularly the adsorber solids and regenerating steam temperatures, are important parameters for the LCOE calculation. Note that many of the top ranking parameters share the common trait of influencing the solid flow rate and/or heat exchanger calculations. This indicates that a system with a high working capacity and good heat transfer characteristics is key to achieving a more efficient system.

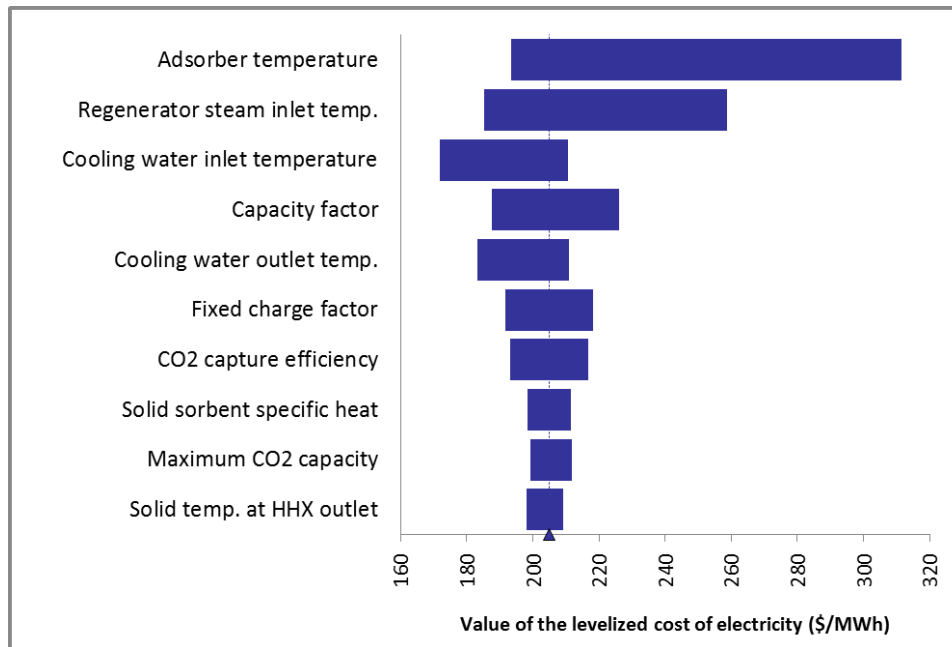


Figure 7.3: A tornado diagram indicating the change in the levelized cost of electricity for a +/- 10% change in the input of ten important parameters.

In practice, the values of performance and cost parameters are not all independent of one another and the properties of the solid sorbent do not occur independently of the system parameters. Moreover, some parameters are more uncertain than others. Thus, several analyses are used to characterize the uncertainty regarding the performance and cost of a full-scale system. First, a probabilistic analysis was undertaken to more realistically characterize the range of key system parameters relative to the deterministic results presented in the previous section.

The parameter distribution functions for this analysis were shown in Tables 5.17 and 6.8 for the performance and cost variables, respectively. Uncertainty distributions were compiled following the methodology outlined by Frey and Rubin (Frey & Rubin, 1991), with distributions inferred either from the literature or estimated by the author. Where data are lacking, expert elicitation was employed to estimate parameter uncertainty based on the elicited values for the best case, worst case, and “best guess” responses. More discussion about uncertainty distributions and the expert elicitation exercise may be found in Appendix A and Appendix I, respectively.

7.4. Probabilistic uncertainty analysis

How much is it likely to cost to produce electricity from a new supercritical pulverized coal (PC) power plant equipped with solid sorbent-based CO₂ capture technology in the U.S. today? The question sounds quite simple. However, one needs to make a great number of assumptions in order to answer it. Different assumptions about power plant design, operation, and financing can have a significant effect on the cost of electricity production. The Present Case scenario (Case #10) represents a current available system employing a hypothetical amine-based solid sorbent subject to degradation. This section details the cumulative probability distribution results based on the performance and cost distributions shown in Tables 5.18 and 6.9, respectively.

The results represent the range of potentially feasible solid sorbent systems capable of delivering 550 MW_{net} of electricity with 90% CO₂ capture using currently available solid sorbent materials. However, note that not every combination of uncertain parameter values results in an operable system. Recall from Figure 5.5, for example, that the rich and lean loading can become equal or even inverted (lean loading is greater than rich loading) for certain combinations of sorbent parameters and vessel conditions, which is not a feasible system. Hence, the results shown in this section represent only combinations of parameters that yield a plausible CCS system.

Figure 7.4 first shows the effect of considering uncertainties and design variability only in the performance parameters of the solid sorbent system (from Table 5.18). It may be noted that most of the distributions for the input parameters are uniform or triangular. The resulting distribution for the levelized cost of electricity has a 90-percentile range of \$167 to \$534 per MWh of net electricity produced. The median cost is \$209 per MWh compared to the deterministic value of \$208 per MWh and the mean value of \$330/MWh. The wide range indicates that the LCOE is quite sensitive to the performance parameters uncertainty and variability. Among the 21 parameters included in this analysis, those with the highest impact on the mean of the distribution curve include the influence of water on the maximum CO₂ capacity, the regenerator CO₂ pressure, and the efficiency of the flue gas blower.

The tails of the distribution extending to the left imply combinations of design conditions and performance parameter values that yield the lowest overall cost. However, these are generally unlikely combinations (*e.g.*, high maximum loading and beneficial water interactions) or too pessimistic (*e.g.* adsorption equilibrium at outlet CO₂ gas pressure and low overall heat transfer coefficients). In contrast, the tail extending to the right indicates that there are multiple parameters and/or combinations of parameters that would cause the system to perform poorly and substantially increase electricity generation costs. Correlations between these parameters are not well quantified, however, and thus the cumulative probability may overstate the extreme values of plausible systems. The median value (and its vicinity) represents a more realistic set of design conditions for current commercial systems. Note that uncertainty in the capacity factor and fixed charge factor would further broaden the distribution.

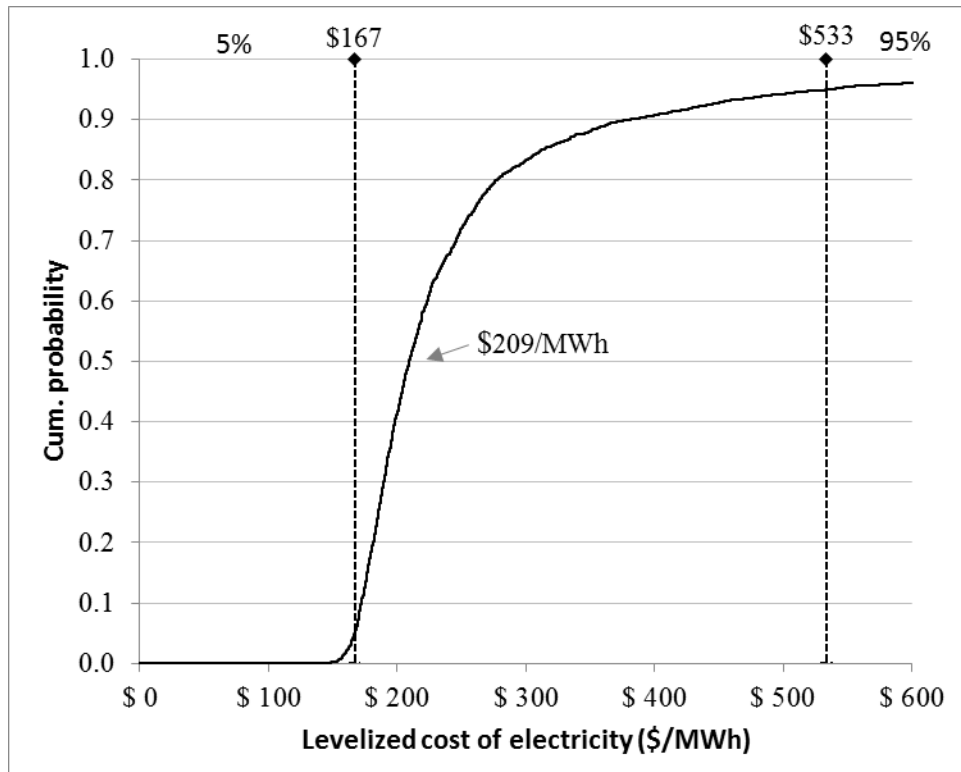


Figure 7.4: Probability distribution for the levelized cost of electricity with only the uncertainties in the performance parameters of the solid sorbent system considered. Values are reported in constant dollars (2011).

Figure 7.5 next considers the probabilistic curves obtained by including uncertainty distributions for only the cost parameters of the capture system. Generally, the cost parameter uncertainties do not have as significant an impact on the levelized cost of electricity compared to the performance parameter uncertainties. Also shown is the probability distribution obtained by varying both the performance and cost parameters. This closely tracks the performance-only distribution and is evidence that the performance parameters are the dominant source of uncertainty in the LCOE uncertainty results shown in Figure 7.5.

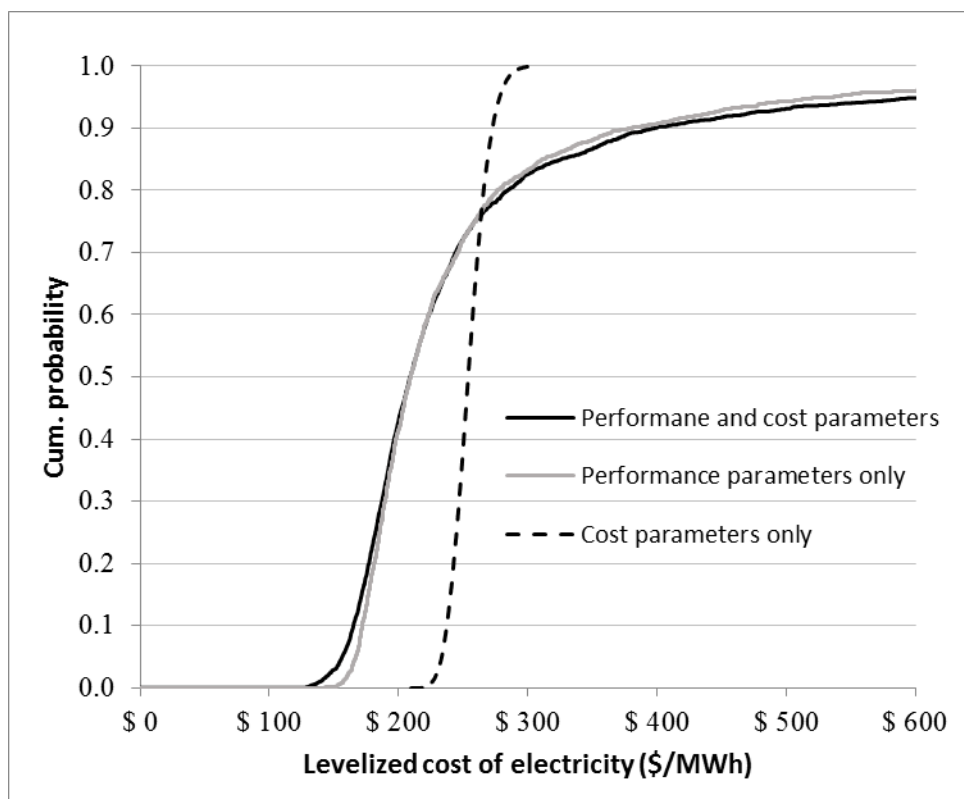


Figure 7.5: Probability distribution for the levelized cost of electricity for the Present Case scenario with the uncertainties in performance and cost parameters of the solids sorbent system considered.

Table 7.11 summarizes the probabilistic results by looking at three representative data points for each curve representing the 90% confidence interval and median value.

Table 7.11: Summary data for the probabilistic LCOE uncertainty distributions representing the 90th percentile and median. All dollars are expressed in 2011 U.S. dollars .

Levelized cost of electricity probability estimates				
Uncertainty Scenario	Mean cost	Median cost (50th percentile)	Cost range (5th and 95th percentile)	Most influential parameters on distribution mean
Performance variables only	\$330	\$209	\$167 - \$534	Lost CO ₂ capacity (water), Regenerator CO ₂ pressure, FG blower efficiency
Cost variables only	\$254	\$254	\$232 - \$278	Total maintenance cost (%TPC), reference regenerator cost, reference HHX cost
Performance and Cost variables	\$355	\$209	\$156 - \$613	Water loss, regenerator CO ₂ pressure, reference regenerator cost

The parameter with the greatest influence on the LCOE calculation is the influence of flue gas water vapor on the solid sorbent's maximum CO₂ capacity. This parameter is important because of its influence on the rich CO₂ loading. A positive value indicates that the benefit of additional CO₂ adsorption pathways is dominant over potential pore blockage caused by capillary action or other negative effects. The propensity of the material to experience one or more of these phenomena depends on the materials and manufacturing methods used make the solid sorbent.

7.5. Estimating future costs

The electricity industry has experienced reductions in the cost of technologies over the past several decades as a result of R&D investments, learning by doing, and other factors (Rubin, et al., 2007). In an effort to understand how a power plant equipped with solid sorbent-based CO₂ capture may perform as a mature, widely deployed system, this thesis uses historical experience curves as the basis for estimating future cost trends and compares the results to target goals set by U.S. DOE for advanced CO₂ capture technologies. The effects of uncertainties in the capital and operating costs on projected cost reductions are also evaluated using sensitivity studies for the currently available solid sorbent technology.

7.5.1. Introduction

Given the growing worldwide interest in CO₂ capture and storage as a potential option for climate change mitigation, the expected future cost of CCS technologies is of significant interest. Like some studies of CO₂ capture and storage (Al-Juaied & Whitmore, 2008), the cost estimates shown in the previous chapters have modelled a first-of-a-kind (FOAK) estimate of the solid sorbent process based on the status of currently available technology. This approach has the advantage of avoiding subjective judgement about unforeseen advances in design, performance, costs, efficiency, and reliability for a technology that is still in early development. On the other hand, reliance on cost estimates for current technology has the disadvantage of not accounting for potential improvements for a given process that can affect the long-term competitiveness of early stage CO₂ capture systems.

To address this problem, many techno-economic assessments of emerging technologies continue to use detailed “bottom-up” cost methods with parameter values that reflect some degree of technological improvement and cost reduction over time. Such studies typically assume low values for parameters like contingency costs and cost of capital to represent a high degree technological maturity (EPRI, 1986; DOE/NETL, 2011; Versteeg, 2012). However, a careful reading of the cost method guidelines published by major organizations (DOE, EPRI, AACE) reveals that such assumptions are not justified (Rubin, 2012). Rather, such parameters are to be based on the current level of knowledge and detail of process design.

An alternative approach, widely used in the literature, is the use of “learning curves” or “experience curves” to estimate future costs based on present knowledge. The approach used in this work is to develop projections of future costs of solid sorbent-based CO₂ capture based on historical observations of other technologies relevant to post-combustion CO₂ separation.

7.5.2. Application of technology learning curves

This section summarizes the learning curve method employed in this thesis for estimating the future capital costs and levelized cost of electricity for a mature solid sorbent technology using the range of probabilistic FOAK costs discussed in Section 7.4. The learning curve method uses mathematical models, also known as experience curves, developed from historical data for similar technologies in similar systems. Learning curves are used to predict the cost of manufactured products after experience is gained using the technology and improving on its capital costs, efficiency, and reliability in following installations. Although these curves were originally developed to project production costs (Wright, 1936), there are many variations used to describe the progression of future costs based on the manner of institutional learning, influence of government investment, and the degree of collaboration among competitors (Ostwald, 1992; Taylor, 2001; Yeh & Rubin, 2012).

The most commonly used type of learning curve is the so-called “one-factor model” based on the premise that a reduction in costs will take place each time the cumulative production is doubled (Rubin, et al., 2004). This is represented mathematically using Equation 7.1:

Equation 7.1

$$Y = AX^{-b}$$

where:

Y = Specific cost of the Xth unit

A = direct person hours, capital cost, or other metric required to produce the FOAK unit

b = Parametric constant

The quantity 2^{-b} is defined as the progress ratio (PR). It implies that each doubling of cumulative production or capacity results in a cost savings of $(1-2^{-b})$. The latter quantity is defined as the learning

rate, (LR). Values of the progress ratio and the learning rate are commonly reported as a fraction or percentage for each doubling of cumulative installed capacity or production (Boston Consulting Group, 1968). While both the progress ratio and learning rate are commonly used in the literature, this work uses learning rates to quantify percentage cost reductions associated with a doubling of cumulative capacity.

In this formulation, the value of LR will vary from technology to technology (Rubin, et al., 2006). Thus, the learning rate for natural gas combined cycle (NGCC) plants is likely to differ from that of liquefied natural gas (LNG) facilities. Likewise, the learning rate for a specific solid sorbent process will possibly differ from the learning rate of Shell's Cansolv process, which is being used for CO₂ capture at SaskPower's Boundary Dam Project. Nevertheless, one would expect learning rates to be closer for similar technologies (DOE/NETL, 2013; Rubin, et al., 2004; Yeh & Rubin, 2012; McDonald & Schratzenholzer, 2001).

To estimate future cost trends for power plants with CO₂ capture, we first decompose the power plant into major process areas. Each area includes the equipment needed to carry out certain functions such as power generation, air pollution control, and CO₂ capture. We then apply separate learning rates to the capital and operating costs of each sub-system based on judgements as to which technologies offer the best analogue to the power plant process area in question. The cost of the total plant is then calculated as the sum of all process area costs for increasing levels of total installed capacity. This approach implicitly assumes that technological learning occurs via incremental improvements to existing technologies, which historically has been the dominant mode of technological innovation (Alic, et al., 2003). Since CO₂ transport and storage technologies are also vital components of a complete CCS system, these components are included in the scope of the present study using technological LRs from the oil and gas extraction industry.

Table 7.12 summarizes the learning rates for capital cost and O&M cost for the process area technologies examined in this study as well as the cumulative installed capacity. Detailed descriptions and discussions of each technology and their historical cost trends are presented elsewhere (Rubin, et

al., 2006). All learning rates used in this study fall within the range reported in the literature for an array of energy-related technologies studied by McDonald and Schratzenholzer (McDonald & Schratzenholzer, 2001). Although the learning rates used here for capital cost are systematically smaller than the median rate of 14%.

Table 7.12: Summary of “best estimate” learning rates for capital and O&M costs from historical case studies and the initial cumulative installed capacity used to calculate future costs of supercritical PC systems equipped with solid sorbent-based CO₂ capture and storage.

Technology	Learning rate*		Current installed capacity (GW)**
	Capital cost	O&M cost	
Balance of plant			
Supercritical pulverized coal boilers	0.06	0.15	120
Air pollution control (APC)	0.12	0.22	230
Fuel	n/a	0.04	120
CO₂ capture and storage			
CO ₂ capture	0.12	0.21	10
CO ₂ compression	0.00	0.00	10
CO ₂ transport and storage	0.04	0.04	10

*Fractional reduction in cost for each doubling of total production or capacity

**Estimated cumulative installed capacity of CO₂ capture systems (Rubin, et al., 2007)

As discussed in the previous section, the reliability of cost estimates for plants equipped with solid sorbent-based CCS is very uncertain since no system has yet to be built and operated at the scale of a modern power plant. Of particular relevance to this study, however, is the percentage contribution of each sub-section to the total costs of construction and operation. These percentages are typically more robust for a given plant design (Rubin, et al., 2007).

Starting with current capital and operating cost estimates for the Present Case with degradation from water and SO₂ (Case Study #10), this study uses the historical learning rates reported in Table 7.12 to project the future costs of each major power plant sub-section (shown in Table 7.13) as a function of

plant capacity (which is proportional to power output at a given capacity factor). This approach allows the cost of different plant sections to change at different rates, reflecting differences in the technological maturity of each plant sub-system. It also reflects the contribution of each component to the total capital requirement and total O&M cost of the plant. Improvements in overall plant efficiency due to improved component design and/or improved plant integration also is reflected in a learning rate for fuel use per megawatt hour of electricity generated.

Table 7.13: Cost estimates for FOAK power plants with CO₂ capture derived for solid sorbent-based systems for the Present Case with water and SO₂ degradation (Case Study #10). Total capital requirement and operating costs are calculated using the percentages reported by (Rubin, et al., 2007) for all non-CCS related equipment.

Technology	Total capital requirement		Total O&M cost	
	(\$M)	% Total	\$M/yr	% Total
Supercritical PC boiler	1,192	35	34	13
AP controls (SCR, ESP, FGD)	224	7	25	9
CO ₂ capture	1,921	56	109	27
CO ₂ compression	35	1	1	41
CO ₂ transport and storage	63	2	27	1
Fuel cost	0	0	72	10
Total	3,437	100	268	100

One drawback of this approach is that it does not explicitly include potential cost increases that may arise when building or combining components that have not yet been proven for solid sorbent application and scale assumed. There are no easy or reliable methods, however, to quantify the magnitude of potential cost increases commonly observed during early commercialization of large-scale technologies (Merrow, et al., 1988). This work assumes that learning begins with the first generation of the plant or process, with the recognition that higher plant costs might be incurred initially and gradually decline via learning-by-doing and continued R&D. Although not addressed here, these initial increases in cost would effectively delay the onset of learning and result in higher costs for a given value of cumulative gross installed capacity.

7.5.3. Future cost results

Figure 7.6 summarizes the resulting reduction in LCOE from the onset of learning (the FOAK plant) based on installed worldwide capacity of supercritical plants equipped with solid sorbent-based CO₂ capture and storage. The capital cost data presented in this figure use a fixed charge factor of 0.113 to indicate a mature system rather than the 0.143 used in previous sections to indicate a FOAK plant. Hence, the cost of the first GW of installed capacity is reduced from the FOAK projection of \$210/MWh to \$182/MWh for the first versus gigawatt (GW) of installed capacity. The first 50 GW of installed capacity reduce the cost to \$147/MWh. A global installed capacity of 230 GW (the estimate for the global installed capacity of supercritical boilers from Table 7.12) yields a LCOE of \$124 per megawatt hour.

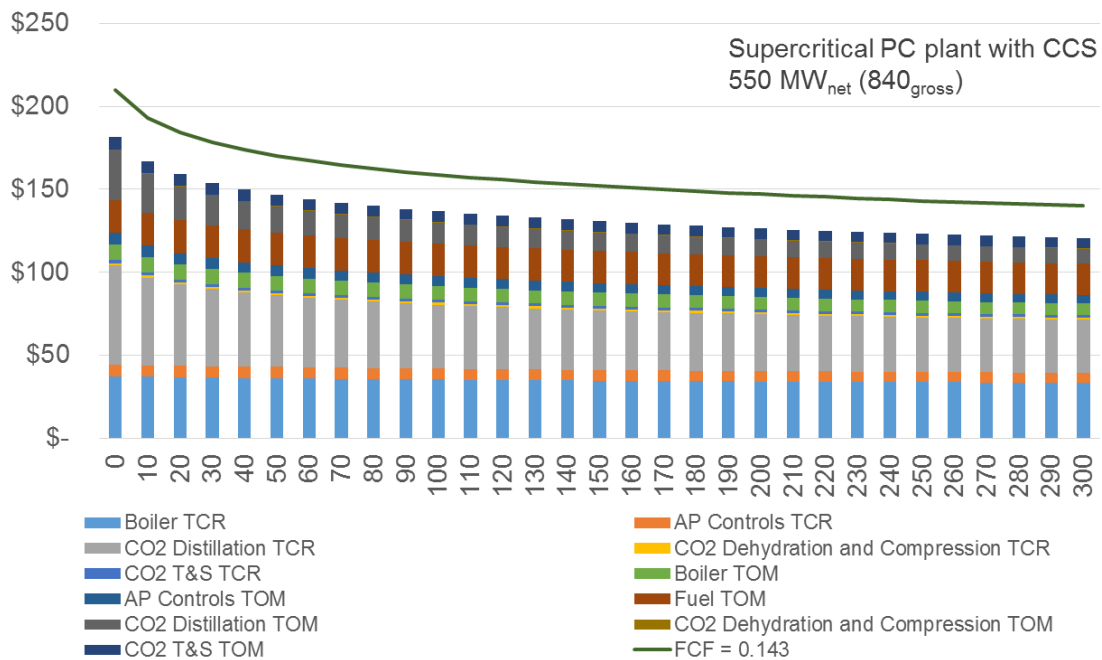


Figure 7.6: Projections of future LCOE for supercritical power plants equipped with solid sorbent-based CO₂ capture and storage. The stacked bars use a fixed charge factor of 0.113 to indicate a mature plant while the line shows the change in LCOE using a fixed charge factor of 0.143.

The LCOE estimates for power generation with solid-based CCS are more expensive than estimates from other research groups for supercritical PC plants equipped with liquid-based CO₂ capture. Table 7.16 shows the results of a recent literature review of post-combustion cost estimates for several recent cost estimates for liquid technologies, which emphasize the higher cost of electricity generation

using mature solid sorbent-based CO₂. Even with installed global capacities of 300 GW (resulting in a LCOE of \$120/MWh), the results of this study indicate that mature plant designs for supercritical PC plants equipped with solid sorbent-based CO₂ capture systems are significantly outside of the range of estimates for NOAK estimates for the currently available technology.

Table 7.14: NOAK cost estimates for the best available CO₂ control technology for post-combustion application. Estimates represent comparable supercritical plants equipped with liquid-based CCS. Values are adjusted to 2011 constant dollars using CPI inflation rate as needed.

Source	Plant efficiency (%HHV)	Representative NOAK LCOE (\$/MWh)	Notes
(Carnegie Mellon University, 2014)	28	105	IECM, v8.0.2 using default CCS settings
(Carnegie Mellon University, 2015)	28	106	IECM v9.0.1 using default CCS values
(Alstom, 2011)	33	88	2020 projection
(MIT, 2007)	29	89	2030 projection
(Rubin, et al., 2015)*	32	113	Based on reported “representative” value
(Versteeg, 2012)	27	105	

*Excludes transport and geological storage costs. The primary author of the cited paper (Rubin) estimates that pipeline transport and geological storage costs add approximately 10-20 USD/MWh

7.6. Achieving low cost solid sorbent-based CO₂ capture

A portion of the Department of Energy’s CCS research and development program is focused on developing advanced technology options that are capable of producing electricity while still capturing 90% of the CO₂ emissions at lower costs than can be achieved using today’s available technologies. To this end, DOE/NETL CCS program is pursuing development options to reduce the cost of post-combustion CO₂ capture to less than a 30% increase in the cost of electricity for mature, fully integrated power plants compared to plants without CO₂ capture and storage (DOE/NETL, 2010). This begs the question: is it plausible that the current generation of solid sorbent-based CO₂ capture and storage systems might achieve this goal? This section analyses this question by evaluating the range of case study costs, probabilistic costs, and learning rates presented throughout this chapter. Then we look at requirements for future generations of the technology to meet DOE goals.

To begin, recall from Section 7.1 that the reference case without CO₂ capture (Case study #0) produces electricity at an LCOE of \$61/MWh and represents a mature (NOAK) electricity generation technology. A 30% increase in the cost of electricity – that is, a cost of \$79/MWh for a supercritical PC plant with post-combustion CCS-- provides a basis for the NOAK cost goal in this section. While this goal is below the LCOE results reported in Figure 7.6, it may be possible to increase the learning rate and/or performance of the system in order to meet this goal.

First, consider the possibility of increasing the learning rate for CO₂ capture systems. This is one of the major goals of the CCSI group, whose purpose is to accelerate the advancement of CO₂ capture technologies by assisting in the development and deployment of advanced computational modelling tools. This effort has the potential to increase the learning rate for solid sorbent systems by avoiding pitfalls that are inherent in technological development and deployment. A successful result from this program might increase the capital and operating cost learning rates for solid sorbent-based CO₂ capture, compression, transport, and storage from the current values listed in Table 7.12 to a new value of 22%. This is the highest learning rate reported among 26 data sets for energy technologies (McDonald & Schratzenholzer, 2001). Note that the learning rates for the balance of plant are not altered.

The higher learning rates for the CCS system components cause the levelized cost of electricity to drop more rapidly as additional generation capacity is installed. Using these higher learning rates, the cost of current technology would fall to an LCOE of \$119/MWh after 100 GW of installed capacity (a level of experience comparable to that for flue gas desulfurization system improvements over a 20-year period, as assumed in Rubin, et al., 2007). Despite this more rapid rate of improvement, the cost of electricity generation would remain well above the \$79/MWh needed to achieve goal of a 30% increase in generation cost.

It may also be possible to increase the initial performance and lower the cost of solid sorbent systems by R&D that enhances the solid sorbent and heat exchange properties of the system. If, for example, the conditions shown in Table 7.15 could be achieved for the present case system without

water or SO₂ degradation (Case study #7), then a power plant equipped with solid sorbent-based CCS could achieve an initial LCOE of \$97/MWh. This FOAK system would be competitive with current (more mature) liquid amine-based CCS systems, although it would still fall short of the DOE cost goals for advanced power plants with CCS. However, if this improved system could also achieve favorable learning rates (22%) for the CCS components, the NOAK cost would fall to \$79/MWh after 100 GW of deployment, thereby meeting DOE's goal for post-combustion CO₂ capture and storage.

Table 7.15: An example of modifications to the solid sorbent-based CO₂ capture system that could result in a system capable of meeting DOE's goals for post-combustion CCS technologies given favorable learning rates and no water or SO₂ degradation.

Performance parameter	Original value (Case study #7)	New value
Maximum CO ₂ capacity (moles CO ₂ /kg solid sorbent)	2.9	5.8
Adsorber kinetic parameter (%)	83	100
Regenerator kinetic parameter (%)	11	0
Overall heat transfer coefficient (W/m ² -K)*	300, 55, 55	450, 450, 450
Flue gas blower efficiency (%)	75	85
Regenerator maximum steam temperature (°C)	135	165

*Values for the adsorber, regenerator, and cross-flow heat exchanger respectively

An additional consideration for the future performance of a supercritical PC plant equipped with solid sorbent-based CO₂ capture is the installed capacity at which costs begin to decline. Recall from Table 7.12 that the initial installed capacity for CO₂ capture technology (10 GW) is based on the cumulative experience for liquid-based CO₂ capture technologies (Rubin et al., 2007). However, major differences relating to the indirect heat transfer and material handling systems distinguish the solid-based process from the historically prevalent liquid-based technology. Thus, a bounding condition for this “best case” scenario would use an initial installed capacity of 550 MW rather than 10 GW. Replacing the initial installed capacity for the CO₂ capture technology with this lower value would result in a facility capable of meeting DOE's cost target goal after 50 GW of installed capacity due to a shaper initial reduction in the cost of the CO₂ capture process.

Achieving the performance goals outlined in Table 7.15 would require overcoming several formidable technological hurdles relating to the performance of the solid sorbent and heat transfer equipment. These parameter values represent goals for materials and process designers. The success of solid sorbent systems hinges on meeting these conditions while still overcoming the significant effects of chemical degradation and thermal oxidation. Efforts to accelerate technological learning so as to more rapidly reduce costs during early deployment can improve the potential for achieving DOE cost goals.

7.7. Technological maturity of solid sorbent systems

As discussed in Section 1.4, solid sorbent CO₂ capture technologies are an active area of materials research, and pilot plants are under construction or soon running though not yet at large scale at the time of this writing. Technological learning for solid sorbents CO₂ capture systems for post-combustion systems requires developing the technology at demonstration and pilot scales and continued material and process development.

The outlook is uncertain for solid sorbent technology. A handful of research and development companies, include RTI International, TRA Research, and ADA Environmental Services are pursuing demonstration plants as part of a wider collaborative effort to validate and improve model designs, but it appears that the learning rates of solid sorbent plants are slowing. Historical evidence with flue gas desulfurization is instructive in the context of CO₂ capture technologies, and shows that many initially promising technologies do not get the opportunity to travel far along a learning curve. A large number of systems and schemes have been proposed but few ever develop to the commercial state and fewer gain a significant amount of market share. For example, an assessment of 189 different flue gas desulfurization processes in 1987 showed that only 11 were being used in power plants, with more than 65% of those being wet limestone or lime FGD systems (Kohl & Nielsen, 1997). Utilities often choose the most mature technologies, making it difficult for vendors of less mature technologies to win contracts (*ibid.*). The system design released by NETL in 2011 is still the standard for solid-based CO₂ capture, but future designs will likely incorporate changes to the processes, further delaying the onset of a first-of-a-

kind plant. These maturity issues should also be considered by process developers when investigating these technologies.

7.8. Chapter conclusion

This chapter reviewed the performance and cost results for a variety of deterministic and probabilistic scenarios relating to solid sorbent-based CO₂ capture and storage presented in this thesis. Examples of the potential impact of performance and cost assumptions on the first generation of plants found that degradation and heat transfer are major issues for solid sorbent systems. When water and SO₂ degradation is excluded from consideration, the levelized cost of electricity for four potential scenarios ranges from \$147 to \$178 per megawatt hour depending on performance and design assumptions and assuming 90% CO₂ capture. With water and SO₂ degradation, the cost of electricity production ranges from \$164 to 210 per megawatt hour.

Table 7.16: An example of modifications to the solid sorbent-based CO₂ capture system that could result in a system capable of meeting DOE's goals for post-combustion CCS technologies given favorable learning rates and no water or SO₂ degradation.

Case	TCR (\$M)	Plant Efficiency (% HHV)	LCOE (\$/MWh)	Case	TCR (\$M)	Plant Efficiency (% HHV)	LCOE (\$/MWh)
1	2,572	29.6	161	8	2,020	28.8	188
2	2,697	29.0	170	9	3,330	27.4	199
3	2,857	28.5	176	10	3,435	27.2	210
4	2,956	28.3	184	11	2,303	29.8	147
5	2,323	24.4	160	12	2,386	29.3	154
6	2,380	24.0	165	13	2,550	28.1	158
7	2,899	29.3	178	14	2,610	27.9	164

A probabilistic analysis revealed that the LCOE for the current generation of solid sorbent technology could result in a 90% percentile ranging from \$167 to \$533 per megawatt hour with an expected value of \$209 per megawatt hour. Comments were made on the maturity of solid sorbent technologies to note that these learning rates are dependent on continuation and acceleration of funding

for solid sorbent systems, which may be slowing. Finally, the analysis in this chapter was completed using the models discussed in previous chapters, and all of the results should be reproducible to users of the model.

8. Summary and conclusions

8.1. Thesis summary

This thesis is intended to be a starting point for estimating the costs for solid sorbent-based post-combustion CO₂ capture, a starting point that will help policy makers, researchers, technology developers, and others to be more informed about the costs of this CO₂ emission mitigation option.

Chapter 1 briefly introduced the connection between CO₂ emissions and global climate change, and established that post-combustion based CCS could be a useful technology for significantly reducing CO₂ emissions at large point sources. Chapter 1 also limited the scope of this thesis to an investigation of the performance and economics of solid sorbent-based post-combustion CO₂ capture.

Chapter 2 provided a review of solid sorbent properties important for CO₂ capture and characterized several materials used in today's largest technology research efforts. The discussion then broadened to include a range of factors which affect the CO₂-capture process, such as the interactions between the solid sorbent and other flue gas components, sorbent degradation, and the influence of reaction kinetics. Finally, the chapter summarized the nominal values and characteristics for a mixed-amine solid sorbent seen as state-of-the-science for currently available materials.

Chapter 3 reviewed the solid sorbent-based CO₂ capture process. Several concepts relating to solid-gas separation systems were summarized, including pressure and temperature-swing operations used for adsorption/desorption systems and types of reactors applicable to post-combustion capture. Chapter 3 concluded by proposing a process design for CO₂ capture that served as the basis of the performance and cost assessment presented in later chapters.

Chapter 4 described the performance model that is the basis for the mass and energy flow rate data. This chapter described the model's design and provided the necessary detail needed to reproduce the model's results for comparison with other scenarios for a solid sorbent based CO₂ capture process.

For a desired CO₂ capture efficiency, specific sorbent, and given operating conditions, the performance model calculates the mass flow rates and energy balances of all the listed process areas.

Chapter 5 demonstrated the functionality of the performance model and highlighted the versatility of a reduced-order model approach described in Chapter 4. Further, this chapter provided context for the solid sorbent-based CO₂ capture system by defining the integrated post-combustion CO₂ capture power plant as it would operate as a first-of-a-kind system. Case studies introduced additional capabilities of the model in response to choices in critical material and equipment performance. This chapter also characterized uncertainty in the performance of a solid sorbent-based CO₂ capture technology based on the case study results and expert elicitations.

Chapter 6 described the cost model used to estimate the capital and operating costs of post-combustion solid sorbent-based CO₂ capture. The model was then exercised in order to examine important relationships between the performance cost model concluding with a discussion of process design and the importance of heat exchange. This chapter also characterized uncertainty for current state of solid sorbent technology based on available literature and expert elicitations.

Chapter 7 compared the performance and cost solid sorbent-based systems. Through a variety of estimates, this chapter showed that pulverized coal plants equipped with solid sorbent-based CO₂ capture require capital and operating costs similar to the combined capital and operating costs for the balance of the plant. This result was found across all deterministic case studies despite wide variation in the performance and cost assumptions. A probabilistic analysis for the levelized cost of electricity also showed a very high likelihood that the initial cost of solid sorbent technology will be more costly than current liquid systems. Projections about future costs of mature solid sorbent systems also showed a very high likelihood that a sorbent-based system would be more costly than mature liquid-based systems based on current sorbents and process designs. Only with major long-term improvements in sorbent properties and large reductions in future equipment cost would solid sorbent-based power plants be able to approach DOE's cost goals for future new post-combustion CCS technologies. Comments were also

made about the maturity of solid sorbent-based systems, and its relevance for cost analysis. The primary conclusions are summarized below.

8.2. Main results and implications

This thesis has modeled solid sorbent-based CO₂ capture technology and has found that a full-scale system using the presently available process will likely have a higher revenue requirement and levelized cost compared to liquid-based systems. While plants equipped with the solid sorbent process were found to have similar efficiencies compared to those equipped with a liquid amine-based process (26-29% by HHV), the levelized cost of electricity is higher for solid sorbents due to higher capital costs. Solid-based CO₂ capture was shown to be a capital intensive process as a result of the challenges of indirect heat transfer with solid sorbents combined with high solid flow rates.

The case studies explored several prominent schools of thought regarding the “best available” design for solid sorbent-systems given the current state of the science. Several system scenarios (represented by the ideal and CCSI series of case studies) are based on tenuous assumptions regarding the performance of the materials and/or equipment design (e.g. solid sorbents that are resistant to oxidation at high temperatures and/or regenerator vessels with favorable heat transfer properties). The solid sorbent process evaluated in this thesis looks less promising than these estimates as well as estimates for mature liquid-based technologies available for PC power plants. The probabilistic levelized cost of electricity analysis explored departures from the nominal performance and cost assumptions and supported the general conclusion that the cost of electricity is higher for plants with solid sorbent –based CO₂ capture systems than for liquid-based systems reported in the literature.

In summary, heat transfer in the current generation of solid sorbent-based CO₂ capture systems is currently performed by indirect heat exchange. This process is challenging due to the low overall heat transfer coefficient combined with the solid sorbent’s susceptibility to degradation and thermal oxidation

despite the lower heat capacity of the solid sorbent. In addition, liquid amine-based technologies are more mature than other post-combustion technologies, and are commercially offered by large companies.

Finally, an important caveat is that the results of this thesis are highly dependent on the specific assumptions used, and may vary for different scenarios. For example, power plant performance and costs for solid sorbent systems would change for improved heat integration of the CO₂ capture system, more efficient solids heat exchange, and higher resistivity to degradation. Similarly, further improvements in the process could alter its cost relative to solvent-based systems. Reduced-order models like those developed in this work and those employed in the IECM can be used to more fully and efficiently explore these and other options.

9. References

Abanades, J. C. & Alvarez, D., 2003. Conversion limits in the reaction between carbon dioxide and lime. *Energy and Fuels*, pp. 308-315.

Acharya, A. & BeVier, W. E., 1985. *Attrition resistant molecular sieve*. USA, Patent No. US 4526877 A.

ADA- ES Inc., 2013. *Pilot scale evaluation of an advanced carbon sorbent-based process for post-combustion carbon capture*, Morgantown, WV: DOE/NETL.

ADA-ES, 2011. *Evaluation of solid sorbents as a retrofit technology for CO₂ capture from coal-fired power plants*, Morgantown, WV: DOE/NETL.

Ahmadalinezhad, A., Tailor, R. & Sayari, A., 2013. Molecular-level insights into the oxidative degradation of grafted amines. *Chem. Eur. J.* , Volume 19, pp. 10543-10550.

Alesi, Jr, W. R. & Kitchin, J. R., 2012. Evaluation of a primary amine-functionalized ion-exchange resin for CO₂ capture. *Ind Eng Chem Res*, 51(19), pp. 6907-6915.

Alic, J. A., Mowery, D. S. & Rubin, E. S., 2003. *US Technology and innovation policies lessons for climate change*, Arlington: Pew Center on Climate Change.

Al-Juaied, M. & Whitmore, A., 2008. *Realistic costs of carbon capture*, Cambridge, MA: Harvard Kennedy School.

Alptekin, G., 2013. *Low-cost high capacity regenerable sorbent for carbon dioxide capture from existing coal-fired power plants*, Wheat Ridge, CO: TDA.

Alstom, 2011. *Cost assessment of fossil power plants*, Milan, Italy: POWER-GEN Europe Conference.

Babcock & Wilcox Power Generation Group, 2011. *Engineering and Economic Evaluation of Oxy-Fired 1100F (593C) Ultra-Supercritical Pulverized Coal Power Plant with CO₂ Capture*, Palo Alto: EPRI.

Banerjee, R. et al., 2008. High-throughput synthesis of zeolitic imidazolate frameworks and application to CO₂ capture. *Science*, Volume 319, pp. 939-943.

Belmabkhout, Y., Guerrero, R. S. & Sayari, A., 2011. Adsorption of CO₂-containing gas mixtures over amine-bearing pore-expanded MCM-41 silica: applicatio for CO₂ separation. *Adsorption*, pp. 395-401.

Belmabkhout, Y. & Sayari, A., 2009. Adsorption of carbon dioxide from dry gases on MCM-41 silica at ambient temperature and high pressure. *Chem Eng Sci*, 64(17), pp. 3729-3735.

Benson, S., 2013. *Evaluation of carbon dioxide capture from existing coal-fired plants by hybrid sorption using physical sorbents*, Minneapolis, MN: DOE/NETL.

Berger, A. H. & Bhowan, A. S., 2011. Comparing physisorption and chemisorption solid sorbents for use separating CO₂ from flue gas using temperature swing adsorption. *Energy Procedia*, Volume 4, p. 562–567.

Berkenpas, M. B. et al., 2009. *IECM Technical Documentation Updates Final Report*, Pittsburgh, PA: National Energy Technology Laboratory.

Bollini, P., Choi, S., Drese, J. & Jones, C. W., 2011. Oxidative degradation of aminosilica adsorbents relevant to post-combusiton carbon dioxide capture. *Energy Fuels*, 25(5), pp. 2416-2425.

Borgert, K., 2015. *Ph.D. Thesis: Performance and cost of oxy-combustion*. Pittsburgh, PA: CMU.

Boston Consulting Group, 1968. *Perspectives on experience*, Boston: BSG.

Bottoms, R., 1930. *Separating acid gases*. USA, Patent No. 1,753,901.

Caplow, M., 1968. Kinetics of carbamate formation and breakdown. *J. Am. Chem. Soc.*, 90(24), p. 6795.

Carbon Dioxide Information Analysis Center, 2013. *Fossil-fuel CO₂ emissions*, Oak Ridge, TN: DOE/ORNL.

Carnegie Mellon University, 2014. *Integrated Environmental Control Model (IECM)*, Pittsburgh: CMU.

Carnegie Mellon University, 2015. *Integrated Environmental Assessment Model (v9.0.2 beta)*. Pittsburgh: CMU.

Cavenati, S., Grande, C. A. & Rodrigues, A. E., 2004. Adsorption equilibrium of methane, carbon dioxide, and nitrogen on zeolite 13X at high pressures. *J. Chem. Eng. Data*, 49(4), pp. 1095-1101.

CCSI, 2015. *Carbon Capture Simulation Initiative Homepage*. [Online]
Available at: <https://www.acceleratecarboncapture.org/>
[Accessed 29 September 2015].

China-OGPE, 2014. *Shell and tube type heat exchanger*. [Online]
Available at: http://www.china-ogpe.com/buyingguide_content/Floating_head_heat_exchanger_1276.html
[Accessed 17 9 2014].

Choi, S., Drese, J. H. & Jones, C. W., 2009. Adsorbent materials for carbon dioxide capture from large anthropogenic point sources. *ChemSusChem*, Volume 2, pp. 798-854.

Choi, S., Drese, J. H. & Jones, C. W., 2009. Solid adsorbent materials for carbon dioxide capture from large anthropogenic point sources. *Chemistry and Sustainable Energy Materials*, 2(9), pp. 796-854.

Chuang, S., 2013. *Metal monolithic amine-grafted silica for CO₂ capture*. Morgantown, WV: DOE/NETL.

CO₂ Capture Project, 2008. *Three basic methods to separate gases*, s.l.: CO₂ Capture Project.

Cook, J. L., Khang, S. J., Lee, S. K. & Keener, T. C., 1996. Attrition and change in particle distribution of lime sorbents in a circulation fluidized bed adsorber. *Powder Technol.*, 89(1), p. 1.

Cozad, A., Chang, Y., Sahinidis, N. & Miller, D., 2010. *Optimization of carbon capture systems using surrogate models of simulated processes*. Pittsburgh, American Institute of Chemical Engineers.

D'Alessandro, D. M., Smit, B. & Long, J., 2010. Carbon dioxide capture: Prospects for new materials. *Angewandte Chemie International Edition*, 49(35), pp. 6058-6082.

Diaf, A. & Beckman, E. J., 1995. Thermally reversible polymeric sorbents for acid gases, IV. Affinity tuning for the selective dry sorption of NO_x. *Reactive polymers*, 25(1), pp. 89-96.

Diaf, A., Garcia, J. L. & Beckman, E. J., 1994. Thermally reversible polymeric sorbents for acid gases: CO₂, SO₂, and NO_x. *J. of Appl. Polymer Sci.*, 53(7), pp. 857-875.

DOE/EERE, 2006. *Gasification-based biomass*, Washington, D.C.: DOE/NETL.

DOE/NETL, 2006. *Nth-of-a-kind cost estimation methodology*, Morgantown, WV: RDS.

DOE/NETL, 2010. *Cost and Performance Baseline for Fossil Energy Plants: Revision 2*, Morgantown, WV: DOE/NETL.

DOE/NETL, 2010. *DOE/NETL Carbon Dioxide Capture and Storage RD&D Roadmap*, Morgantown, WV: United States DOE/NETL.

DOE/NETL, 2011. *Carbon capture simulation initiative for accelerating the commercialization of carbon capture technology*. [Online]

Available at: <http://204.154.137.14/newsroom/labnotes/2011/10-2011.html>

[Accessed 12 March 2015].

DOE/NETL, 2011. *Quality guidelines for energy system studies: Cost estimation methodology for NETL assessments of power plant performance*, Pittsburgh: DOE/NETL.

DOE/NETL, 2012. *NETL ARRA report on the development of a process design of a solid sorbent carbon capture process*, Morgantown, WV: NETL.

DOE/NETL, 2012. *Technology readiness assessment - analysis of active research portfolio for the clean coal research program*, Morgantown, WV: DOE/NETL.

DOE/NETL, 2013. *Advanced carbon dioxide capture R&D program: Technology update, May 2013*, Morgantown, WV: DOE/NETL.

DOE/NETL, 2013. *Cost and Performance Baseline for Fossil Energy Plants, Volume 1: Bituminous Coal and Natural Gas to Electricity*, Morgantown/ WV: U.S. Department of Energy.

DOE/NETL, 2013. *DOE/NETL Advanced Carbon Dioxide R&D Program: Technology Update*, Morgantown, WV: DOE/NETL.

DOE/NETL, 2013. *Quality guidelines for energy system studies: Technology learning curve (FOAK to NOAK)*, Morgantown, WV: DOE/NETL.

DOE/NETL, 2015. *Cost and performance baseline for fossil energy plants. Volume 1: Revision 3*, Morgantown: DOE/NETL.

DOE/NETL, August, 2007. *Cost and Performance Baseline for Fossil Energy Plants. Volume 1: Bituminous Coal*, Morgantown, WV: s.n.

DOE, 2010. *Department of Energy Announces \$67 Million Investment for Carbon Capture Development*. [Online]

Available at: <http://energy.gov/articles/department-energy-announces-67-million-investment-carbon-capture-development>

[Accessed 2 May 2014].

DOE, 2014. *Advanced combustion energy systems*. [Online]

Available at: <http://www.netl.doe.gov/research/coal/energy-systems/advanced-combustion/oxy-combustion>

DOE, 2015. *Energy.gov Regional Carbon Sequestration Partnerships*. [Online]

Available at: <http://energy.gov/fe/science-innovation/carbon-capture-and-storage-research/regional-partnerships>

[Accessed 19 2015].

Donaldson, T. L. & Nguyen, Y. N., 1980. Carbon dioxide reaction kinetics and transport in aqueous amine membranes. *Ind. Eng. Chem. Res.*, 19(3), pp. 260-266.

Drage, T. C., Smith, K. M., Arenillas, A. & Snape, C. E., 2009. Developing strategies for the regeneration of polyethylenimine based carbon dioxide adsorbents. *Energy Procedia*, 1(1), pp. 875-880.

Drage, T. C. et al., 2012. Materials challenges for the development of solid sorbents for post-combustion carbon capture. *J. Mater. Chem.*, Volume 22, p. 2815–2823.

Dreisbach, F., Staudt, R. & Keller, J. U., 1999. High pressure adsorption data of methane, nitrogen, carbon dioxide, and their ternary mixture on activated carbon. *Adsorption*, 5(3), pp. 215-227.

EARPC, 2013. *America's Dirtiest Power Plants*, s.l.: Environment America Research and Policy Center.

Elliott, J., 2013. *Low-cost sorbent for capturing CO2 emissions generated by coal-fired power plants*, Morgantown, WV: DOE/NETL.

EPRI, 1986. *Technical assessment guide (TAG) Vol. 1: Electricity supply*, Palo Alto, CA: Electric Power Research Institute.

EPRI, 2011. *Advanced Coal Power Systems with CO₂ Capture: EPRI's CoalFleet for Tomorrow(R) Vision-- 2011 Update*, Palo Alto, CA: EPRI.

Finkenrath, M., 2011. *Cost and performance of carbon dioxide capture from power generation*, Paris: IEA.

Frey, H. C. & Rubin, E. S., 1991. *Modeling IGCC system performance, emissions, and cost using probabilistic engineering models*. Pittsburgh, PA, CMU.

Gerdes, K. & Nichols, C., 2009. *Water requirements for existing and emerging thermoelectric plant technologies: U.S. Department of Energy National Laboratory Report 402/080108*, Morgantown, WV: DOE/NETL.

Glier, J. C. & Versteeg, P. L., 2012. *Comparison of liquid amines and solid sorbents for carbon dioxide capture for new, supercritical coal-fired power plants: A life cycle assessment*. Tacoma, WA, American Council for Life Cycle Assessment.

Global CCS Institute, 2015. *Large scale CCS project database*, Docklands, Australia: Global CCS Institute.

Grace, J. R., 1986. Contacting modes and behaviour classification of gas-solid and other two-phase suspensions. *Canadian Journal of Chemical Engineering*, 64(3), pp. 353-363.

Gray, M. L. et al., 2008. Performance of immobilized tertiary amine solid sorbents for the capture of carbon dioxide. *Int. J. Greenhouse Gas Control*, 2(1), pp. 3-8.

Green, D. W., 2008. *Perry's Chemical Engineers' Handbook*. 8th ed. Blacklick(OH): McGraw-Hill Professional Publishing.

Hicks, J. C. et al., 2008. Designing adsorbents for carbon dioxide capture from flue gas - hyperbranched aminosilicas capable of capturing carbon dioxide reversibly. *Journal of the American Chemical Society*, 130(10), pp. 2902-2903.

Hoffman, J., 2014. [Interview] (13 August 2014).

Hornbostel, M. D. et al., 2013. Characteristics of an advanced carbon sorbent for carbon dioxide capture. *Carbon*, Volume 56, pp. 77-85.

IEA Clean Coal Centre, 2014. *IEA Clean Coal Centre's CoalPower database*, London: IEA.

IEA, 2013. *International energy outlook 2013 with projections to 2040*, Washington, DC: DOE/IEA.

IEA, 2014. *Energy, climate change, an environment*, Paris, France: IEA.

IPCC, 2005. *Special report on carbon dioxide capture and storage*, Geneva, Switzerland: Cambridge University Press.

IPCC, 2007. *Climate Change 2007: Synthesis Report*, New York: Cambridge University Press.

IPCC, 2014. *Climate change 2014 synthesis report. Contribution of Working Groups I, II, and III to the Fifth Assessment Report of the Intergovernmental Panel on Climate Change [core writing team, R.K. Pachuri and L.A. Meyer (eds.)]*, Geneva, Switzerland: IPCC.

ITFCCS, 2010. *Executive summary: Report of the interagency task force on carbon capture and storage*, s.l.: s.n.

Jones, A., 2014. *Personal interview* [Interview] (13 3 2014).

Jones, C., 2013. *Rapid temperature swing adsorption using polymeric/supported amine hollow fiber materials*. Atlanta, GA: DOE/NETL.

Khatri, R. A., Chuang, S. C., Soong, Y. & Gray, M., 2005. Carbon dioxide capture by diamine-grafted SBA-15: A combined Fourier transform infrared and mass spectrometry study. *Ind. Eng. Chem. Res.*, 44(10), p. 3702.

Kim, S., Ida, J., Gulians, V. & Lin, J. Y. S., 2005. Tailoring pore properties of MCM-48 silica for selective adsorption of carbon dioxide. *J Phys Chem B*, Volume 109, pp. 6287-6293.

Kohl, A. & Nielsen, R., 1997. *Gas Purification*. 5th ed. Houston(Texas): Gulf Publishing Co..

Krishnan, G., 2013. *Development of novel carbon sorbents for CO₂ capture*, Menlo Park, CA: SRI International.

Lang, D., 2013. *Carbon dioxide removal from flue gas using microporous metal organic frameworks*, Des Plaines, IL: UOP LLC, a Honeywell Company.

Lee, A., Mebane, D., Fauth, D. & Miller, D., 2011. *A model for the adsorption kinetics of CO₂ on amine-impregnated mesoporous sorbents in the presence of water*. Pittsburgh, DOE/NETL.

Lee, S. K., Jiang, X., Keener, T. C. & Khang, S. J., 1993. Attrition of Lime Sorbents during Fluidization in a Circulating Fluidized Bed Adsorber. *Ind. Eng. Chem. Res.*, 32(11), p. 2758.

Li, B., Duan, Y., Luebke, D. & Morreale, B., 2013. Advances in CO₂ capture technology: A patent review. *Applied Energy*, Volume 102, pp. 1439-1447.

Lin, L., Sears, J. T. & Wen, C., 1980. Elutriation and attrition of char from a large fluidized bed. *Powder Technol.*, 27(1), pp. 105-115.

Li, Y., Ju, Z., Wu, B. & Yuan, D., 2013. A water and thermally stable metal-organic framework featuring selective CO₂ adsorption. *Crystal growth and design*, 13(9), pp. 4125-4130.

Lu, C. et al., 2008. Comparative study of carbon dioxide capture by carbon nanotubes, activated carbons, and zeolites. *Energy and Fuels*, Volume 22, pp. 3050-3056.

Marx, D., Joss, L., Hefti, M. & Mazzotti, M., 2013. The role of water in adsorption-based capture systems. *Energy Procedia*, Volume 37, pp. 107-114.

Mather, K. B. & Epstein, N. eds., 1974. *Sprouted Beds*. New York: Academic Press.

McCabe, W. L., Smith, J. C. & Harriott, P., 2005. *Unit operations of chemical engineering*. 7th ed. New York: McGraw-Hill.

McCoy, S., 2009. *Ph.D. Thesis: The economics of carbon dioxide transport by pipeline and storage in saline aquifers and oil reservoirs*. Pittsburgh, PA: ProQuest Dissertations And Theses.

McDonald, A. & Schrattenholzer, L., 2001. Learning rates for energy technologies. *Energy Policy*, Volume 29, pp. 255-261.

Merrick, D. & Highley, J., 1974. Particle Size Reduction and Elutriation in a Fluidized Bed Process. *AIChE Symp. Ser.*, 70(137), pp. 366-378.

Morrow, E. W., McDonnell, L. & Yilmaz Arguden, R., 1988. *Understanding the outcomes of megaprojects*, Santa Monica: RAND Corp..

MIT, 2007. *The future of coal*, Cambridge, MA: MIT Press.

MIT, 2015. *Carbon capture and sequestration project database*, Cambridge, MA: MIT.

Morgan, M. G., Henrion, M. & Small, M., 1990. *Uncertainty: A guide to dealing with uncertainty in quantitative risk and policy analysis*. Cambridge, UK: Cambridge University Press.

NAS, 2011. *Understanding earth's deep past: Lessons for our climate future*, Washington, DC: National Academies Press.

Nelson, T., 2013. *Bench-scale development of an advanced solid sorbent-based CO₂ capture process for coal-fired power plants*. Morgantown, WV: DOE/NETL.

Nelson, T., 2013. *Development of a dry sorbent-based post-combustion CO₂ capture technology for retrofit in existing power plants*. [Online]

Available at: <http://www.netl.doe.gov/research/coal/carbon-capture/post-combustion/dry-regen>

[Accessed 22 February 2015].

Nelson, T. et al., 2009. The dry carbonate process: Carbon dioxide recovery from power plant flue gas. *Energy Procedia*, 1(1), pp. 1305-1311.

Ostwald, P. F., 1992. *Engineering cost estimating*. 3 ed. Upper Saddle River, NJ: Prentice Hall Engineering/Science/Mathematics.

Pennline, H. & Hoffman, J., 2000. *Carbon dioxide capture process with regenerable solid sorbents*. US, Patent No. 6,387,337.

Pennline, H. W. et al., 2011. *Regenerable sorbent technique for capturing CO₂ using immobilized amine sorbents*. USA, Patent No. US8500854.

Plaza, M. G. et al., 2007. Carbon dioxide capture by adsorption with nitrogen enriched carbons. *Fuels*, 86(14), pp. 2204-2212.

Qi, G., Fu, L. & Giannelis, E., 2014. Sponges with covalently tethered amines for high-efficiency carbon capture. *Nature Communications*, Volume 5.

Radosz, M., Hu, X., Krutkramelis, K. & Shen, Y., 2008. Flue-gas carbon capture on carbonaceous sorbents: Toward a low-cost multifunctional carbon filter for "green" energy producers. *Ind. Eng. Chem. Res.*, 47(10), pp. 3783-3794.

Rao, A., 2003. *Ph.D. Thesis: Techno-economic assessment of amine-based carbon capture*. Pittsburgh, PA: Carnegie Mellon University.

Ray, Y. C., Jiang, T. S. & Wen, C. Y., 1987. Particle attrition phenomena in a fluidized bed. *Power Technol.*, 49(3), pp. 193-206.

RFF, 2003. *The prospects for carbon capture and storage technologies*, Washington, D.C.: RFF.

Ritter, J., 2013. *Bench-scale development and testing of rapid pressure swing adsorption for carbon capture*. Morgantown, WV: DOE/NETL.

Rochelle, G., 2009. Amine Scrubbing for CO₂ Capture. *Science*, 325(5948), pp. 1652-1654.

Rubin, E. S., 2012. Understanding the pitfalls of CCS cost estimates. *Int. J. Greenhouse Gas Control*, Volume 10, pp. 181-190.

Rubin, E. S., Antes, M. K., Yeh, S. & Berkenpas, M. B., 2006. *Estimating future trends in the cost of CO₂ capture technologies*, Cheltenham, UK: IEA Greenhouse Gas R&D Programme (IEA GHG).

Rubin, E. S., Davison, J. E. & Herzog, H. J., 2015. The Cost of CO₂ Capture and Storage. *International Journal of Greenhouse Gas*.

Rubin, E. S., Taylor, M. R., Yeh, S. & Hounshell, D., 2004. Learning curves for environmental technology and their importance for climate policy analysis. *Energy*, 29(9), pp. 1551-1559.

Rubin, E. S. et al., 2007. Estimating future costs of CO₂ capture systems using historical experience curves. *Proceedings of GHGT-8, Int'l conf. on greenhouse gas control technologies*.

Rubin, E. S. & Zhai, H., 2011. *The cost of CCS for natural gas-fired power plants*. Pittsburgh, PA, CMU.

Samanta, A. et al., 2012. Post-combustion carbon dioxide capture using solid sorbents: A review. *I&EC*, 51(4), pp. 1438-1463.

Sanz, R., Calleja, A., Arencibia, A. & Sanz-Perez, E. S., 2010. Carbon dioxide adsorption on branched polyethyleneimine-impregnated mesoporous silica SBA-15. *Applied Surface Science*, Volume 256, pp. 5323-5328.

Seider, W., 2014. *Product and process design lecture 6: Equipment sizing and capital cost estimation*, State College, PA: University of Pennsylvania.

Serna-Guerrero, R., Da'na, E. & Sayari, A., 2008. New insights into the interactions of carbon dioxide with amine-functionalized silica. *Ind. Eng. Chem. Res.*, 47(23), p. 9406–9412.

Shamlou, P. A., Liu, Z. & Yates, J. G., 1990. Hydrodynamic influences on particle breakage in fluidized beds. *Chem. Eng. Sci.*, 45(4), pp. 809-817.

Shen, D. et al., 2000. Comparison of experimental techniques for measuring isosteric heat of adsorption. *Adsorption*, 6(4), pp. 275-286.

Shigemoto, N., Yanagihara, T., Sugiyama, S. & Hayashi, H., 2006. Material balance and energy consumption for carbon dioxide recovery from moist flue gas employing K₂CO₃-on-activated carbon and its evaluation for practical adaptation. *Energy & Fuels*, 20(2), pp. 721-726.

Shih, H. H., Chu, C. Y. & Hwang, S. J., 2003. Solids circulation and attrition rates and gas bypassing in an internally circulating fluidized bed. *Ind. Eng. Chem. Res.*, 42(23), pp. 5915-5923.

Sintef, 2013. *Technology report and assessment for piloting of carbon dioxide capture technologies*, Trondheim, Norway: Sintef.

Siriwardane, R. V., Shen, M. S., Fisher, E. P. & Poston, J. A., 2001. Adsorption of carbon dioxide on molecular sieves and activated carbon. *Energy & Fuels*, 15(2), pp. 279-284.

Sjostrom, S. & Krutka, H., 2010. Evaluation of solid sorbents as a retrofit technology for CO₂ capture. *Fuel*, Volume 89, pp. 1298-1306.

Sjostrom, S., Krutka, H., Starns, T. & Campbell, T., 2011. Pilot Test Results of Post-Combustion CO₂ Capture Using Solid Sorbents. *Energy Procedia*, Volume 4, pp. 1584-1592.

Solex Thermal Science, 2015. *Solex homepage*. [Online]
Available at: www.solexthermal.com
[Accessed 22 June 2015].

SRI International, 2013. *NETL post-combustion carbon capture research project*. [Online]
Available at: <http://www.netl.doe.gov/research/coal/carbon-capture/post-combustion/de-fe00013123>
[Accessed 2014 5 May].

SRI International, 2013. *Pilot scale evaluation of an advanced carbon sorbent-based process for post-combustion carbon capture*, Morgantown, WV: DOE/NETL.

Srinivasachar, S. et al., 2014. *Evaluation of carbon dioxide capture from existing coal-fired plants by hybrid sorption using solid sorbents (CACHYS)*. Pittsburgh, PA, DOE/NETL.

Starns, T., Sjostrom, S., Krutka, H. & Wilson, C., 2012. *Solid sorbents as a retrofit CO₂ capture technology: Update on 1 MWe pilot progress*, Highlands Ranch, CO: ADAES.

Tarka, T. J. & Ciferno, J. P., 2005. *Carbon dioxide capture systems utilizing amine-enriched solid sorbents*, Morgantown, WV: DOE/NETL.

Taylor, M., 2001. *Ph.D. Thesis: Influence of government on environmental technological innovation*. Pittsburgh: Carnegie Mellon University.

Tribe, M. A. & Alpine, R. L. W., 1986. Scale economies and the "0.6 rule". *Engineering costs and production economies*, 10(1), pp. 271-278.

U.S. Energy Information Administration, 2015. *Energy Power Annual 2013*, Washington, D.C.: U.S. EIA.

Vaidya, P. D. & Kenig, E. Y., 2007. Carbon dioxide-alkanolamine reaction kinetics: A review of recent studies. *Ind. Eng. Chem. Res.*, 30(11), p. 1467.

Versteeg, P., 2012. *Ph.D. Thesis: Advanced amines and ammonia systems for greenhouse gas control at fossil fuel power plants*, Pittsburgh: Carnegie Mellon University.

Viguri-Fuente, J. R., n.d. *Chemical Process Design, Subject 7: Equipment Sizing and Costing*.
[Online]

Available at: <http://ocw.unican.es/enseñanzas-tecnicas/procesos-quimicos-de-fabricacion/materiales/Subject%207.%20Equipment%20Sizing%20and%20Costing%20OCW.pdf>

[Accessed 9 April 2015].

Wei, J. et al., 2008. Adsorption of carbon dioxide on organically functionalized SBA-16. *Microporous Mesoporous Mater.*, 116(1-3), pp. 394-399.

Wilcox, J., 2012. *Carbon Capture*. New York: Springer.

WRI, 2015. *Global coal risk assessment*. [Online]

Available at: <http://www.wri.org/publication/global-coal-risk-assessment>

[Accessed 20 September 2015].

Wright, T., 1936. Factors affecting the cost of airplanes. *Journal of Aeronautical Science*, Volume 3, pp. 122-128.

Xiaochun, X. et al., 2002. Novel polyethylenimine-modified mesoporous molecular sieve of MCM-41 type as high-capacity adsorbent for CO₂ capture. *Energy Fuels*, 16(6), pp. 1463-1469.

Xu, X. et al., 2003. Preparation and characterization of novel "molecular basket" adsorbents based on polymer-modified mesoporous molecular sieve MCM-41. *Microporous Mesoporous Mater.*, 62(1-2), pp. 29-45.

Xu, X. et al., 2005. Adsorption separation of carbon dioxide from flue gas of natural gas-fired boiler by a novel nanoporous “molecular basket” adsorbent. *Fuel Process Technol.*, 86(14-15), pp. 1457-1472.

Yang, Q., Xue, C., Zhong, C. & Chen, J. F., 2007. Molecular simulation of separation of CO₂ from flue gases in CU-BTC metal-organic framework. *AIChE J*, 53(11), pp. 2832-2840.

Yang, R. T., 2003. *Adsorbents: fundamentals and applications*. Hoboken, NJ: Wiley.

Yeh, S. & Rubin, E., 2012. A review of uncertainties in technology experience curves. *Energy Economics*, Volume 34, pp. 762-771.

Yeh, S., Rubin, E. S., Taylor, M. R. & Hounshell, D. A., 2005. Technology innovations and experience curves for nitrogen oxides control technologies. *J. of Air and Water Manage. Assoc.*, 55(12), pp. 1827-1838.

Yue, M. B. et al., 2008. Promoting the CO₂ adsorption in the amine-containing SBA-15 by hydroxyl group. *Microporous and Mesoporous Materials*, 114(1-3), pp. 74-81.

Zhao, Y., Ding, H. & Zhong, Q., 2012. Preparation and characterization of aminated graphite oxide for CO₂ capture. *Applied Surface Science*, 258(10), pp. 4301-4307.

10. Appendices

Appendix A: Characterization of uncertainty and variability

The term “uncertainty” is a vast umbrella that covers a variety of concepts. Uncertainty often arises from various sources including lack of complete information, conflicting sources of information, variability in a process or an object, linguistic imprecision, and approximations incorporated in a model to simplify the real life situations (Morgan, et al., 1990). Uncertainty in an empirical quantity is usually expressed using a probability distribution.

Any techno-economic analysis, and especially that of new energy and environmental controls that are still in the research phase, involves uncertainties regarding the performance and costs. These uncertainties come from incomplete data and numerous assumptions and approximations built into simulations. Some parameters, especially the cost parameters, are influenced by a larger set of factors outside of the scope of this particular study, and fluctuations in these quantities may be seen as “inert randomness” when viewed within this limited focus area. In addition, there may be significant variability in plant or process design assumptions across different studies or organizations.

Uncertainty and variability are often ignored or treated in a limited way using sensitivity analysis. However, sensitivity suffers from shortcomings resulting from the difficulty in evaluating the effect of simultaneous variations in several parameters and the lack of insight into the likelihood of obtaining any particular result.

A more robust approach is to present uncertainties and/or variability in model parameters using probability distributions. Using probabilistic simulation techniques, simultaneous uncertainties in any number of input parameters can be propagated through a model to determine their combined effect on model output parameters and information about the likelihood of obtaining various results. The development of ranges and probability distributions for model input parameters can be based on

information available in published studies, statistical data analysis, and/or the judgments of process engineers with relevant experience.

One of the distinguishing features of this modelling effort is a probabilistic capability that allows model inputs to be represented by probability distributions rather than single deterministic values. Depending upon the parameter, these distributions reflect the ranges of values reported in the literature, modelling approximations, and evolving nature of the technology, practical considerations in running such plants and variety of plant or process design assumptions. Some of the distributions are also based on an expert elicitation exercise (explained in Chapter 7) in which experts were asked about the nominal values and possible ranges for several important parameters characterizing the performance of current commercial solid sorbent-based systems capturing 90% CO₂ from the flue gas of a typical coal-fired power plant.

While designing a solid sorbent-based CO₂ capture system for a given flue gas (from a power plant application), there are certain parameters that could be specified independent of others. For example, the solid purge fraction, CO₂ capture efficiency target, SO₂ adsorption and desorption efficiency, temperature and pressure of the reactor vessels, etc. Distributions for such parameters reported in different studies essentially represent variability. Experts' technical judgments were useful in defining these distributions.

Probability distributions for parameters such as the efficiencies of fans, pumps or compressors represent the possibility of encountering fluctuations in the performance due to inherent characteristics of these devices in an operating plant. Uncertainties arising from real plant operating conditions and approximations in process simulations are also reflected in the distributions for parameters such as water capture and regeneration, removal efficiencies for other reactive flue gas constituents, and the pressure drop across the adsorber bed.

In case of cost parameters such as capital costs, O&M costs, cost of reagents (including solid sorbent) and cost of disposal, the distributions represent both variability and uncertainty arising from disagreement in data sources and inherent characteristics of market mechanisms.

Then there are certain process parameters that are interdependent. For example, the CO₂ capture efficiency (η_{C,CO_2}) is a function of various operating variables of the system for a given adsorber design as shown in Equation 10.20.

Equation 10.1:

$$\eta_{C,CO_2} = f(p_{CO_2}^A, T^A, q_{adj.max.}, k_A)$$

where:

$p_{CO_2}^A$ = Equilibrium partial pressure of CO₂ in the adsorber

T^A = Temperature of the adsorber

$q_{adj.max.}$ = Adjusted maximum loading of CO₂ at equilibrium, standard conditions

k_A = Kinetic parameter in the adsorber

In the process model shown here, the CO₂ capture efficiency (η_{C,CO_2}) is a user-defined parameter (treated as an independent parameter) and the circulation of solids is estimated using Equation 10.21.

Equation 10.2:

$$m_{solid}^{A,in} = f(\eta_{C,i}, \eta_{R,i}, m_i^{A,in}, X_{solid\ purge})$$

Similarly, the partial pressure of CO₂ at equilibrium is estimated using Equation 10.22:

Equation 10.3:

$$p_{CO_2}^A = f(\eta_{C,CO_2}, T^A, q_{adj,max}, k_A)$$

Probability distributions for these calculated parameters are not explicitly defined. Instead, the probability distributions on the independent parameters are propagated to these parameters throughout the model.

Appendix B: Expert elicitation form

Thank you for agreeing to assist us in our work on characterizing the uncertainty and variability associated with the performance of solid sorbent-based CO₂ capture technology. We plan to use your answers and those of other experts as inputs to engineering-economic models we have developed to characterize the performance and cost of these systems. While we will acknowledge the experts who have assisted us in this effort, we will not identify any expert with any specific response. If you have questions or concerns, please contact me:

Attn: Justin Glier

129 Baker Hall

Carnegie Mellon University

5000 Forbes Ave

Pittsburgh, PA 15213

Alternatively, if you prefer, we can schedule a time when I can call or visit your office and note down your responses.

In the pages that follows we:

1. Provide some background information on the problem
2. List the key assumptions we are using in our model and ask you to comment on their appropriateness *for current systems*
3. Ask you to make judgments about the likely values of a number of key coefficients *for future systems*

Part 1: Background

Development of improved technology to capture and store the CO₂ emitted by power plants using fossil fuels, particularly coal, is the subject matter of major research efforts worldwide. The attraction of this option is that it would allow abundant world resources of fossil fuels to be used for power generation and other applications without contributing significantly to atmospheric emissions of greenhouse gases. The two key barriers to carbon capture and storage (CCS), however, are the high cost of current CO₂ capture technologies, and uncertainties regarding the technical, economic, and political feasibility of storage options.

As part of the USDOE's efforts to explore alternative CCS options, we have developed an integrated modeling framework to evaluate the performance and cost of alternative CCS technologies for fossil-fueled power plants in the context of multi-pollutant control requirements. This model (called the IECM) allows for explicit characterization of the uncertainty or variability in any or all model input parameters. One of the purposes of this exercise is to improve the understanding of both the technical and policy communities about the magnitude of CCS cost and the various factors that affect it. We also want to explore the potential for reducing costs through targeted R&D.

At this stage, many of the model parameter values and uncertainty distributions have been based on information gathered from the literature. This approach has its limitations owing to the limited availability of data and possibility of inconsistent assumptions across different studies. An alternative

method elicits the judgment of experts to develop a more robust analysis of uncertainty and variability. Here, we want to understand how experts in this field would characterize some of the key parameters that affect the performance and cost of a particular CO₂ capture technology namely, solid sorbent-based adsorption of CO₂ from flue gas. We are interested in both current and improved future designs that you might envision.

Please briefly review the *Supplementary Information* in the next section to make sure that we use a consistent terminology during this exercise.

Supplementary Information

Among the many process technology options used for CO₂ capture from flue gases, there is significant interest in using solid sorbent-based processes as an alternative separation technique. Like the liquid solvent system, the *adsorption* processes (as opposed to *absorption*) reversibly captures CO₂ using a pressure and/or temperature swing approach. The CO₂ is later purified and compressed for storage at the generation station. This process is thought to have several potential advantages compared to other separation techniques, the foremost advantage being reduced energy consumption in the regeneration process (DOE/NETL, 2013). Most notably, solid sorbents may have lower costs for implementation (ADA- ES Inc., 2013; Tarka & Ciferno, 2005).

Process description

The default solid sorbent system used in this work is an adaptation of the design developed by the Carbon Capture Simulation Initiative (CCSI). This work represents the best available design for a large-scale solid sorbent system and as such, it is the best available source for a full-scale design. A description of the CCSI work can be found in the American Recovery and Reinvestment Act (ARRA) NETL report (DOE/NETL, 2012). The process flow diagram of the adapted system is shown in Figure 1. A bubbling fluidized-bed reactor and a moving-bed reactor are used for the adsorber and regenerator, respectively. The flue gas stream that is coming from the power plant, [G1], is comprised of nitrogen,

water vapor, and trace constituents. The flow rate, composition, and thermodynamic conditions are calculated by the power plant model within the Integrated Environmental Control Model (IECM) and are a function of upstream power plant processes. Flue gas first enters a pre-treatment step in which the concentration of SO₂ is reduced to negligible levels using a lime slurry, [W1], whose product, [W2], is mixed with the processed FGD wastewater. The flue gas is cooled by the limestone slurry from 55°C to ~45°C resulting in an exit water vapour concentration of approximately 11% by volume. The flue gas stream exits pre-treatment, [G2], and is compressed to overcome the pressure drop required by the adsorber and stack. The compressed flue gas stream, [G3], passes into the adsorber through a gas distributor and a CO₂-depleted gas stream, [G4], produced via gas-solid contacting is sent to cyclone and then released to the environment [G5]. A small amount of separated solid is returned to adsorber from the cyclone [S2].

The solid sorbent stream, [S1], is introduced to the adsorber and adsorbs CO₂ and other constituents from the flue gas, yielding the loaded sorbent stream, [S3]. The CO₂-rich solids and any absorbed species are conveyed by a solid moving system, *e.g.*, a bucket elevator, pneumatic conveyor, or some other means, to the cold-side heat exchanger. The solids stream is heated indirectly by thermal contact with steam, [X4], via heat exchanging tubes circulating between the solids heat exchangers. The steam undergoes a phase change to water and is then pumped to the hot-side heat exchanger, [X5]. The water is then heated and converted back to steam from heat recovered from hot solids exiting the regenerator. The pre-heated solid stream, [S4], enters the regenerator and achieves full heating via thermal contact with in-reactor heat exchanging tubes.

In the tube side of the regenerator, hot steam, [X1], extracted at the IP/LP crossover in the power plant turbines is used as a heat source. Once used to heat the solids, this steam is then returned to steam cycle for reheating [X2]. The effect of heating the solid causes the CO₂ to be desorbed, yielding a regenerated solid stream. In addition, a mild condition steam, [X3], is also injected into the regenerator as direct contact steam in order to enhance desorption by reducing the mole fraction of gaseous CO₂. The

injected steam and desorbed species are drawn through a gas collector, [G6], and sent to a dehydration and compression stage.

The CO₂-lean solid stream, [S5], exits the regenerator and is conveyed to the hot-side heat exchanger. The solids are cooled via thermal contact with cooling water circulating between the hot- and cold-side heat exchangers. The cooled solids, [S6], are then sent to a degraded solids separation unit where a small slipstream, [S7], is removed and processed to remove discard solids. The majority of the CO₂-lean solid stream, [S8], is sent to a solid staging area and mixed with make-up solids before being returned to the adsorber.

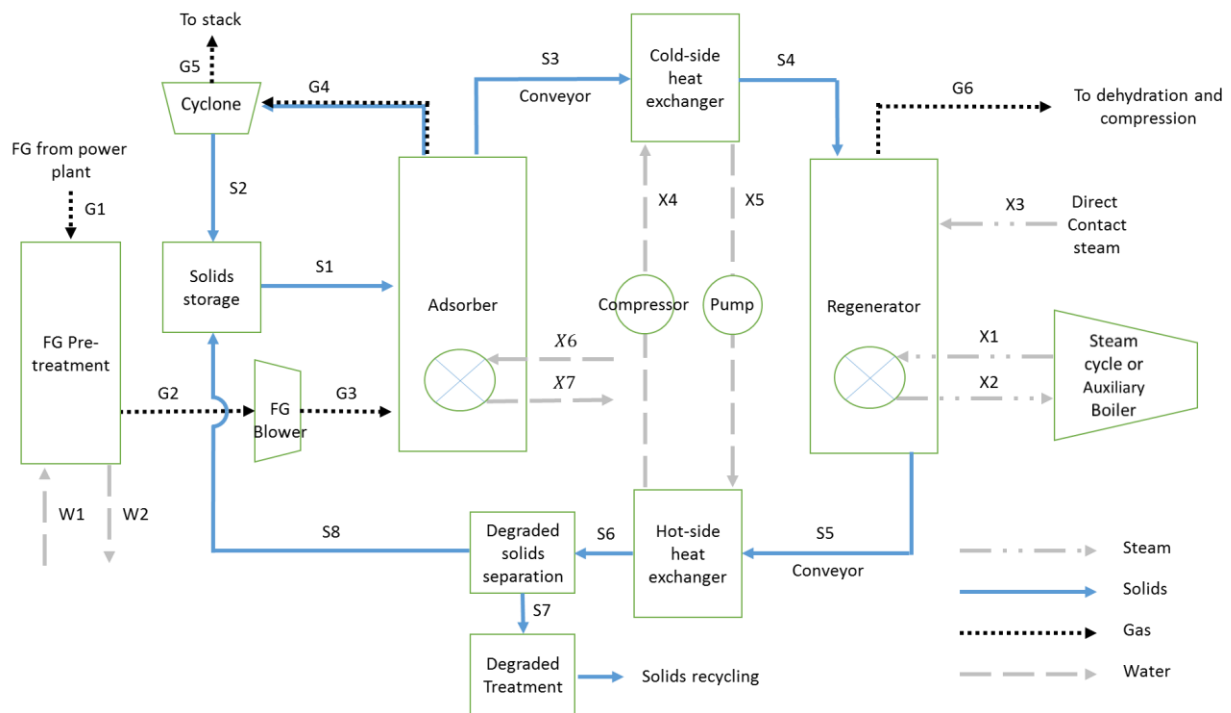


Figure 10.1: Process flow diagram for solid sorbent-based CO₂ capture adapted from the CCSI design (DOE/NETL, 2012).

Part 2: Current solid sorbent systems

To begin, please consider a CO₂ capture system which:

- Uses a supported amine-based solid sorbent
- Treats the flue gas stream from a coal-combustion source which has a CO₂ concentration of about 15% (by volume) and which has been pre-treated for removal of SO_x and cooled to a desired inlet temperature with a reduced water vapor concentration (~10% by volume).
- And removes 90% of CO₂ from the flue gas stream

In the table that follows we have summarized the base case key parameters that we ask you to comment upon. These parameters are intended to characterize the performance of a current commercial system as described above in the supplemental information given earlier.

Please indicate whether you find each of these nominal values and ranges to be reasonable. If not, please indicate the value you would prefer and provide us with a brief explanation. If you prefer to use different units than the one shown here, please indicate clearly the measure that you prefer.

Parameter	Acceptability		If not OK, New Value	Explanation of change
Maximum sorbent loading after repeated adsorption/desorption cycles. Please assume standard adsorption conditions (1 atm. CO ₂ and 25°C)				
Nominal value = 2.9 moles CO ₂ /kg sorbent (~13 g CO ₂ /100 g sorbent)	OK	Not OK		

Range = 2.5-3.3 moles CO ₂ /kg sorbent (11-15 g CO ₂ /100 g sorbent)	OK	Not OK		
Influence of water on actual maximum loading				
Nominal value = -0.5 moles/kg (-2 g CO ₂ /100 g sorbent)	OK	Not OK		
Range = -1.0 moles CO ₂ /kg to +0.5 moles CO ₂ /kg (-4 g CO ₂ to 2 g CO ₂ /100 g sorbent)	OK	Not OK		
The actual rich loading will be ____% below the equilibrium rich loading				
Nominal value = 100%	OK	Not OK		
Range = 85-100%	OK	Not OK		

The actual lean loading will be ____% above the equilibrium lean loading				
Nominal value = 0%	OK	Not OK		
Range = 0%-15%	OK	Not OK		
Solid sorbent price				
Nominal value = \$2.3 /kg (~\$5.0 / lb)	OK	Not OK		
Range = \$1.4/kg – \$3.2/kg (\$3.0 - \$7.0 / lb)	OK	Not OK		

Adsorber overall heat transfer coefficient				
Nominal range = 300 W/m ² -K (95 btu/hr-sqft)	OK	Not OK		
Range = 250-350 W/m ² - K (80-110 Btu/hr-sqft)	OK	Not OK		
Regenerator overall heat transfer coefficient				
Nominal range = 60 W/m ² -K (19 Btu/hr-sqft)	OK	Not OK		
Range = 40-80 W/m ² -K (13-25 Btu/hr-sqft)	OK	Not OK		

Part 3: Judgments about future solid sorbent systems

In this section, we would like to obtain your technically informed probabilistic judgments about several key parameters of a future amine solid-based CO₂ capture system built around the year 2025. We would like you to consider all of the parameters listed, but feel free to skip any parts that you are not comfortable with. Also, if you prefer to use some different unit of measurement in your answer, please mention it clearly.

In producing your answers please assume that:

- We are still talking about an amine sorbent-based plant that treats the flue gas stream from a coal-combustion source, which is about 15% CO₂ and which has been pre-treated for the removal of SO_x and water vapor, and removes 90% of CO₂ from the flue gas stream.
- The plant has been optimized for the lowest overall cost of CO₂ avoidance (\$/tonne CO₂ avoided), considering both capital and operating costs (including energy costs) over the life of the plant.
- R&D support for this technology continues to steadily increase at a modest rate through 2025, and includes several new large-scale applications to coal-fired power plants.

Parameter 1: Maximum solid sorbent loading

First please give us your highest estimate of the maximum loading that could be achieved for an amine-based solid sorbent under standard temperature and pressure conditions by 2025.

$\frac{\text{moles } CO_2}{\text{kg solid sorbent}}$
--

Suppose that we have a clairvoyant who can look ahead to 2025 and tells you that the actual number is 1.15 times this value. Can you think of any plausible story of how that might have happened?

--

If you answered yes, briefly what is the story:

Is there at least a 5% probability that this story could turn out to be true?

	No		Yes
--	----	--	-----

Next, we'd like your lowest estimate of the maximum loading that could be achieved for an amine-based solid sorbent under standard temperature and pressure conditions by 2025.

	$\frac{\text{moles } CO_2}{\text{kg solid sorbent}}$
--	--

Suppose that we have a clairvoyant who can look ahead to 2025 and tells you that the actual number is 0.85 times this value. Can you think of any plausible story of how that might have happened?

	No		Yes
--	----	--	-----

If you answered yes, briefly what is the story:

Is there at least a 5% probability that this story could turn out to be true?

	No		Yes
--	----	--	-----

Finally, we'd like your best estimate of the value that you think the maximum loading might be for a commercially available solid sorbent for CCS application by 2025.

	$\frac{\text{moles } CO_2}{\text{kg solid sorbent}}$
--	--

Parameter 2: Influence of water on maximum CO₂ loading

First, please give us your estimate of the most detrimental influence that water will have on a sorbent's capacity for CO₂ acting in a state-of-the art operating plant in 2025.

	$\frac{\text{moles } CO_2}{\text{kg solid sorbent}}$
--	--

Suppose that we have a clairvoyant who can look ahead to 2025 and tells you that the actual number is 1.15 times this value. Can you think of any plausible story of how that might have happened?

	No		Yes
--	----	--	-----

If you answered yes, briefly what is the story:

Is there at least a 5% probability that this story could turn out to be true?

	No		Yes
--	----	--	-----

Next, we'd like your most positive estimate for the influence that water will have on a sorbent's capacity for CO₂ acting in a state-of-the art operating plant in 2025.

	$\frac{\text{moles } CO_2}{\text{kg solid sorbent}}$
--	--

Again, suppose that we have a clairvoyant who can look ahead to 2025 and tells you that the actual number is 1.15 times this value. Can you think of any plausible story of how that might have happened?

	No		Yes
--	----	--	-----

If you answered yes, briefly what is the story?

Is there at least a 5% probability that this story could turn out to be true?

	No		Yes
--	----	--	-----

Finally, we'd like your best estimate of the influence that water will have on a commercially available solid sorbent in a state-of-the-art operating plant built in 2025.

	$\frac{\text{moles } CO_2}{\text{kg solid sorbent}}$
--	--

Parameter 3: The actual rich loading will equal ____% of the equilibrium rich loading

First, please give us your worst case estimate of how the actual rich loading will compare to the equilibrium rich loading in a state-of-the-art system operating in 2025.

Actual loading is _____% below equilibrium rich loading

Suppose that we have a clairvoyant who can look ahead to 2025 and tells you that the actual number is 15% worse (your answer x 1.15) than this value. Can you think of any plausible story of how that might have happened?

	No		Yes
--	----	--	-----

If you answered yes, briefly what is the story?

Is there at least a 5% probability that this story could turn out to be true?

	No		Yes
--	----	--	-----

Next, we'd like your best case estimate of how the actual rich loading will compare to the equilibrium rich loading in a state-of-the-art system operating in 2025.

Actual loading is _____% below equilibrium rich loading

Again, suppose that we have a clairvoyant who can look ahead to 2025 and tells you that the actual number is 15% better (your answer x 0.85) than this value. Can you think of any plausible story of how that might have happened?

	No		Yes
--	----	--	-----

If you answered yes, briefly what is the story?

Is there at least a 5% probability that this story could turn out to be true?

	No		Yes
--	----	--	-----

Finally, we'd like your best estimate of how close the actual rich loading will be to the equilibrium rich loading for a commercial amine solid sorbent in a state-of-the-art system built in 2025.

Actual loading is _____% below the equilibrium rich loading

Parameter 4: The actual lean loading will be ____% above the equilibrium lean loading

First, please give us your worst case estimate of how the actual lean loading will compare to the equilibrium lean loading in a state-of-the-art system operating in 2025.

Actual loading will be _____% above equilibrium lean loading
--

Suppose that we have a clairvoyant who can look ahead to 2025 and tells you that the actual number is 15% worse (your answer x 1.15) than this value. Can you think of any plausible story of how that might have happened?

	No		Yes
--	----	--	-----

If you answered yes, briefly what is the story?

--

Is there at least a 5% probability that this story could turn out to be true?

	No		Yes
--	----	--	-----

Next, we'd like your best case estimate of how the actual lean loading will compare to the equilibrium lean loading in a state-of-the-art system operating in 2025.

Actual loading is _____% above the equilibrium lean loading

Again, suppose that we have a clairvoyant who can look ahead to 2025 and tells you that the actual number is 15% better (your answer x 0.85) than this value. Can you think of any plausible story of how that might have happened?

	No		Yes
--	----	--	-----

If you answered yes, briefly what is the story?

--

Is there at least a 5% probability that this story could turn out to be true?

	No		Yes
--	----	--	-----

Finally, we'd like your best estimate of how close the actual lean loading will be to the equilibrium rich loading for a commercial amine solid sorbent in a state-of-the-art system built in 2025.

Actual loading is _____ % above equilibrium lean loading

Parameter 5: Cost of solid sorbent (US\$/kg)

First, please give us your lowest estimate of what you think the cost of solid sorbent might be in a state-of-the-art operating plant in 2025.

	\$/kg solid sorbent
--	---------------------

Suppose that we have a clairvoyant who can look ahead to 2025 and tells you that the actual number is 0.85 times this value. Can you think of any plausible story of how that might have happened?

	No		Yes
--	----	--	-----

If you answered yes, briefly what is the story?

Is there at least a 5% probability that this story could turn out to be true?

	No		Yes
--	----	--	-----

Next, we'd like your highest estimate of what you think the cost of solid sorbent might be in a state-of-the-art operating plant in 2025.

	\$/kg solid sorbent
--	---------------------

Suppose that we have a clairvoyant who can look ahead to 2025 and tells you that the actual number is 1.15 times this value. Can you think of any plausible story of how that might have happened?

	No		Yes
--	----	--	-----

If you answered yes, briefly what is the story?

Is there at least a 5% probability that this story could turn out to be true?

	No		Yes
--	----	--	-----

Finally, we'd like your best estimate of the average price of solid sorbent in a state-of-the-art facility operating in 2025.

	\$/kg solid sorbent
--	---------------------

Parameter 6: Adsorber overall heat transfer coefficient

Please give us your highest estimate of what the overall heat transfer coefficient might be between the solid and cooling water in a state-of-the-art bubbling fluidized bed adsorber operating in 2025.

	W/m ² - K
--	-------------------------

Suppose that we have a clairvoyant who can look ahead to 2025 and tells you that the actual number is 1.15 times this value. Can you think of any plausible story of how that might have happened?

	No		Yes
--	----	--	-----

If you answered yes, briefly what is the story?

Is there at least a 5% probability that this story could turn out to be true?

	No		Yes
--	----	--	-----

Next, we'd like your lowest estimate of what the overall heat transfer coefficient might be between the solid and cooling water in a state-of-the-art bubbling fluidized bed adsorber operating in 2025.

	W/m ² - K
--	-------------------------

Suppose that we have a clairvoyant who can look ahead to 2025 and tells you that the actual number is 0.85 times this value. Can you think of any plausible story of how that might have happened?

	No		Yes
--	----	--	-----

If you answered yes, briefly what is the story?

--

Is there at least a 5% probability that this story could turn out to be true?

	No		Yes
--	----	--	-----

Finally, we'd like your best estimate of the value that you think the average overall heat transfer coefficient might be in a state-of-the-art adsorber operating in 2025.

	W/m ² - K
--	-------------------------

Parameter 7: regenerator overall heat transfer coefficient

Please give us your highest estimate of what the overall heat transfer coefficient might be between the solid and steam in a state-of-the-art moving bed regenerator operating in 2025.

	W/m ² - K
--	-------------------------

Suppose that we have a clairvoyant who can look ahead to 2025 and tells you that the actual number is 1.15 times this value. Can you think of any plausible story of how that might have happened?

--

If you answered yes, briefly what is the story?

--

Is there at least a 5% probability that this story could turn out to be true?

	No		Yes
--	----	--	-----

Next, we'd like your lowest estimate of what the overall heat transfer coefficient might be between the solid and steam in a state-of-the-art adsorber operating in 2025.

	W/m ² - K
--	-------------------------

Suppose that we have a clairvoyant who can look ahead to 2025 and tells you that the actual number is 0.85 times this value. Can you think of any plausible story of how that might have happened?

	No		Yes
--	----	--	-----

If you answered yes, briefly what is the story?

--

Is there at least a 5% probability that this story could turn out to be true?

No	Yes
----	-----

Finally, we'd like your best estimate of the value that you think the average overall heat transfer coefficient might be in a state-of-the-art moving bed regenerator operating in 2025.

	W/m ² -K
--	---------------------

Part 4: Other solid sorbents

The preceding questions have all focused on amine-based solid sorbents. Today, there is much research being directed at developing alternative solid sorbents for post-combustion CO₂ capture from flue gas. How likely do you think it is that by 2025 there will be some other commercially available sorbent (other than amine-based) that significantly out-performs amine-based solid sorbents in CO₂ capture from flue gas and which is economically competitive? (Please mark an X on the line)



If your answer was less than 0.5, do you think that some other commercially available and economically competitive solid sorbent will become available sometime after 2025?

- No
- Yes, in approximately the year 20__
m.

Works Cited

ADA- ES Inc., 2013. Pilot Scale Evaluation of an Advanced Carbon Sorbent-based Process for Post-Combustion Carbon Capture, Morgantown, WV: DOE/NETL.

DOE/NETL, 2012. NETL ARRA report on the development of a process design of a solid sorbent carbon capture process, Morgantown, WV: NETL.

DOE/NETL, 2013. DOE/NETL Advanced Carbon Dioxide R&D Program: Technology Update, s.l.: DOE/NETL.

Tarka, T. J. & Ciferno, J. P., 2005. CO₂ capture systems utilizing amine-enriched solid sorbents, Morgantown, WV: DOE/NETL.

Appendix C: Flue gas pre-treatment (Direct Contact Cooler and Polishing Scrubber)

The following was written by Kyle Borgert and is included in this work as documentation of the pre-treatment process that will be coded as a common module in the IECM. Further documentation will become available when technical reports are released documenting these ongoing changes to the IECM. This work references the oxy-combustion process, which is the original application for the direct contact cooler and SO₂ polishing unit (referred to in this work as the pre-treatment process).

General application

Whether a traditional pulverized coal facility needs to decrease the relative humidity of the flue gas exiting the stack to conform to opacity limits or an amine-based CO₂ scrubbing system needs an ultra-low sulfur concentration flue gas to avoid heat stable salt formation; direct contact coolers and polishing scrubbers are an important component of modern electricity generation units. Their value is tied to the ability to accomplish three operations simultaneously: trace sulfur removal, bulk flue gas cooling, and reducing the concentration of water in the exiting flue gas. Furthermore, the latter two operations are physically linked; the concentration of water in the exiting flue gas being a function of the exiting flue gas temperature.

Direct contact coolers utilize the saturation properties of water to condense out any liquid water that is formed as the gaseous water in the flue gas stream is cooled and changes phase. This process is

illustrated in Figure 10.1. as the entering flue gas (red diamond) is gradually cooled until the water saturation pressure curve is encountered. As further cooling of the flue gas occurs, the maximum partial pressure of water vapor in the flue gas is reduced. This means that the flue gas water, no longer able to stay in gaseous form, condenses out of the mixture as liquid water. This simultaneous reduction of temperature and gaseous water in the flue gas is continued until the desired exiting concentration of water is present (yellow diamond).

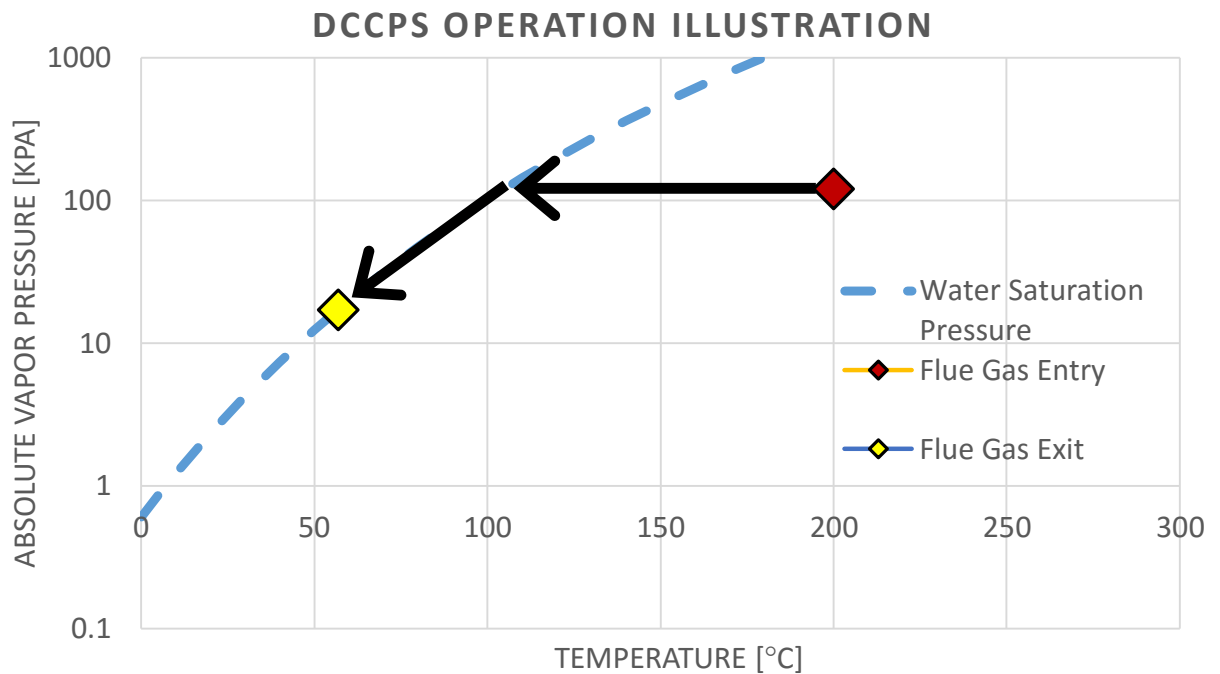


Figure 10.2: Illustration of the flue gas pre-treatment process.

The trace sulfur removal is performed using a well understood and often used chemical reaction for the formation of sodium sulfite. This chemical process involves adding sodium hydroxide, commonly referred to as caustic soda, in order to react with the residual sulfur dioxide in the flue gas. This combination of a chemical and physical process allows DCCPS systems to accomplish their three tasks of trace sulfur removal, bulk flue gas cooling, and water concentration reduction in the exiting gas stream.

Oxyfuel application

The current generation of oxyfuel systems require the use of flue gas recirculation (FGR) to moderate temperature inside the boiler and to ensure that the heat transfer mechanisms are maintained closely to the air-fired conditions for which today's boilers were designed. To that end, the flue gas which is recycled to the boiler must have an acceptable temperature and water concentration to ensure proper thermal regulation and to allow uninterrupted performance of the downstream traditional pollution control equipment. This last consideration is especially important for oxyfuel systems utilizing either a sub-bituminous or lignite coal with a high moisture content. Such coal types typically have a low enough sulfur content to permit the use of a spray-dry absorption system for sulfur removal in lieu of a wet system. This is positive for plant heat rate, but a direct contact cooler must then be used to reduce FGR water content. FGR water concentration reduction is necessary to ensure that a sufficient approach temperature be maintained so that the SDA may continue to function at the desired level of sulfur removal.

Performance model development

Modelling Approach

The direct contact cooler and polishing scrubber model uses or calculates the nine inlet and outlet streams depicted in Figure 10.2. These process flow streams are delineated for ease of mass and energy accounting and calculation but are not necessarily reflective of real-world DCCPS operation. The entering flue gas stream is passed to the model from the IECM fully defined: meaning that the stream is fully defined with composition, temperature, and pressure data along with the mass flow rate. There are then two main parameters which need to be specified prior to the first calculation for cooling and condensing: an anticipated pressure drop across the contacting column and either a desired exit temperature for the flue gas exiting the DCCPS or a desired water concentration in the exiting flue gas. If sulfur polishing is desired, the concentration of sulfur dioxide exiting the DCCPS must also be specified in units of parts per million.

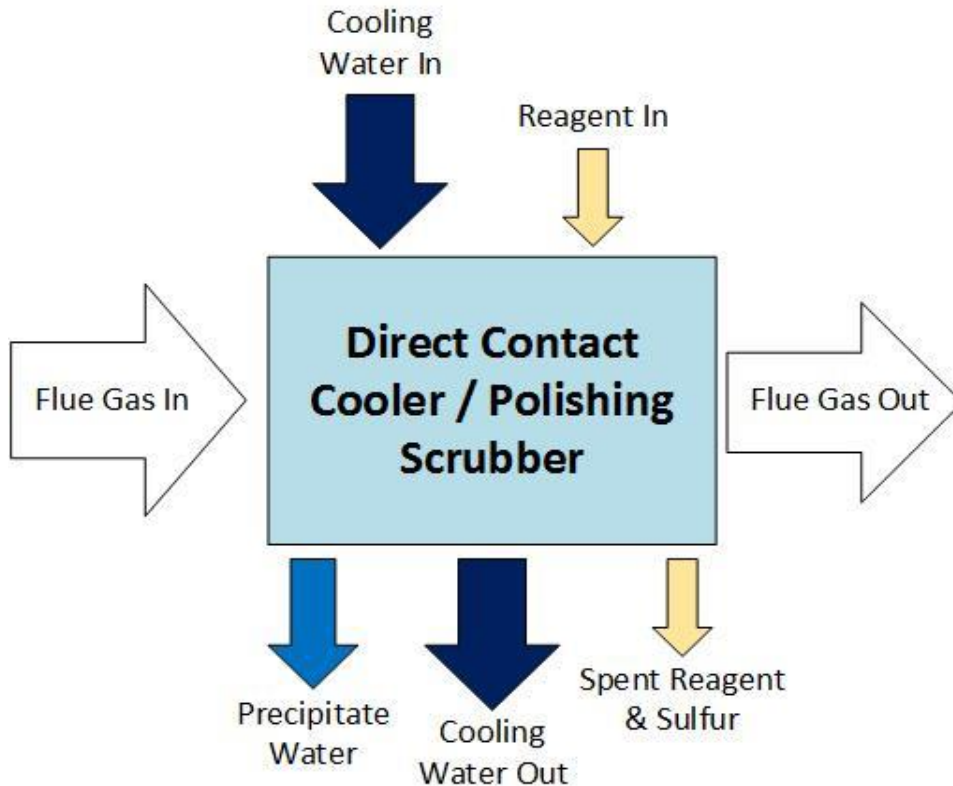


Figure 10.3: Block flow diagram representing the stream flows accounted for in the direct contact cooler and polishing scrubber model.

The model then steps through a series of calculations involving the saturation pressure curve of water to determine the non-specified value of either exit flue gas temperature or exit water concentration in the flue gas. From there, the model calculates the mass balance of all streams in the model along with the composition of gases, liquids, and/or solids in each stream. The energy balance is then completed in a two-step calculation process. First, changes in latent and sensible heat for each stream are calculated using a combination of the Shomate relations, heat capacity data, and the latent heat of condensation model (Borgert, 2015). Secondly, the amount of cooling load required to offset the total latent and sensible heat increase is calculated treating the DCCPS as an adiabatic heat exchanger. Lastly, the amount of cooling water can be calculated from the required cooling load and can be reported along with the rest of the fully defined process flow streams.

Limitations

There were a number of simplifying assumptions made in the creation of this model which would limit its accuracy for forecasting real-world operation. As was previously noted, the nine process flow streams have been delineated for mass and energy accounting purposes and are not indicative of operation in practice. Specifically, the reagent and cooling water inlet streams would be a premixed solution entering the top of the contacting column and the cooling water out, precipitate water, and spent reagent streams would be an admixture at the bottom of the contacting column. Furthermore, many studies involving a DCCPS of the size required for a coal plant equipped with carbon capture (Babcock & Wilcox Power Generation Group, 2011; DOE/NETL, 2013) have indicated that it is desirable from both a cost and simplicity standpoint to construct a dedicated cooling system and water handling services for the contacting tower(s). This is in part due to the issues previously raised about the reagent stream and cooling water being combined in practice. Thus having a dedicated system to handle the caustic-doped water and precipitated solids (sodium sulfite) would be desirable. There are also balance of plant and layout considerations from the volume of cooling water required which bolster the case for a dedicated cooling water system.

Treating the DCCPS system as an adiabatic heat exchanger for purposes of calculating the heat balance also limits the applicability of the model to real world conditions. The weather conditions (including ambient water and air temperature, and associated maximum cooling water delta) will affect the quantity of cooling water required and associated parasitic load of pumping and processing that cooling water. However, absent very detailed weather data, anticipating the effect of the weather is beyond the capabilities of this analysis. For those concerned with not underestimating the effects of an undersized cooling system for the DCCPS, a heat transfer efficiency factor $\alpha_{Cooling}$ has been provided to allow the user to enter what amounts to a cooling water safety factor into their analysis.

Saturation Pressure of Water

The maximum concentration of water vapor which can be contained in a gas mixture is a function of the gas temperature and pressure. This relationship is illustrated by the water vapor saturation pressure curve presented in Figure 10.3. There are numerous scientific methods for describing the relationship between vapor pressure and temperature for pure components. For this work we have chosen to use the Antoine equation (Equation 10.1), which is derived from the Clausius-Clapeyron relation.

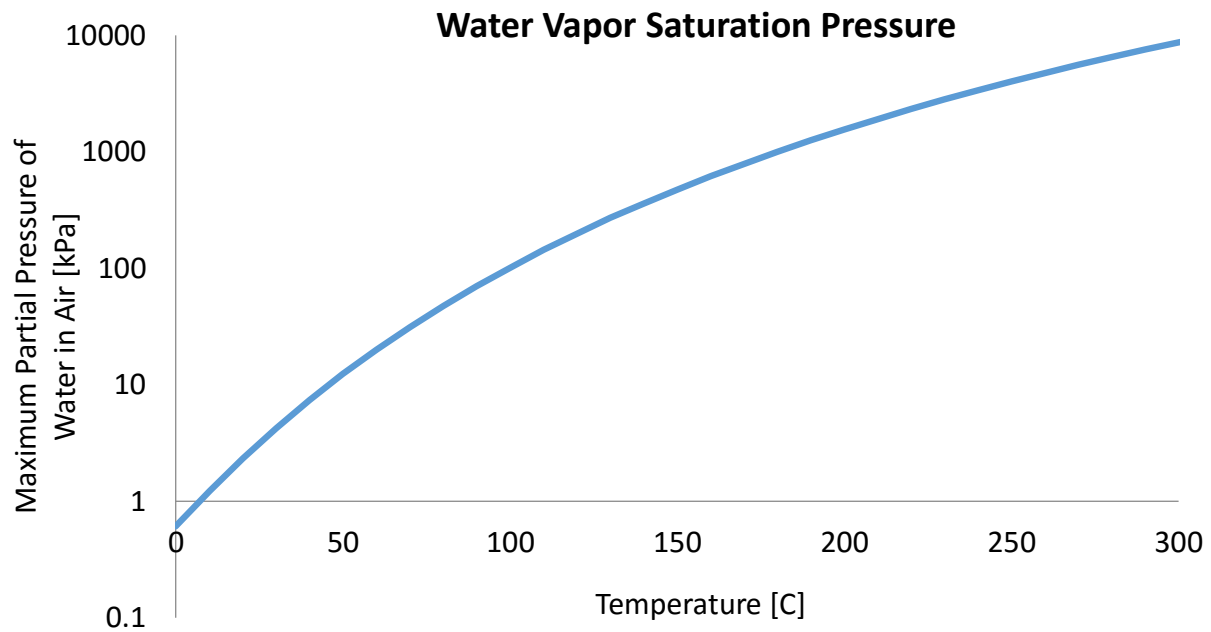


Figure 10.4: Water vapor saturation curve used in the flue gas pre-treatment process.

Due to tradition, the units of pressure of the Antoine coefficients (A, B, and C) are reported in millimeters of mercury [mmHG]. A conversion factor (γ) allows for the below version of the Antoine equation to report pressures in units of kilopascals rather than millimeters of mercury.

$$\gamma = 0.133322368$$

Equation 10.4:

$$P_{saturation} = p_{H_2O} = 10^A \left[A - \frac{B}{(C + T)} \right]$$

The Antoine equation reports a saturation pressure which is here interpreted as the maximum partial pressure of water vapor in the flue gas mixture. The partial pressure of any given component of a gas mixture can be calculated directly given the total pressure of the gas stream and the molar fraction using Dalton's Law of Partial Pressures.

Latent Heat of Water Condensation

A reduction in the concentration of water in the flue gas is accomplished by causing the water vapor to change phase and condense out as liquid water. The amount of heat required to cause a liquid to vaporize is known as the latent heat of vaporization (LHOV). The latent heat of condensation (LHOC) is equivalent in magnitude to the (LHOV) for a pure component, but of the opposite sign. In the case of water vapor in the DCCPS, we are concerned with the amount of heat which must be removed in order to induce a change of phase from vapor to liquid. The LHOC is temperature dependent for water. As can be seen in Figure 10.4, the LHOC of water displays a gradual decline in magnitude as temperature is increased. However, as the triple point is approached, the LHOC rapidly converges toward zero.

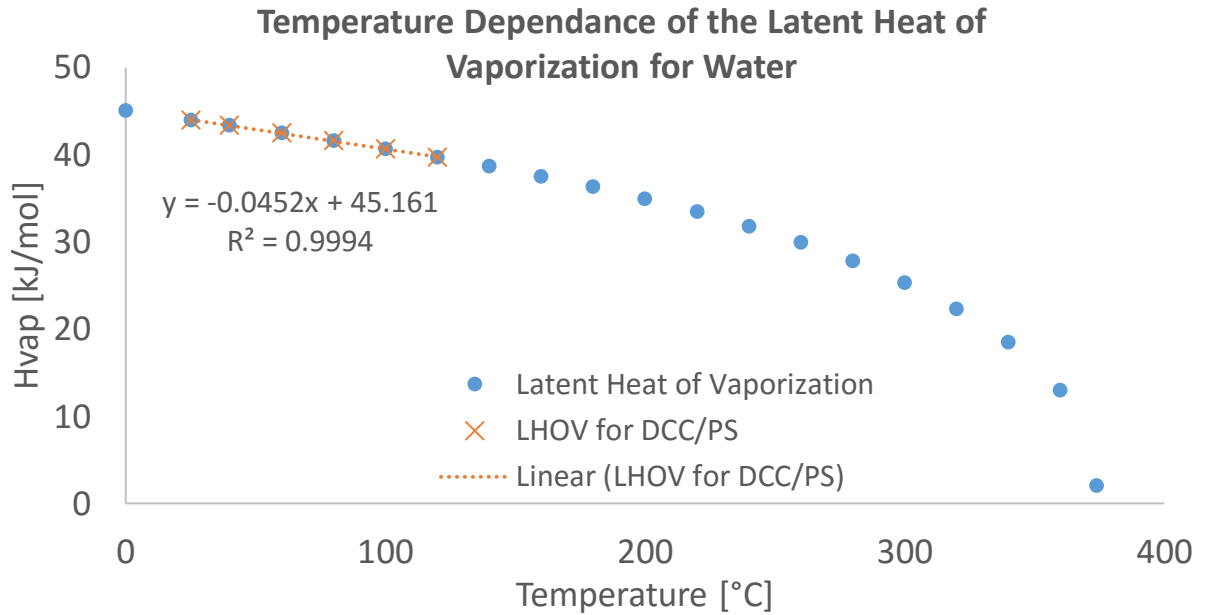


Figure 10.5: The latent heat of vaporization of water is temperature dependent (Marsh, 1987). The decline in LHOV magnitude is very linear over the temperature window expected during operation of the DCCPS.

Flue gas temperatures entering the DCCPS rarely exceed 170°C and the temperature zone where water condensation occurs from these entry conditions will typically be below 120°C. This operational temperature window allows us to simplify the LHOV relation of water to the linear region. A linear regression taken from 20 - 120°C provides a nearly perfect fit ($R^2 > 0.99$) over our condensation regime. This regression is shown in Equation 10.2.

Equation 10.5:

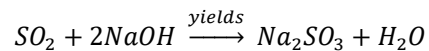
$$\text{Latent Heat of Condensation} \left[\frac{\text{kJ}}{\text{mol}} \right] = -45.161 + 0.0452 * T_{\text{Condensation}}$$

In practice, the phase change to liquid water would not occur at a single temperature, but across a range defined by the interplay between maximum partial pressure and temperature. In our model we use a mean temperature for $T_{\text{Condensation}}$ in Equation 10.2 for calculating the LHOC for water. This mean

temperature is the average between the DCCPS exit temperature (T_{sat_exit}) and the temperature at which the inlet flue gas first encounters the water vapor saturation curve during cooling (T_{sat_enter}).

Sulfur Removal Calculation Strategy

Deep sulfur scrubbing with sodium hydroxide (NaOH) can be enabled as a concurrent process to flue gas cooling in the updated DCCPS model. The amount of sodium hydroxide, also referred to as caustic soda or caustic, required for polishing is determined on a strictly mass balance basis according to the mass of sulfur to be removed from the flue gas. The kinetics are assumed to be sufficiently fast as to not preempt the completion of the following reaction:



The heat of reaction from the formation of solid sodium sulfite (Na_2SO_3) and water is also neglected in determining the required cooling load of the DCCPS unit. However, the water formed has been assumed to be in the gaseous state and is therefore accounted for in the latent heat removal formulation.

A desired exiting sulfur concentration, in parts per million (ppm), may be specified when using the DCCPS model. This volumetric concentration, along with the entering flue gas composition, is then used to determine the mass of sulfur which must be removed from the flue gas stream per unit time. Because the quantity of sulfur in the DCCPS exit stream is much, much less than the total quantity of gas in the exit stream; the number of sulfur moles can be calculated with sufficient accuracy based upon the balance of gas moles in the exit stream.

Performance model

Performance Input and Output Parameters

Input Parameters

The key input parameters defining the performance of the DCCPS are as follows:

\dot{M}_{fg_enter}	Mass flow rate of flue gas entering the contacting tower [kgmol/hr]
x_{i,fg_enter}	Mole fraction of all species (i) in the entering flue gas
P_{fg_enter}	Absolute pressure [kPa] of the entering flue gas
P_{drop_DCCPS}	Absolute pressure drop across the contacting tower [kPa]
x_{SO_2,fg_exit}	Molar concentration of sulfur dioxide in exiting flue gas [ppm]
PMC	Moisture content in the sodium sulfite slurry [mass fraction]
$\alpha_{cooling}$	Heat transfer efficiency of the DCCPS system (unity being ideal heat transfer)
$\Delta T_{max,cooling\ water}$	Largest acceptable cooling water temperature increase [°C]

Additionally, one of the following two parameters must be specified about the exit flue gas stream:

T_{fg_exit}	Temperature of exiting flue gas [°C]
x_{H_2O,fg_exit}	Mole fraction of water vapor in exiting flue gas

Output Parameters

The model will then calculate or report the following key output parameters:

\dot{M}_{fg_exit}	Mass flow rate of flue gas exiting the contacting tower [kgmol/hr]
x_{i,fg_exit}	Mole fraction of all species (i) in the exiting flue gas

P_{fg_exit}	Absolute pressure [kPa] of the exiting flue gas
T_{fg_exit}	Temperature of exiting flue gas [°C]
$\varphi_{H2O_Condensed}$	Molar flow rate of water condensed out of flue gas [mol/sec]
$\varphi_{Na2SO3,precipitant}$	Molar flow rate of sodium sulfite produced from sulfur treatment [mol/sec]
$\varphi_{H2O,precipitant}$	Molar flow rate of water produced for sulfur treatment [mol/sec]
\dot{M}_{NaOH}	Mass flow rate of sodium hydroxide required for sulfur treatment [kg/sec]
\dot{M}_{Slurry}	Mass flow rate of sodium sulfite slurry produced by sulfur treatment [kg/sec]
$Cooling\ Load_{total}$	Total cooling load requirement of DCCPS [kJ/sec]
$\dot{M}_{Cooling\ water}$	Mass flow rate of cooling water required for DCCPS cooling [kg/sec]
$\dot{M}_{water_generated}$	Mass flow rate of water generated during DCCPS operation [kg/sec]

Mass and Energy Balance Calculation Strategy

Flue Gas Mass & Energy Balance

The DCCPS model has been designed so that either a desired water concentration of the exiting flue gas or a desired exiting flue gas temperature may be specified by the user. These two variables are co-dependent and cannot be specified independently. Regardless of starting information, the Antoine Equation is then utilized to determine either the exit concentration or exit temperature of the flue gas leaving the DCCPS.

Table 10.1: The constants used in the Antoine Equation are temperature dependent across the range of expected operation of the DCCPS.

Antoine Constants for Water [°C and mmHG]		
	1 – 100 °C	99 – 374 °C
A	8.07131	8.14019
B	1730.63	1810.94
C	233.426	244.485

Starting Equations Given: fully defined inlet (pressure, temperature, composition, mass flow rate), pressure drop across DCCPS, and desired flue gas exit composition as shown in Equations 10.3 and 10.4.

Equation 10.6

$$p_{H_2O,fg_exit} = x_{H_2O,fg_exit} * (P_{fg_enter} - P_{drop_DCCPS})$$

Equation 10.7

$$T_{fg_exit} = T_{sat_exit} = \frac{B}{A - (\log_{10}(p_{H_2O,fg_exit}/\gamma))} - C$$

Starting Equations Given: fully defined inlet, pressure drop across DCCPS, desired flue gas exit temperature as shown in Equations 10.5 and 10.6.

Equation 10.8

$$p_{H_2O,fg_exit} = \gamma \left[10^{\left(A - \frac{B}{(C + T_{fg_exit})} \right)} \right]$$

Equation 10.9

$$x_{H_2O,fg_exit} = \frac{p_{H_2O,fg_exit}}{(P_{fg_enter} - P_{drop_DCCPS})}$$

Once one of the above sequences has been followed, the temperature at which the incoming flue gas reaches the water vapor saturation curve during cooling must be calculated using Equation 10.7.

Equation 10.10

$$T_{sat_enter} = \frac{B}{A - (\log_{10}(p_{H_2O,fg_enter}/\gamma))} - C$$

Gas Stream Flow Rate Calculations

At this point, the temperature, pressure, and composition of the flue gas has been either calculated or specified at the three important states of the DCCPS. The mass flows through the system must now be balanced:

Inlet stream needs to be in [mol/sec] for each compound. This conversion can be accomplished utilizing Equation 10.8 if total mass flow is in [kgmol/hr].

Equation 10.11

$$\varphi_{i,fg_enter} = x_{i,fg_enter} * \frac{\dot{M}_{fg_enter}}{3.6}$$

where:

φ_{i,fg_enter} is the molar flow rate [mol/sec] of species i in the entering flue gas

x_{i,fg_enter} is the mole fraction of species (i) in the entering flue gas

\dot{M}_{fg_enter} is the total mass flow rate [kgmol/hr] of flue gas into the DCCPS

The flue gas exit molar flow rate can then be calculated using the below for all gaseous species other than water and sulfur dioxide as shown in Equation 10.9.

Equation 10.12

$$\varphi_{i,fg_exit} = \varphi_{i,fg_enter}$$

For water, Equation 10.10 is used to determine the exit flue gas molar flow rate.

Equation 10.13

$$\varphi_{H_2O,fg_exit} = \frac{x_{H_2O,fg_exit} * \sum_j \varphi_{i,fg_exit}}{1 - x_{H_2O,fg_exit}}$$

where:

$\sum_j \varphi_{i,fg_exit}$ is the total flow rate of all non-water gas species in the exiting flue gas (neglecting sulfur)

The molar flow rate of water condensed out of the DCCPS is then calculated by subtracting the outlet flue gas flow rate from the inlet flow rate as shown in Equation 10.11.

Equation 10.14

$$\varphi_{H_2O_Condensed} = \varphi_{H_2O,fg_enter} - \varphi_{H_2O,fg_exit}$$

The sulfur dioxide molar flow rate in the exiting flue gas is then defined using Equation 10.12.

Equation 10.15

$$\varphi_{SO_2,fg_exit} = x_{SO_2,fg_exit} [ppm] * \frac{\sum_k \varphi_{i,fg_exit}}{1,000,000}$$

where:

$\sum_k \varphi_{i,fg_exit}$ is the total flow rate of all gas species in the exiting flue gas (neglecting sulfur)

x_{SO_2,fg_exit} [ppm] is the desired concentration of sulfur dioxide in the exiting flue gas in ppm

The mass flow rate [kgmol/hr] of the exiting flue gas stream can now be calculated by taking the sum across all component gas molar flow rates and multiplying by their respective molecular weights as shown in Equation 10.13.

Equation 10.16

$$\dot{M}_{fg_exit} = 3.6 * \sum (\varphi_{i,fg_exit} * MW_i)$$

where:

φ_{i,fg_exit} is the molar flow rate [mol/sec] of species (i) in the exiting flue gas

MW_i is the molecular weight of species (i) [g/mol]

\dot{M}_{fg_exit} is the total mass flow rate [kgmol/hr] of flue gas exiting the DCCPS

Reagent Stream Flow Rate Calculations

The amount of sodium hydroxide (NaOH) added for sulfur removal in the DCCPS model is assumed to be equal to the stoichiometric requirement. In practice, a surplus quantity of caustic would be supplied to the DCCPS in the recycled cooling water to ensure sufficient availability to achieve the stipulated exiting sulfur dioxide concentration. For ease of calculation however, we have assumed that the stoichiometric quantity of caustic closely approximates steady state behavior for caustic consumption in the DCCPS model as shown in Equation 10.14.

Equation 10.17:

$$\varphi_{NaOH} = 2 * (\varphi_{SO_2,fg_enter} - \varphi_{SO_2,fg_exit})$$

The mass flow rate of required sodium hydroxide added as reagent is then quantified using Equation 10.15.

Equation 10.18:

$$\dot{M}_{NaOH} \left[\frac{kg}{sec} \right] = 0.04 \left[\frac{kg}{mol} \right] * \varphi_{NaOH}$$

Precipitant Stream Flow Rate Calculations

The precipitant stream is assumed to be comprised of only water and the sodium sulfite solid created by the removal of sulfur from the incoming flue gas. The quantity of sodium sulfite can be calculated based upon the difference in sulfur dioxide flow rate between the entering and exiting flue gas. This is true because SO₂ and Na₂SO₃ are equimolar in reaction (A). Additionally, an equivalent number of moles of water are generated in the production of sodium sulfite which must be added to the molar flow rate of precipitate water as shown in Equation 10.16.

Equation 10.19:

$$\varphi_{Na_2SO_3, precipitant} = \varphi_{SO_2, fg_enter} - \varphi_{SO_2, fg_exit} = \varphi_{H_2O_SO_2removal}$$

The molar flow rate of all precipitate water can then be calculated by adding the water generated by the creation of sodium sulfite to the condensed water calculated previously as shown in Equation 10.17.

Equation 10.20:

$$\varphi_{H_2O, precipitant} = \varphi_{H_2O_Condensed} + \varphi_{H_2O_SO_2removal}$$

For reporting mass flow rates from the model, it is necessary to convert the molar flow rates of the above streams. In practice, a fraction of the water produced in the formation of sodium sulfite remains

with the solid to form a slurry. This fraction, denoted as Precipitant Moisture Content [mass fraction], may be specified by the user but carries a default value of 25%. A lower limit of 14.3% is stipulated for Precipitant Moisture Content (PMC) because this represents the equimolar mixture of sodium sulfite and water which would be produced simultaneously when sodium hydroxide reacts with sulfur. Therefore, absent drying, a PMC of less than 14.3% is not possible. For PMC's greater than 14.3% additional water from the DCCPS is entrained with the precipitant slurry. For a generic PMC the resulting precipitant slurry mass flow rate is defined using Equation 10.18.

Equation 10.21:

$$\dot{M}_{slurry} \left[\frac{kg}{sec} \right] = 0.126 \left[\frac{kg}{mol} \right] * \varphi_{Na_2SO_3, precipitant} + 0.018 \left[\frac{kg}{mol} \right] * \left(\frac{PMC}{14.3} \right)$$

Because the sodium sulfite is produced in a slurry, rather than as a dry product, there is no excess water created from the removal of sulfur which can be returned to the DCCPS. In fact, for all PMC's greater than the minimum value, the sulfur removal process is water negative. The required slurry water must be subtracted from the overall water balance and is calculated using Equation 10.19.

Equation 10.22:

$$\dot{M}_{slurry_water} \left[\frac{kg}{sec} \right] = 0.018 \left[\frac{kg}{mol} \right] * \varphi_{H_2O_SO_2removal} * \left(\frac{PMC}{14.3} - 1 \right)$$

Calculating the Required Cooling Load

To determine the amount of cooling which must be provided to the DCCPS, we define the system as an adiabatic heat exchanger. This allows us to neglect any second order effects of environmental temperature fluctuations and focus on the primary bulk fluid heat transfer required. The cooling load is made up of a sensible heat component (temperature change) and a latent heat component (phase change). The sensible heat change of each of the non-reactive gas species is calculated using the Shomate equation to determine the enthalpy of each component at the entering and exiting states of the

DCCPS. To then calculate the change in sensible heat of all the non-reactive gas (NRG) species we assume ideal gas behavior and apply the Gibbs-Dalton law for calculating the combined enthalpy of a gas stream shown in Equation 10.20

Equation 10.23:

$$H = mh = m_1h_1 + m_2h_2 + \dots + m_kh_k = \sum_{i=1}^k m_ih_i$$

The difference in enthalpy of each component of the entering and exiting flue gas can then be multiplied by their respective mass flow rates to calculate the total sensible heat which must be removed from the non-reactive gas species while in the DCCPS as shown in Equation 10.21.

Equation 10.24:

$$\Delta \text{Sensible Heat}_{NRG} = H_{enter_NRG} - H_{exit_NRG}$$

The sensible heat delta calculation for sulfur dioxide is calculated using the same formula as the non-reactive gases. Theoretically, there should be some accounting for the reduction in moles of SO₂ gas as the flue gas passes through the DCCPS which would result in a slightly lower value for the sensible heat of SO₂ than calculated using the non-reactive gases methodology. However, due to the diminutive mass flow rate of SO₂ even before removal, the reduction in the system heat balance through precise mass accounting is negligible (<0.1%). We therefore chose to use the following relation to calculate the sensible heat delta of the sulfur dioxide gas in the flue gas stream as shown in Equation 10.22.

Equation 10.25:

$$\Delta \text{Sensible Heat}_{SO_2} = \varphi_{SO_2,fg_enter} * [h_{SO_2}(T_{fg_enter}) - h_{SO_2}(T_{fg_exit})]$$

The sensible heat delta from water in the flue gas is calculated in three parts. Two of which correspond to the vapor and liquid phase of the condensing water, while the third accounts for the bulk cooling of the non-condensing water vapor (NCV) in the flue gas. The third part is the most straightforward and is calculated in identical fashion to the sensible heat of sulfur dioxide save that the molar flow rate used is the exiting, rather than entering, gas flow rate of water vapor from the DCCPS as shown in Equation 10.23

Equation 10.26:

$$\Delta \text{Sensible Heat}_{H_2O_NCV} = \varphi_{H_2O_NCV,fg_exit} * [h_{H_2O}(T_{fg_enter}) - h_{H_2O}(T_{fg_exit})]$$

The remaining two sensible heat components for water relate to the vapor (CV) and then liquid water (CL) which is condensed out of the incoming flue gas. The vapor phase of the condensate water sensible heat change is calculated in a similar fashion to the non-reactive gaseous components using the Shomate relations. The specific calculation varies in that the final temperature of the water vapor is not assumed to be the exit temperature of the DCCPS, but rather the average condensation temperature as shown in Equation 10.24.

Equation 10.27:

$$T_{\text{Condensation}} = \frac{T_{\text{sat_enter}} + T_{\text{sat_exit}}}{2}$$

The sensible heat of the condensing vapor is quantified using Equation 10.25.

Equation 10.28:

$$\text{Sensible Heat}_{H_2O_CV} = \varphi_{H_2O_Condensed} * [h_{H_2O}(T_{fg_enter}) - h_{H_2O}(T_{\text{Condensation}})]$$

The liquid phase of the condensate sensible heat change is calculated using the heat capacity of liquid water as shown in Equation 10.26.

Equation 10.29:

$$C_{p_{H_2O_liquid}} \left[\frac{kJ}{mol * K} \right] = 0.075$$

The heat capacity of liquid water is close enough to constant over the range of temperature involved within the DCCPS to allow us to safely assume a fixed specific heat for liquid water. The sensible heat change of the liquid water can be calculated using the change in temperature of the condensate and the molar flow rate as shown in Equation 10.27.

Equation 10.30:

$$\Delta \text{Sensible Heat}_{H_2O_CL} = \phi_{H_2O_Condensed} * C_{p_{H_2O_liquid}} * (T_{Condensation} - T_{fg_exit})$$

Latent Heat of Water

Calculating the latent heat required to be removed from a gas stream in order to have a specified fraction of a component condense is not a straight-forward calculation to obtain an exact answer. In order to simplify the calculation of the latent heat of cooling, $T_{Condensation}$ was assumed to be the temperature at which all water vapor was condensed out of the flue gas within the DCCPS. This assumption preempts the use of a much more computationally intensive, iterative method which could capture continuous changes in water vapor concentration as a function of temperature. It was determined that this degree of precision was not appropriate given the inherent uncertainty of the electrical generation unit as a whole and therefore a decision was made in favor of computational economy.

The total latent heat of condensation for the water condensed out of the flue gas is calculated for the new DCCPS model using the molar flow rate of the precipitated water and the molar flow rate of water created by the sulfur removal process chemistry. The water created by the formation of sodium sulfite is very small in comparison (typically 3 orders of magnitude less) but is included here as the sole means of thermally accounting for the exothermic removal of sulfur in the model. The sum of these two molar flow

rates is then combined with the latent heat of condensation correlation detailed earlier to calculate the required cooling load for the latent heat of water condensation. The formula for calculating the latent heat is shown in Equation 10.28.

Equation 10.31:

$$\Delta \text{ Latent Heat} = (\varphi_{H2O_Condensed} + \varphi_{H2O_SO2removal}) * (-45.161 + 0.0452 * T_{Condensation})$$

Cooling Water Requirement Calculation Strategy

At this point all of the mass and energy streams have been calculated with the exception of the cooling water flow rate. The required flow rate of cooling water is a function of four parameters:

$\alpha_{Cooling}$ heat transfer efficiency of the DCCPS system (unity being ideal heat transfer)

$Cooling\ Load_{total}$ sum of all latent and sensible cooling loads in the DCCPS system

$\Delta T_{max,Cooling\ water}$ largest acceptable temperature increase of cooling water

$Cp_{Cooling\ water}$ specific heat of cooling water, default value of 4.2 [kJ/kg K]

The total cooling load is the first piece of information which is required to be calculated. It can be found by taking the sum of all the latent and sensible heat deltas calculated in the previous section to get a total cooling load in kilojoules per second as shown in Equation 10.29.

Equation 10.32:

$$Cooling\ Load_{total} \left[\frac{kJ}{SEC} \right] = \Delta SH_{NRG} + \Delta SH_{SO2} + \Delta SH_{H2O_NCV} + \Delta SH_{H2O_CV} + \Delta SH_{H2O_CL} + \Delta LH$$

The required mass flow of cooling water can then be calculated using Equation 10.30.

Equation 10.33

$$\dot{M}_{\text{Cooling water}} \left[\frac{\text{kg}}{\text{sec}} \right] = \frac{\text{Cooling Load}_{\text{total}}}{\alpha_{\text{cooling}} * C_{p_{\text{Cooling water}}} * \Delta T_{\text{max, Cooling water}}}$$

Water Balance

One of the primary functions of the DCCPS is to reduce the moisture content in the entering flue gas. It follows logically then that a substantial amount of liquid water ($\varphi_{H_2O_Condensed}$) is produced during normal operation. However, as discussed previously, the reaction to sodium sulfite can be a water consuming process if a water-rich slurry is specified. However, the creation of sodium sulfite slurry is a secondary process compared to the precipitation of flue gas moisture under typical operating conditions and has correspondingly little effect on the net water produced during operation. Equation 10.31 calculates the flow rate of generated water.

Equation 10.34:

$$\dot{M}_{\text{water_generated}} = \left(0.018 \left[\frac{\text{kg}}{\text{mol}} \right] * \varphi_{H_2O_Condensed} \right) - \dot{M}_{\text{Slurry_water}} \left[\frac{\text{kg}}{\text{sec}} \right]$$

The input and output variables for the DCCPC processmodel are shown in Table 10.6.

Table 10.2: Input and output properties for the DCCPC process model

Input variable	Units	Description
$M_{CO_2(gas)}^{DCC,in}$	kmol/hr	Molar flow rate of CO ₂ at the adsorber inlet
$M_{N_2(gas)}^{DCC,in}$	"	" " " N ₂ " " "
$M_{O_2(gas)}^{DCC,in}$	"	" " " O ₂ " " "
$M_{NO_X(gas)}^{DCC,in}$	"	" " " NO _X " " "
$M_{SO_2(gas)}^{DCC,in}$	"	" " " SO ₂ " " "
$M_{H_2O(gas)}^{DCC,in}$	"	" " " H ₂ O " " "

$M_{inert(gas)}^{DCC,in}$	“	“ “ “ inert gas “ “ “
$T_{gas}^{DCC,in}$ or $P_{gas}^{DCC,in}$	K or Pa	Flue gas temperature or pressure
Output variable	Units	Description
$M_{CO_2(gas)}^{DCC,in}$	Kmol/hr	Molar flow rate of CO ₂ at the adsorber outlet
$M_{N_2(gas)}^{DCC,in}$	“	“ “ “ N ₂ “ “ “
$M_{O_2(gas)}^{DCC,in}$	“	“ “ “ O ₂ “ “ “
$M_{NO_X(gas)}^{DCC,in}$	“	“ “ “ NO _x “ “ “
$M_{SO_2(gas)}^{DCC,in}$	“	“ “ “ SO ₂ “ “ “
$M_{H_2O(gas)}^{DCC,in}$	“	“ “ “ H ₂ O “ “ “
$M_{inert(gas)}^{DCC,in}$	“	“ “ “ inert gas “ “ “
$P_{gas}^{DCC,in}$ or $T_{gas}^{DCC,in}$	Pa or K	Flue gas pressure or temperature

Appendix D: Flue gas blower design

The added cooling load is estimated using the temperature and pressure data from the equipment specifications shown in Table 10.2. This data is based on the work completed by the Carbon Capture Simulation Initiative (CCSI) (DOE/NETL, 2012).

Table 10.3: Specifications for the induced draft blower developed by CCSI.

Design Data	Centrifugal blower type	
Identification	Feed	Product
Quantity (kmol/hr)	743,599	743,599
Composition	Mole fraction	
CO ₂	0.1177	0.1177
H ₂ O	0.1417	0.1417
N ₂	0.7406	0.7406
Temperature (K)	427	454
Pressure (Pa)	110,000	129,000

In this model, the total pressure change is limited to half an atmosphere and the correlation between temperature and pressure is assumed to be linear over this range according to the following relationship:

$$\frac{\Delta P}{T} = \frac{129,000 - 110,000}{454 - 427} = 704 \frac{Pa}{K}$$

Appendix E: Heat exchanger design

Specifications for the cold- and hot-side heat exchanger designs are based on the work completed by CCSI are shown in Tables 10.3 and 10.4 below. . The heat exchanger specifications shown here are the same as those reported in the 2012 Report (DOE/NETL, 2012). Note that this work uses an overall heat exchange coefficient (U) value of 60 W/m²-K in order to maintain consistency with design assumptions for the regenerator.

Table 10.4: Specifications for the cold-side cross-flow heat exchanger

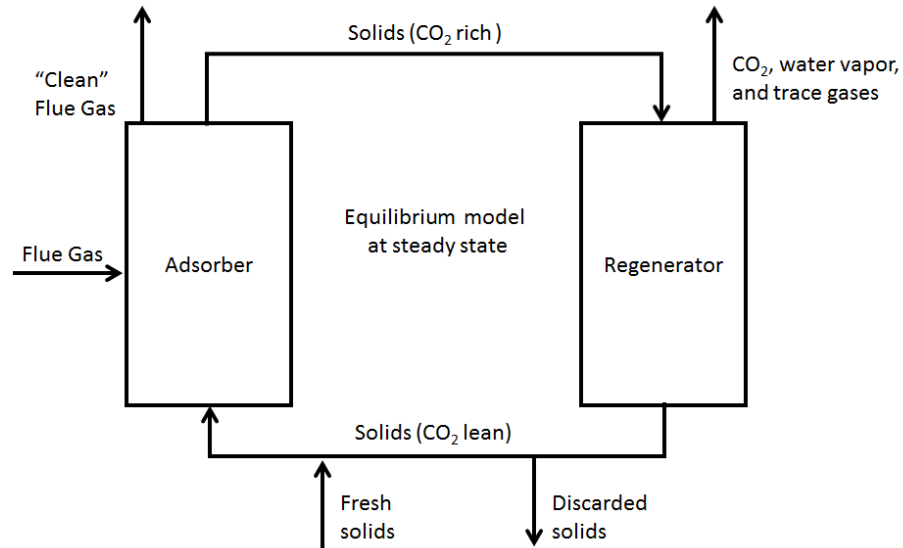
Cold-side heat exchanger					
Function	Solids heat exchanger before the regenerator				
Operation	Continuous				
	Feed	Product		Feed	Product
Materials	Shell side (Saturated Steam)		Tube side (Solids)		
Quantity (kmol/hr)	743,599	743,599	Quantity (kg/hr)	594,231	594,231
Temperature (K)	401	384	Temperature (K)	327	342
Pressure (kPa)	150	130	Pressure (Pa)	101,000	101,000
Design Data	Floating heat shell-and-tube design				
Material of construction	Carbon steel				
Tube length (m)	3.7				
U (W*m ⁻² *K)	300				
LMTD (K)	58				
HX Area (m ²)	208				

Table 10.5: Specifications for the hot-side heat exchanger

Hot-side heat exchanger					
Function	Solids heat exchanger after the regenerator				
Operation	Continuous				
	Feed	Product		Feed	Product
Materials	Shell side (Saturated Steam)		Tube side (Solids)		
Quantity (kmol/hr)	743,599	743,599	Quantity (kg/hr)	594,231	594,231
Temperature (K)	384	384	Temperature (K)	408	391
Pressure (kPa)	130	150	Pressure (kPa)	101	101
Design Data	Floating heat shell-and-tube design				
Material of construction	Carbon steel				
Tube length (m)	3.7				
U ($W \cdot m^{-2} \cdot K$)	300				
LMTD (K)	13.6				
HX Area (m^2)	870				

Appendix F: Derivation of the degraded solid flow rate at the adsorber inlet

With the exception of CO₂ and N₂, calculation of the quantity of most of the adsorbed flue gas species may be expressed using the following procedure for steady state conditions. As a matter of context, the diagram below shows the inlets and outlets of solids and gases in the CO₂ capture system. The calculations shown here will focus on the flow rates of solids in the lower half of this diagram.



First, it is necessary to define the flow rate of SO_2 entering the system as flue gas.

Mass flow rate of SO_2 entering the system

In this example, let:

Total flue gas flow rate = 115,000 kmol/hr

SO_2 concentration = 1 ppmv

The flow rate of SO_2 at the adsorber inlet can be calculated as:

$$m_{\text{SO}_2(\text{gas})}^{A,\text{in}} = 115,000 \frac{\text{kmol}}{\text{hr}} * 1 * 10^{-6} \frac{\text{kmol SO}_2}{\text{kmol FG}} * 64 \frac{\text{kg SO}_2}{\text{kmol}} = 7.4 \text{ kg/hr}$$

Mass flow rate of adsorbed SO_2 at the adsorber inlet

Next, calculate the flow rate of adsorbed SO_2 . The following sequence of equations shows the mass balance for the adsorbed species at various points of interest in the CO_2 capture system.

Solid flow rate of species, i	Equation
Adsorber inlet	$m_{i(solid)}^{A,in}$
Adsorber outlet	$m_{i(solid)}^{A,in} + m_{i(gas)}^{A,in} * \eta_{C,i}$
Regenerator outlet	$(m_{i(solid)}^{A,in} + m_{i(gas)}^{A,in} * \eta_{C,i}) * (1 - \eta_{R,i})$
After solid separation	$(m_{i(solid)}^{A,in} + m_{i(gas)}^{A,in} * \eta_{C,i}) * (1 - \eta_{R,i}) * (1 - X_{solid\ purge})$
Adsorber inlet	$\left(\frac{\eta_{C,i} - \eta_{C,i}\eta_{R,i} + \eta_{C,i}\eta_{R,i}X_{solid\ purge} - \eta_{C,i}X_{solid\ purge}}{\eta_{R,i} + X_{solid\ purge} - \eta_{R,i}X_{solid\ purge}} \right) * m_{i(gas)}^{A,in}$

where:

$m_{i(solid)}^{A,in}$ = Mass flow rate of adsorbed species at the adsorber inlet (kg/r)

$m_{i(gas)}^{A,in}$ = Mass flow rate of the species in the flue gas at the adsorber inlet (kg/hr)

$\eta_{C,i}$ = Adsorption efficiency

$\eta_{R,i}$ = Regeneration efficiency

$X_{solid\ purge}$ = Solid purge fraction

In this example, let:

$i = \text{SO}_2$

$\eta_{C,i} = 1.0$

$\eta_{R,i} = 0.0$

$X_{solid\ purge} = 4 * 10^{-5}$

The flow rate of adsorbed SO_2 at the adsorber inlet is calculated using the last equation from the previous table.

$$m_{SO_2(solid)}^{A,in} = \left(\frac{\eta_{C,SO_2} - \eta_{C,SO_2}\eta_{R,SO_2} + \eta_{C,SO_2}\eta_{R,SO_2}X_{solid\ purge} - \eta_{C,SO_2}X_{solid\ purge}}{\eta_{R,SO_2} + X_{solid\ purge} - \eta_{R,SO_2}X_{solid\ purge}} \right) * m_{SO_2(gas)}^{A,in}$$

$$m_{SO_2(solid)}^{A,in} = \frac{1.0 - 1.0 * 0 + 1.0 * 0.0 * 4 * 10^{-5} - 1.0 * 4 * 10^{-5}}{0.0 + 4 * 10^{-5} - 0.0 * 4 * 10^{-5}} * 7.4 \frac{kg\ SO_2}{hr} = 185,000 \frac{kg\ SO_2}{hr}$$

Mass flow rate of degraded solid sorbent

The mass flow rate of degraded solid sorbent is calculated using the equation below.

$$m_{solid-SO_2}^{A,in} = M_{SO_2(solid)}^{A,in} * 1000 \frac{moles}{kmol} * q_{max}$$

Note that the molar flow rate of SO₂ is required in this section and so 185,000 kg SO₂/hr calculated above is converted to the molar flow rate of 2,881 kmol/hr. The maximum capacity of the solid sorbent in this example is 2.9 moles/kg.

$$m_{solid-SO_2}^{A,in} = 2,881 * 1000 \frac{moles}{kmol} * 2.9 = 993,000 \frac{kg}{hr}$$

Solid composition

The composition and flow rates of solids relating to the removal of degraded solids are shown in the table below. Note that the mass flow rate of SO₂ leaving the system (7.4 kg/hr) is equivalent to the inlet flow rate of SO₂ entering the system as flue gas (7.4 kg/hr).

Solid composition and flow rates (kg/hr)	
<u>Adsorber solid inlet</u>	<u>Regenerator solid outlet</u>
CO ₂ : 242,000	CO ₂ : 242,000

SO ₂ : 184,000	SO ₂ : 184,000
Clean solid: 6,900,000	Clean solid: 6,900,000
Degraded solid: 993,000	Degraded solid: 993,000
Total: 8,340,000	Total: 8,340,000
<u>Fresh solids</u>	<u>Discarded solids</u>
CO ₂ : 0	CO ₂ : 10
SO ₂ : 0	SO ₂ : 7.4
Clean solid: 317	Clean solid: 277
Degraded solid: 0	Degraded solid: 40
Total: 317	Total: 334

Sensitivity to purge fraction

Changes to the solid purge fraction will change the solid flow rate of the system. The table below shows three examples in which the solid purge fraction is varied between 0.001% and 0.01%. This range bounds the value that minimizes the levelized cost of electricity. The mass balance with respect to SO₂ is complete as demonstrated by the equivalent input and output SO₂ mass flow rates in the system.

$m_{CO_2(gas)}^{A,in}$	X_{purge}	$m_{SO_2(gas)}^{A,in}$	$m_{SO_2(solid)}^{discarded}$	$m_{CO_2(solid)}^{discarded}$	$m_{clean(solid)}^{discarded}$	m_{purge}	m_{fresh}	$m_{solid}^{A,in}$
616,000	0.001	7.5	7.5	2	71	121	111	12,130,000
603,000	0.004	7.4	7.4	10	317	334	317	8,340,000
601,000	0.01	7.3	7.3	24	729	760	729	7,600,000

In a solid sorbent system, degraded solid sorbent cannot be separated from the clean solids. In order to visualize why this is true, picture a bottle filled with layered red and blue sand. Once this bottle is shaken, it is not possible to separate the red sand from the blue sand. The same is true of the degraded

and clean solid sorbent. And so, in order to complete the mass balance, most of the solids exiting the system is clean. A smaller purge fraction will allow a greater buildup of degradation products in the system and therefore require more solid sorbent to capture the requisite 90% CO₂. A larger solid purge fraction will reduce the solid flow rate of the system.

With the exception of CO₂ and N₂, calculation of the quantity of most of the adsorbed flue gas species existing as a solid may be expressed using the equations shown in Table 10.7.

Table 10.6: Calculations used to calculate the flow rate of adsorbed flue gas constituents.

Solid flow rate of species, i	Equation
Adsorber inlet	$m_{i(solid)}^{A,in}$
Adsorber outlet	$m_{i(solid)}^{A,in} + m_{i(gas)}^{A,in} * \eta_{C,i}$
Regenerator outlet	$(m_{i(solid)}^{A,in} + m_{i(gas)}^{A,in} * \eta_{C,i}) * (1 - \eta_{R,i})$
After solid separation	$(m_{i(solid)}^{A,in} + m_{i(gas)}^{A,in} * \eta_{C,i}) * (1 - \eta_{R,i}) * (1 - X_{solid\ purge})$
Adsorber inlet	$\left(\frac{\eta_{C,i} - \eta_{C,i}\eta_{R,i} + \eta_{C,i}\eta_{R,i}X_{solid\ purge} - \eta_{C,i}X_{solid\ purge}}{\eta_{R,i} + X_{solid\ purge} - \eta_{R,i}X_{solid\ purge}} \right) * m_{i(gas)}^{A,in}$

Appendix G: CCSI performance and cost model data matching exercise

As part of a data validation procedure, the CCSI case studies developed as part of this work were vetted using performance parameters and results published by CCSI (DOE/NETL, 2012). The goal of this exercise was to reproduce the material performance and operational conditions from CCSI's deterministic results within ±10% of the reported performance metrics. The performance and cost parameter values used in this exercise are based on CCSI's report when available. Table 10.23 compares the results of this exercise.

Table 10.7: The results from a data validation procedure in which the performance variables were adjusted in order to reproduce the results published by CCSI. This data is reported in NETL's 2012 report on their solid sorbent system design (DOE/NETL, 2012).

Value	Units	CCSI's Published Data	Case Study Matched Results
CCS System Performance			
Working Capacity	moles CO ₂ /kg solid sorbent	1.8	1.8
Specific Solid Requirement	kg solid/kmol captured CO ₂	573	574
Auxiliary Electrical Load	MW	80	95
Electrical Equivalent Loss	MW _e	160	163
Total Electrical Loss	MW	240	258
Power Plant Summary			
Net Power Output	MW	410	385
Total Capital Cost*	\$Millions	2,200	1,900
LCOE*	\$/MWh	157	156

*CCSI costs are reported in their original 2007 values. The case study using CCSI's values are reported in 2011 dollars.

The first step in this result model matching exercise was equating the flue gas flow rate entering the CO₂ capture system. Next, the solid sorbent characteristics, including the maximum CO₂ capacity and heat of reaction were adjusted based on available data. The adsorber temperature and inlet pressure were then adjusted to match CCSI's reported values. The rich loadings were then set equal by adjusting the adsorber kinetic parameter. Next, a similar exercise was complete for the regenerator by matching the regenerator temperature and product CO₂ concentration. The regenerator kinetic parameter was then adjusted such that the lean loadings predicted by the two models were equal. These steps ensured that the solid sorbent flow rates were equal.

Next, the water adsorption efficiency was adjusted such that the concentrations of water vapor in the flue gas at the adsorber exit were equal. Next, the water regeneration efficiency was adjusted such that the two models predicted the same loading of adsorbed water at the adsorber inlet. At this point, the mass flow rates of gas and solid in the CO₂ capture system are the same.

The next step used to calibrate the CCSI case studies was to ensure that the conditions of the cooling water in the adsorber are similar. This was accomplished by adjusting the cooling water inlet and outlet temperatures to match the values reported by CCSI. Similarly, the inlet and outlet steam enthalpies for heating steam in the regenerator were matched. Finally, the temperatures of the solids and gases in the cross-flow heat exchanger were adjusted to match the conditions reported by CCSI. The resulting total electrical loss and net power output of the models systems are within the reasonable 10% range, suggesting that the overall energy demand of the systems are comparable.

A notable difference between these results are the relative balance between auxiliary electrical load and electrical equivalent loss. These differences can be attributed to assumptions regarding the performance of the equipment used in the IECM (used for this work) compared to contrasting assumptions used by CCSI. Specific data regarding the electrical demand of these components, however, has not been reported. Instead, CCSI's results report a cumulative 80 MW of electricity use in the CCS process of which 56 MW is attributed to the dehydration and compression stage.

The matching case study from this work predicts a comparable compressor electrical requirement (56 MW). However, this work also predicts significant additional electrical demand caused by the induced draft (ID) blower at 31 MW. The electrical load of the ID blower is more than the combined 24 MW of electrical load reported for the pumps, blowers and compressors simulated in the CCSI model resulting in an 18 MW difference between the electrical demands of these models. This difference is largest source of discrepancy between these models and.

The net power output of these two simulated plants are separated by 25 MW of net electrical output (a difference of 6% when normalized by CCSI's predicted net electrical output of 410 MW), allowing for a reasonable comparison between the plant-level costs. Itemized cost breakdowns of CCSI's system, however, are not publically available and so process-level comparisons are speculative. On the other hand, both studies report capital costs pertaining to the power plant excluding CCS which allows for a high level comparison between the CO₂ process capital cost and overall system costs. CCSI reports a

total system cost of \$2.2 billion (2011) of which \$1.4 billion (2011) is attributed to the base plant without CCS. The matching case study developed in this work predicts a total cost of 1.9 billion (2011) of which \$1.2 billion (2011) is base-plant costs. Hence, one may infer that the capital cost estimated for both models is approximately \$0.7-0.8 billion.

Appendix H: Adsorber response surface model

Matching CCSI adsorber modelling results

This section outlines the work done to integrate CCSI's adsorber model into this work based on a series of sensitivity studies on a more recent version of CCSI's solid sorbent-based CO₂ capture model. This effort was made possible by Yang Chen and David Miller at NETL, who kindly donated their time in order to provide supplemental data regarding the adsorber process simulated in Aspen Custom Modeler® Version 8. This data was used in order to develop a regression model that predicts the rich loading achieved in the adsorber as a function of the inlet and outlet solid temperature as well as the inlet CO₂ partial pressure. The regression equation was then used to estimate the kinetic parameter as a means of adjusting the equilibrium rich loading predicted by this work to match the rich loading predicted by CCSI's model.

The regression equation predicts the rich loading as a function of four parameters as shown in Equation 10.35. This equation is capable of predicting the rich loading results determined by CCSI's Aspen model with a residual squared value of 97.92%.

Equation 10.35

$$q_{rich,regression} = -8.26 + 0.2547 * P_{CO_2}^{A,in} + 4.207 * \eta_{C,CO_2} + 0.2213 * T^A - 0.00906 * (P_{CO_2}^{A,in})^2 - 0.001319 * (T^A)^2 - 0.0653 * \eta_{C,CO_2} * T^A$$

where:

$q_{rich,regression}$ = Loading of CO₂ on the solid exiting the adsorber predicted by the regression equation (moles * kg⁻¹)

$P_{CO_2}^{A,in}$ = Partial pressure of CO₂ at the adsorber inlet (kPa)

η_{C,CO_2} = Capture efficiency of CO₂ in the flue gas (fraction)

T^A = Adsorber temperature (°C)

Note that the temperatures and pressures used in this equation are in degrees Celsius and kilopascals rather than Kelvin and Pascals used in the rest of this work. It was found that units were necessary because of significant figure limitations for the coefficients in the Minitab software.

Next, the regression equation is used to predict the adsorber kinetic parameter as a function of the adsorber equilibrium CO₂ loading as shown in Equation 10.36.

Equation 10.36

$$k_A = \frac{q_{rich,regression}}{q_{equilibrium}}$$

where:

κ_A = kinetic parameter for the adsorber (fraction) defined in Equation 4.48

$q_{equilibrium}$ = Equilibrium loading of CO₂ on the solid sorbent defined in Equation 4.43 using the adsorber conditions.

Ideally, the kinetic parameter calculated for each scenario would be the same for all of the scenarios shown in Table 10.24. However, slight variation does exist which can be attributed to variation between these two models. Nonetheless, the variability is relatively small and the mean value ($\kappa_A = 81\%$) is close to the mean value derived from the expert elicitation exercise ($\kappa_A = 83\%$). A summary analysis of

the kinetic parameter calculated using the CCSI data is shown in Table 10.24. For this work, the mean value, 0.81, is used as the nominal value for the CCSI case studies.

Table 10.8: Summary of the kinetic parameter value calculated for each of the 49 sensitivity cases derived using CCSI's adsorber model.

Kinetic parameter statistical indicator	Value
Maximum	0.85
Minimum	0.73
Mean	0.81
Median	0.81
Mode	0.81

CCSI adsorber sensitivity analysis data

The input data set used by CCSI's Aspen model adsorber module is shown in Table 10.25.

Table 10.9: Aspen Custom Modeler input parameters used by CCSI to predict loading response in the adsorber.

Parameter	Value	Units	Parameter	Value	Units
Inlet flue gas flow rate	100,377	Kmol/hr	Diameter of adsorber	15	m
Inlet flue gas mole fraction			Height of bottom adsorber	4.2	m
CO ₂	0.118	fraction	Height of middle adsorber	4.2	m
H ₂ O	0.142	fraction	Height of top adsorber	4.2	m
N ₂	0.74	fraction	Number of adsorber trains	15	
Inlet flue gas temperature	54	C	HX tube diameter	0.0275	m
Inlet flue gas pressure	101,325	Pa	HX tube spacing	0.4	m
Inlet sorbent loading			Sorbent inlet type	Bottom	
Bicarbonate	0.124	mol/kg solid	Sorbent outlet type	Overflow	
Carbonate	0.741	mol/kg solid			
Water	0.254	mol/kg solid			

The outputs produced by this model are shown in Table 10.26.

Table 10.10: Outputs of NETL's solid sorbent-based CO₂ capture adsorber model.

Result	Value	Units
CO ₂ removal fraction	0.9208	
Outlet sorbent temperature	73.84	°C
Outlet sorbent loading		
Bicarbonate	0.2481	mol/kg-solid
Carbonate	1.8287	mol/kg-solid
Water	0.5299	mol/kg-solid
Outlet clean gas temperature	73.52	°C
Outlet clean gas mole fraction		
CO ₂	0.0121	
H ₂ O	0.0294	
N ₂	0.9585	

The sensitivity cases used to develop the regression equation shown in Equation 10.1 are shown in Tables 10.27 through 10.31 below. This data reflects 49 model iterations run by varying 5 different model parameters.

Table 10.11: Case studies varying the solid sorbent flow rate

Case 1: Solid sorbent flow rate						
Input	Outputs					
Flue gas flow rate (kmol/hr)	CO ₂ removal efficiency (fraction)	Temperature of solids at adsorber outlet (°C)	Bicarbonate loading (mol/kg)	Carbonate loading (mol/kg)	Water loading (mol/kg)	CO ₂ rich loading (mol/kg)
400000	0.7263	65.61	0.3378	1.9610	0.6720	2.30
450000	0.7865	67.76	0.3075	1.9375	0.6169	2.25
500000	0.8400	69.85	0.2835	1.9081	0.5765	2.19
550000	0.8854	71.89	0.2641	1.8721	0.5479	2.14
600000	0.9208	73.84	0.2481	1.8287	0.5299	2.08
650000	0.9451	75.60	0.2345	1.7786	0.5205	2.01
700000	0.9597	77.05	0.2223	1.7253	0.5165	1.95
750000	0.9680	78.15	0.2110	1.6731	0.5148	1.88
800000	0.9728	78.95	0.2006	1.6246	0.5135	1.83
850000	0.9758	79.51	0.1911	1.5805	0.5117	1.77

900000	0.9778	79.90	0.1823	1.5406	0.5095	1.72
--------	--------	-------	--------	--------	--------	------

Table 10.12: Case studies varying the flue gas flow rate entering the adsorber

Case 2: Inlet flue gas flow rate						
Input	Output					
Flue gas flow rate (kmol/hr)	CO ₂ removal efficiency (fraction)	Temperature of solids at adsorber outlet (°C)	Bicarbonate loading (mol/kg)	Carbonate loading (mol/kg)	Water loading (mol/kg)	CO ₂ rich loading (mol/kg)
80302	0.9768	76.13	0.2163	1.6771	0.5424	1.89
85320	0.9700	75.76	0.2263	1.7237	0.5377	1.95
90339	0.9589	75.19	0.2348	1.7660	0.5329	2.00
95358	0.9424	74.51	0.2419	1.8013	0.5299	2.04
100377	0.9208	73.84	0.2481	1.8287	0.5299	2.08
105396	0.8958	73.23	0.2538	1.8490	0.5329	2.10
110415	0.8692	72.71	0.2593	1.8640	0.5381	2.12
115434	0.8423	72.26	0.2646	1.8752	0.5449	2.14
120452	0.8160	71.87	0.2698	1.8838	0.5527	2.15

Table 10.13: Case studies varying the inlet flue gas CO₂ mole fraction

Case 3: Inlet flue gas CO₂ mole fraction								
Input			Output					
Inlet flue gas CO ₂ mole fraction	Inlet flue gas water mole fraction	Inlet flue gas N ₂ fraction	CO ₂ removal efficiency (fraction)	Temperature of solids at adsorber outlet (°C)	Bicarbonate loading (mol/kg)	Carbonate loading (mol/kg)	Water loading (mol/kg)	CO ₂ rich loading (mol/kg)
0.0944	0.142	0.7636	0.9637	74.17	0.2229	1.6567	0.5995	1.88
0.1003	0.142	0.7577	0.9580	74.29	0.2308	1.7059	0.5797	1.94
0.1062	0.142	0.7518	0.9493	74.24	0.2376	1.7519	0.5611	1.99
0.1121	0.142	0.7459	0.9369	74.07	0.2433	1.7931	0.5443	2.04
0.118	0.142	0.74	0.9208	73.84	0.2481	1.8287	0.5299	2.08
0.1239	0.142	0.7341	0.9017	73.59	0.2523	1.8588	0.5179	2.11
0.1298	0.142	0.7282	0.8809	73.35	0.2560	1.8842	0.5080	2.14
0.1357	0.142	0.7223	0.8591	73.14	0.2594	1.9058	0.4997	2.17
0.1416	0.142	0.7164	0.8373	72.94	0.2626	1.9247	0.4927	2.19

Table 10.14: Case studies varying the inlet flue gas water concentration

Case 4: Inlet flue gas H₂O mole fraction								
Input			Output					
Inlet water mole fraction	Inlet CO ₂ mole fraction	Inlet N ₂ mole fraction	CO ₂ removal efficiency (fraction)	Temperature of solids at adsorber outlet (°C)	Bicarbonate loading (mol/kg)	Carbonate loading (mol/kg)	Water loading (mol/kg)	CO ₂ rich loading (mol/kg)
0.1	0.118	0.782	0.9151	73.46	0.2495	1.8198	0.5443	2.07
0.11	0.118	0.772	0.9164	73.55	0.2492	1.8219	0.5409	2.07
0.12	0.118	0.762	0.9178	73.64	0.2489	1.8240	0.5375	2.07
0.13	0.118	0.752	0.9192	73.73	0.2485	1.8261	0.5340	2.07
0.14	0.118	0.742	0.9205	73.82	0.2482	1.8283	0.5306	2.08
0.142	0.118	0.74	0.9208	73.84	0.2481	1.8287	0.5299	2.08
0.15	0.118	0.732	0.9219	73.91	0.2479	1.8304	0.5271	2.08
0.16	0.118	0.722	0.9233	74.01	0.2475	1.8326	0.5237	2.08
0.17	0.118	0.712	0.9247	74.11	0.2472	1.8347	0.5202	2.08
0.18	0.118	0.702	0.9260	74.21	0.2468	1.8369	0.5167	2.08

Table 10.15: Case studies varying the inlet solid sorbent temperature

Case 5: Inlet sorbent temperature						
Input	Output					
Temperature of solids at the adsorber inlet (°C)	CO ₂ removal efficiency (fraction)	Temperature of solids at adsorber outlet (°C)	Bicarbonate loading (mol/kg)	Carbonate loading (mol/kg)	Water loading (mol/kg)	CO ₂ rich loading (mol/kg)
35	0.9714	70.53	0.2886	1.8548	0.6271	2.14
45	0.9581	71.52	0.2764	1.8495	0.5950	2.13
55	0.9409	72.63	0.2627	1.8407	0.5623	2.10
65	0.9208	73.84	0.2481	1.8287	0.5299	2.08
75	0.8985	75.12	0.2334	1.8141	0.4984	2.05
85	0.8745	76.46	0.2187	1.7972	0.4681	2.02
95	0.8494	77.83	0.2045	1.7783	0.4393	1.98
105	0.8235	79.23	0.1910	1.7578	0.4121	1.95
115	0.7969	80.66	0.1781	1.7356	0.3866	1.91
125	0.7699	82.09	0.1661	1.7122	0.3629	1.88

Appendix I: Probability distributions for solid sorbent system performance model parameters

This section briefly explains the basis for the probability distributions for various model parameters (Table 5.8 and Table 6.7) used in the Present-case and Future-case probabilistic analyses presented in Chapter 7. As mentioned in Appendix A, these distributions take into account the data reported in literature, modelling assumptions, and experts' technical judgments (especially when sufficient data is not available).

CO₂ capture efficiency (%)

Almost all of the studies report CO₂ capture efficiency of 90%. This seems to be the optimum capture level in the MEA-based CO₂ capture systems, especially for Flour-Daniel's process using 30% MEA solvent. Few studies mention desired capture efficiency of 85% or less (Rao, 2003). Only the Kerr-McGee/ ABB Lummus amine process using 20% MEA solvent is reported to capture as high as 96% CO₂. This work uses 90% as the default value for this parameter and does not specify any distribution.

Maximum CO₂ loading (moles CO₂/kg dry solid sorbent)

The Department of Energy publishes periodic updates about ongoing research projects called the Advanced Carbon Capture R&D Program: Technology Update. In the May, 2013 edition of this publically available report lists some two dozen ongoing projects relating to solid-based CO₂ capture mechanisms (DOE/NETL, 2013). Data for the amine resin and activated carbon solid sorbents discussed in this work were derived from the maximum reported loadings for these solid sorbents from projects NT0004343 and NT0005578 respectively. The tethered amine solid sorbent was described in a recent paper published in *Nature Communications* (Qi, et al., 2014). The distribution provided for the solid sorbent used in the Present-Case elicitation was derived using the expert elicitation exercise. The maximum and minimum values represent the average for these values as reported by the experts. A graphical representation of these answers for the present case is shown in Figure 10.5. The average high value for maximum loading was 3.4 moles CO₂/kg. The low value was 2.4 moles/kg. The average best estimate value was 2.8 moles/kg. The deterministic present-case value uses the average best estimate.

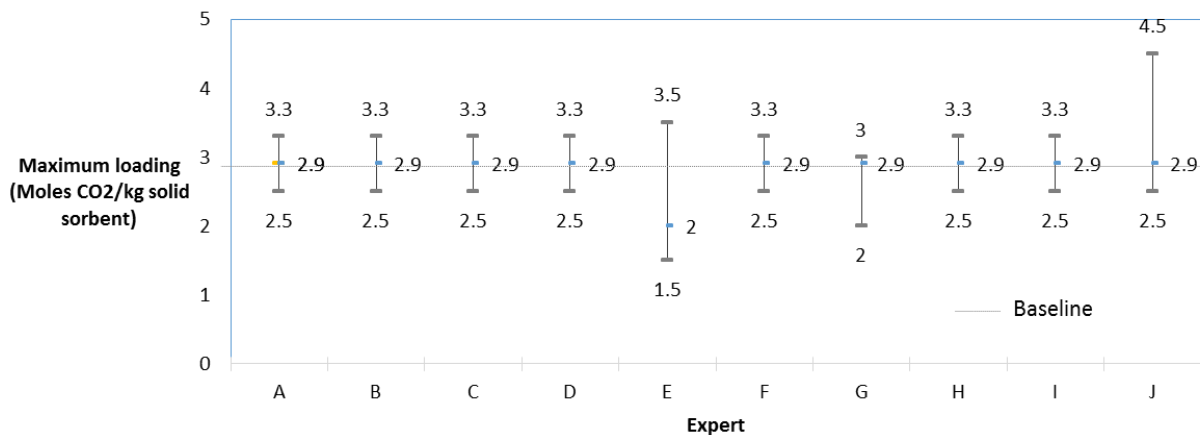


Figure 10.6: Elicited responses for the Present Case maximum CO₂ loading.

For the future-case scenario, the best estimate was 3.9 moles/kg. The high value was 5.1 moles/kg. The low value was 2.8 moles/kg. Figure 10.6 shows a visual representation of the experts' responses.

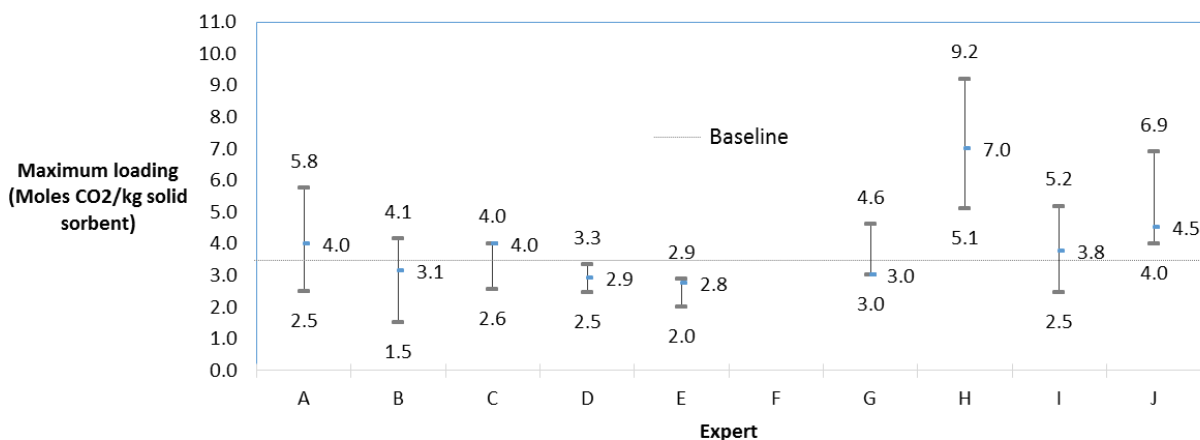


Figure 10.7: Elicited responses for the Future Case maximum CO₂ loading.

Heat of reaction

The heat of reaction of CO₂ by amines is a well studied thermodynamic property and commonly reported in the existing literature. Choi, Drese and Jones provide a comprehensive review of solid sorbents including the various types of amine structures under review at the time of their publication

(Choi, et al., 2009). The heat of adsorption of CO₂ by amines dissolved in aqueous solution has been reported to be in the range of -48 to -84 kJ/mol (Kohl & Nielsen, 1997). The highest heat of adsorption of -73 kJ/mol for chemically tethered amines was reported by Shi for diamine-functionalized sorbents by differential scanning calorimetry (DSC) analysis at 333K (Wei, et al., 2008) although more recent work has characterized the heat of adsorption for some tethered amines at values as high as 75 kJ/mol (Qi, et al., 2014). The lowest heat of adsorption reported, -48 kJ/mol, was also reported for diamine silica (SBA-15) (Khatri, et al., 2005). However, this value was estimated by FTIR analysis by subtracting desorption spectra from adsorption spectra and inferring CO₂ capacities, and should be considered a lower bound on the binding energy. Heats of adsorption for monoamine and triamine silicas have been reported between these two values. Shu observed an increase in the heat of adsorption of diamine functionalized SBA-16 as amine loading increased (Wei, et al., 2008) and Chaffee (Serna-Guerrero, et al., 2008) observed a similar increase as the number of tethered amines per unit area for triamine-functionalized HMS. Higher heats of adsorption have been reported for CO₂ adsorbed by amino acids with values as high as -81 kJ/mol [Guo Thee]. The range chosen in this work (-40 to -80 kJ/mol) is meant to reflect the wide range of nitrogen based solid sorbents currently under investigation today. The deterministic value of -60 kJ/mol reflects the specific value reported by Sjostrom and Krutka (Sjostrom & Krutka, 2010) for their ongoing investigation of this solid sorbent at the pilot project operating at Plant Miller.

Solid heat capacity

The heat capacity of the solids circulating through the CO₂ capture system is an important parameter for quantifying the sensible heat load in each process where solids are involved in heat exchange. For this work, the nominal value for the sensible heat capacity is derived from material data provided by ADA as part of their reporting requirements to the Department of Energy (ADA- ES Inc., 2013). The range of heat capacities (0.7 – 1.5 kJ/kg-K) used in this work represent the heat capacities published for DOE-funded solid sorbent research at the time this DOE report was published (May, 2013).

The majority of reported values, however, are between 0.9-1.1 kJ/kg-K and so a normal distribution with a mean of 1.0 kJ/kg-K and a standard deviation of 0.1 kJ/kg-K is the range used in the sensitivity analysis.

Adsorber Temperature

The temperature of the solids in the adsorber is necessary in order to quantify many performance and cost values in the CO₂ capture model. This model assumes cooling water is provided at 10°C and a reasonable limit on the temperature approach is between 10 and 20°C, thus resulting in a practical upper bound of 20-30 °C. However, results from this study have shown that adsorption temperatures in this range do not improve the cost of the system (See Section 6.3) due to the larger cooling requirements. As an alternative, the lower limit for the adsorber temperature is instead defined by the process conditions reported for the amine-resin used in this work (40°C). The upper bound is set at 70°C, which is temperature at which the rich loading and lean loading are equal in the default case. The nominal value of 54°C is the same value published by CCSI as the adsorber outlet temperature of the solids (DOE/NETL, 2012).

Adsorber equilibrium CO₂ pressure

The equilibrium CO₂ pressure in the adsorber is a difficult parameter to define. The limiting upper and lower bounds are represented by the two reactor ideal adsorber reactor (i.e. the plug-flow reactor and the well-mixed stirred-tank reactor), and the equilibrium CO₂ pressure is calculated at the inlet and outlet gas pressure and CO₂ concentration respectively. However, the actual equilibrium pressure in a non-ideal design is determined by the by the process design and the true equilibrium pressure will be somewhere between these two values. The nominal value for this parameter is based on the adsorber inlet CO₂ concentration and pressure conditions.

Adsorber pressure drop

The pressure drop in the adsorber is required in order to determine the electrical load of the flue gas blower. The default value of 30 kPa is equal to the pressure drop specified by CCSI in their process design. However, the pressure drop of the system depends upon the adsorber design. The lower bound of 6 kPa is the value used for the liquid amine-based adsorption process developed by Peter Versteeg for CO₂ capture (Versteeg, 2012). Given the limited availability of data, the upper bound is set to 40 kPa in order to represent the additional pressure drop that would accompany a multi-stage, co-current flow design (such as a bubbling bed). A triangular distribution is used with a maximum probability set to the default CCSI value (30 kPa) and the bounding conditions of 6 and 40 kPa representing the unlikely lower and upper distribution boundaries.

Adsorption Kinetics

The adsorber kinetic parameter is an adjustment to the equilibrium loading in order to account for the limited retention time of the solids in the adsorber. The value of this parameter depends upon the vessel design as well as the properties of the solid sorbent. This work uses two methods to estimating the adsorber kinetic parameter. The first method uses a series of sensitivity studies based on NETL's adsorber model developed in Aspen Custom Modeler. Values derived from this method are applied to Cases #5 and #6, the sensitivity analysis included in Chapters 5 and 7, and serve as the default method for determining the adsorber kinetic value in the IECM. More information about this exercise is available in Appendix H.

The second method estimates values for the adsorption kinetic parameter using the expert elicitation exercise described in Appendix B. The results of this exercise for the Present-Case Scenario are described in Figure 10.7. The average high value provided by the experts was 87% and the average low value was 75%. The average best guess value was 83%. These values are used as the upper, lower, and nominal values for the Present Case scenario.

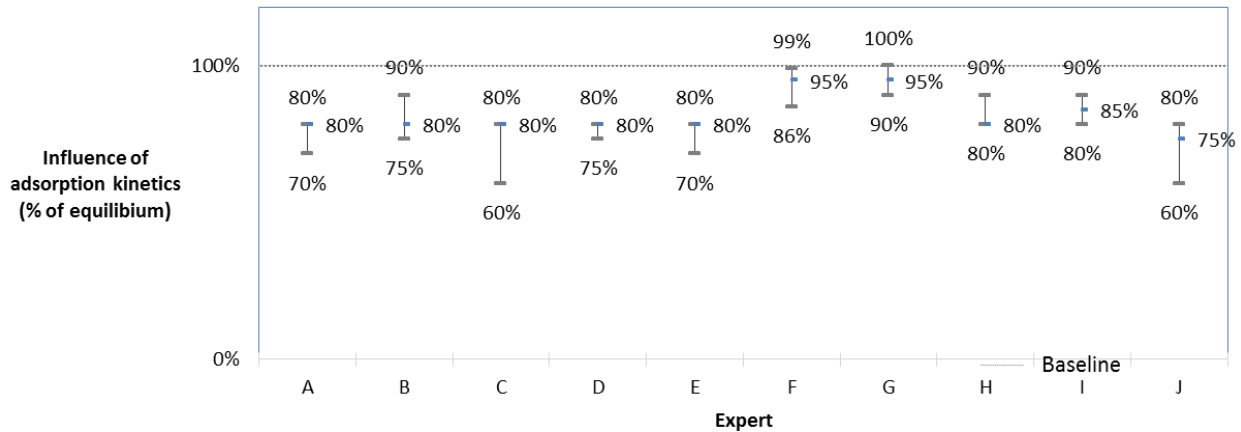


Figure 10.8: Elicited responses for the Present-Case adsorber kinetic parameter.

For the future-case scenario, the best estimate was 90%. The high value was 95%. The low value was 67%. Figure 10.8 shows a visual representation of the experts' responses.

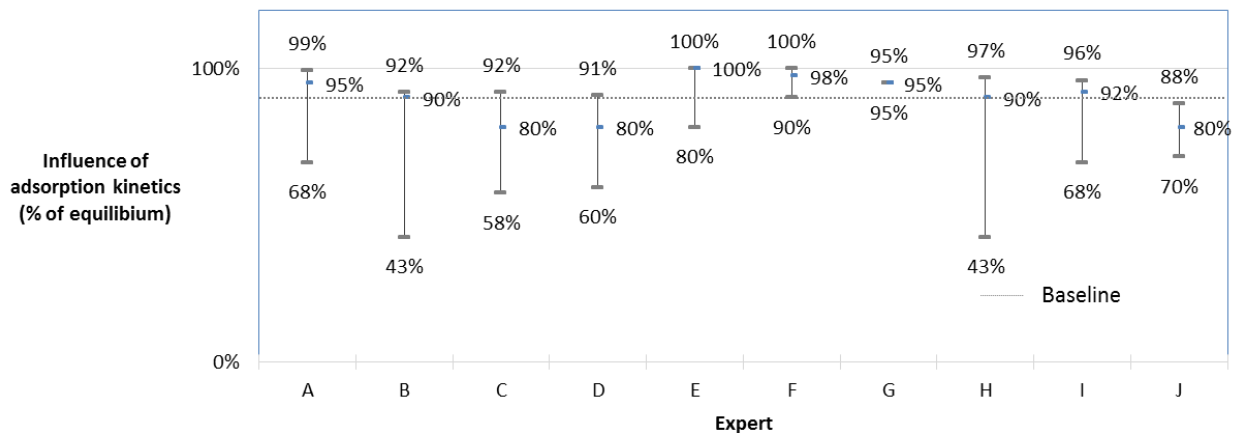


Figure 10.9: Elicited responses for the Future Case kinetic parameter.

Adsorber overall heat transfer coefficient

The overall heat transfer coefficient in the adsorber was another of the seven parameters estimated using the expert elicitation exercise. This method was chosen due to the lack of available data regarding the heat exchange properties of indirect solid-liquid heat transfer for the types of fluidized beds discussed in this work. The elicited responses provided by experts for the Present Case are shown in Figure 10.9. The average response for the high value was 392 W/m²-K. The average low value response

was 250 W/m²-K. The average best guess was 300. These values are used as the upper, lower, and nominal values for the Present Case scenario.

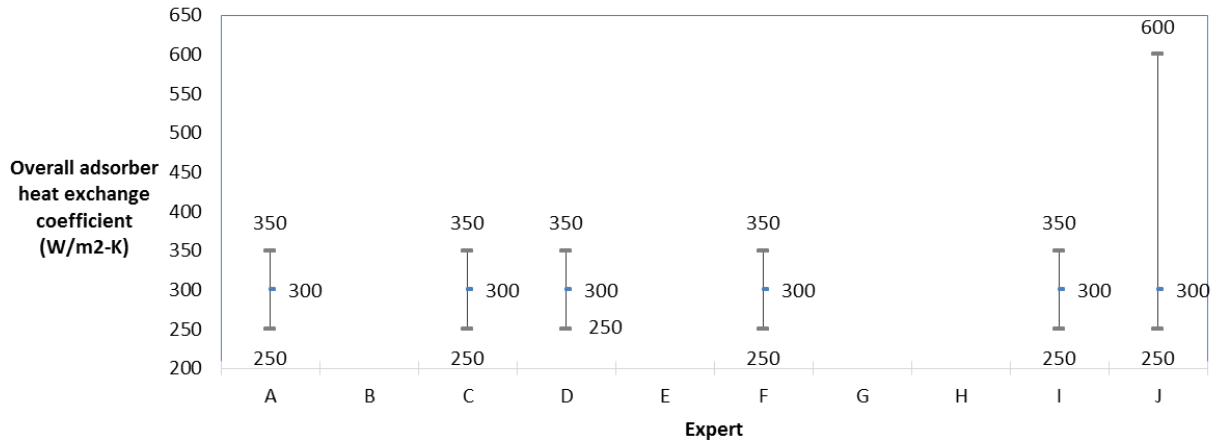


Figure 10.10: Expert elicitation responses for the Present Case overall adsorber heat transfer coefficient.

For the Future Case scenario, the best estimate was 385 W/m²-K. The high value was 460 W/m²-K. The low value was 232 W/m²-K. Figure 10.10 shows a visual representation of the experts' responses.

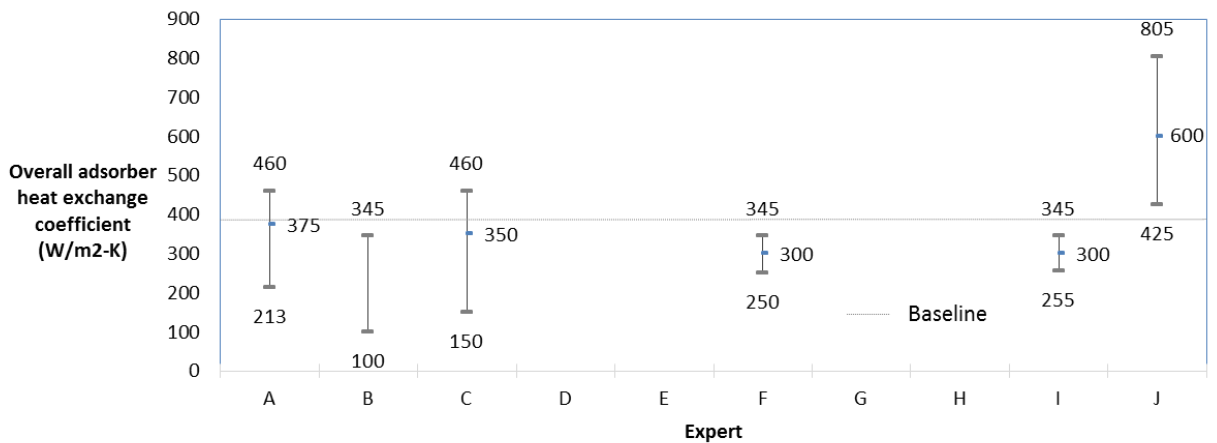


Figure 10.11: Expert elicitation responses for the Future Case overall adsorber heat transfer coefficient.

Regeneration temperature

The final temperature of the solids in the regenerator is nominally set at 393 K (120°C) since this value is considered the maximum temperature sustainable for amine functional groups before degradation occurs. However, it is also possible that degradation may begin to occur at temperatures as low as 378 K (108°C). Since degradation of the solid sorbent is not desirable, the solids must be kept at a temperature lower than the degradation limit. At the same time, a higher temperature is required in order to drive off CO₂ and maintain a low lean loading. As such, the degradation range of 378 – 393 K is used as the low and high limits of the regenerator temperature.

CO₂ outlet pressure

The pressure of CO₂ at the regenerator outlet is one of the parameters used to determine the lean loading of the solid at the regenerator exit. The nominal value is 42 kPa, which is the pressure specified at the regenerator outlet in CCSI's process design (DOE/NETL, 2012). The minimum value is 20 kPa as a representation of a low pressure system based on the author's judgement regarding the practical limits of a the system's operation. The majority of the product gas in such a system would consist of water vapor which would be removed as part of the dewatering/compression process. The maximum CO₂ pressure is set to 101 kPa, which represents a pure CO₂ environment under atmospheric conditions.

Regeneration kinetics

The kinetic parameter in the regenerator is estimated based on the expert elicitation exercise discussed in the next section. For the Present Case scenario, the nominal value is equal the average "best guess" value provided by the experts (11%). The regenerator kinetic parameter is 17% as the average "worst case" scenario and 4% as the best case. These values should be interpreted as a percentage increase in the lean loading above the equilibrium. The responses provided by the experts are shown in Figure 10.11.

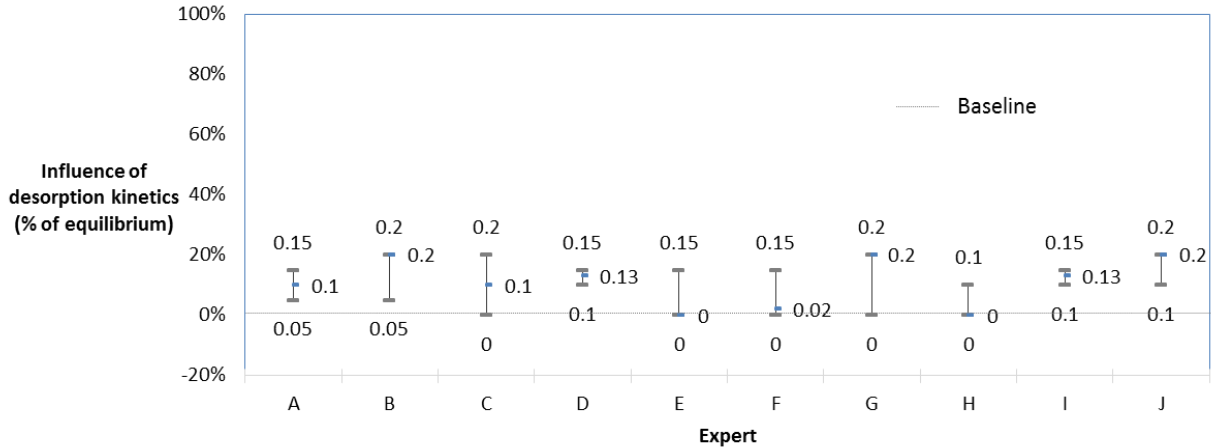


Figure 10.12: Expert responses for the present case regeneration (desorption) kinetic parameter.

A similar exercise was performed for the Future Case scenario and responses from the experts are shown in Figure 10.13. The average best guess for this scenario is 10%. The average high value is 31% and the average low value is 6%.

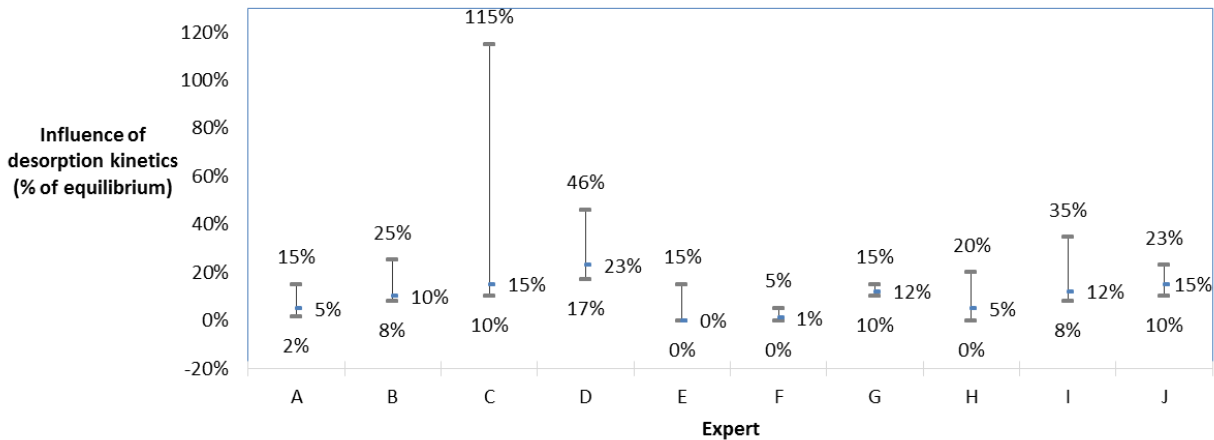


Figure 10.13: Expert responses for the Future Case regenerator (desorption) kinetic parameter.

Regenerator overall heat transfer coefficient

The regenerator overall heat transfer coefficient is used in order to calculate the heat exchange area and cost of the regenerator vessel. This parameter was estimated using the expert elicitation exercise. The average “best guess” provided by the experts for the Present Case scenario is 55 W/m²-K. The average low value is 40 W/m²-K and the average high value is 80 W/m²-K. These values are used as

the nominal, minimum, and maximum values for the Present Case scenario respectively. The responses for each expert are shown in Figure 10.13.

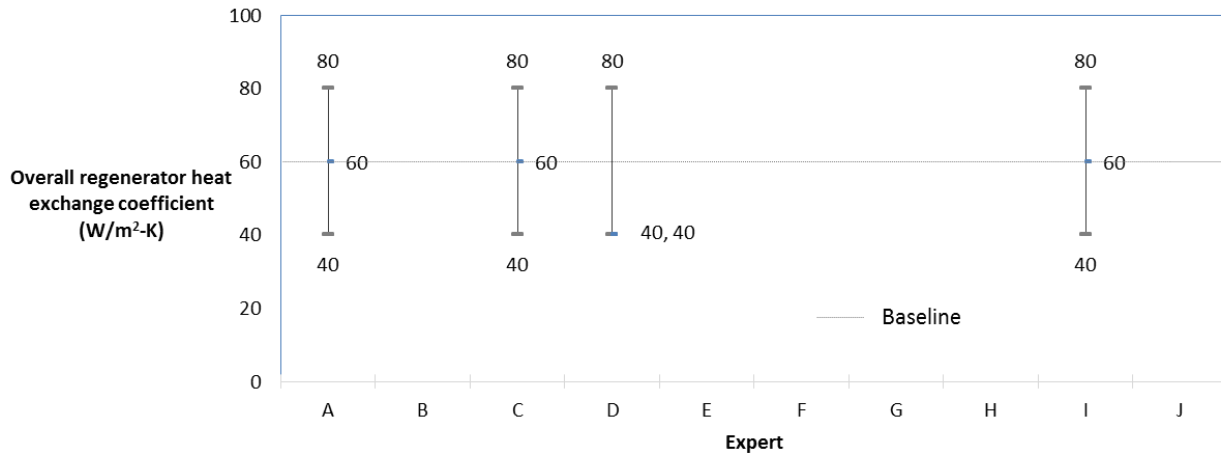


Figure 10.14: Expert responses for the Present Case regenerator overall heat transfer coefficient.

Responses for the Future Case Scenario are shown in Figure 10.15. The average “best guess” response was 73 W/m²-K. The average low value reported by experts was 37 W/m²-K and the average high value was 202 W/m²-K. These values were used as the nominal and bounding conditions for the Future Case.

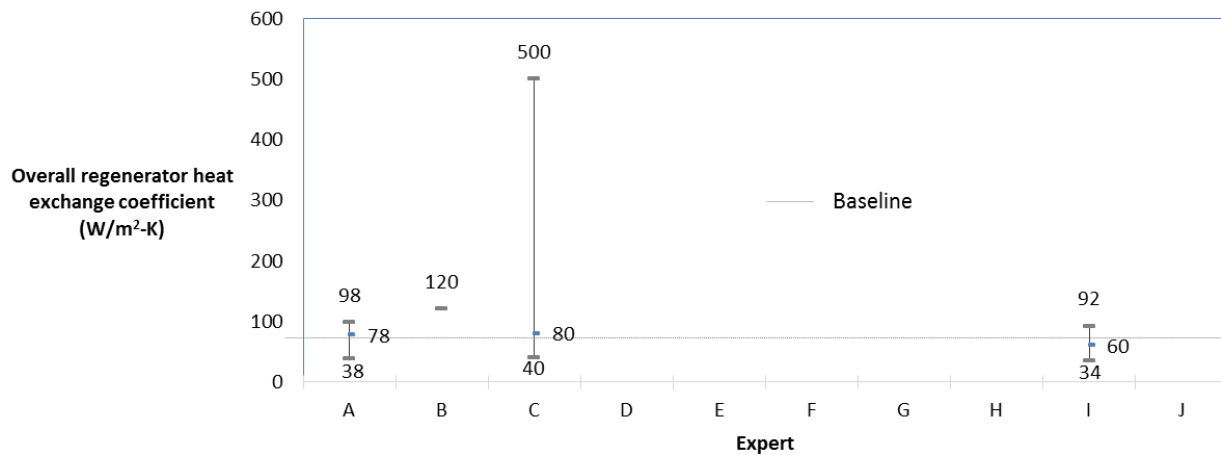


Figure 10.15: Expert responses for the Future Case regenerator overall heat transfer coefficient.

Cross-flow HX solid temp. at hot-side outlet

The solid temperature at the hot-side heat exchanger outlet is required in order to determine the size and cooling duty of the hot-side heat exchanger. The nominal value is 360 K (87°C), which is the average of the nominal solid temperatures at the outlets of the adsorber and regenerator. Excluding the sensitivity analysis for the cross-flow heat exchanger described in Section 7.4, the temperature of the solids exiting the hot-side heat exchanger is always calculated in this manner. This method deviates from the single deterministic value of 391 K (118°C) provided by CCSI because of conflicting assumptions regarding the feasibility of high solid sorbent temperatures (>120°C) in the regenerator. In this model, the maximum solid temperature in the regenerator is 393 K (120°C) because of evidence that higher temperatures cause a breakdown in the amine functional groups. In contrast, CCSI's uses a solid temperature of 408 K (135°C). Because this model used a lower regeneration temperature, the solid temperature in the hot-side heat exchanger is lower than the reported CCSI value (391 K or 118°C) in order to allow for the continued use of the cross-flow heat exchange system as a design option in keeping with CCSI's process design.

Flue gas blower efficiency

The flue gas blower efficiency is modeled based on the performance and cost values for previous studies using the IECM framework. Similarly, the nominal value and distribution for the blower efficiency are the same as the values used in these studies. Specifically, these values are the same as those used by Dr. Anand Rao in his liquid amine-based CCS system (Rao, 2003).

Solids purge fraction

The solid purge fraction is required in order to prevent the build-up of degradation products in the solid stream. In case studies in which degradation is occurring, the solid purge fraction is set to 0.004% in order to minimize the levelized cost of electricity. However, this value is specific to the Present Case

scenario and is only an approximation of the optimal value when applied to the wide range of degradation scenarios shown throughout this work. Section 6.3 discusses the sensitivity of the cost of electricity as a function of the purge fraction, and based on this work, it is the author's judgement that a range of 0.001-0.005 is reasonable in order to capture the optimal value for the range of cases in which degradation is occurring.

Water uptake (% removed from flue gas)

For the Present and Future Case scenarios, water uptake by the solid sorbent is estimated based on the modeling efforts of CCSI. The process model published by CCSI estimates that approximately 70% of water vapor entering the system is removed by the adsorption process. However, this removal efficiency is provided in a context of an ideal flue gas consisting of 6% water vapor at the adsorber inlet. To the author's knowledge, these results have yet to be validated in the context of an actual operating system and there is no published data regarding the true uptake for any solid sorbent under actual operating conditions. As such, the true water removal efficiency is largely unknown. For the Present and Future Case studies, water uptake is therefore nominally set to 70% in keeping with CCSI's published values and a range of 30% to 90% is applied based on the author's judgement in order to capture a wide range of potential solid sorbents (such as hydrophobic substrates), flue gas pre-treatment options, and operating conditions.

Water regeneration efficiency

This parameter is required in order to calculate the heating requirement in the regenerator and the mass flow rate of purge steam. Although the regenerator always operates above 373 K (100°C), the actual operating conditions may be such that water remains entrained with the solid sorbent due to the partial pressure of water in the regenerator due to the high partial pressure of water. In a patent filed in 2000, for example, Hoffman and Pennline estimate that 50% of the entrained water entering from the adsorber remains associated with the solid upon exiting the regenerator (Pennline & Hoffman, 2000).

Likewise, CCSI estimates that the solid sorbent exiting the regenerator retains nearly 20% of the entrained water while 80% of the entrained water exits the regenerator as part of the product gas stream.

The nominal water regeneration efficiency is set to 80% in keeping with the published CCSI results. The range applied to the water regeneration efficiency is 30-100% in order to account for a wide range of solid sorbents, water loadings, and regenerator operating conditions.

Water influence on CO₂ Capacity

The influence of water on CO₂ capacity is required in order to calculate the adjusted equilibrium CO₂ loading. This parameter was estimated using the expert elicitation exercise. The average “best guess” provided by the experts for the Present Case scenario is no change in CO₂ loading as a result of water uptake. The average low value is -0.4 mole CO₂ per kg solid sorbent and the average high value is 0.4 mole CO₂ per kg of solid sorbent. These values are used as the nominal, minimum, and maximum values for the Present Case scenario respectively. The responses for each expert are shown in Figure 10.15.

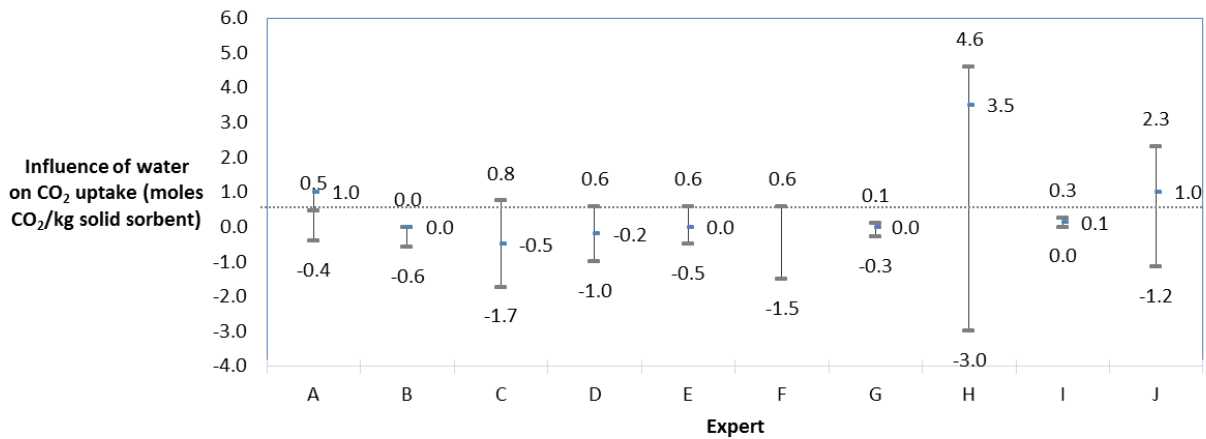


Figure 10.16: Expert responses for the Present Case influence of water on CO₂ loading.

A similar exercise was performed for the Future Case scenario and responses from the experts are shown in Figure 10.16. The average best guess for this scenario is 0.6 moles of CO₂ per kilogram of

solid sorbent. The average high value is 1.0 mole of CO₂ per kg solid sorbent and the average low value is -1.0 mole of CO₂ per kilogram of solid sorbent.

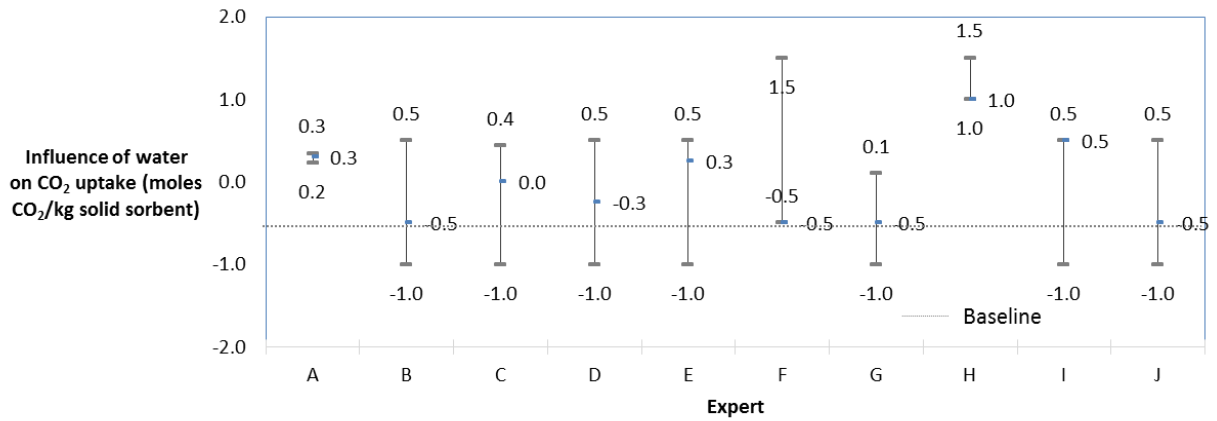


Figure 10.17: Expert responses for the Future Case influence of water on CO₂ loading.

CO₂ product pressure

The final CO₂ product pressure is required in order to calculate the energy requirement of the CO₂ compressor. This is the pressure of the gas in the pipeline once the gas has been separated from the flue gas, purified and compressed for geologic storage. The nominal value and potential range for this parameter is derived from previous techno-economic evaluations performed using the IECM framework. Specifically, these values are derived from the work of Anand Rao and his estimation of the performance and cost of liquid amine-based CO₂ capture and storage (Rao, 2003).

CO₂ compressor efficiency

The performance and costs of the CO₂ compressor are derived from previous techno-economic studies that have used the IECM framework. In this case, the nominal value for the compressor efficiency is 80% and the range of possible values is 75%-88% based on Anand Rao's work on liquid amine technology (Rao, 2003).

Solid sorbent cost

The cost of solid sorbent was derived using the expert elicitation exercise. For the Present Case scenario, the average “best guess” response was \$4.30 per kilogram. The average low value reported by experts was \$3.10 per kilogram and the average high response was \$5.8 per kilogram. These values are used for the nominal, minimum, and maximum cost of fresh solid sorbent material respectively.

Responses from the experts are shown in Figure 10.17.

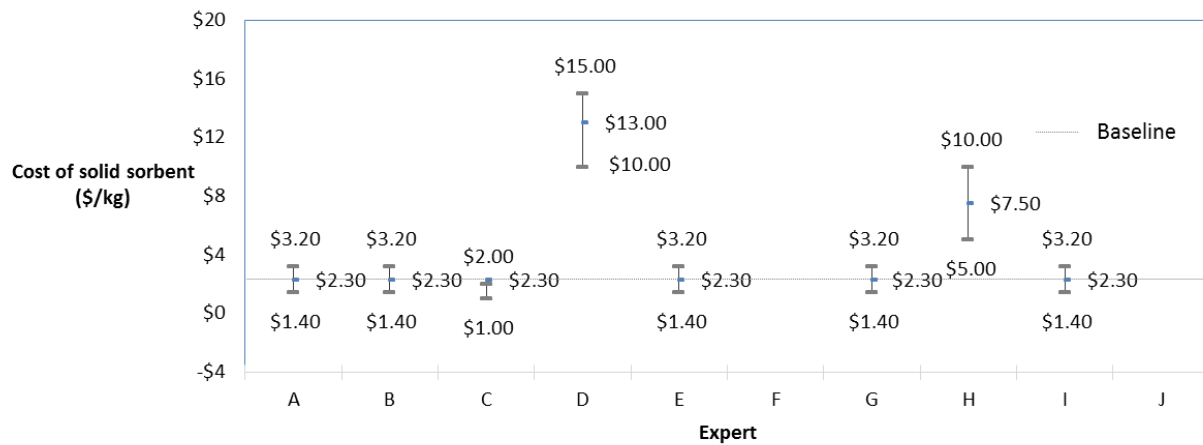


Figure 10.18: Present Case expert elicitation responses regarding the cost of solid sorbent.

For the Future Case scenario, the average “best guess” response for solid sorbent cost was \$2.7 per kilogram. The average low value estimate was \$1.5 per kilogram and the average high value was \$6.4 per kilogram. Likewise, these value are used as the basis for the nominal, low, and high estimates for the cost of solid sorbent. Responses from the individual experts are shown in Figure 10.18.

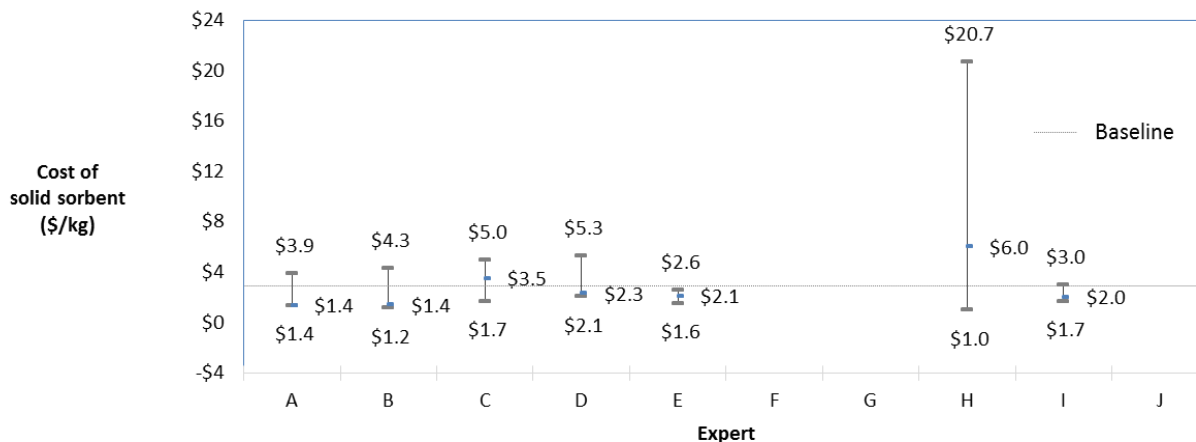


Figure 10.19: Future Case expert elicitation responses for the cost of solid sorbent.

CO₂ transport cost

There is a wide range of reported values for the cost of transporting the concentrated stream of CO₂ product. Most of the variability may be explained in terms of assumptions about the location of the pipeline and design parameters (safety factors, spare capacity, etc.). Dr. Rao performed a similar techno-economic study for a liquid amine system (Rao, 2003). After reviewing this data, Dr. Rao determined that an appropriate representation of this data requires a nominal value for the cost of CO₂ transport is \$0.02 per km per tonne CO₂ with a triangular distribution of (0.004,0.02,0.08).

Appendix J: Case study generation and cost data

Case study #1: Ideal solid sorbent system without degradation

For the PC power plant with an ideal solid sorbent-based CO₂ capture system, a number of default parameters values must be specified to generate Case Study No. 1. These parameters and their values are shown in Table 10.8. With respect to the maximum uptake of CO₂, note that the laboratory studies performed by ADA-ES include moisture in the simulated flue gas stream. However, laboratory conditions are often poor representations of full-scale. Hence, the maximum CO₂ capacity values used in

this case represent a system in which the behavior of the solid mimics the performance seen in the laboratory setting.

Table 10.16: Nominal performance and cost values for Case study #1.

Input variable	Value	Units
Configuration		
Adsorber CO ₂ removal efficiency	90	%
CO ₂ product compressor used?	Yes	
Direct contact cooler used?	No	
Flue gas pre-treatment		
Pressure drop across the pre-treat unit	0	Pa
Solid sorbent material	Amine-based resin	
SO ₂ polisher outlet concentration	237	ppmv
SO ₂ polisher used?	No	
Temperature exiting DCC	327	K
Water vapor mole fraction at adsorber inlet	15.5	%
Sorbent properties		
Heat capacity	1	kJ/kg dry solid-K
Heat of reaction	-60	kJ/mol CO ₂
Langmuir isotherm parameter (b ₀)	4.92*10 ⁻¹⁴	Pa ⁻¹
Maximum CO ₂ loading	2.9	moles CO ₂ /kg dry solid
CO₂ capture system		
<u>Adsorber</u>		
Adsorber operating temperature	313	K
Adsorber pressure drop	29	kPa
CO ₂ equilibrium pressure*	15.7	kPa
Effective adsorption kinetics (% equilib. capacity)	100	%
Overall heat transfer coefficient	300	W/m ² -K
<u>Regenerator</u>		
CO ₂ pressure in product gas stream	81	kPa
Effective desorption kinetics	0	%
Overall heat transfer coefficient	60	W/m ² -K
Regenerator operating temperature	393	K
Steam inlet temperature	408	K
Steam temperature approach	20	K

Cross-flow heat exchanger

Overall heat transfer coefficient	60	W/m ² -K
Temperature of solids at hot-side HX outlet	353	K

Auxiliary

Flue gas blower efficiency	75	%
----------------------------	----	---

System-wide constants and variables

Ambient air pressure	101,325	Pa
Ambient air temperature	298	K
Coal heat value	30840	kJ/kg
Cooling water temp. in	283	K
Cooling water temp. out	308	K
Cost of caustic	507.5	\$/tonne
Cost of water	0.3033	\$/tonne
FG Heat capacity	0.036	kJ/kmol
FG pressure entering CCS system	101,325	Pa
FG temp. entering CCS system	326.5	°C
Latent heat of vaporization of water	2260	kJ/kg
Plant capacity factor	0.75	fraction
Steam temperature	773	K
Universal gas constant	8,314	m ³ -Pa/kmol-K
Water heat capacity	4.18	kJ/kg-K

* Calculated value equal to $P_{A,in} * M_{CO_2}^{A,in} / \sum M_i^{A,in}$ where i=all flue gas constituents at the adsorber inlet

Case study #2: Ideal with SO₂ degradation

Table 10.17: Nominal performance and cost values for Case study #2.

Input variable	Value	Units
Configuration		
Adsorber CO ₂ removal efficiency	90	%
CO ₂ product compressor used?	Yes	
Solid sorbent material	Amine-based resin	
Flue gas pre-treatment		
Direct contact cooler used?	Yes	
Pressure drop across the pre-treat unit	6,894	Pa
SO ₂ polisher used?	Yes	
SO ₂ polisher outlet concentration	1	ppmv
Temperature exiting DCC	316.5	K
Water vapor mole fraction at adsorber inlet	10	%
Sorbent properties		
Heat capacity	1	kJ/kg dry solid-K
Heat of reaction	-60	kJ/mol CO ₂
Langmuir isotherm parameter (b ₀)	4.92*10 ⁻¹⁴	Pa ⁻¹
Maximum CO ₂ loading	2.9	moles CO ₂ /kg dry solid
CO₂ capture system		
<u>Adsorber</u>		
Adsorber operating temperature	313	K
Adsorber pressure drop	29	kPa
CO ₂ equilibrium pressure*	15.7	kPa
Effective adsorption kinetics (% equilib. capacity)	100	%
Overall heat transfer coefficient	300	W/m ² -K
<u>Regenerator</u>		
CO ₂ pressure in product gas stream	81	kPa
Effective desorption kinetics	0	%
Overall heat transfer coefficient	60	W/m ² -K
Regenerator operating temperature	393	K
Steam inlet temperature	408	K
Steam temperature approach	20	K

Cross-flow heat exchanger		
Overall heat transfer coefficient	60	W/m ² -K
Temperature of solids at hot-side HX outlet	353	K
	<u>Auxiliary</u>	
Flue gas blower efficiency	75	%
	Degradation	
Solid purge fraction	0.004	%
	<u>SO₂</u>	Yes
SO ₂ Capture Efficiency (moles in - moles out)/moles in	100	%
SO ₂ gas release in regenerator (moles in -moles out as gas)/moles in	0	%
	<u>O₂</u>	No
O ₂ Capture Efficiency (moles in - moles out)/moles in	0	%
O ₂ gas release in regenerator (moles in -moles out as gas)/moles in	100	%
	<u>N₂</u>	No
CO ₂ :N ₂ Selectivity Ratio (moles adsorbed CO ₂ /moles adsorbed N ₂)	10,000,000,000	Ratio
	<u>NO_x (NO + NO₂)</u>	No
NO _x Capture Efficiency (moles in - moles out)/moles in	0	%
NO _x gas release in regenerator (moles in -moles out as gas)/moles in	100	%
	<u>Water adsorption</u>	No
Water uptake (% removed from flue gas)	0	%
Water regeneration efficiency	100	%
Competitively Adsorbed Water (Influence on CO ₂ Capacity)	0	moles CO ₂ /kg solid sorbent
System-wide constants and variables		
Ambient air pressure	101,325	Pa
Ambient air temperature	298	K
Coal heat value	30840	kJ/kg
Cooling water temp. in	283	K
Cooling water temp. out	308	K
Cost of caustic	507.5	\$/tonne
Cost of water	0.3033	\$/tonne
FG Heat capacity	0.036	kJ/kmol
FG pressure entering CCS system	101,325	Pa

FG temp. entering CCS system	326.5	°C
Latent heat of vaporization of water	2260	kJ/kg
Plant capacity factor	75	%
Steam temperature	773	K
Universal gas constant	8,314	m ³ -Pa/kmol-K
Water heat capacity	4.18	kJ/kg-K

* Calculated value equal to $P_{A,in} * M_{CO_2}^{A,in} / \sum M_i^{A,in}$ where i=all flue gas constituents at the adsorber inlet

Case study #3: Ideal with water degradation

Table 10.18: Nominal performance and cost values for Case study #3.

Input variable	Value	Units
Configuration		
Adsorber CO ₂ removal efficiency	90	%
CO ₂ product compressor used?	Yes	
Solid sorbent material	Amine-based resin	
<u>Flue gas pre-treatment</u>		
Direct contact cooler used?	Yes	
Pressure drop across the pre-treat unit	6,894	Pa
SO ₂ polisher used?	No	
SO ₂ polisher outlet concentration	237	ppmv
Temperature exiting DCC	316.5	K
Water vapor mole fraction at adsorber inlet	10	%
Sorbent properties		
Heat capacity	1	kJ/kg dry solid-K
Heat of reaction	-60	kJ/mol CO ₂
Langmuir isotherm parameter (b ₀)	4.92*10 ⁻¹⁴	Pa ⁻¹
Maximum CO ₂ loading	2.9	moles CO ₂ /kg dry solid
CO₂ capture system		
<u>Adsorber</u>		
Adsorber operating temperature	313	K
Adsorber pressure drop	29	kPa
CO ₂ equilibrium pressure*	15.7	kPa
Effective adsorption kinetics (% equilib. capacity)	100	%

Overall heat transfer coefficient	300	W/m ² -K
<u>Regenerator</u>		
CO ₂ pressure in product gas stream	81	kPa
Effective desorption kinetics	0	%
Overall heat transfer coefficient	60	W/m ² -K
Regenerator operating temperature	393	K
Steam inlet temperature	408	K
Steam temperature approach	20	K
<u>Cross-flow heat exchanger</u>		
Overall heat transfer coefficient	60	W/m ² -K
Temperature of solids at hot-side HX outlet	353	K
<u>Auxiliary</u>		
Flue gas blower efficiency	75	%
Degradation		
Solid purge fraction	0.00001	%
<u>SO₂</u>		
SO ₂ Capture Efficiency (moles in - moles out)/moles in	0%	%
SO ₂ gas release in regenerator (moles in -moles out as gas)/moles in	100	%
<u>O₂</u>		
O ₂ Capture Efficiency (moles in - moles out)/moles in	0	%
O ₂ gas release in regenerator (moles in -moles out as gas)/moles in	100	%
<u>N₂</u>		
CO ₂ :N ₂ Selectivity Ratio (moles adsorbed CO ₂ /moles adsorbed N ₂)	10,000,000,000	Ratio
<u>NO_x (NO + NO₂)</u>		
NO _x Capture Efficiency (moles in - moles out)/moles in	0	%
NO _x gas release in regenerator (moles in -moles out as gas)/moles in	100	%
<u>Water adsorption</u>		
Water uptake (% removed from flue gas)	30	%
Water regeneration efficiency	30	%
Competitively Adsorbed Water (Influence on CO ₂ Capacity)	-0.5	moles CO ₂ /kg solid sorbent
System-wide constants and variables		
Ambient air pressure	101,325	Pa

Ambient air temperature	298	K
Coal heat value	30,840	kJ/kg
Cooling water temp. in	283	K
Cooling water temp. out	308	K
Cost of caustic	507.5	\$/tonne
Cost of water	0.3033	\$/tonne
FG Heat capacity	0.036	kJ/kmol
FG pressure entering CCS system	101,325	Pa
FG temp. entering CCS system	326.5	°C
Latent heat of vaporization of water	2260	kJ/kg
Plant capacity factor	75	%
Steam temperature	773	K
Universal gas constant	8,314	m ³ -Pa/kmol-K
Water heat capacity	4.18	kJ/kg-K

* Calculated value equal to $P_{A,in} * M_{CO_2}^{A,in} / \sum M_i^{A,in}$ where i=all flue gas constituents at the adsorber inlet

Case study #4: Ideal with SO₂ and water degradation

Table 10.19: Nominal performance and cost values for Case study #4.

Input variable	Value	Units
Configuration		
Adsorber CO ₂ removal efficiency	90	%
CO ₂ product compressor used?	Yes	
Solid sorbent material	Amine-based resin	
<u>Flue gas pre-treatment</u>		
Direct contact cooler used?	Yes	
Pressure drop across the pre-treat unit	6,894	Pa
SO ₂ polisher used?	Yes	
SO ₂ polisher outlet concentration	1	ppmv
Temperature exiting DCC	316.5	K
Water vapor mole fraction at adsorber inlet	10	%
Sorbent properties		
Heat capacity	1	kJ/kg dry solid-K

Heat of reaction	-60	kJ/mol CO ₂
Langmuir isotherm parameter (b ₀)	4.92*10 ⁻¹⁴	Pa ⁻¹
Maximum CO ₂ loading	2.9	moles CO ₂ /kg dry solid

CO₂ capture system

Adsorber

Adsorber operating temperature	313	K
Adsorber pressure drop	29	kPa
CO ₂ equilibrium pressure*	15.7	kPa
Effective adsorption kinetics (% equilib. capacity)	100	%
Overall heat transfer coefficient	300	W/m ² -K

Regenerator

CO ₂ pressure in product gas stream	81	kPa
Effective desorption kinetics	0	%
Overall heat transfer coefficient	60	W/m ² -K
Regenerator operating temperature	393	K
Steam inlet temperature	408	K
Steam temperature approach	20	K

Cross-flow heat exchanger

Overall heat transfer coefficient	60	W/m ² -K
Temperature of solids at hot-side HX outlet	353	K

Auxiliary

Flue gas blower efficiency	75	%
----------------------------	----	---

Degradation

Solid purge fraction	0.004	%
----------------------	-------	---

SO₂

SO ₂ Capture Efficiency (moles in - moles out)/moles in	100	%
SO ₂ gas release in regenerator (moles in -moles out as gas)/moles in	0	%

O₂

O ₂ Capture Efficiency (moles in - moles out)/moles in	0	%
O ₂ gas release in regenerator (moles in -moles out as gas)/moles in	100	%

N₂

CO ₂ :N ₂ Selectivity Ratio (moles adsorbed CO ₂ /moles adsorbed N ₂)	10,000,000,000	Ratio
--	----------------	-------

NO_x (NO + NO₂)

No

NO _x Capture Efficiency (moles in - moles out)/moles in	0	%
NO _x gas release in regenerator (moles in -moles out as gas)/moles in	100	%
	<u>Water adsorption</u>	Yes
Water uptake (% removed from flue gas)	30	%
Water regeneration efficiency	30	%
Competitively Adsorbed Water (Influence on CO ₂ Capacity)	-0.5	moles CO ₂ /kg solid sorbent

System-wide constants and variables

Ambient air pressure	101,325	Pa
Ambient air temperature	298	K
Coal heat value	30,840	kJ/kg
Cooling water temp. in	283	K
Cooling water temp. out	308	K
Cost of caustic	507.5	\$/tonne
Cost of water	0.3033	\$/tonne
FG Heat capacity	0.036	kJ/kmol
FG pressure entering CCS system	101,325	Pa
FG temp. entering CCS system	326.5	°C
Latent heat of vaporization of water	2260	kJ/kg
Plant capacity factor	75	%
Steam temperature	773	K
Universal gas constant	8,314	m ³ -Pa/kmol-K
Water heat capacity	4.18	kJ/kg-K

* Calculated value equal to $P_{A,in} * M_{CO_2}^{A,in} / \sum M_i^{A,in}$ where i=all flue gas constituents at the adsorber inlet

Case study #5: CCSI model without SO₂ degradation

Table 10.20: Nominal performance and cost values for Case study #5.

Input variable	Value	Units
Configuration		
Adsorber CO ₂ removal efficiency	90	%
CO ₂ product compressor used?	Yes	
Solid sorbent material	32D supported amine	

Flue gas pre-treatment

Direct contact cooler used?	Yes	
Pressure drop across the pre-treat unit	6,894	Pa
SO ₂ polisher used?	Yes	
SO ₂ polisher outlet concentration	1	ppmv
Temperature exiting DCC	316.5	K
Water vapor mole fraction at adsorber inlet	10	%

Sorbent properties

Heat capacity	1	kJ/kg dry solid-K
Heat of reaction	-67	kJ/mol CO ₂
Langmuir isotherm parameter (b ₀)	4.92*10 ⁻¹⁴	Pa ⁻¹
Maximum CO ₂ loading	3.5	moles CO ₂ /kg dry solid

CO₂ capture system

Adsorber

Adsorber operating temperature	327	K
Adsorber pressure drop	29	kPa
CO ₂ equilibrium pressure*	15.7	kPa
Effective adsorption kinetics (% equilib. capacity)	65	%
Overall heat transfer coefficient	300	W/m ² -K

Regenerator

CO ₂ pressure in product gas stream	42	kPa
Effective desorption kinetics	11	%
Overall heat transfer coefficient	60	W/m ² -K
Regenerator operating temperature	408	K
Steam inlet temperature	438	K
Steam temperature approach	85	K

Cross-flow heat exchanger

Overall heat transfer coefficient	300	W/m ² -K
Temperature of solids at hot-side HX outlet	391	K

Auxiliary

Flue gas blower efficiency	75	%
----------------------------	----	---

Degradation

Solid purge fraction	0.00001	%
----------------------	---------	---

SO₂

No

SO ₂ Capture Efficiency (moles in - moles out)/moles in	0	%
SO ₂ gas release in regenerator (moles in -moles out as gas)/moles in	0	%
	<u>O₂</u>	No
O ₂ Capture Efficiency (moles in - moles out)/moles in	0	%
O ₂ gas release in regenerator (moles in -moles out as gas)/moles in	100	%
	<u>N₂</u>	No
CO ₂ :N ₂ Selectivity Ratio (moles adsorbed CO ₂ /moles adsorbed N ₂)	10,000,000,000	Ratio
	<u>NO_x (NO + NO₂)</u>	No
NO _x Capture Efficiency (moles in - moles out)/moles in	0	%
NO _x gas release in regenerator (moles in -moles out as gas)/moles in	100	%
	<u>Water adsorption</u>	Yes
Water uptake (% removed from flue gas)	92	%
Water regeneration efficiency	79	%
Competitively Adsorbed Water (Influence on CO ₂ Capacity)	0	moles CO ₂ /kg solid sorbent

System-wide constants and variables

Ambient air pressure	101,325	Pa
Ambient air temperature	298	K
Coal heat value	30,840	kJ/kg
Cooling water temp. in	305	K
Cooling water temp. out	320	K
Cost of caustic	507.5	\$/tonne
Cost of water	0.3033	\$/tonne
FG Heat capacity	0.036	kJ/kmol
FG pressure entering CCS system	101,325	Pa
FG temp. entering CCS system	326.5	°C
Latent heat of vaporization of water	2260	kJ/kg
Plant capacity factor	75	%
Steam temperature	773	K
Universal gas constant	8,314	m ³ -Pa/kmol-K
Water heat capacity	4.18	kJ/kg-K

* Calculated value equal to $P_{A,in} * M_{CO_2}^{A,in} / \sum M_i^{A,in}$ where i=all flue gas constituents at the adsorber inlet

Case study #6: CCSI model with SO₂ degradation

Table 10.21: Nominal performance and cost values for Case study #6.

Input variable	Value	Units
Configuration		
Adsorber CO ₂ removal efficiency	90	%
CO ₂ product compressor used?	Yes	
Solid sorbent material	32D supported amine	
<u>Flue gas pre-treatment</u>		
Direct contact cooler used?	Yes	
Pressure drop across the pre-treat unit	6,894	Pa
SO ₂ polisher used?	Yes	
SO ₂ polisher outlet concentration	1	ppmv
Temperature exiting DCC	316.5	K
Water vapor mole fraction at adsorber inlet	10	%
Sorbent properties		
Heat capacity	1	kJ/kg dry solid-K
Heat of reaction	-67	kJ/mol CO ₂
Langmuir isotherm parameter (b ₀)	4.92*10 ⁻¹⁴	Pa ⁻¹
Maximum CO ₂ loading	3.5	moles CO ₂ /kg dry solid
CO₂ capture system		
<u>Adsorber</u>		
Adsorber operating temperature	327	K
Adsorber pressure drop	29	kPa
CO ₂ equilibrium pressure*	15.7	kPa
Effective adsorption kinetics (% equilib. capacity)	65	%
Overall heat transfer coefficient	300	W/m ² -K
<u>Regenerator</u>		
CO ₂ pressure in product gas stream	42	kPa
Effective desorption kinetics	11	%
Overall heat transfer coefficient	60	W/m ² -K

Regenerator operating temperature	408	K
Steam inlet temperature	438	K
Steam temperature approach	85	K
<u>Cross-flow heat exchanger</u>		
Overall heat transfer coefficient	300	W/m ² -K
Temperature of solids at hot-side HX outlet	391	K
<u>Auxiliary</u>		
Flue gas blower efficiency	75	%
Degradation		
Solid purge fraction	0.00001	%
<u>SO₂</u>		
	Yes	
SO ₂ Capture Efficiency (moles in - moles out)/moles in	100	%
SO ₂ gas release in regenerator (moles in -moles out as gas)/moles in	0	%
<u>O₂</u>		
	No	
O ₂ Capture Efficiency (moles in - moles out)/moles in	0	%
O ₂ gas release in regenerator (moles in -moles out as gas)/moles in	100	%
<u>N₂</u>		
	No	
CO ₂ :N ₂ Selectivity Ratio (moles adsorbed CO ₂ /moles adsorbed N ₂)	10,000,000,000	Ratio
<u>NO_x (NO + NO₂)</u>		
	No	
NO _x Capture Efficiency (moles in - moles out)/moles in	0	%
NO _x gas release in regenerator (moles in -moles out as gas)/moles in	100	%
<u>Water adsorption</u>		
	Yes	
Water uptake (% removed from flue gas)	92	%
Water regeneration efficiency	79	%
Competitively Adsorbed Water (Influence on CO ₂ Capacity)	0	moles CO ₂ /kg solid sorbent
System-wide constants and variables		
Ambient air pressure	101,325	Pa
Ambient air temperature	298	K
Coal heat value	30,840	kJ/kg
Cooling water temp. in	305	K
Cooling water temp. out	320	K
Cost of caustic	507.5	\$/tonne

Cost of water	0.3033	\$/tonne
FG Heat capacity	0.036	kJ/kmol
FG pressure entering CCS system	101,325	Pa
FG temp. entering CCS system	326.5	°C
Latent heat of vaporization of water	2260	kJ/kg
Plant capacity factor	75	%
Steam temperature	773	K
Universal gas constant	8,314	m ³ -Pa/kmol-K
Water heat capacity	4.18	kJ/kg-K

* Calculated value equal to $P_{A,in} * M_{CO_2}^{A,in} / \sum M_i^{A,in}$ where i=all flue gas constituents at the adsorber inlet

Case study #7: Present case without degradation

Table 10.22: Nominal performance and cost values for Case study #7.

Input variable	Value	Units
Configuration		
Adsorber CO ₂ removal efficiency	90	%
CO ₂ product compressor used?	Yes	
Solid sorbent material	Amine-based resin	
<u>Flue gas pre-treatment</u>		
Direct contact cooler used?	No	
Pressure drop across the pre-treat unit	0	Pa
SO ₂ polisher used?	No	
SO ₂ polisher outlet concentration	237	ppmv
Temperature exiting DCC	327	K
Water vapor mole fraction at adsorber inlet	15.5	%
Sorbent properties		
Heat capacity	1	kJ/kg dry solid-K
Heat of reaction	-60	kJ/mol CO ₂
Langmuir isotherm parameter (b ₀)	4.92*10 ⁻¹⁴	Pa ⁻¹
Maximum CO ₂ loading	2.9	moles CO ₂ /kg dry solid
CO₂ capture system		
<u>Adsorber</u>		

Adsorber operating temperature	327	K
Adsorber pressure drop	29	kPa
CO ₂ equilibrium pressure*	15.7	kPa
Effective adsorption kinetics (% equilib. capacity)	83	%
Overall heat transfer coefficient	300	W/m ² -K
<u>Regenerator</u>		
CO ₂ pressure in product gas stream	42	kPa
Effective desorption kinetics	11	%
Overall heat transfer coefficient	55	W/m ² -K
Regenerator operating temperature	383	K
Steam inlet temperature	408	K
Steam temperature approach	20	K
<u>Cross-flow heat exchanger</u>		
Overall heat transfer coefficient	55	W/m ² -K
Temperature of solids at hot-side HX outlet	355	K
<u>Auxiliary</u>		
Flue gas blower efficiency	75	%
Degradation		
Solid purge fraction	0.00001	%
<u>SO₂</u>		
SO ₂ Capture Efficiency (moles in - moles out)/moles in	0	%
SO ₂ gas release in regenerator (moles in -moles out as gas)/moles in	100	%
<u>O₂</u>		
O ₂ Capture Efficiency (moles in - moles out)/moles in	0	%
O ₂ gas release in regenerator (moles in -moles out as gas)/moles in	100	%
<u>N₂</u>		
CO ₂ :N ₂ Selectivity Ratio (moles adsorbed CO ₂ /moles adsorbed N ₂)	10,000,000,000	Ratio
<u>NO_x (NO + NO₂)</u>		
NO _x Capture Efficiency (moles in - moles out)/moles in	0	%
NO _x gas release in regenerator (moles in -moles out as gas)/moles in	100	%
<u>Water adsorption</u>		
Water uptake (% removed from flue gas)	0	%

Water regeneration efficiency	100	%
Competitively Adsorbed Water (Influence on CO ₂ Capacity)	0	moles CO ₂ /kg solid sorbent

System-wide constants and variables

Ambient air pressure	101,325	Pa
Ambient air temperature	298	K
Coal heat value	30,840	kJ/kg
Cooling water temp. in	283	K
Cooling water temp. out	308	K
Cost of caustic	507.5	\$/tonne
Cost of water	0.3033	\$/tonne
FG Heat capacity	0.036	kJ/kmol
FG pressure entering CCS system	101,325	Pa
FG temp. entering CCS system	326.5	°C
Latent heat of vaporization of water	2260	kJ/kg
Plant capacity factor	75	%
Steam temperature	773	K
Universal gas constant	8,314	m ³ -Pa/kmol-K
Water heat capacity	4.18	kJ/kg-K

* Calculated value equal to $P_{A,in} * M_{CO_2}^{A,in} / \sum M_i^{A,in}$ where i=all flue gas constituents at the adsorber inlet

Case study #8: Present case with SO₂ degradation

Table 10.23: Nominal performance and cost values for Case study #8.

Input variable	Value	Units
Configuration		
Adsorber CO ₂ removal efficiency	90	%
CO ₂ product compressor used?	Yes	
Solid sorbent material	Amine-based resin	
Flue gas pre-treatment		
Direct contact cooler used?	Yes	
Pressure drop across the pre-treat unit	6,894	Pa
SO ₂ polisher used?	Yes	
SO ₂ polisher outlet concentration	1	ppmv

Temperature exiting DCC	316.5	K
Water vapor mole fraction at adsorber inlet	10	%
Sorbent properties		
Heat capacity	1	kJ/kg dry solid-K
Heat of reaction	-60	kJ/mol CO ₂
Langmuir isotherm parameter (b ₀)	4.92*10 ⁻¹⁴	Pa ⁻¹
Maximum CO ₂ loading	2.9	moles CO ₂ /kg dry solid
CO₂ capture system		
Adsorber		
Adsorber operating temperature	327	K
Adsorber pressure drop	29	kPa
CO ₂ equilibrium pressure*	15.7	kPa
Effective adsorption kinetics (% equilib. capacity)	83	%
Overall heat transfer coefficient	300	W/m ² -K
Regenerator		
CO ₂ pressure in product gas stream	42	kPa
Effective desorption kinetics	11	%
Overall heat transfer coefficient	55	W/m ² -K
Regenerator operating temperature	383	K
Steam inlet temperature	408	K
Steam temperature approach	20	K
Cross-flow heat exchanger		
Overall heat transfer coefficient	55	W/m ² -K
Temperature of solids at hot-side HX outlet	355	K
Auxiliary		
Flue gas blower efficiency	75	%
Degradation		
Solid purge fraction	0.004	%
<u>SO₂</u>	Yes	
SO ₂ Capture Efficiency (moles in - moles out)/moles in	100	%
SO ₂ gas release in regenerator (moles in -moles out as gas)/moles in	0	%
<u>O₂</u>	No	
O ₂ Capture Efficiency (moles in - moles out)/moles in	0	%

O ₂ gas release in regenerator (moles in -moles out as gas)/moles in	100	%
<u>N₂</u>	No	
CO ₂ :N ₂ Selectivity Ratio (moles adsorbed CO ₂ /moles adsorbed N ₂)	10,000,000,000	Ratio
<u>NO_x (NO + NO₂)</u>	No	
NO _x Capture Efficiency (moles in - moles out)/moles in	0	%
NO _x gas release in regenerator (moles in -moles out as gas)/moles in	100	%
<u>Water adsorption</u>	No	
Water uptake (% removed from flue gas)	0	%
Water regeneration efficiency	100	%
Competitively Adsorbed Water (Influence on CO ₂ Capacity)	0	moles CO ₂ /kg solid sorbent

System-wide constants and variables

Ambient air pressure	101,325	Pa
Ambient air temperature	298	K
Coal heat value	30,840	kJ/kg
Cooling water temp. in	283	K
Cooling water temp. out	308	K
Cost of caustic	507.5	\$/tonne
Cost of water	0.3033	\$/tonne
FG Heat capacity	0.036	kJ/kmol
FG pressure entering CCS system	101,325	Pa
FG temp. entering CCS system	326.5	°C
Latent heat of vaporization of water	2260	kJ/kg
Plant capacity factor	75	%
Steam temperature	773	K
Universal gas constant	8,314	m ³ -Pa/kmol-K
Water heat capacity	4.18	kJ/kg-K

* Calculated value equal to $P_{A,in} * M_{CO_2}^{A,in} / \sum M_i^{A,in}$ where i=all flue gas constituents at the adsorber inlet

Case study #9: Present case with water degradation

Table 10.24: Nominal performance and cost values for Case study #9.

Input variable	Value	Units
----------------	-------	-------

Configuration		
Adsorber CO ₂ removal efficiency	90	%
CO ₂ product compressor used?	Yes	
Solid sorbent material	Amine-based resin	
<u>Flue gas pre-treatment</u>		
Direct contact cooler used?	Yes	
Pressure drop across the pre-treat unit	6,894	Pa
SO ₂ polisher used?	No	
SO ₂ polisher outlet concentration	237	ppmv
Temperature exiting DCC	316.5	K
Water vapor mole fraction at adsorber inlet	10	%
Sorbent properties		
Heat capacity	1	kJ/kg dry solid-K
Heat of reaction	-60	kJ/mol CO ₂
Langmuir isotherm parameter (b ₀)	4.92*10 ⁻¹⁴	Pa ⁻¹
Maximum CO ₂ loading	2.9	moles CO ₂ /kg dry solid
CO₂ capture system		
<u>Adsorber</u>		
Adsorber operating temperature	327	K
Adsorber pressure drop	29	kPa
CO ₂ equilibrium pressure*	15.7	kPa
Effective adsorption kinetics (% equilib. capacity)	83	%
Overall heat transfer coefficient	300	W/m ² -K
<u>Regenerator</u>		
CO ₂ pressure in product gas stream	42	kPa
Effective desorption kinetics	11	%
Overall heat transfer coefficient	55	W/m ² -K
Regenerator operating temperature	383	K
Steam inlet temperature	408	K
Steam temperature approach	20	K
<u>Cross-flow heat exchanger</u>		
Overall heat transfer coefficient	55	W/m ² -K
Temperature of solids at hot-side HX outlet	355	K
<u>Auxiliary</u>		

Flue gas blower efficiency	75	%
Degradation		
Solid purge fraction	0.004	%
<u>SO₂</u>		
SO ₂ Capture Efficiency (moles in - moles out)/moles in	No	
SO ₂ gas release in regenerator (moles in -moles out as gas)/moles in	0	%
	100	%
<u>O₂</u>		
O ₂ Capture Efficiency (moles in - moles out)/moles in	No	
O ₂ gas release in regenerator (moles in -moles out as gas)/moles in	0	%
	100	%
<u>N₂</u>		
CO ₂ :N ₂ Selectivity Ratio (moles adsorbed CO ₂ /moles adsorbed N ₂)	No	
	10,000,000,000	Ratio
<u>NO_x (NO + NO₂)</u>		
NO _x Capture Efficiency (moles in - moles out)/moles in	No	
NO _x gas release in regenerator (moles in -moles out as gas)/moles in	0	%
	100	%
<u>Water adsorption</u>		
Water uptake (% removed from flue gas)	Yes	
Water regeneration efficiency	92	%
Competitively Adsorbed Water (Influence on CO ₂ Capacity)	79	%
	-0.02	moles CO ₂ /kg solid sorbent
System-wide constants and variables		
Ambient air pressure	101,325	Pa
Ambient air temperature	298	K
Coal heat value	30,840	kJ/kg
Cooling water temp. in	283	K
Cooling water temp. out	308	K
Cost of caustic	507.5	\$/tonne
Cost of water	0.3033	\$/tonne
FG Heat capacity	0.036	kJ/kmol
FG pressure entering CCS system	101,325	Pa
FG temp. entering CCS system	326.5	°C
Latent heat of vaporization of water	2260	kJ/kg
Plant capacity factor	75	%
Steam temperature	773	K

Universal gas constant	8,314	m ³ -Pa/kmol-K
Water heat capacity	4.18	kJ/kg-K

* Calculated value equal to $P_{A,in} * M_{CO_2}^{A,in} / \sum M_i^{A,in}$ where i=all flue gas constituents at the adsorber inlet

Case study #10: Present case with SO₂ and water degradation

Table 10.25: Nominal performance and cost values for Case study #10.

Input variable	Value	Units
Configuration		
Adsorber CO ₂ removal efficiency	90	%
CO ₂ product compressor used?	Yes	
Solid sorbent material	Amine-based resin	
<u>Flue gas pre-treatment</u>		
Direct contact cooler used?	Yes	
Pressure drop across the pre-treat unit	6,894	Pa
SO ₂ polisher used?	Yes	
SO ₂ polisher outlet concentration	1	ppmv
Temperature exiting DCC	316.5	K
Water vapor mole fraction at adsorber inlet	10	%
Sorbent properties		
Heat capacity	1	kJ/kg dry solid-K
Heat of reaction	-60	kJ/mol CO ₂
Langmuir isotherm parameter (b ₀)	4.92*10 ⁻¹⁴	Pa ⁻¹
Maximum CO ₂ loading	2.9	moles CO ₂ /kg dry solid
CO₂ capture system		
<u>Adsorber</u>		
Adsorber operating temperature	327	K
Adsorber pressure drop	29	kPa
CO ₂ equilibrium pressure*	15.7	kPa
Effective adsorption kinetics (% equilib. capacity)	83	%
Overall heat transfer coefficient	300	W/m ² -K
<u>Regenerator</u>		
CO ₂ pressure in product gas stream	42	kPa

Effective desorption kinetics	11	%
Overall heat transfer coefficient	55	W/m ² -K
Regenerator operating temperature	383	K
Steam inlet temperature	408	K
Steam temperature approach	20	K
<u>Cross-flow heat exchanger</u>		
Overall heat transfer coefficient	55	W/m ² -K
Temperature of solids at hot-side HX outlet	355	K
<u>Auxiliary</u>		
Flue gas blower efficiency	75	%
Degradation		
Solid purge fraction	0.004	%
<u>SO₂</u>		
SO ₂ Capture Efficiency (moles in - moles out)/moles in	100	%
SO ₂ gas release in regenerator (moles in -moles out as gas)/moles in	0	%
<u>O₂</u>		
O ₂ Capture Efficiency (moles in - moles out)/moles in	0	%
O ₂ gas release in regenerator (moles in -moles out as gas)/moles in	100	%
<u>N₂</u>		
CO ₂ :N ₂ Selectivity Ratio (moles adsorbed CO ₂ /moles adsorbed N ₂)	10,000,000,000	Ratio
<u>NO_x (NO + NO₂)</u>		
NO _x Capture Efficiency (moles in - moles out)/moles in	0	%
NO _x gas release in regenerator (moles in -moles out as gas)/moles in	100	%
<u>Water adsorption</u>		
Water uptake (% removed from flue gas)	92	%
Water regeneration efficiency	79	%
Competitively Adsorbed Water (Influence on CO ₂ Capacity)	-0.02	moles CO ₂ /kg solid sorbent
System-wide constants and variables		
Ambient air pressure	101,325	Pa
Ambient air temperature	298	K
Coal heat value	30,840	kJ/kg
Cooling water temp. in	283	K

Cooling water temp. out	308	K
Cost of caustic	507.5	\$/tonne
Cost of water	0.3033	\$/tonne
FG Heat capacity	0.036	kJ/kmol
FG pressure entering CCS system	101,325	Pa
FG temp. entering CCS system	326.5	°C
Latent heat of vaporization of water	2260	kJ/kg
Plant capacity factor	75	%
Steam temperature	773	K
Universal gas constant	8,314	m ³ -Pa/kmol-K
Water heat capacity	4.18	kJ/kg-K

* Calculated value equal to $P_{A,in} * M_{CO_2}^{A,in} / \sum M_i^{A,in}$ where i=all flue gas constituents at the adsorber inlet

Case study #11: Future case without degradation

Table 10.26: Nominal performance and cost values for Case study #11.

Input variable	Value	Units
Configuration		
Adsorber CO ₂ removal efficiency	90	%
CO ₂ product compressor used?	Yes	
Solid sorbent material	Amine-based resin	
<u>Flue gas pre-treatment</u>		
Direct contact cooler used?	No	
Pressure drop across the pre-treat unit	0	Pa
SO ₂ polisher used?	No	
SO ₂ polisher outlet concentration	237	ppmv
Temperature exiting DCC	327	K
Water vapor mole fraction at adsorber inlet	15.5	%
Sorbent properties		
Heat capacity	1	kJ/kg dry solid-K
Heat of reaction	-60	kJ/mol CO ₂
Langmuir isotherm parameter (b)	4.92*10 ⁻¹⁴	Pa ⁻¹
Maximum CO ₂ loading	3.9	moles CO ₂ /kg dry solid

CO₂ capture system

Adsorber

Adsorber operating temperature	327	K
Adsorber pressure drop	29	kPa
CO ₂ equilibrium pressure*	15.7	kPa
Effective adsorption kinetics (% equilib. capacity)	90	%
Overall heat transfer coefficient	385	W/m ² -K

Regenerator

CO ₂ pressure in product gas stream	42	kPa
Effective desorption kinetics	10	%
Overall heat transfer coefficient	73	W/m ² -K
Regenerator operating temperature	383	K
Steam inlet temperature	408	K
Steam temperature approach	20	K

Cross-flow heat exchanger

Overall heat transfer coefficient	73	W/m ² -K
Temperature of solids at hot-side HX outlet	355	K

Auxiliary

Flue gas blower efficiency	75	%
----------------------------	----	---

Degradation

Solid purge fraction	0.00001	%
----------------------	---------	---

SO₂

	No	
SO ₂ Capture Efficiency (moles in - moles out)/moles in	0	%
SO ₂ gas release in regenerator (moles in -moles out as gas)/moles in	100	%

O₂

	No	
O ₂ Capture Efficiency (moles in - moles out)/moles in	0	%
O ₂ gas release in regenerator (moles in -moles out as gas)/moles in	100	%

N₂

	No	
CO ₂ :N ₂ Selectivity Ratio (moles adsorbed CO ₂ /moles adsorbed N ₂)	10,000,000,000	Ratio

NO_x (NO + NO₂)

	No	
NO _x Capture Efficiency (moles in - moles out)/moles in	0	%
NO _x gas release in regenerator (moles in -moles out as gas)/moles in	100	%

	<u>Water adsorption</u>	No	
Water uptake (% removed from flue gas)		0	%
Water regeneration efficiency		100	%
Competitively Adsorbed Water (Influence on CO ₂ Capacity)		0	moles CO ₂ /kg solid sorbent

System-wide constants and variables

Ambient air pressure	101,325	Pa
Ambient air temperature	298	K
Coal heat value	30,840	kJ/kg
Cooling water temp. in	283	K
Cooling water temp. out	308	K
Cost of caustic	507.5	\$/tonne
Cost of water	0.3033	\$/tonne
FG Heat capacity	0.036	kJ/kmol
FG pressure entering CCS system	101,325	Pa
FG temp. entering CCS system	326.5	°C
Latent heat of vaporization of water	2260	kJ/kg
Plant capacity factor	75	%
Steam temperature	773	K
Universal gas constant	8,314	m ³ -Pa/kmol-K
Water heat capacity	4.18	kJ/kg-K

* Calculated value equal to $P_{A,in} * M_{CO_2}^{A,in} / \sum M_i^{A,in}$ where i=all flue gas constituents at the adsorber inlet

Case study #12: Future case with SO₂ degradation

Table 10.27: Nominal performance and cost values for Case study #12.

Input variable	Value	Units
Configuration		
Adsorber CO ₂ removal efficiency	90	%
CO ₂ product compressor used?	Yes	
Solid sorbent material	Amine-based resin	
<u>Flue gas pre-treatment</u>		
Direct contact cooler used?	Yes	
Pressure drop across the pre-treat unit	6,894	Pa

SO ₂ polisher used?	Yes	
SO ₂ polisher outlet concentration	1	ppmv
Temperature exiting DCC	316.5	K
Water vapor mole fraction at adsorber inlet	15.5	%
Sorbent properties		
Heat capacity	1	kJ/kg dry solid-K
Heat of reaction	-60	kJ/mol CO ₂
Langmuir isotherm parameter (b ₀)	4.92*10 ⁻¹⁴	Pa ⁻¹
Maximum CO ₂ loading	3.9	moles CO ₂ /kg dry solid
CO₂ capture system		
<u>Adsorber</u>		
Adsorber operating temperature	327	K
Adsorber pressure drop	29	kPa
CO ₂ equilibrium pressure*	15.7	kPa
Effective adsorption kinetics (% equilb. capacity)	90	%
Overall heat transfer coefficient	385	W/m ² -K
<u>Regenerator</u>		
CO ₂ pressure in product gas stream	42	kPa
Effective desorption kinetics	10	%
Overall heat transfer coefficient	73	W/m ² -K
Regenerator operating temperature	383	K
Steam inlet temperature	408	K
Steam temperature approach	20	K
<u>Cross-flow heat exchanger</u>		
Overall heat transfer coefficient	73	W/m ² -K
Temperature of solids at hot-side HX outlet	355	K
<u>Auxiliary</u>		
Flue gas blower efficiency	75	%
Degradation		
Solid purge fraction	0.004	%
<u>SO₂</u>		
SO ₂ Capture Efficiency (moles in - moles out)/moles in	100	%
SO ₂ gas release in regenerator (moles in - moles out as gas)/moles in	0	%
<u>O₂</u>		
	No	

O ₂ Capture Efficiency (moles in - moles out)/moles in	0	%
O ₂ gas release in regenerator (moles in -moles out as gas)/moles in	100	%
	<u>N₂</u>	No
CO ₂ :N ₂ Selectivity Ratio (moles adsorbed CO ₂ /moles adsorbed N ₂)	10,000,000,000	Ratio
	<u>NO_x (NO + NO₂)</u>	No
NO _x Capture Efficiency (moles in - moles out)/moles in	0	%
NO _x gas release in regenerator (moles in -moles out as gas)/moles in	100	%
	<u>Water adsorption</u>	No
Water uptake (% removed from flue gas)	0	%
Water regeneration efficiency	100	%
Competitively Adsorbed Water (Influence on CO ₂ Capacity)	0	moles CO ₂ /kg solid sorbent

System-wide constants and variables

Ambient air pressure	101,325	Pa
Ambient air temperature	298	K
Coal heat value	30,840	kJ/kg
Cooling water temp. in	283	K
Cooling water temp. out	308	K
Cost of caustic	507.5	\$/tonne
Cost of water	0.3033	\$/tonne
FG Heat capacity	0.036	kJ/kmol
FG pressure entering CCS system	101,325	Pa
FG temp. entering CCS system	326.5	°C
Latent heat of vaporization of water	2260	kJ/kg
Plant capacity factor	75	%
Steam temperature	773	K
Universal gas constant	8,314	m ³ -Pa/kmol-K
Water heat capacity	4.18	kJ/kg-K

* Calculated value equal to $P_{A,in} * M_{CO_2}^{A,in} / \sum M_i^{A,in}$ where i=all flue gas constituents at the adsorber inlet

Case study #13: Future case with water degradation

Table 10.28: Nominal performance and cost values for Case study #13.

Input variable	Value	Units
Configuration		
Adsorber CO ₂ removal efficiency	90	%
CO ₂ product compressor used?	Yes	
Solid sorbent material	Amine-based resin	
<u>Flue gas pre-treatment</u>		
Direct contact cooler used?	Yes	
Pressure drop across the pre-treat unit	6,894	Pa
SO ₂ polisher used?	No	
SO ₂ polisher outlet concentration	237	ppmv
Temperature exiting DCC	316.5	K
Water vapor mole fraction at adsorber inlet	10	%
Sorbent properties		
Heat capacity	1	kJ/kg dry solid-K
Heat of reaction	-60	kJ/mol CO ₂
Langmuir isotherm parameter (b ₀)	4.92*10 ⁻¹⁴	Pa ⁻¹
Maximum CO ₂ loading	3.9	moles CO ₂ /kg dry solid
CO₂ capture system		
<u>Adsorber</u>		
Adsorber operating temperature	327	K
Adsorber pressure drop	29	kPa
CO ₂ equilibrium pressure*	15.7	kPa
Effective adsorption kinetics (% equilib. capacity)	90	%
Overall heat transfer coefficient	385	W/m ² -K
<u>Regenerator</u>		
CO ₂ pressure in product gas stream	42	kPa
Effective desorption kinetics	10	%
Overall heat transfer coefficient	73	W/m ² -K
Regenerator operating temperature	383	K
Steam inlet temperature	408	K
Steam temperature approach	20	K

Cross-flow heat exchanger

Overall heat transfer coefficient	73	W/m ² -K
Temperature of solids at hot-side HX outlet	355	K
<u>Auxiliary</u>		
Flue gas blower efficiency	75	%
Degradation		
Solid purge fraction	0.004	%
<u>SO₂</u>		
SO ₂ Capture Efficiency (moles in - moles out)/moles in	0	%
SO ₂ gas release in regenerator (moles in -moles out as gas)/moles in	100	%
<u>O₂</u>		
O ₂ Capture Efficiency (moles in - moles out)/moles in	0	%
O ₂ gas release in regenerator (moles in -moles out as gas)/moles in	100	%
<u>N₂</u>		
CO ₂ :N ₂ Selectivity Ratio (moles adsorbed CO ₂ /moles adsorbed N ₂)	10,000,000,000	Ratio
<u>NO_x (NO + NO₂)</u>		
NO _x Capture Efficiency (moles in - moles out)/moles in	0	%
NO _x gas release in regenerator (moles in -moles out as gas)/moles in	100	%
<u>Water adsorption</u>		
Water uptake (% removed from flue gas)	92	%
Water regeneration efficiency	79	%
Competitively Adsorbed Water (Influence on CO ₂ Capacity)	0.6	moles CO ₂ /kg solid sorbent

System-wide constants and variables

Ambient air pressure	101,325	Pa
Ambient air temperature	298	K
Coal heat value	30,840	kJ/kg
Cooling water temp. in	283	K
Cooling water temp. out	308	K
Cost of caustic	507.5	\$/tonne
Cost of water	0.3033	\$/tonne
FG Heat capacity	0.036	kJ/kmol
FG pressure entering CCS system	101,325	Pa

FG temp. entering CCS system	326.5	°C
Latent heat of vaporization of water	2260	kJ/kg
Plant capacity factor	75	%
Steam temperature	773	K
Universal gas constant	8,314	m ³ -Pa/kmol-K
Water heat capacity	4.18	kJ/kg-K

* Calculated value equal to $P_{A,in} * M_{CO_2}^{A,in} / \sum M_i^{A,in}$ where i=all flue gas constituents at the adsorber inlet

Case study #14: Future case with SO₂ and water degradation

Table 10.29: Nominal performance and cost values for Case study #14.

Input variable	Value	Units
Configuration		
Adsorber CO ₂ removal efficiency	90	%
CO ₂ product compressor used?	Yes	
Solid sorbent material	Amine-based resin	
<u>Flue gas pre-treatment</u>		
Direct contact cooler used?	Yes	
Pressure drop across the pre-treat unit	6,894	Pa
SO ₂ polisher used?	Yes	
SO ₂ polisher outlet concentration	1	ppmv
Temperature exiting DCC	316.5	K
Water vapor mole fraction at adsorber inlet	10	%
Sorbent properties		
Heat capacity	1	kJ/kg dry solid-K
Heat of reaction	-60	kJ/mol CO ₂
Langmuir isotherm parameter (b ₀)	4.92*10 ⁻¹⁴	Pa ⁻¹
Maximum CO ₂ loading	3.9	moles CO ₂ /kg dry solid
CO₂ capture system		
<u>Adsorber</u>		
Adsorber operating temperature	327	K
Adsorber pressure drop	29	kPa
CO ₂ equilibrium pressure*	15.7	kPa
Effective adsorption kinetics (% equilib. capacity)	90	%

Overall heat transfer coefficient	385	W/m ² -K
<u>Regenerator</u>		
CO ₂ pressure in product gas stream	42	kPa
Effective desorption kinetics	10	%
Overall heat transfer coefficient	73	W/m ² -K
Regenerator operating temperature	383	K
Steam inlet temperature	408	K
Steam temperature approach	20	K
<u>Cross-flow heat exchanger</u>		
Overall heat transfer coefficient	73	W/m ² -K
Temperature of solids at hot-side HX outlet	355	K
<u>Auxiliary</u>		
Flue gas blower efficiency	75	%
Degradation		
Solid purge fraction	0.004	%
<u>SO₂</u>		
SO ₂ Capture Efficiency (moles in - moles out)/moles in	100	%
SO ₂ gas release in regenerator (moles in -moles out as gas)/moles in	0	%
<u>O₂</u>		
O ₂ Capture Efficiency (moles in - moles out)/moles in	0	%
O ₂ gas release in regenerator (moles in -moles out as gas)/moles in	100	%
<u>N₂</u>		
CO ₂ :N ₂ Selectivity Ratio (moles adsorbed CO ₂ /moles adsorbed N ₂)	10,000,000,000	Ratio
<u>NO_x (NO + NO₂)</u>		
NO _x Capture Efficiency (moles in - moles out)/moles in	0	%
NO _x gas release in regenerator (moles in -moles out as gas)/moles in	100	%
<u>Water adsorption</u>		
Water uptake (% removed from flue gas)	92	%
Water regeneration efficiency	79	%
Competitively Adsorbed Water (Influence on CO ₂ Capacity)	0.6	moles CO ₂ /kg solid sorbent
System-wide constants and variables		
Ambient air pressure	101,325	Pa

Ambient air temperature	298	K
Coal heat value	30,840	kJ/kg
Cooling water temp. in	283	K
Cooling water temp. out	308	K
Cost of caustic	507.5	\$/tonne
Cost of water	0.3033	\$/tonne
FG Heat capacity	0.036	kJ/kmol
FG pressure entering CCS system	101,325	Pa
FG temp. entering CCS system	326.5	°C
Latent heat of vaporization of water	2260	kJ/kg
Plant capacity factor	75	%
Steam temperature	773	K
Universal gas constant	8,314	m ³ -Pa/kmol-K
Water heat capacity	4.18	kJ/kg-K

* Calculated value equal to $P_{A,in} * M_{CO_2}^{A,in} / \sum M_i^{A,in}$ where i=all flue gas constituents at the adsorber inlet

Appendix K: Financial assumptions for the baseline power plant

The default financial assumptions used for the power plant throughout this thesis are based on a widely-used set of baseline plant characteristics specified by the U.S. Department of Energy (DOE/NETL, August, 2007) as shown in the table below. The fixed charge factor reflects whether these plants are financially considered to be a relatively low risk (plants without CCS) or relatively high risk (plants with CCS), with higher fixed charge factors used for plants with CCS owing to the increased complexity of these systems and to the shortage of commercially proven CO₂ capture technology at large scales. All costs are evaluated in \$2011 constant dollars.

This analysis does not consider inflation when calculating the cost of electricity. The wide variety of ownership costs that are sometimes included in other financial analyses are not included here for simplicity and clarity. For more detailed estimates for any power plant, ownership costs specific to the project would typically be included. Table 10.22 lists the financial assumptions about the baseline power plant congruent with previous IECM-based modelling work (Versteeg, 2012).

Table 10.30: Baseline plant financial assumptions

Plant specification	PC Power Plant w/o CCS	PC Power Plant w/ CCS
Power plant specifications		
Ambient air pressure (kPa)	101.3	101.3
Ambient air temperature (K)	298	298
Capacity factor (%)	75%	75%
Constant flue gas heat capacity (kJ/kmol)	0.036	0.036
Cooling	Wet cooling tower	Wet cooling tower
Environmental controls	SCR, fabric filter, wet FGD	SCR, fabric filter, wet FGD
Fuel cost (2011\$/GJ)	\$2.1	\$2.1
Fuel type	Illinois No. 6	Illinois No. 6
Fuel cost nominal escalation (real escalation plus inflation %)	0%	0%
Fuel heating value as received (HHV, kJ/kg)	30,840	30,840
Nominal net power plant output (MWe)	550	550
Steam cycle	Supercritical	Supercritical
Financial assumptions		
Annual inflation rate	N/A	N/A
Cost year and type	2011 constant dollars	2011 constant dollars
Fixed charge factor*	0.113	0.143
Percentage debt	50%	45%
Percentage equity	50%	55%
Real bond interest rate	4.5%	5.5%
Real escalation rate	0%	0%
Real stock return	12%	12%
Plant book life	30	30
Weighted cost of capital before taxes	8.25%	9.075%
Years of construction	5	5
Tax rates		
Federal tax rate (%)	36%	36%
State tax rate (%)	6%	6%
Property tax rate	0%	0%
CO₂ capture system specifications		
CO ₂ product pressure (MPa)	N/A	13.79

CO ₂ transportation distance (km)	N/A	100
Flue gas CO ₂ capture requirement	N/A	90%
Flue gas CO ₂ concentration into CO ₂ capture system	N/A	13.5%
Project contingency (%)	N/A	55%
Process contingency (%)	N/A	40%

*The fixed charge factor is calculated based on the year end carrying charges and a present worth factor according to the equation: $FCF = [CC_1(1+i)^{-1} + CC_2(1+i)^{-2} + \dots + CC_n(1+i)^{-n}] / a_n$ where n is the book life of the plant, i is the interest rate, CC is the year by year carrying charges of the plant and a_n is the present worth factor for a uniform series. The year by year carrying charges are the sum of: (the return on debt, the return on equity, the payable income taxes, book depreciation, property tax, and insurance)/the total plant cost (TPC). The value of a_n is calculated according to the following equation $a_n = [(1+i)^n - 1] / [i(1+i)^n]$ (EPRI, 1986). A value of 0.113 represents financing assumptions for a mature system while 0.143 represents a first-of-a-kind plant (FOAK). See (Borgert, 2015; Versteeg, 2012) for details.